THE UNIVERSITY
of EDINBURGH

Microbial Stress in Rock Habitats

Casey C. Bryce

Doctor of Philosophy
The University of Edinburgh
2015

Lay Summary

Micro-organisms are the most abundant form of life on Earth and they have an incredible ability to tolerate stressful conditions, allowing them to colonise many extreme environments. Microbial processes change the chemistry of the environment which can have a big influence on the Earth as a whole. On the other hand, the environment has a big effect on how micro-organisms behave and evolve.

This thesis explores how microbial life is influenced by its environment, with particular focus on the interaction between microbes and rocks. These are an excellent system in which to explore this interaction as they are very common habitats, both today and throughout the Earth's history, and are relatively simple. Although rocks provide micro-organisms somewhere to live, these environments can be very stressful. This thesis focusses on the response of micro-organisms to 3 types of stress faced in rock environments: exposure to UV radiation from the sun, exposure to changes in the amount of different chemicals in the environment, and to lack of essential nutrients.

The first exposes samples to conditions outside the International Space Station to show that it would be possible for photosynthetic bacteria (which need light for energy) to survive on the early surface of the Earth, despite UV radiation being much higher than today. The latter two studies use a technique called "proteomics" to investigate how cells change the types of proteins they make in response to lack of nutrients or changing chemistry caused by reactions with water and rock, two common stresses in rock habitats. Together these results further our understanding of the relationship between micro-organisms and rocks, both today and over geological time.

Abstract

Micro-organisms are the most abundant and diverse form of life on Earth. Their ability to tolerate stress has enabled them to colonise many inhospitable environments. Microbial processes alter the chemistry of the environment which has left a lasting mark on the geological record. On the other hand, microbial life is heavily influenced by environmental conditions. Indeed, the history of the Earth is shaped by the co-evolution of microbial and geological processes.

This thesis explores how micro-organisms are influenced by their environment, with particular reference to microbial rock habitats. Rock habitats are an interesting system to understand the inter-relationship between microbial life and it's environment as they are relatively simple and very common. Rock-dwelling communities are also exposed to numerous stresses such as surface UV exposure, desiccation, temperature fluctuations, low nutrient availability or toxicity from elements leached from the rocks themselves. Three specific aspects of microbial stress in rock environments are investigated here: 1) The use of rocks as a shield from surface UV radiation stress, 2) The microbial response to chemical changes during water-rock interactions, 3) The effect of simultaneous limitation of more than one nutrient.

The first uses exposure facilities aboard the International Space Station to provide empirical evidence that colonisation of the early land masses by phototrophs was not inhibited by high surface UV radiation. The latter studies use quantitative proteomics to investigate the cellular response of a heterotrophic bacterium to nutrient deficiency and element leaching, two common stresses in rock habitats. Together these results further our understanding of the relationship between micro-organisms and rocks, both today and over geological time.

Declaration

I declare that this thesis was composed by myself, that the work contained herein is my own except where explicitly stated otherwise in the text, and that this work has not been submitted for any other degree or professional qualification except as specified.

Parts of this work have been published in [1, 2].

(*Casey C. Bryce, 2015*)

Acknowledgements

During my time at Edinburgh I have been fortunate to benefit from the kindness, patience and enthusiasm of so many inspiring people.
Firstly, I am extremely grateful for the guidance of my supervisor Charles Cockell who provided so much support and encouragement throughout this project. Thank you for giving me the opportunity to do so many interesting and varied pieces of work. It has been a real pleasure to be a part of your group.
Thanks also to my fellow members of the Astrobiology group, past and present, who helped shape this project in so many big and small ways over the years.
I also want to thank Thierry Le Bihan and Sarah Martin for introducing me to the fascinating world of proteomics, for their endless patience and enthusiasm, and for always attempting to answer my many questions.
In terms of technical advice and assistance, I would like to thank Lorna Eades for assisting with ICP-OES, Jesse Harrison for help with multivariate statistics, and Bryan Spears and Alanna Moore for helping to finally solve the phosphorus mystery. I would also like to thank the group at SCK.CEN, especially Natalie Leys and Bo Byloos, for lending their expertise with *Cupriavidus* and for always holding my work to their high standards.
In general, I would like to thank everyone in ICMCS for extending such a warm welcome to a non-physicist. You have given me a whole new perspective on what it means to understand something, and a confidence in my opinions I never knew I could have. I am extremely grateful to have had the opportunity to be part of this department and for the many friends I made here. Particular thanks to the "Cottage Club" for all the board game days and pub nights, and just generally being great.
To Mum, Dad, Gran, Granda; thank you for your unwavering support and patience always.
And finally thanks to Tim, for everything.

Contents

List of Figures

List of Tables

Chapter 1

Introduction

Micro-organisms colonise a large variety of environments on Earth, from hot springs [5, 6] to polar deserts [7], the deep sub-surface [8] and glacial environments [9] as well as inhospitable man-made environments such as metal contaminated sites [10], radioactive waste [11] and acid mine drainage [12]. Central to the capability of micro-organisms to colonise these extreme environments is their ability to cope with extreme conditions. Micro-organisms can survive at extreme temperatures from 121°C [13] down to around -20°C [14, 15], under extremely alkaline [16] and acidic conditions [17], in high salinity [18] and with very few sources of energy or nutrients [19].

Micro-organisms have persisted in extreme environments for billions of years and have developed diverse approaches for coping with such environmental stresses. They can alter the cell membrane in response to temperature stress, repair DNA damage in response to radiation exposure and produce osmoprotectant molecules to aid in desiccation survival [20]. They can also pump out toxic metals and salts or selectively uptake specific nutrients to tightly regulate intracellular chemistry under conditions of toxicity or nutrient deficiency [20].

The adaptability of micro-organisms and their ability to thrive in almost any

environment makes them the most abundant and diverse form of life on Earth [21]. It is estimated that there are up to 6×10^{30} prokaryotic cells on Earth [21]. In extreme environments micro-organisms are typically the only form of life which can survive, thus many key processes in these environments are carried out exclusively by micro-organisms. For example, methane production under the Antarctic Ice Sheet is carried out exclusively by methanogenic archaea [22]. The incredible abundance of micro-organisms means that they control the global cycling of numerous key elements such as carbon, nitrogen, phosphorus, sulfur and iron [23], and consequently have shaped the fundamental chemistry of the Earth over geological time. For example, without micro-organisms the atmosphere would not be oxygenated [24].

Micro-organisms have been present on the Earth since at least 3.2 billion years ago. Indeed, all life was microbial until around 1.1 billion years ago [25] and fossil evidence of complex life on land dates from only around 475 million years ago [26]. Over this long history, micro-organisms have actively influenced the planet; extruding gases, cycling elements and dissolving or precipitating minerals in the Earth's crust. In this way, micro-organisms can be considered to be geological agents, similar to water, wind or ice, which are responsible for the redistribution of elements, minerals and rocks on the Earth surface over geological time [27].

Although micro-organisms influence geological processes, their evolution has, in turn, been shaped by environmental conditions. For example, the concentration of biologically important elements in the environment is rarely adequate to supply optimal nutrient and energy sources to micro-organisms. Thus, micro-organisms have been forced to evolve sophisticated mechanisms for coping with nutrient starvation. Alternatively, the environment may contain high concentrations of salts or toxic elements, forcing micro-organisms to evolve the ability to pump toxins out of the cell. Physical stresses such as surface UV exposure, desiccation and temperature stress, particularly in poorly buffered surface habitats, are also common and require complex microbial responses.

This thesis attempts to understand the capabilities micro-organisms need to

cope with the stresses imposed by their environment, with a particular focus on life in rock environments. Rocky habitats represent all of the habitable space within the crust of the Earth. Biofilms on, or near, to rock surfaces were likely the first habitats on the surface of the land masses [28]. Furthermore, microbial life in the continental and ocean crust is thought to represent a large proportion of the Earth's biomass [21, 29]. Thus, rock-associated environments are a particularly ancient and common microbial habitat. However, rocks are reactive substrates which will evolve over time and alter surrounding chemistry. They can simultaneously provide nutrients and a habitat, but also have associated stresses. This makes them an interesting system in which to understand the inter-relationship between microbial life and it's environment. A number of key open research questions exist.

- What capabilities do micro-organisms need to survive and grow in rocky habitats?
- What cellular machinery have micro-organisms evolved to cope with rock-associated stresses such as toxicity or nutrient limitation?
- How might the interaction with rocks benefit or stress the microbial community?
- Does exposure to a number of stressors elicit a different response compared to exposure to a single stress?
- How would micro-organisms have coped in the geological past when problems such as UV stress were more pronounced and cellular machinery likely more primitive?

This thesis presents three studies which broadly approach these open questions. Each of the three studies presented investigate different aspects of stress in the rock environment:

1. The first investigates the mitigation of UV stress in rock environments, with particular reference to the importance of rocks as a UV shield on the early Earth when the UV flux was higher than today.

2. The second study investigates the effects of rock-induced changes in fluid chemistry on the bacterial proteome.

3. The third study investigates the effect of both single and multiple element limitation on the bacterial proteome.

A vast amount of literature has previously been generated which investigates microbial responses to stress. However, most of these studies test the response to one stress at a time. For example, they investigate the response to limitation of one nutrient or exposure to one physical stressor such as temperature, UV or pressure. However, the natural environment is much more complex and often numerous stresses will exist simultaneously. For example, microbial colonisers of deep subsurface rock environments are subject to high pressure and extreme nutrient limitation [8], and colonisers of rock surfaces are exposed to UV radiation, desiccation and temperature fluctuations [28]. Thus, without investigating the effect of multiple stressors simultaneously, we cannot adequately understand how combinations of extremes in rocky habitats will influence the survivability and stress responses of micro-organisms.

This thesis adopts a novel approach where micro-organisms are exposed to controlled combinations of stresses. Each of the three studies are conducted in a controlled setting with model strains but include exposure to multiple potential stressors. Chapter 4 investigates the survival of a rock-dwelling cyanobacterium under extreme UV radiation exposure, temperature fluctuations and desiccation. Chapter 5 investigates microbial response to rock-induced changes in fluid chemistry by introducing igneous rock, which leaches numerous different cations, into the cultures. Chapter 6 investigates the response of micro-organisms to multiple simultaneous nutrient stress.

Together these results demonstrate that the rock environment can be beneficial for micro-organisms by providing protection from external physical stressors and by providing nutrients. However, the rock environment is, in itself, capable of inflicting complex chemical stresses on micro-organisms which require tightly regulated cellular responses.

Chapter 2

Background

2.1 Introduction

This thesis explores the microbial adaptations required to cope with the complex stresses encountered in rock environments through investigation of three key stresses: 1) UV exposure, 2) rock-induced changes in fluid chemistry and 3) multiple nutrient limitation. This chapter discusses the background literature relevant to these topics. I provide a brief history of life on Earth before outlining the importance of microbe-rock interactions in the Earth system, both past and present. As part of this outline, I discuss the ways in which rock habitats may both protect micro-organisms from stress and how they may cause it. A general overview of microbial stress responses is provided, with discussion on the lack of experimental focus on combined stressors.

2.2 Brief History of Life on Earth

The oldest evidence for life on Earth dates to around 3.8-3.5 billion years ago [30–33]. While the evidence of life 3.8 billion years ago is controversial, most authors agree that microbial life was present on Earth by around 3.2 billion years ago [34].

When early micro-organisms evolved, the Earth was very different [35]. Until around 2.4 billion years ago, the atmosphere contained only trace amounts of oxygen and was, instead, dominated by nitrogen and carbon dioxide [36–39]. The lack of oxygen in the atmosphere, which now acts to form the ozone shield, would have resulted in a significantly more damaging dose of UV radiation reaching the surface of the Earth than it does today [40]. However, an intermittent hydrocarbon "haze" may have provided some short-lived protection during some parts of the early history of life on Earth [41]. The oceans would have been primarily anoxic and have very different chemistry from today, in particular they would have contained abundant iron [42].

The earliest estimates for the first life also coincide with a period known as the 'Late Heavy Bombardment'. During this time, the Earth was subjected to a much higher occurrence of asteroid and comet impacts than today [43]. This bombardment is thought to have been most intense around 3.9 billion years ago but may even have continued to around 3.2 billion years ago, well into the range of the Earth's oldest fossils [44]. Much debate surrounds the nature of this early asteroid bombardment and its effect of the origin of life. One hypothesis is that it may have caused a high temperature bottle-neck whereby only thermophilic (heat-loving) micro-organisms could survive and give rise to the rest of the history of life [45]. Alternatively, another hypothesis suggests that the Earth's surface may have been sterilised by these impacts which, if correct, places constraints on the timing or location of the origin of life on Earth [46].

2.3 Microbial Influence on Geological Processes

Conditions on the Earth today are clearly very different from those when life first evolved and organisms have been forced to adapt to these changing environments, eventually leading to the complex life observed today. However, micro-organisms were not only influenced by changes in environmental conditions, they were often the main cause. This section outlines how microbial processes lead to global changes in geological processes.

2.3.1 Micro-organisms and the Evolution of the Atmosphere

An excellent example of microbial influences on the Earth system is the oxygenation of the atmosphere. Oxygen concentrations rose from almost zero to present levels in two sudden events, the first of which is termed "The Great Oxidation Event". This was a key transition in the history of life on Earth and occurred around 2.4 billion years ago. Figure 2.1 shows the predicted oxygen composition of the atmosphere over geological time [39]. This record was established using various proxies (clues from the rock record which indicate the oxygen concentrations but do not measure them directly) [47, 48] and reveals two sudden increases in oxygen concentration in the atmosphere. The first occurred around 2.4 billion years ago and the second occurred around 0.85 billion years ago.

Oxygen is produced via oxygenic photosynthesis. This is a complex process whereby carbon dioxide and water are converted into carbohydrates using energy from the sun. This reaction produces oxygen as a waste product. Oxygenic photosynthesis had probably evolved by around 2.7 billion years ago [49] but may have been around for even longer (potentially up to 3 billion years ago) [48]. The sudden rise in oxygen therefore represents a tipping point in the balance between oxygen sources and oxygen sinks in the Earth system.

The first rise in oxygen (to levels around 1% of present) fundamentally and permanently changed environmental conditions. The appearance of oxygen caused ozone to form high in the atmosphere [24]. This formed a shield from incoming short-wave UV radiation [40]. The new oxygen level caused a shortage of iron to micro-organisms because a great deal of the soluble iron was oxidised and no longer readily available to life [42]. Additionally, because oxygen is toxic to most anaerobic life, the Great Oxidation Event limited primitive anaerobes to the remaining anoxic habitats, forced them to evolve to cope with oxygen stress or caused them to go extinct [50]. It is likely that the oxidation of the atmosphere resulted in the extinction of a huge number of microbial species [50].

In this way the oxidation of the atmosphere serves as an excellent example of the co-evolution of life and the Earth system; the evolution of oxygen-producing micro-organisms changed the composition of the atmosphere in such a way that the environmental conditions, in turn, forced life to develop new traits.

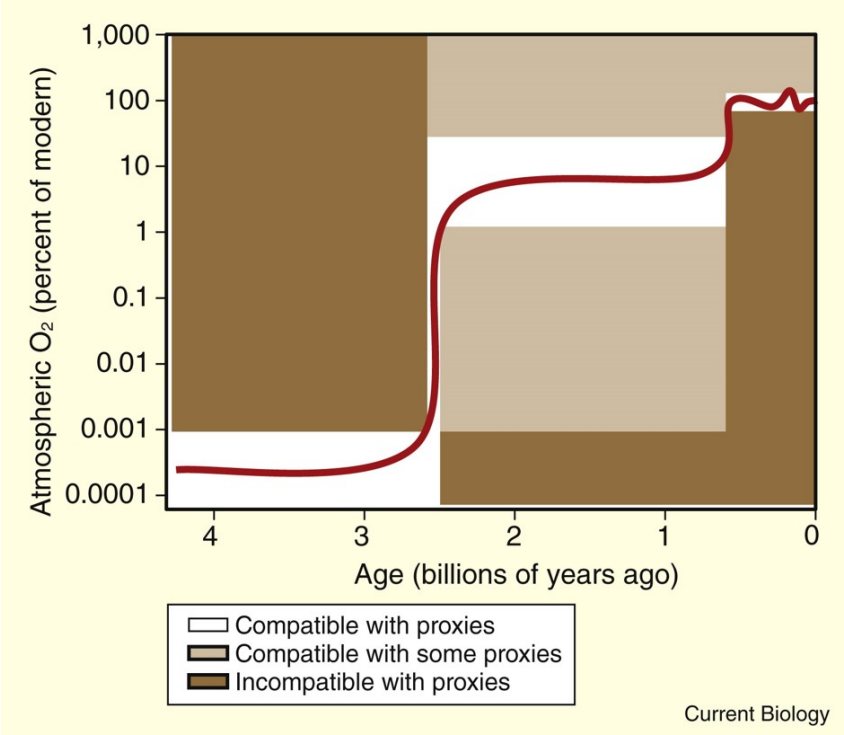

Figure 2.1 Oxygen concentrations over geological time from Sessions *et al* (2009) as inferred from various geological proxies. White = estimate compatible with proxies; beige = compatible with some proxies, therefore some doubt exists on absolute O_2 concentrations; brown = not compatible with proxies, therefore these concentrations are unlikely. This figure shows two sudden rises in atmospheric oxygen concentrations. O_2 rose from trace levels to around 1% of present at approximately 2.4 billion years ago. It rose again to around modern day levels at approximately 0.85 billion years ago.

2.3.2 Micro-organisms as Geological Agents

The oxidation of the atmosphere is just one example of how microbial processes exert control on global chemistry. However, the cycling of almost every element on Earth is, in some way, under microbial control [23]. Micro-organisms exert such a strong control on the Earth that they can be considered geological agents, similar to water or ice, which act to redistribute elements, rocks and minerals around the Earth's surface [27]. For example, microbial rock dissolution reactions transform CO_2 in the atmosphere to bicarbonate which is then stored away in

sediments. It has been suggested that removal of atmospheric CO_2 by microbially enhanced rock dissolution was essential for reducing early Earth temperatures to levels suitable for complex life [51]. This section explores how microbial energy and nutrient acquisition drive changes in geological processes.

Microbial Energy Acquisition

Micro-organisms display a huge diversity of metabolic capabilities. Types of metabolism are defined based on what an organism uses as a source of energy and what they use as a source of carbon. An organism which obtains energy from sunlight is a phototroph whilst organisms which obtain energy from molecules in the environment are chemotrophs. Many chemotrophs respire using redox reactions. In a redox reaction, the oxidation of one compound is coupled to the reduction of another. For example, iron reducing micro-organisms couple the reduction of Fe^{3+} to the oxidation of an organic compound. In this example, the organic compound is referred to as the electron donor and iron as the electron acceptor. Chemotrophs are further sub-divided depending on which electron donor they use: organotrophs use organic compounds, lithotrophs use inorganic compounds. In all aerobic organisms, oxygen is the electron acceptor. In anaerobic organisms, alternative electron acceptors such as sulfate (SO_4^{2-}), nitrate (NO_3^-) or sulphur (S) can be used [52]. Organisms which use organic compounds as a carbon source are heterotrophs whereas organisms which obtain carbon from CO_2 in the atmosphere are autotrophs. These definitions can be grouped together to give complete descriptions of an organism's metabolism. For example, a chemolithoautotroph is an organism which uses inorganic compounds from the environment as an energy source and fixes atmospheric CO_2 as a carbon source. Table 2.1 shows the definitions of different types of microbial metabolism.

This diversity of metabolism allows micro-organisms to colonise a vast array of extreme habitats. For example, chemolithotrophy allows micro-organisms to live

Table 2.1 Naming conventions for different types of microbial metabolism

Energy source	Sunlight Environmental compounds	photo- chemo-			-troph
Electron donor	Organic compounds Inorganic compounds		organo- litho-		
Carbon source	Organic compounds Carbon dioxide			hetero- auto-	

at hydrothermal vents deep in the oceans where they use inorganic elements from the hot fluids to gain energy. This often forms the base of the food chain for other more complex animals [53]. These energy acquisition processes are key to understanding how microbial processes influence the wider Earth system. For example, microbial iron reduction may be responsible for as much as 70% of the anaerobic recycling of organic matter in soils and sediments [54]. Lithotrophy is one of the primary ways in which micro-organisms dissolve [55] or precipitate minerals [10, 56]. The influence of microbial metabolism on dissolution and precipitation of minerals is discussed later in this section.

Microbial Nutrient Requirements

In addition to needing chemical sources of energy, micro-organisms have many other chemical requirements they must satisfy in order to build biomass. Satisfying these nutrient requirements is another way in which micro-organisms influence global chemistry. For example, in some areas of the ocean the iron requirement of heterotrophic bacteria leads them to assimilate more than 50% of the dissolved iron [57].

All life requires carbon, hydrogen, nitrogen, oxygen, phosphorus and sulfur [58]. In addition to these, many "micronutrients" are also required. These are mostly metals which are used in redox reactions within the cell. Iron, for example, is essential for the functioning of cytochromes (iron-containing proteins responsible for ATP production via electron transport) [59]. Magnesium is essential for numerous key cellular processes such as ATP utilisation, genome stability and

maintenance of membranes and ribosomes [60]. Furthermore, an estimated 16% of all microbial enzymes use magnesium as a cofactor [61]. Magnesium is also used in chlorophyll, essential for photosynthesis [62]. Most of the elements required by microbial life can be found within rocks but they are locked within the matrices of the minerals and not readily available. Micro-organisms have evolved numerous mechanisms to enhance the breakdown of rocks and minerals in order to release elements they require. This is discussed in detail in the next section.

Micro-organisms and Mineral Alteration

Minerals and rocks can break down abiotically through reactions with water resulting in the leaching of cations and silica, hydration of minerals and pH changes. However, this important process can be significantly enhanced by microbial activity [63–67]. This occurs via three primary mechanisms:

1) Altering pH to dissolve rock surfaces

Bacterial metabolism can produce a number of by-products which can act to alter the rock surface by changing the pH which in turn enhances dissolution. For example, the CO_2 produced by microbial aerobic respiration can combine with water to form carbonic acid. Since the solubility of minerals is often dependent on pH, this in turn contributes to the dissolution of the rocks and minerals.

2) Altering the redox state of elements

Chemolithotrophs specialize in the use of metal ions as electron donors and acceptors to serve their energetic requirements. In the process of oxidising or reducing metals, organisms can alter the speciation and therefore solubility of certain elements. For example, iron commonly exists as two different ions; Fe^{3+} and Fe^{2+}. Fe^{3+}, oxidised iron, is insoluble in water. Fe^{2+}, the reduced ion, is soluble in water. The conversion of Fe^{3+} to Fe^{2+} by iron

reducing micro-organisms will turn the iron into its soluble form where it can then be washed away and precipitated elsewhere. In the opposite reaction, iron oxidizing micro-organisms will turn soluble Fe^{2+} to insoluble Fe^{3+} and precipitate iron minerals from solution.

Microbial redox reactions leading to the precipitation of minerals are common in the geological record. For example, large banded deposits of iron sulfide minerals (called banded iron formations) deposited early in geological history may have been formed by such a process [68]. Micro-organisms may also be responsible for forming valuable mineral deposits. For example, consortia of sulfate reducing bacteria can precipitate almost pure zinc sulfide from dilute groundwater [69] and the Gram-negative bacterium *Cupriavidus metallidurans* CH34 (used for work in most of this thesis) can precipitate gold nanoparticles from solution [70]. These reactions are also exploited in bioremediation of metal contaminated sites by causing immobilisation of toxic metal species [71]. This mobilisation/immobilisation of elements exerts control over element fluxes to other parts of the Earth system, particularly the elemental composition of oceans, rivers and pore waters [72].

3) Production of chelating agents

Chelating agents are compounds which strongly bind to metal ions and transport them into the bacterial cell. The most intensely studied chelating agents are siderophores [64] which have a very high and specific affinity for iron. These compounds will be secreted by organisms to scavenge elements from the surrounding environment and transport them into the cell. Siderophores are extremely important for global iron cycling. For example, almost all of the Fe^{3+} dissolved in the surface of the oceans is bound to siderophores [73].

The formation of biofilms on rock surfaces is a key facilitator of these microbial rock weathering mechanisms. By ensuring adhesion to the rock surface, these

assist in concentrating the chemical effects of microbial activity directly on the rock surface, enhancing weathering effects [28].

2.4 Geological Influence on Microbial Processes

The previous section outlined the ways in which microbial metabolism influences geological processes. However, this is a two-way interaction. Overall the story of life on Earth is a story of feedbacks between geological processes and life. Investigation of the metabolic and stress-tolerance strategies of micro-organisms cannot be undertaken out-with the context of the environment. The key focus of this thesis is the interaction between rock habitats and microbial life. Rock habitats provide an ideal model system for understanding microbe-environment interactions because of their simplicity. In this section I provide some background to rock habitats and the benefits and stresses imposed by rocks on microbial life.

2.4.1 Rocks Provide Microbial Habitats

One way in which geology influences microbial life is by providing many different habitats [72]. The following short descriptions outline broad examples of microbial rock habitats and aim to aid in the appreciation of the great variety of microbe-rock interactions on Earth.

Biofilms on rock surfaces

Microbial life on rock surfaces is everywhere and a thin microbial film will exist on almost any rock surface [28, 74]. Indeed, even rock freshly created in volcanic eruptions is colonised by micro-organisms within a matter of weeks [75]. These habitats are poorly buffered from environmental stresses, thus communities on rock surfaces are exposed to UV radiation exposure, temperature fluctuations, wind and desiccation [76–79].

Endoliths

Endolithic communities are those contained within cracks and pore spaces in rocks rather than on the surface. These communities are buffered from external stresses experienced in surface rock biofilm habitats and thus are most commonly associated with harsh environments in which these factors limit growth on rock surfaces [76–79]. For example, in the Antarctic Dry Valleys microbial life is rare on the surface but commonly found under quartz stones [80] or inside sandstones [81]. Communities also inhabit salt crusts in extremely dry regions such as the Atacama Desert [82]. Additionally, endoliths have been found in impact craters in the High Arctic [83, 84], igneous rocks in Svalbard and Iceland [85, 86] and silicious volcanic deposits [87–89]. These communities are some of the simplest ecosystems known [90]. They typically contain several photosynthetic species (cyanobacteria, blue green algae, fungi, lichens) along side a larger number of non-photoautotrophic bacteria [91]. The prevalence of photosynthetic organisms in almost all endolithic communities suggests a minimum requirement for light [92].

Sub–surface habitats

It has only become accepted in the last few decades that the biosphere consists of more than what is observed in the near-surface environment. Early estimates thought even the hardiest micro-organisms could only survive a few tens of metres underground [93] but abundant, diverse microbial communities have now been observed deep in the continental and oceanic crust [8, 94–96]. Recent estimates suggest between 2% and 19% of the total biomass on Earth is in the terrestrial deep sub–surface and that the abundance of prokaryotes in the oceanic sub–surface is at least equal to that of seawater [29]. Deep sub–surface environments are typically very isolated and receive little external light or energy input. Potential energy sources may be buried organic carbon or H_2 which can

be released via serpentenization of basaltic rocks deep in the crust [97]. Cell turnover times can be on geological timescales [19]. Diverse microbial communities kilometres below glacial ice have also recently been observed [98]. These sub-glacial environments experience nutrient stress and high pressures similar to crustal sub–surface habitats but additionally expose the organisms to extremely cold temperatures.

2.4.2 Rock Habitats Protect Micro-organisms From Stress

Common Physical Stresses

Rock habitats impose many different stresses on microbial communities. Surface rock environments, for example, are poorly shielded from the wind and the sun thus microbial communities on rock surfaces are subject to stresses such as desiccation, temperature fluctuations and radiation exposure [74]. Microbial communities in the deep sub–surface are exposed to high pressure and low energy and nutrient fluxes [19]. However, rocks may also protect micro-organisms from stress.

In Chapter 4 of this thesis I focus on the protection afforded by rocks to UV radiation stress in particular. This is particularly interesting in the context of understanding the early evolution of life as UV stress on the surface of the Earth was much higher before the formation of a protective ozone layer around 2.4 billion years ago [24]. The rest of this section further explores surface UV radiation in rock environments and the microbial response to such a stress.

Micro-organisms and UV Radiation Stress

Most humans are familiar with the damage induced by extended exposure to the sun's UV radiation which damages DNA. DNA damage, as well as damage

to other cellular structures, is also common in micro-organisms. Exposure to UV radiation causes damage to essential biomolecules such as DNA, RNA and proteins. In cyanobacteria, UV exposure is associated with destruction of photosystem proteins and light harvesting pigments as well as decreased efficiency of chlorophyll synthesis, nitrogen fixation, energy production and cell differentiation [99].

Ultraviolet (UV) radiation is electromagnetic radiation within the wavelength range 400nm - 10nm. Biologically relevant wavelengths of UV are those which fall into the UVC (280–100nm), UVB (315–280nm) and UVA (400–315nm) ranges. The extent of damage during UV exposure is correlated with the wavelength of UV, shorter wavelengths cause more damage than longer ones [40].

Long-wavelength UVA radiation is the dominant form of UV on the Earth today, followed by UVB which is mostly absorbed by the atmosphere before reaching the Earth's surface. Today, all UVC radiation is absorbed by the atmosphere but this was different early in Earth history when the atmosphere contained much less oxygen than today [24].

UV History of the Earth

As discussed earlier in this chapter, the Earth today is protected from UV radiation by the ozone shield [24]. Ozone reduces the biological damage caused by incoming UV radiation by three orders of magnitude [100]. However, the nitrogen and carbon dioxide atmosphere dominant prior to the Great Oxidation Event could not block incoming UV as effectively [40]. Organisms attempting to survive on the Earths surface prior to the rise in oxygen would receive a radiation dose up to 1000 times more damaging to DNA than today [40]. The problem is significant even accounting for lower solar luminosity early in Earth history [101]. Indeed, it was originally proposed that the intense UV radiation flux experienced on the early Earth might have prevented the colonization of the land masses until after oxidation of the atmospshere [102].

However, cyanobacteria had already evolved prior to the oxygenation of the atmosphere [103] and significant microbial colonisation of the land masses is thought to have occurred by at least 2.7-2.8 billion years ago [104]. How then did micro-organisms survive on land under these harsh UV conditions?

UV Avoidance Strategies

An understanding of how micro-organisms cope with high levels of UV radiation today can provide some clues as to how micro-organisms may have dealt with this problem in the past.
Numerous methods for actively repairing DNA damage induced by UV exposure are observed in prokaryotes today [99]. However, given the severity of the UV flux on the early Earth, these mechanisms would likely have become overwhelmed in organisms directly exposed on the surface of the land masses [40]. It is therefore likely that any surface or near-surface dwelling life at this time would require some kind of UV avoidance strategy.

In high UV environments on Earth today, micro-organisms are commonly found in locations where there is a physical barrier between the micro-organisms and the incident UV radiation. Some organisms, for example, achieve protection within thick laminated structures called stromatolites. These are large (up to 1m across) mound-like structures formed in shallow water by the trapping and cementation of sediment by microorganisms, mostly cyanobacteria, to form thick mats. The structures grow as the cyanobacteria are buried by the trapped sediment and must move up to continue to access light.
This has long been recognized as a potential means for micro-organisms to survive the early intense UV radiation, in part due to the discovery of fossil evidence of micro-organisms in ancient stromatolites in Western Australia [105–107].
Alternatively, environments which experience harsh surface conditions often display excellent examples of organisms growing in the interior of rocky substrates

or under them which are known as endoliths and hypoliths, respectively [79, 80, 108]. As mentioned previously, endolithic communities contain photosynthetic organisms at a depth in the rock where they can still access some light but where they are buffered from the extremes on the surface.
This ability to grow phototrophically in the sub–surface whilst being shielded from most of the incident UV radiation led to the suggestion that endolithic habitats may have been useful on the early surface of the Earth [1, 83, 84, 86, 109, 110]. Assessing the suitability of endolithic habitats for protecting phototrophs from early Earth UV conditions is the main focus of the first study in this thesis.

2.4.3 Chemical Stress in Microbial Rock Habitats

As discussed in section 2.3, micro-organisms have many nutrient requirements. Often, in rock habitats, these nutrient requirements are satisfied by elements abiotically leaching out of rocks. If abiotic processes do not supply the required nutrients, micro-organisms can enhance this supply by dissolving the rock surface. However, these processes may still not supply an adequate amount of the required nutrients and consequently nutrient deficiency is a common stress in the environment [74, 111–116]. Furthermore, the dissolution of rocks often releases other toxic chemicals such as heavy metals [117]. In this section I outline the concepts of nutrient deficiency and toxicity in the context of microbial rock habitats.

Nutrient Deficiency in the Environment

Although rocks can supply nutrients, most environments on Earth remain nutrient limited [115, 118]. Over time, soils initially rich in rock-derived nutrients will become irreversibly depleted as these elements are washed away to the oceans [119, 120]. Rock-derived nutrients in the oceans will be increasingly exhausted

the further the region is from the continental margins. Sub-surface habitats are typically very isolated and not regularly replenished with external nutrient and energy sources [19]. Nutrient stress is therefore a key environmental stress for microbial life. Microbial responses to nutrient stress are investigated in Chapter 6 of this thesis. The next section outlines the concepts surrounding nutrient deficiency in micro-organisms.

Concepts in Nutrient Deficiency

The term "nutrient limitation" is commonly used to refer to a situation in which the scarcity of nutrients results in a reduction in the growth rate of the population. This occurs because low extracellular concentrations mean less nutrient reaches the cell surface to be transported into the interior of the cell. This reduces the intracellular concentration of that nutrient and limits the growth rate [118].

The effect of nutrient availability on growth rate can be described by a saturating relationship [121]. This means that, at low nutrient concentration, the growth rate will increase as more nutrient is added and, in this circumstance, the concentration of the nutrient could be considered to be limiting. When nutrient concentration is high, the micro-organisms will see no improvement in the growth rate when more nutrient is added as the growth has become "saturated".

Chapter 6 of this thesis focuses on understanding multiple nutrient stress. Most nutrient stress experiments in the lab test the effects of deficiency of one nutrient [122–124]. However, increasingly abundant evidence from bottle incubations and *in situ* gene/protein expression studies show that, often, more than one nutrient can influence the microbial growth in the environment [111, 114–116, 125]. The term "nutrient co-limitation" is typically used to describe conditions where two or more nutrients are required to stimulate the growth of the micro-organisms or where the addition of two or more nutrients results in greater increase in growth rate/yield than the addition of any one nutrient alone [118, 126].

Two differing philosophies exist regarding how micro-organisms are expected to

respond to limitation of multiple elements. The first suggests that the effect on growth rate would be multiplicative such that both elements will influence the overall growth rate [121]. Alternatively, the co-limited growth rate could be determined by the growth rate of the most limiting of the nutrients. This is known as "Liebig's Law of the Minimum" [127]. Significant debate exists in the literature around which of these approaches is more realistic [126].

Very few studies have investigated the physiological response to multiple nutrient stress but, in the few studies conducted, differences between single and multiple limitation have been observed. For example, in *Pseudomonas putida*, PHA accumulation differs under carbon, nitrogen and dual carbon-nitrogen stress [128]. Experiments investigating the physiological response of micro-organisms to limitation by multiple nutrients could indicate whether one nutrient had a more dominant effect on the cell. This would help establish whether the response to multiple nutrient limitation is influenced by both elements or follows Liebig's Law of the Minimum. In addition to providing insights into nutrient controls on microbial population dynamics, investigation of physiological changes during multiple nutrient limitation can take us a step closer to understanding the capabilities micro-organisms require to cope with complex stresses in the environment.

Toxicity Caused by Elemental Leaching

Although the rock environment can supply nutrients, the leaching of elements may be excessive and cause toxicity to the microbial community. For example, most rocks contain trace amounts of metals which can be toxic in high concentrations [117]. In leaching bio-essential elements, non-essential elements may also be leached and cause stress. For example, mobilisation of arsenic from igneous rocks is extremely common, particularly in Asia, and causes severe human suffering as well as stress to microbial communities [129]. Indeed, it has been suggested that multiple metal stress resistance mechanisms, typically found in

microbial colonisers of anthropogenic metal contaminated sites, originally evolved to respond to metal leaching from rocks in volcanic environments [117].

Water-rock interactions also often lead to particularly alkaline or acidic environments. For example, where sulfide minerals are exposed to the surface by mining, solutions containing sulfuric-acid and dissolved toxic metals. Indeed, formation of these solutions is primarily driven by sulfide-oxidizing bacteria such as *Thiobacillus* [12]. This is known as acid mine drainage and contains diverse microbial communities adapted to these extreme conditions [12]. Experiments presented in Chapter 5 explore the response of micro-organisms to chemical changes induced by water-rock interactions.

2.5 Microbial Response to Stress

I have outlined the numerous types of stress which micro-organisms have to be able to cope with in the environment. In order to understand how micro-organisms cope with the different types of stress studied in this thesis, a general overview of microbial stress responses is required. This section will only broadly discuss stress responses in bacteria. Bacteria possess a wide variety of responses to stresses they may encounter in their environment which is the subject of a correspondingly enormous body of literature [20, 59, 122–124, 130].

Micro-organisms possess two broad stress adaptation approaches: a specific or general response. Specific responses encompass a very specific regulation component which regulates expression of specific genes associated with the original stress, with the aim of repairing the damage or regaining homeostasis within the cell. However bacteria also have a number of broad stress responses which are more focussed on prevention of stress than avoidance of it [131, 132]. The global regulators triggered by these broad stress responses are responsible for general restructuring of cellular processes such that the cells are generally more resistant to stress.

This section attempts to give a broad overview of different approaches adopted by bacteria to respond to environmental stress. Each individual specific or general stress response has a very large associated body of literature and there will be no attempt to cover that here. Even in their very specific review of the general stress response in *E.coli*, Battesti *et al* [131] emphasise their need to be selective on the literature even when just discussing one type of response in one organism. The aim of this section is only to familiarise the reader with typical broad strategies employed to deal with environmental stresses.

2.5.1 How do Bacteria Sense and Respond to the Environment?

Protein Synthesis

Micro-organisms only have a limited ability to alter their environment. Therefore, when they find themselves exposed to a stressor (such as UV stress, nutrient deficiency or toxicity) they must be able to alter the cell in order to cope. Central to this ability is the synthesis of proteins. Proteins are macromolecular structures formed of long chains of amino acids which carry out cellular processes. Thus, when a stress is encountered, the micro-organism will alter the abundance of proteins designed to deal with that stress.

The instructions for making proteins are encoded on DNA. When a protein is required, the code for the protein is transcribed from DNA to RNA. First, the RNA polymerase protein binds to the promoter region of the DNA, the part that initiates transcription of a specific gene. The RNA polymerase separates the two DNA strands and matches RNA nucleotides to the DNA nucleotides of one DNA strand. The RNA nucleotides are linked by a sugar-phosphate back bone to form an RNA strand. The RNA strand then breaks away from the DNA strand and is known as messenger RNA (mRNA).

This mRNA strand can then be "translated" into protein. Every three nucleotides in the RNA code for one amino acid and, together, are called a "codon". During translation, the ribosome (a complex of proteins and RNA which synthesises proteins) assembles around the mRNA. Transfer RNA (tRNA) attaches to the corresponding mRNA, bringing the amino acid coded by the 3 bases with it. The ribosome then moves on to the next codon, joining the amino acids together as it goes. When the ribosome reaches the codon which indicates the end of the protein, it releases the amino acid chain. This chain is then folded to form an active protein.

Regulation of Gene Expression

Some genes are continually transcribed into proteins in relatively constant amounts. Typically these are genes for proteins required for maintenance of the cell. However, some genes are expressed (turned into protein) only when they are required, and are typically induced in response to environmental signals.
As discussed above, protein synthesis proceeds in 3 stages: transcription (DNA to mRNA), translation (mRNA to protein) and post–translational modification (folding of protein etc). When micro-organisms sense a stress, they can enhance or inhibit the synthesis of proteins at any of these stages [4]. Alternatively, micro-organisms may selectively degrade proteins which are no longer required.
Regulation at the transcriptional level controls the rate of conversion of DNA to RNA. A number of mechanisms exist to increase or decrease transcription rate and they primarily involve factors which inhibit or assist the binding of the RNA polymerase [4]. Post-transcriptional regulation controls gene expression at the RNA level, typically by promotion or inhibition of mRNA degradation or by controlling the abundance of protein translated from mRNA [133]. After protein synthesis has occurred, proteins can be selectively degraded when they are not needed [133].

Types of Proteins

A huge variety of proteins exist with an equally diverse array of functions. The database used in Chapter 6 groups proteins into "product types". Despite some overlap in definition, this provides a good framework for describing the variety of functions proteins carry out.

This database primarily classifies proteins as: enzymes, carriers, transporters, receptors, factors, regulators, structures, membrane components, lipoproteins or cell process proteins. Enzymes are the most abundant type of proteins and are responsible for catalysing biochemical reactions in the cell. Carrier proteins facilitate the movement of ions, small molecules or macromolecules. Transporters facilitate transport of molecules in and out of the cell. Receptors are proteins which bind substances for transport across the cell membrane. Factors, or transcription factors, are proteins which bind to DNA sequences to control the rate of transcription whereas the regulator class includes proteins which control gene expression at other stages or via different mechanisms. Lipoproteins are complexes consisting of lipids and proteins, typically associated with the membrane. Membrane components include proteins integral to the membrane, most of which are electron transport chain proteins or transmembrane proteins. Structural proteins are those which form macromolecular structures in the cell such as ribosomes or flagella. Cellular process proteins are those essential for key processes such as replication and chemotaxis.

Different types of proteins come together to adapt to environmental conditions. Some adaptations are very well characterised. An overview of typical stress responses is provided in the following sections.

2.5.2 The General Stress Response

The General Stress Response, best studied in *E.coli*, is a global response which induces broad changes in metabolism and gene expression that protect the cells from a variety of different stresses, such as the transition from exponential to stationary phase, induction of starvation, high/low pH, temperature stress or DNA damage [131].

The general response is triggered by accumulation of sigma factor RpoS. A sigma factor (σ-factor) is a protein required only for the initation of RNA transcription which typically regulates a large number of genes. The sigma factor used to initiate transcription of specific genes will depend on the gene and the external trigger. Every bacteria will have a house-keeping sigma factor which will ensure transcription of genes needed for normal growth. Other sigma factors will be increased or decreased dependent on the genes required. The number of sigma factors varies between organisms. For example, *E. coli* has seven whereas *Cupriavidus metallidurans* has 18.

The collection of genes regulated by sigma factor RpoS is termed the RpoS "regulon". The RpoS regulon contains genes responsible for numerous stress adaptations. For example, induction of RpoS induces genes for oxidative stress and desiccation tolerance [131]. The RpoS-mediated general response also affects cell morphology and the cell envelope, resulting in a transition to small, ovoid cells in *E. coli* [134].

2.5.3 The Stringent Response

The stringent response is adopted by bacteria to quickly reorganise translational machinery in response to nutrient stress. The trademark of this response is the production of the molecules ppGpp (guanosine 5'-diphosphate 3'-diphosphate) and pppGpp (guanosine 5'-triphosphate 3'diphosphate), together known as

(p)ppGpp [132, 135]. (p)ppGpp is a secondary messenger, triggered by the original stress cue.

Typically, induction of the stringent response results in down-regulation of translational machinery such as ribosomes and factors promoting growth and division, as well as up-regulation of stress response genes. Both the stringent response and general response can occur simultaneously. This is because RpoS (the general stress sigma factor) induces production of (p)ppGpp (the stringent response regulator).

2.5.4 Specific Stress Responses

Instead of, or in addition to, the broad adaptive responses, micro-organisms may employ responses with the specific aim of countering the specific stress experienced. For example, in response to low temperatures, bacteria employ a variety of mechanisms to replace saturated fatty acids (no double bonds) with unsaturated fatty acids (at least one double bond) in the membrane. Phospholipids with unsaturated fatty acids have lower melting points and greater flexibility than those with saturated fatty acids, thus countering the temperature effects on membrane fluidity.

Another example of a stress with a specific response is oxidative stress. This stress is the result of an imbalance in the pro-oxidants and anti-oxidants in the cell due to high concentrations of reactive oxygen species such as superoxide anions (O_2^-), hydrogen peroxide (H_2O_2) or hydroxyl radicals (HO), or low concentrations of antioxidant molecules or enzymes such as glutathione. Typically this occurs as a by-product of respiration or during exposure to UV radiation. The oxidative stress response induces expression of numerous genes for direct detoxification, production of antioxidants such as glutathione and repair of cellular structures like DNA.

Specific responses exist for a huge variety of environmental stressors, each with

its own background body of work. These include responses to acid stress [136], osmotic stress [137], DNA damage [138] and temperature stress [139, 140]. The response becomes even more specific in the case of metal toxicity or nutrient deprivation where the response is unique to the element of interest. For example, deprivation of iron induces a separate and unique response to phosphorus deprivation [59, 141], and response to metal toxicity will be unique to each element [142].

2.6 Multiple Simultaneous Stresses

As demonstrated in the previous section, significant understanding of the response mechanisms to a large variety of stresses has already been gained. However, there are very few studies which investigate the collective impact of multiple simultaneous stresses on micro-organisms. This is extremely important as most environments on Earth (including but not exclusive to "extreme" environments) are characterised by numerous co-existing stressors. Indeed, "polyextremophiles", micro-organisms which tolerate multiple extreme conditions, are common [143]. For example, desert environments will expose microbial communities to desiccation, UV radiation exposure and extreme temperatures (either hot or cold). Even in the soil environment, micro-organisms are exposed to nutrient stress (potentially of more than one nutrient). Indeed, the most unrealistic situation is the study of rich, rapidly growing cultures in the laboratory.

2.6.1 Multiple Physical and Chemical Stresses

The small number of studies which have investigated microbial growth and survival under multiple stressors have found that combinations of extremes can have surprising effects. For example, iron limitation and micro-aerobic conditions lead to reduced sensitivity to high temperatures in *Halomonas hydrothermalis*

[144]. *Shewanella gelidimarina* has a higher tolerance to elevated temperature when cultivated under high salinity due to increased membrane lipid packing and fatty acid content which aids in resistance to both stresses [145]. *Natranaerobius thermophilus* uses alternative pH regulation strategies (antiporters or solute accumulation) to tolerate alkalinity under different temperature and pressure regimes [146].

Part of the reason for increased tolerance to one stressor during exposure to another, is likely the cross-resistance conferred by numerous stress responses. For example, heat shock proteins induced under temperature stress also confer resistance to desiccation [147].

Experiments conducted in Chapters 4, 5 and 6 of this thesis expose the model strains to multiple physical and chemical stresses simultaneously. In Chapter 4, the model cyanobacterium is exposed to intense UV radiation exposure, extreme temperature fluctuations and prolonged desiccation. In Chapter 5, the model bacterium is cultured in the presence of rock which leaches out numerous cations, alters the pH and sequesters essential nutrients. In Chapter 6, the bacterium is exposed to limitation of multiple essential nutrients.

2.7 Use of Proteomics for Understanding Microbial Stress Responses

As discussed, the primary way micro-organisms respond to a stress is by increasing or decreasing production of proteins related to that stress. For example, when an organism senses high extracellular concentrations of toxic metals, it can produce more proteins which pump toxic metals out of the cell [148]. Therefore, directly comparing protein abundances under different conditions can provide clues as to how micro-organisms respond to different stresses.

The problem is that micro-organisms typically express thousands of proteins

simultaneously. Until recently, the technology did not exist to investigate expression of such a large number of proteins. This led to a reliance on gene expression studies using techniques such a DNA micro-arrays rather than protein expression. These have benefits as they use a specially designed micro-array chip which will bind messenger RNA from every gene in the genome. However, RNA is only the instructions for a process whereas proteins are the molecules which carry out the process. Because a significant proportion of regulation occurs post-transcriptionally, looking only at RNA abundance does not give an accurate picture of the processes actually occurring in the cell. Indeed, it has been observed that gene expression and protein expression results are poorly correlated when analysed from the same treatment [149].

The past decade has seen advances in 'omics' technologies which have revolutionised the study of microbiology. Advances in genomics have enabled the sequencing of an ever growing list of microbial genomes and revealed great microbial diversity in the environment. Metagenomics is now expanding on that by potentially sequencing *all* genes in an environment, allowing reconstruction of microbial metabolisms and lifestyles in different habitats. Transcriptomics enables researchers to identify which of the genes present in the genome are triggered under different circumstances. Advances in mass spectrometry and bioinformatics have now revolutionised the study of protein expression. It is now possible to accurately identify and quantify more than one thousand proteins from a complex sample with very minimal sample preparation. The large scale analysis of the protein complement of the cell is known as proteomics.

The use of large-scale protein expression studies has yielded fresh insights into a wide variety of stresses such as salt stress [150], osmotic stress [151], oxidative stress [152] and metal resistance [153], to name just a few.

2.8 Thesis Focus

This chapter has outlined the ways in which micro-organisms interact with, influence and are influenced by the materials which make up planet Earth, specifically with regards to strategies of stress and stress avoidance in the environment. In the remainder of this thesis, three studies are presented which investigate different aspects of stress in the rock environment:

1) UV exposure

The first study attempts to understand the importance of rocks as a UV-shielded habitat for primitive cyanobacteria on the early Earth. The UV radiation flux to the surface of the Earth was higher and more damaging before the atmosphere became oxygenated around 2.4 billion years ago. It has been suggested this would have inhibited phototrophs, which require light energy to survive, from colonising the Earth's land masses prior to this time. However, shelter within cracks and pore space in rocks with some light transmissivity have been hypothesised as a solution to this problem. To empirically test whether these rocks could provide adequate protection for early phototrophs, facilities on board the International Space Station were used to expose cyanoacterial endoliths to extremely high UV fluxes. Through post-flight analysis of viability, morphology and biomarker preservation, this thesis provides the first empirical refutation of the proposal that colonisation of the land by phototrophs was delayed by the high UV flux on the early Earth.

2) Rock-induced changes in chemistry

Secondly, this thesis attempts to understand how the addition of rock to cultures of micro-organisms in defined growth media alters fluid chemistry and thus molecular processes within a model bacterial strain. This chapter demonstrates that the addition of rock is both stressful and beneficial for

the microbial population. The rock is useful as it provides nutrients such as iron and magnesium which improves growth rate and yield in nutrient deficient cultures. However, the addition of rock to optimal media (i.e. all nutrients adequately supplied) results in reduced growth rate and yield compared to the optimal media with no rock added. Detailed chemical analysis of the effects of rock on fluid chemistry reveal that this is caused by adsorption of phosphorus on to the rock surface and by increases in pH. Analysis of the proteome, the protein complement of the cells, revealed that exposure to rock required micro-organisms to actively scavenge phosphorus and reorganise energy metabolism due to rock-induced nutrient limitation.

3) Nutrient deficiency

Finally, having observed the importance of phosphorus limitation in rock environments, this thesis investigates the molecular response of a model bacterium to deficiency of one or more nutrients. The proteome response to different severities of phosphorus, iron and magnesium stress is catalogued before comparing simultaneous deficiency of two of these elements simultaneously i.e. magnesium and phosphorus limitation, iron and magnesium limitation or phosphorus and iron limitation. In comparing protein expression under single and multiple nutrient limitation, this thesis demonstrates that the response is dominated by just one nutrient. This has important implications for the representation of micro-organisms in environmental models and provides a novel insight into microbial capabilities under multiple nutrient stress.

The approach adopted in this thesis differs from that commonly employed in studies of microbial stress by attempting to incorporate some of the complexity of the natural environment into controlled studies. In Chapter 5, for example, the response of micro-organisms to rock-induced stress is assessed by exposing a model bacterium to liquid containing a typical rock with all of its inherent complexity. This exposes the model organism to changes in numerous different

elements, both increases and decreases, simultaneously. However, the controlled laboratory setting and use of a single bacterial species enables detailed analysis of the experiment from different analytical perspectives and allow us to unravel the relationship between chemistry and cellular response.

This approach is also adopted in the space experiments in Chapter 4, where exposure to UV radiation occurs in tandem with other space exposure effects such as temperature fluctuations and desiccation, and in Chapter 6, where typical controlled nutrient experiments are expanded to include multiple simultaneously limiting nutrients.

This thesis represents a significant advancement in our understanding of the microbial capabilities required to cope with stress in microbial rock habitats.

Chapter 3

Methodology

3.1 Introduction

This chapter describes the principles of some of the key experimental and analytical techniques adopted in this thesis. As the exact protocols used differ in each of the following chapters, specific details of each experiment or analysis is included within the methodology section of the relevant chapter. This chapter instead aims to provide an overview of the principles behind the techniques used and walk the reader through the typical workflow.

3.2 Bacteria and Culture Media

3.2.1 Bacterial Strains

The cyanobacterium *Chroococcidiopsis* CCMEE 029 was used for the experiments discussed in Chapter 4. This was obtained by Prof. Charles Cockell from the Culture Collection of Micro-organisms in Extreme Environments established by

E. Imre Friedmann and now maintained at the University of Rome Tor Vergata. The beta-proteobacterium *Cupriavidus metallidurans* CH34 (wild-type) was used for the experiments discussed in Chapter 5 and Chapter 6. This was obtained from Liebniz Institute DSMZ - German Culture Collection of Micro-organisms and Cell Cultures.

3.2.2 Culture Media

Cupriavidus metallidurans CH34 was grown in Tris Salts Minimal Mineral Medium (MM284) [154]. The composition of this medium is shown in Table 3.1. The composition of the SL 7 Trace element solution included in this medium [155] is shown in Table 3.2. The medium was adjusted to pH 7 and autoclaved at 121°C for 20 minutes prior to use. If iron (III) chloride was used as the iron source, this was filter sterilised and added after autoclaving. Modified MM284 medium was used to test various nutrient-limitation effects in Chapters 5 and 6 and is discussed in the relevant chapters. For MM284 solid medium, 1.5% Bacteriological Agar (Sigma-Aldrich, UK) was added to the liquid medium prior to autoclaving.

Chroococcidiopsis is cultured in BG-11 medium. The composition of this medium is displayed in Table 3.3. This was corrected to pH 7.1 and autoclaved at 121°C for 20 minutes prior to use.

Table 3.1 Composition of MM284 medium for growth of *Cupriavidus metallidurans* CH34

Component	Amount in 1L media
Trizma hydrochloride	6.6 g
Sodium chloride	4.68 g
Potassium chloride	1.49 g
Ammonium chloride	1.07 g
Sodium sulfate	0.43 g
Magnesium chloride hexahydrate	0.2 g
Calcium(II) chloride dihydrate	0.03 g
Sodium phosphate dibasic dihydrate	0.04 g
SL 7 Trace element solution*	1 ml
Sodium gluconate	2 g
Ferric ammonium citrate	4.8 mg
OR	
Iron(III) chloride	2.52 mg

* Composition of SL7 Trace element solution is shown in Table 3.2.

Table 3.2 Composition of SL7 trace element solution

Component	Amount in 1L stock
36% Hydrochloric acid	1.3 ml
Zinc sulfate heptahydrate	144 mg
Manganese(II) chloride tetrahydrate	100 mg
Boric acid	62 mg
Cobalt(II) chloride hexahydrate	190 mg
Copper(II) chloride dihydrate	17 mg
Nickel(II) chloride hexahydrate	24 mg
Sodium molybdate	36 mg

Table 3.3 Composition of BG-11 growth medium

Component	Amount in 1L
$NaNO_3$	15 g
K_2HPO_4	0.4 g
$MgSO_4.7H_2O$	0.75 g
$CaCl_2.\ 2H_2O$	0.36 g
Citric Acid	0.06 g
Ammonnium Iron (III) Citrate	0.06 g
EDTA	0.01 g
Na_2CO_3	0.2 g
H_3BO_3	2.86 mg
$MnCl.4H_2O$	1.81 mg
$ZnSO_4.7H_2O$	0.222 mg
$Na_2MoO_4.2H_2O$	0.039 mg
$CuSO_4.5H_2O$	0.079 mg
$Co(NO_3).6H_2O$	0.0496 mg

3.2.3 Long Term Storage of Bacteria

C. metallidurans cells were frozen at -80°C in 20% glycerol for long-term storage. To prepare these: 10 ml of a stationary phase culture was centrifuged at 13,000 g for 5 minutes. The supernatant was discarded and 10 ml fresh MM284 medium added. Eight hundred microlitres of washed cells were vortexed with 800 microlitres 20% glycerol solution in sterile cryotubes. Before use, an inoculating loop was flame-sterilised and inserted into the cryotube. This was then transferred, without sterilisation, to fresh sterile medium. This was cultured at 30°C, shaken at 90rpm for 3 days until stationary phase. This was further transferred to fresh medium to a concentration of approximately 0.01% v/v cells (as determined from comparison to a previously prepared standard curve of optical density vs colony forming units) and grown to stationary phase as before. When this culture had reached stationary phase it was ready to be used in an experiment. At each transfer stage, cells from the culture were streaked onto MM284 agar to visually check for contamination.

3.3 Raman Spectroscopy

Raman spectroscopy is used in Chapter 4 to detect biosignatures on impact shocked rocks. This technique is based on the principle that if a molecule is illuminated with a monochromatic light source, most of the light will be scattered without a change in wavelength (an effect known as Rayleigh Scattering) but a small fraction of the photons will exchange energy with the molecular vibrations in the sample and the scattered light will have a slightly shifted wavelength (Raman scattering) [156]. The resultant "Raman shift" will depend on the mass of the atoms, the strength of the bonds and a molecule's interaction with nearby atoms. This will give a characteristic spectra of Raman peaks which identify the molecular composition of the material.

A resonance effect is exploited in Chapter 4. In Resonance Raman Spectroscopy, scattering occurs as in non-Resonance Raman but the frequency of the incident radiation is selected to be near a frequency of an electronic transition in a molecule. This excites the molecule into a higher energy state and the subsequent scattered light will be amplified [156].
The suitability of Raman spectroscopy for the applications in this thesis is discussed in the relevant chapter. More detail on the use of Raman spectroscopy for the study of biomolecules can be found in Niaura (2006) [156].

3.4 Principles of ICP-OES

Changes in cation concentrations in solution during rock leaching are measured in Chapter 5 by Inductively Coupled Plasma Optical Emission Spectroscopy (ICP-OES). This is a common method for simultaneous measurement of many metals in complex solutions [157]. During ICP-OES analysis, the sample (always in solution) is injected into an argon plasma. As the sample mist reaches the plasma it is rapidly dried, vaporized and atomized. The atoms then become excited and ionized. When this occurs, radiation is emitted from the excited atoms. This emitted radiation is sampled for spectrometric measurements using a complex array of mirrors and lenses, in either a radial mode (sampled side on to the plasma, normal working orientation) or in axial mode (end on to the plasma, good for low detection limits).
The wavelength of the emitted radiation is unique to the element which was initially excited and thus acts as a fingerprint for that element. The intensity of the signal is proportional to the abundance of the element. Solutions containing known concentrations of each element of interest are run alongside the test samples to produce a calibration curve against which experimental samples can be measured. Further detail on ICP-OES analysis can be found in Hou and Jones (2000) [158].

3.5 Shotgun Proteomics

3.5.1 What is Proteomics?

Proteomics is the large-scale analysis of the entire protein complement of a cell and is used extensively in Chapters 5 and 6 of this thesis. Proteomics provides a snapshot of the processes occurring inside a cell and is extremely useful in identifying microbial responses to environmental changes. There are many variations on the proteomics workflow and significant discussion in the literature about the pros and cons of each approach [159, 160]. This is beyond the scope of this thesis. Here I will only discuss the mass-spectrometry based shotgun proteomics approach adopted in this thesis and the specific data analysis conducted here. Shotgun proteomics involves the analysis of large numbers of proteins, usually using mass spectrometry. The methodology used here is closely based on methods developed by Le Bihan *et al* (2010) [161] at the Centre for Synthetic and Systems Biology where the proteomics work for this thesis was conducted.

3.5.2 Collection of Proteome Data

Protein Extraction and Digestion

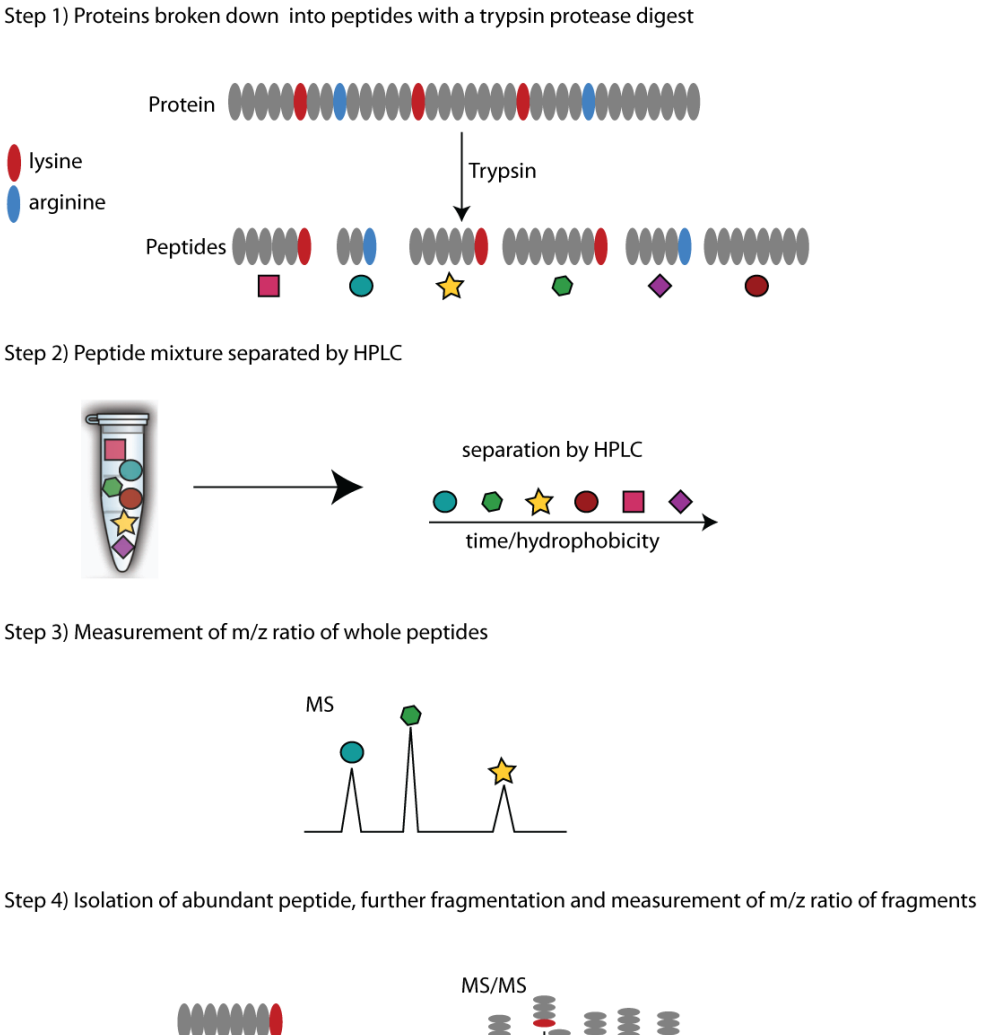

Figure 3.1 Schematic of the workflow for proteomics data collection. 1) Proteins are long chains of amino acids. They are first broken down into peptides by trypsin (a protease enzyme) which cuts at the C-terminal side of lysine and arginine residues. 2) The peptide mixture is then separated based on hydrophobicity by Liquid Chromatography. 3) The first mass spectrometry step measures the m/z ratio of the whole peptides (precursor ions). 4) Abundant ions are isolated for the second mass spectrometry step where the peptide is further fragmented. The m/z ratios of these fragment ions are measured and provide a fingerprint which can be used for peptide identification. Adapted from T. Le Bihan [3]

.

A schematic of the proteomics workflow is shown in Figure 3.1. First, proteins are released from the cells by addition of 8M urea, vortexing and sonication. The addition of urea also acts to unfold the proteins, making them easier to break down during the protease digest. A trypsin digest was employed to break proteins down to smaller, more easily analysed, peptides. Trypsin is an proteolytic enzyme which will cut (cleave) a peptide bond at the C-terminal side of lysine and arginine residues [162] (Figure 3.2).

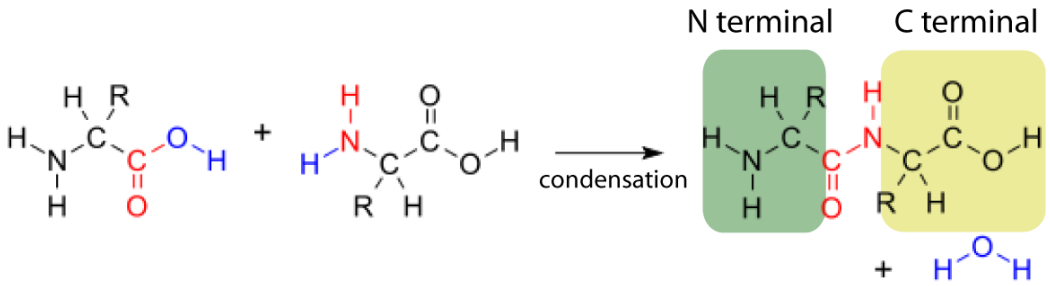

Figure 3.2 Reaction of two amino acids to form a peptide. Occurs via a condensation reaction where H_2O is removed and the amino acids are joined by a peptide bond (in red). The side of the peptide containing the amine group (-NH_2) is known as the N terminal end and the side with the carboxyl group (-COOH) as the C-terminal end [4]. Trypsin cuts proteins at the C-terminal end of lysine and arginine residues.

Trypsin is the most popular choice in mass-spectrometry based proteomics studies because it is highly specific, stable under a variety of conditions and results in peptides in the mass range most favourable for mass spectrometry [163]. Additionally, trypsin cuts the protein in such a way that each peptide is likely to have at least two charged ions. This allows the peptide to be distinguished from interfering substances (which typically have one charge) and allows the mass spectrometer to measure m/z ratios of ions fragmented from different ends of the peptide.

Peptide Clean Up

For mass spectrometry it is important that interfering substances such as salts or DNA are removed. In Chapter 5, peptides were cleaned with Millipore C18 Zip Tips (Sigma Aldrich, UK). Zip Tips are 10 μl pipette tips embedded with chromatography resin. In this process the sample is passed through the chromatography resin to which the peptides bind. The peptides on the column are rinsed and then eluted into fresh buffer (75% Acetonitrile/0.1% Trifluoroacetic acid), separating the peptides from the interfering substances remaining in the digest. A similar clean-up protocol is scaled up in Chapter 6 using Bond Elut C18 columns (Agilent, UK). These contain similar chromatography resin to the Zip Tips but allow the entire digest to be purified instead of just a 10 μg sub-sample.

Reverse Phase Liquid Chromatography

Liquid Chromatography is used to separate peptides based on their hydrophobicity prior to injection into the mass spectrometer. The purified peptide sample is passed through a thin fused silica tube containing chromatography resin on the way to the mass spectrometer. In the Reverse Phase Liquid Chromatography used in this analytical set up, hydrophobic molecules (ones that do not dissolve readily in water) are bound more tightly to the column and hydrophilic molecules (which dissolve readily in water) are bound less tightly. Over the course of the mass spectrometry run, increasing concentrations of organic solvent will be passed through the column, eluting ever more hydrophobic peptides. For this reason hydrophilic peptides are eluted from the column first and are referred to as having a short retention time. The more hydrophobic the molecule, the longer it will be retained on the column, the more organic solvent will be required for elution and thus the longer the retention time.

This additional step prior to mass spectrometry improves the quality of the mass spectrometry data which can be compromised if too many different species are

introduced at once.

Mass Spectrometry

Mass spectrometry, the next step in the proteomics workflow, is a commonly used technique to determine the intensity of ions with a certain "mass–to–charge" *(m/z)* ratio. The mass–to–charge ratio is the molecular or atomic mass number of the ion (m), divided by the charge of the ion (z). Many types of mass spectrometers exist for the analysis of a huge diversity of sample types. They are typically comprised of 3 parts: an ionizer which converts the atoms or molecules to ions, a mass analyser which separates the ions depending on their mass to charge (m/z) ratio and a detector which measures the abundance of the separate ions based on the intensity of some signal [163].
The approach adopted in this thesis uses Electrospray Ionization (ESI) coupled to an Orbitrap Mass Analyzer [164]. Electrospray Ionization uses electrical energy to transfer ions from solution to gaseous phase before they are injected into the Orbitrap [165]. The general principle of the Orbitrap analyser is that the injected ions orbit around, and oscillate along, a central electrode such that the frequency of the oscillations depends on the m/z ratio of the ions [164, 166]. The current generated by the oscillations is used to determine the abundance of ions with that m/z ratio.

Tandem Mass Spectrometry

Although the type of mass spectrometry above is useful in determining the abundance of ions with specific m/z ratios, it can be difficult to identify the specific peptide based on this information. Tandem Mass Spectrometry (MS/MS) can be used to solve this problem. This involves an additional step where the m/z ratio of the whole ion is measured as above (the precursor scan) before it is further fragmented and scanned again to determine the m/z ratio of the

fragmented ions (the fragmentation scan) [167]. This second fragmentation scan allows much more reliable peptide identification.

3.5.3 Data Analysis

Pre-processing

Mass spectrometry data must be pre-processed using various steps before interpretation can begin. All of the pre-processing in the following studies is conducted using Progenesis LC-MS software (version 4.0, Nonlinear Dynamics, UK). An overview of the pre-processing steps are shown in Figure 3.3. The first step in this pre-processing workflow is peak alignment. As the mass spectrometry runs progress, there may be some drift in the retention time. This means that the same feature could be present at a slightly different point on the chromatogram of separate samples. As the ultimate goal is to compare the abundance of individual features between samples, the mass spectrum for each sample is aligned to a reference sample (preferably one with abundant features which was run close to the middle of the analysis time). Each of the runs are then normalised to one another to correct for any discrepancies in the amount of protein injected. This process assumes that most features will not differ in abundance such that the average abundance of protein should be the same. In Progenesis normalisation, the average of all of the intensities for each spectrum is calculated and the spectrum shifted up or down such that average intensity is the same for all samples.

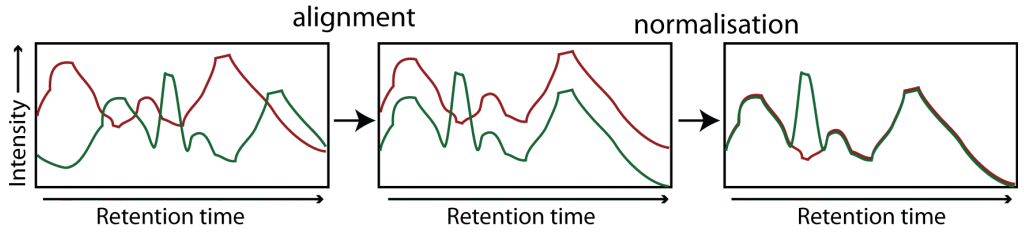

Figure 3.3 Examples of the alignment and normalisation pre-processing steps in Progenesis LC-MS. During alignment, matching features in each sample run are aligned to correct for drifts in retention time during analysis. During normalisation the baseline of the spectra are shifted up or down such that all spectra have the same average intensity. The final plot shows two spectra which match in most features. However, the green spectrum has one feature not detected in the red spectrum.

These steps are conducted using the built in algorithms of Progenesis LC-MS. There are many options for which algorithms to use at each of these stages. However, this thesis is focussed only on interpreting biological response so these will not be discussed here. This section aims only to provide a broad overview of each step in the proteomics workflow to assist in the understanding of the following chapters.

Peptide Identification

The output from each mass spectrometry run is a huge number of mass spectra and fragmentation spectra which, alone, are not very biologically interesting. In order to use this data to interpret the effect of the treatments on cells, the peptides must be identified and matched to their parent protein. There are a number of ways to approach this problem [168] but, in the studies used here, a database searching approach is adopted. This is the most common approach for peptide identification in large shotgun proteomics studies.

This method is summarised in Figure 3.4 and involves searching the experimental fragment spectra against theoretical fragment spectra in a database. Protein

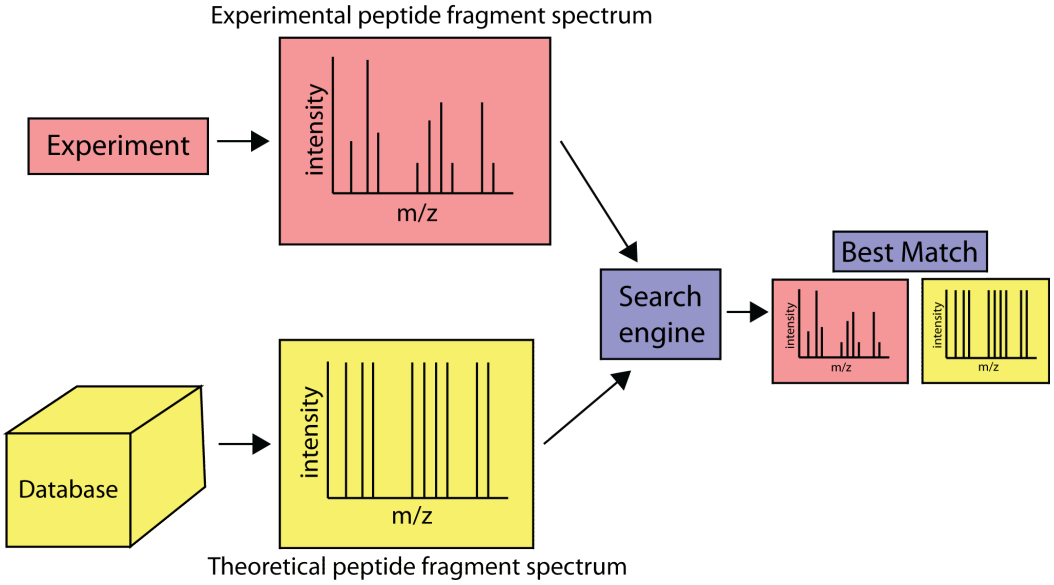

Figure 3.4 Schematic of the identification process for experimental peptide fragment spectra. Experimental fragment spectra are compared to theoretical fragment spectra based on the "theoretical digest" of proteins encoded by the genome. The search engine finds the best match in the database.

databases are constructed from the genome sequence of an organism. For best results, the original genome annotation should have identified the protein-coding sequences in the genome. These can then be translated into protein sequences. The database will then contain the amino acid sequence for all of the known proteins encoded by the genome. In the work presented here, the MASCOT search engine was used to match experimental MS/MS data (from the fragment ion scan) to proteins predicted in the NCBI protein database subset [169] for *Cupriavidus metallidurans*. This contains 6766 amino acid sequences for proteins encoded by the *C. metallidurans* CH34 genome, the organism used in these studies.

In order to match sequences, the search algorithm theoretically digests each of the proteins into its constituent peptides and uses this to predict a theoretical fragment spectrum. The protease enzyme used in the digest will determine where the proteins should break apart and this information must be provided during the search. MASCOT matches each experimental spectrum to a theoretical spectrum and awards the match a "score". This proprietary algorithm takes into account

a number of factors such as the quality of the fragment spectrum, the length of the peptide and the size of the database. The higher the score the less probable the result is a false positive. A global false discovery rate, i.e. the likelihood that a significant match is a random event, was established by comparing the MS/MS spectra to a decoy database of randomly generated sequences. For the data presented here, a peptide with a MASCOT score of 20 has a false discovery rate of approximately 0.1%.

Peptides to Proteins

After the peptides have been identified from their fragment spectra, these have to be matched up to their parent protein. It is possible that the same peptide sequence would come from different proteins. Therefore, peptide sequences are identified which are unique to one protein. Adequate identification can be assumed if a protein has been identified by two or more unique peptides and meets the MASCOT score threshold [160]. A confidence score on the protein identification is obtained from the sum of the MASCOT scores on all of the peptides used for protein quantification [160].
A spectral counting approach is used to quantify proteins [160]. This is based on the idea that more abundant peptides are selected for fragmentation, therefore more abundant peptides have a higher number of fragment spectra. This means the number of fragments is proportional to protein abundance [170]. To quantify each protein, Progenesis LC-MS sums all of the unique peptide ion abundances identified to be from that specific protein.

Comparing Between Experiments

In order to determine how protein expression varies in different experimental treatments, the normalised abundance of the protein in one condition is compared to the normalised abundance in another condition. Significance criteria is based

on that used in LeBihan *et al* (2010) [161]. In all of the experiments in this thesis, changes in protein expression are reported relative to a control (cells grown in optimal MM284 medium). If a protein has a higher normalised abundance in the test condition than in the control it is referred to as "up-regulated". If the normalised abundance in the test condition is lower than in the control it is referred to as "down-regulated". The fold change in the protein abundance is simply calculated by dividing the average normalised abundance in the test condition by the average normalised abundance in the control and is therefore the ratio of the experimental abundance to the control abundance. In Chapter 5, up or down-regulated fold changes are indicated by a + or − sign. In Chapter 6, where fold changes were manually calculated, an up-regulated protein shows a fold change greater than 1 and a down-regulated protein shows a fold change less than one. For example, if the fold change between the experimental treatment and the control is 0.5, the abundance of protein in the experimental treatment is half that in the control.

The significance of the differences in abundance is calculated by one way analysis of variance (ANOVA) on arcsinh transformed protein intensities. In Chapter 5 this is done automatically in Progenesis LC-MS and in Chapter 6 it is calculated manually in MS Excel. One-way ANOVA determines whether there is any significant difference between the means of different groups. In this work, the replicates in the experimental treatments are compared to the replicates from the control. In this thesis, the difference between treatments is considered significant if the P value is less than 0.05.

Four criteria must be satisfied for a protein to be considered significantly up or down-regulated:

1. The protein must have been identified by two or more unique peptides.

2. The protein must have a MASCOT score of at least 20, however a score of at least 40 is ideal.

3. The difference between the experimental treatment and the control must be 2 fold or greater.

4. The P value, calculated by one-way ANOVA, must be below 0.05

Comparison of Overall Similarity of Treatments

In Chapter 5 and Chapter 6, the similarity of the protein profiles in different treatments is demonstrated using multivariate statistical analysis. The Bray-Curtis dissimilarity index determines how similar the protein abundance profiles are for each treatment. A score of 100 indicates that they are exactly the same. A score of 0 indicates that they have no similarity. These results are visualised on an nMDS plot which is a 2-dimensional representation of the n-dimensional Bray-Curtis similarity matrix. The closer the points are on the nMDS (non-metric multidimensional scaling) plot, the more similar they are.
Following non-metric multidimensional scaling ordination, post-hoc pairwise comparisons were performed by 2-way nested permutational analysis of variance (PERMANOVA; [171]). The 2-way nested PERMANOVA calculates the significance of the treatment type accounting for the replicate samples in each treatment.

Functional Annotation

Once identification and quantification has been conducted and differentially regulated proteins highlighted, the biological function of proteins can then be identified. Annotation of function, and hence identification of important cellular responses, relies on previous annotation efforts from other authors. Protein functions in this thesis were primarily assigned using expert manual annotation of the *C. metallidurans* CH34 genome, available on the MaGe platform [172]. This database contains information on the protein name, description and protein

functions.

Chapter 4

Rocks as a UV Shielded Habitat on Early Earth

4.1 Introduction

As described in Chapter 2, endolithic communities are buffered from external stresses such as radiation, temperature fluctuations, wind and desiccation [76–79]. Thus, they are most commonly associated with harsh environments in which these factors limit growth on rock surfaces [80–86].

This ability to grow phototrophically in the subsurface whilst being shielded from most of the incident UV radiation led to the suggestion that endolithic habitats may have been useful on the early surface of the Earth when the UV radiation was thought to be much higher (See Chapter 2) [1, 83, 84, 86, 109, 110].

Although this strategy offers a plausible mechanism for phototrophs to exist on the early land masses, the usefulness of this habitat as a refuge for early surface-dwelling life has not been tested over long periods. In this chapter I outline work which aims to empirically test whether photosynthetic organisms could have survived on the land masses of the early Earth (before atmospheric oxidation

around 2.4 billion years ago) by sheltering just millimetres below the surface in rocks.

Samples were obtained from the European Space Agency's EXPOSE-R mission. EXPOSE-R is a facility mounted outside of the International Space Station which was used to expose a variety of different biological and chemical samples to space conditions. The EXPOSE-R mission was the first use of this facility.Samples were exposed to space conditions for 833 days.

In the experiments discussed here, cyanobacteria were integrated into a known endolithic substrate and exposed to a putative "worse than worst-case" early Earth-like UV radiation flux. This chapter describes the post-flight analysis of these samples and discusses their implications for the early colonisation of the land masses by phototrophs. The work presented in this chapter was published in the International Journal of Astrobiology as part of a Special Issue on EXPOSE-R [1].

4.2 Background

4.2.1 Low Earth Orbit as an Early Earth Analogue

Exposure of samples to the conditions outside the International Space Station (ISS) presents a good analogue for studies of early earth-like UV radiation flux. The ISS orbits the Earth at an altitude of around 450 km, in a region termed low Earth orbit. Conditions here are characterised by low pressures (10^{-6} to 10^{-4} Pa), intense radiation bombardment from solar and galactic sources (including the full spectrum of UV radiation) and extreme and variable temperatures [100]. Indeed, the International Space Station itself is designed to withstand temperatures from $+120°C$ to $-120°C$ [100].

Using the high UV radiation flux in low Earth orbit, it is possible to recreate the early Earth UV radiation environment using various filters. This allows more

natural exposure conditions than can be artificially created on Earth as even the most sophisticated UV radiation lamps fail to exactly mimic the UV spectrum emitted by the sun [40]. By taking the samples above the atmosphere we can expose them to the full extraterrestrial spectrum and use cut-off filters to create an analogue for the early Earth UV environment.

4.2.2 The EXPOSE-R Mission

Overview

A detailed description of the European Space Agency's EXPOSE-R mission can be found in Rabbow *et al.*, (2014) [173]. To summarise, EXPOSE-R is a box-shaped core facility with dimensions 48cm x 39cm x 14cm (l x w x h). The lower part of the facility houses the electronics and the upper parts contain 3 sample exposure trays. The top tray is exposed to all parameters of space including UV radiation and the bottom two are exposed to all of the parameters except UV exposure. A schematic of the EXPOSE-R facility is shown in Figure 4.1.

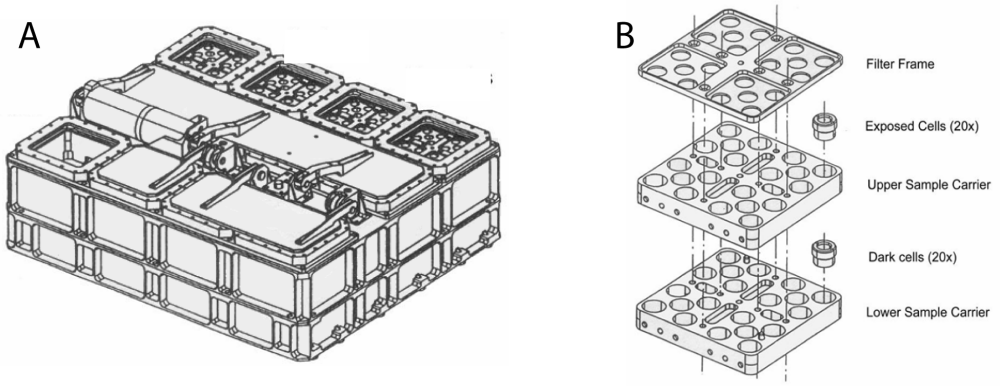

Figure 4.1 Features of the EXPOSE-R facility A) Facility is composed of many cells which each contain 3 layers of trays B) Drawing of an individual compartment showing a top UV exposed layer and a lower dark layer. There is another dark layer below this (source: smsc.cnes.fe/EXPOSE)

The top (UV exposed) tray has windows which allow definition of the amount

and wavelength of radiation which can pass through to the samples.

Before the launch the compartments were filled with argon gas to a pressure of 102kPa. Some of the compartments were fitted with venting line valves to allow evacuation to space vacuum during exposure and some remained sealed for the duration.

Samples were integrated into the facility at the German Aerospace Centre (DLR), Cologne on August 14th 2008. The entire, sealed exposure facility was then transferred to Baikonur, Kazakhstan in a protective cover and launched on November 26th 2008. The samples were placed outside of the ISS on March 10th 2009 and the experiment was active until January 21st 2011. The complete, sealed EXPOSE facility was returned to Earth on March 9th 2011 and received by DLR 3 days later. Samples were removed from the facility and kept at room temperature during return to research teams in April 2011.

Nine hundred and fifty days passed between closure and re-opening of the sample trays. Exposure to UV radiation occurred for 833 days making this the longest exposure of biological samples outside of the International Space Station to date. Images of EXPOSE-R during different stages of the mission are shown in Figure 4.2.

Figure 4.2 The EXPOSE-R facility A) During sample integration B) Awaiting launch C) Outside of the International Space Station (source: NASA)

ROSE-1 ENDO

The specific samples obtained for this chapter were one of six experiments in the ROSE consortium (Response of Organisms to Space Environment) and consisted of glass discs and discs of impact-shocked gneiss to which cells of the polyextremophile phototroph *Chroococcidiopsis* sp. CCMEE 029 had been added. A total of 36 0.5cm glass discs and 12 1cm rock discs were tested. Half of the glass discs were housed in containers which were vented to allow exposure to the vacuum of space whilst half were in sealed containers filled with argon gas. These experiments therefore investigate the effects of UV radiation alone, but do not take into account any potential confounding effects of interactions between UV radiation and atmospheric components that might have been present in the early Earth atmosphere such as carbon dioxide. Twelve glass discs in each condition were exposed to UV radiation whilst the rest were kept dark.

Of the 12 UV exposed glass discs, half were exposed to UV wavelengths greater than 110nm whilst half were only exposed to wavelengths greater than 200nm. The >110nm cut-off was achieved using MgF_2 windows (MaTeck GmbH, Germany; Wisag AG, Switzerland). The >200nm cut-off was achieved using quartz glass windows.

Neutral density filters made from MgF_2 (MaTeck GmbH, Germany; Wisag AG, Switzerland) or coated quartz (Moltech GmbH, Germany) were used to reduce intensity of all wavelengths equally to 0.01 or 1% of the incident radiation whilst some samples had no neutral density filter and thus were exposed to 100% of the incident radiation of the prescribed wavelength.

Three glass discs in each container (sealed or vented) were exposed to 100% of the UV wavelengths greater than 200 nm, two exposed to 1% of the UV wavelengths greater than 200 nm and three exposed to 0.01% of the UV wavelengths greater than 200 nm. These conditions were repeated for UV wavelengths greater than 110 nm to investigate the effects of very short wavelengths of UV radiation.

All of the samples on rock discs were housed in vented containers. Six rock

discs were exposed to 100% of the UV radiation greater than 110 nm and the remaining six kept dark. These rocks were exposed to 80 nm (110-190 nm) of UVC radiation not expected to have been encountered on the early Earth and therefore experienced a UV spectrum on their surface more severe than the worst-case early Earth spectrum. Identically prepared control samples were kept dark in the laboratory for the duration of the experiment.

Exposure Conditions

Various instruments were employed to monitor temperature, cosmic radiation and UV radiation exposure throughout the experiment. A problem with the on board computer system meant that approximately 42% of this data was lost. A private company were contracted to model whole mission data based on the 58% of data which was not lost [173].

The details of exposure conditions are discussed in detail in Rabbow *et al.*, (2014) [173] and are summarised below. These data are included here and not in the Methods or Results sections of this chapter as the investigation of exposure conditions was conducted by other EXPOSE-R teams and is not the focus of this thesis.

Temperature sensors were installed below each tray and were designed to shut down the electronics at temperatures > 52°C to avoid further heating. Heaters were triggered at temperatures below -25°C to keep the electronics functioning. Maximum temperature reached was +49.47°C and the minimum was -24.65°C. A slow oscillation between high and low temperatures was observed due to the position of the ISS relative to the Sun. This was overlain by a faster oscillation with a period of approximately 90 minutes due to day/night cycles as the ISS orbited the Earth.

The simulations calculated the temperature range in the trays to be between -27 to 46 °C (based on the average temperatures across multiple sensors at different positions). Overall average temperature was +19°C. The simulated average tray

temperature predicts that 285 freeze-thaw cycles were exprienced during the experiment. This included 274 short duration cycles and 11 long-duration freeze periods.

UV dose at each of the sample sites was modelled based on the available data. These data included measured doses from the EXPOSE-R UV dosimeters, ISS mission flight data of ISS position and attitude, positions of solar arrrays and radiators and data about visiting space craft and their docking positions. Calculated UV fluences for the samples relevant to this experiment are shown in Table 4.1.
These values incorporate the influence from window contamination which occurred in vented containers during the course of the experiment [174] and blocked some transmission in these compartments.

Table 4.1 Average radiation doses encountered by each sample type

Sample type	**Cut off wavelength**	**% of incident**	**UVA (kJ m^{-2})**	**UVB (kJ m^{-2})**	**UVC (kJ m^{-2})**	**UV 100-400nm (kJ m^{-2})**	**PAR (kJ m^{-2})**	**Total irradiation (kJ m^{-2})**
Glass disc	110nm	100	$4.6x10^5$ ($\pm$ $1x10^5$)	$8.5x10^4$ ($\pm$ $2.2x10^4$)	$3.1x10^4$ ($\pm$ 9266)	$5.7x10^5$ ($\pm$ $1.3x10^5$)	$3.7x10^6$ ($\pm$ $7x10^5$)	$8.2x10^6$ ($\pm$ $1.5x10^6$)
Glass disc	110nm	1	$4x10^3$ ($\pm$ 777)	867 ($\pm$ 176)	205 ($\pm$ 52)	6034 ($\pm$ 1004)	$5.1x10^4$ ($\pm$ 5055)	$1.3x10^5$ ($\pm$ $1x10^4$)
Glass disc	110nm	0.01	51 ($\pm$ 9.1)	8.8 ($\pm$ 2)	2.1 ($\pm$ 0.6)	61 ($\pm$ 12)	521 ($\pm$ 70)	1314 ($\pm$ 160)
Glass disc	200nm	100	$3.9x10^5$ ($\pm$ $8x10^4$)	$6.9x10^4$ ($\pm$ $1.7x10^4$)	$2.4x10^4$ ($\pm$ 6732)	$4.8x10^5$ ($\pm$ $1x10^5$)	$3.3x10^6$ ($\pm$ $6.2x10^5$)	$7.3x10^6$ ($\pm$ $1.3x10^6$)
Glass disc	200nm	1	4270 ($\pm$ 487)	709 ($\pm$ 129)	166 ($\pm$ 37)	5132 ($\pm$ 649)	$4.6x10^4$ ($\pm$ 3499)	$1.1x10^5$ ($\pm$ 7588)
Glass disc	200nm	0.01	44 ($\pm$ 6.6)	7.3 ($\pm$ 1.5)	1.7 ($\pm$ 0.4)	53 ($\pm$ 8)	479 ($\pm$ 58)	1176 ($\pm$ 137)
Rock disc	110nm	100	$3.7x10^5$ ($\pm$ $7x10^4$)	$5.2x10^4$ ($\pm$ 9676)	$1.5x10^4$ ($\pm$ $2.9x10^3$)	$4.3x10^5$ ($\pm$ $8.1x10^4$)	$3.8x10^6$ ($\pm$ $7x10^5$)	$8.7x10^6$ ($\pm$ $1.6x10^6$)

4.2.3 Substrate Selection

The substrate used for the rock discs was taken from the Haughton Impact Crater in the Canadian High Arctic located on Devon Island in Nunavut (75 °22'N, 89 °41'W). This formed during an asteroid impact around 23 million years ago [175]. The discs are composed of highly impact-shocked gneiss which formed during the impact. The rocks used in this study were obtained from the private collection of Professor Charles Cockell and are the same rocks discussed in Cockell *et al.*, (2002). This work compared the characteristics of low-shocked gneiss and high-shocked gneiss which had experienced shock levels less than 10GPa and greater than 20GPa respectively. This work suggested that the impact resulted in geological changes which were ultimately beneficial for endolithic life.
The main differences were:

1. Low shocked gneiss is very dark, almost black, whereas high shocked gneiss is grey or white.

2. Porosity was 25 times higher in shock levels >20 GPa than at shock levels <10 GPa.

3. 22% of incident light passed through 0.5 mm of rocks shocked >20 GPa compared to 0.2% in rocks shocked <10 GPa.

4. Presence of green bands of endolithic phototrophs was much more prevalent in high shocked rocks compared to low shocked rocks.

Cockell *et al.*, (2002) [83] ascribe the prevalence of endoliths in highly shocked rocks to the creation of microhabitats in the new pore spaces and increased light transmissivity which provides adequate light for photosynthesis.
These rocks were chosen for this study for 3 reasons.

1. The field observations of endolithic phototrophs in these rocks show that

this habitat is at least good enough to support phototrophic growth in one of the most extreme environments found on Earth today. Therefore, it could be a good candidate for a UV-shielded habitat on the early Earth.

2. Impact cratering is likely to have been even more common on the early Earth than it is today [176]. Therefore, when life appeared, impact craters would have been widespread. These could contain impact shocked rocks which are more easily colonised than the crystalline lithologies which dominated the early land masses [43].

3. Impact craters are a universal phenomenon, therefore the use of these rocks enables us to discuss the possibility that impact shocked rocks could provide UV-shielded habitats on any rocky planet lacking an atmospheric UV shield.

4.2.4 Organism Selection

The use of the polyextremotolerant cyanobacterium *Chroococcidiopsis* sp.CCMEE 029 is particularly appropriate for this study. *Chroococcidiopsis* is one of the most tolerant to extremes of all of the known cyanobacteria. It is very versatile with strains having been described from a wide range of extreme habitats such as hypersaline [177] and freshwater [178] environments and hot and cold deserts [179–181]. In the most extreme hot, cold, arid and saline habitats on Earth, it is generally found to be the dominant cyanobacterium [182]. It is also very common for *Chroococcidiopsis* to adopt an endolithic lifestyle [179].

The long-term survival of *Chroococcidiopsis* aboard the ISS has been previously demonstrated as part of the EXPOSE-E mission where cells of *Chroococcidiopsis* sp. 029 were used to artificially augment a natural phototroph biofilm which was exposed to space conditions [183]. Viable cells were cultured after 534 days in low Earth orbit, exposed to the full extraterrestrial UV radiation spectrum in a set up similar to that used here [183].

The previous experiments differ from those reported here in that the exposure

time was extended (22 months compared to 18 for EXPOSE-E) and pure cultures of *Chroococcidiopsis* used in sample preparation instead of exposure of *Chroococcidiopsis* as part of a biofilm.

4.3 Methods

4.3.1 Sample Preparation

Chroococcidiopsis sp. CCMEE 029 was obtained from the Culture Collection of Microorganisms from Extreme Environments (CCMEE) established by E. Imre Friedmann and now maintained at the University of Rome Tor Vergata. Cells were cultured in BG-11 medium as described in Chapter 3.

An aliquot of cells (around $1.5x10^6$ cells) were transferred evenly onto the surface of 0.5 cm-diameter sterile glass discs or 1 cm-diameter discs of impact-shocked gneiss (Figure 4.3). The impact-shocked gneiss was 5 mm thick, a thickness within which visible light transmission in the majority of the substrate is sufficient to support photosynthetic growth in natural communities that inhabit these rocks [83].

A complete set of replica samples were prepared in tandem and stored in the laboratory until the space-exposed samples were returned. These steps occurred prior to the commencement of this PhD project.

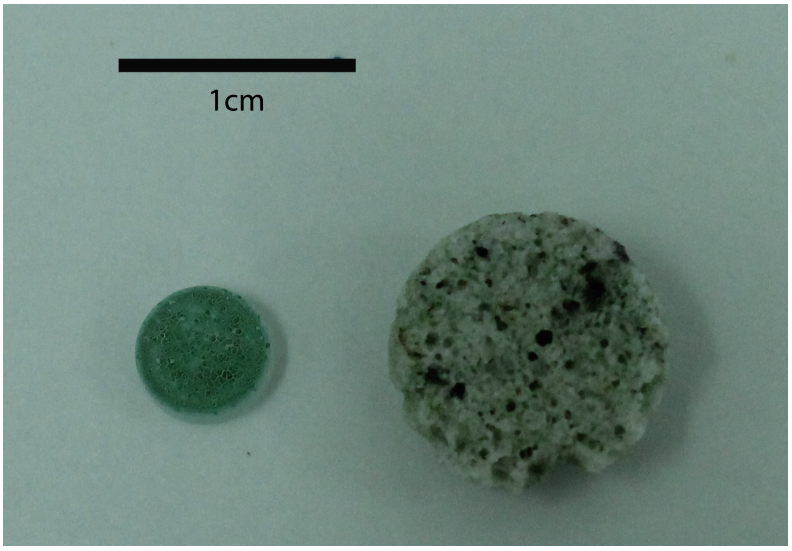

Figure 4.3 Examples of rock and glass discs used as substrates for the experiment

4.3.2 Post-flight Culturing

On return, the rock discs were split into three using a flame-sterilised hammer and chisel. One-third of each rock disc was placed in 100 ml of BG-11 medium with triplicate cultures for each exposure condition: UV-exposed in low Earth orbit, dark in low Earth orbit and a lab control (prepared at the same time as the space samples and stored in the dark at room temperature until sample return). Cultures were incubated at room temperature for 4 months.

Subsequent growth was confirmed using bright field microscopy. Cells were unevenly distributed throughout the pore space and rock samples had to be split to provide enough samples for analysis. Therefore, calculation of the exact number of viable cells on each fragment of rock used for the inoculation was not possible. A positive or negative result for growth is reported here. For the glass discs, one disc for each exposure condition was added to fresh BG-11 medium.

4.3.3 Raman Spectroscopy

To determine whether or not essential biomolecules had been damaged by exposure to the UV exposure in low Earth orbit, Raman spectroscopy was used to establish whether carotenoids had been destroyed in each sample. The principles behind Raman Spectroscopy are outlined in Chapter 3.

Carotenoids as a Proxy for UV Destruction

Carotenoids, the target biomarkers of this study, are a group of ubiquitous coloured pigments which are particularly common in photosynthetic organisms like cyanobacteria and plants [184]. These compounds have two main functions: as light harvesting pigments in photosynthesis and for protection against photo-oxidative stress.

One problem in using traditional Raman Spectroscopy to analyse complex biological samples is that the signals are often noisy, difficult to detect in low abundances or obscured by fluorescence effects caused by excitation in visible laser wavelengths. However, carotenoids make an excellent biomarker in a study such as this, as a Resonance Raman effect can be exploited.

In Resonance Raman, scattering occurs as in non-Resonance Raman but the frequency of the incident radiation is selected to be near a frequency of an electronic transition in a molecule. This excites the molecule into a higher energy state and the subsequent scattered light will be amplified. Excitation of a carotenoid containing sample at 514nm will reveal a characteristic spectrum (Figure 4.4), where the peaks relate to the stretching of the C=C and C-C bonds and to the bending of the C-CH groups within the molecule [85].

This technique has been used by numerous authors to detect cyanobacterial biomarkers from extreme environments and has proved extremely useful for the analysis of complex, low abundance biological samples, particularly within

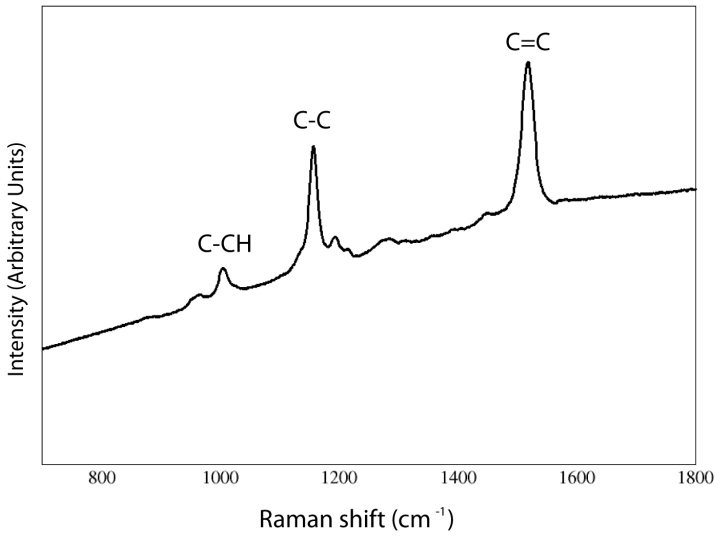

Figure 4.4 Raman spectrum of typical carotenoid signature obtained from a lawn of *Chroococcidiopsis* sp.029 on BG-11 agar

mineral matrices [82, 85, 183, 185]. The technique is also non-destructive and therefore excellent for this study where samples are extremely precious.

Analysis Details

A Renishaw inVia laser Raman microscope (Renishaw, UK) was used and samples were excited at a wavelength of 514 nm. The laser was typically operated at 5% power with each spectrum being an average of ten acquisitions. Data were analysed using the commercial WiRE 3.2 software package (Renishaw, UK).
Before analysis of the rock discs, a cross-section was obtained with a sterile chisel. A positive or negative result for the carotenoid spectra both on the UV-exposed surface of the disc and the interior was recorded. Selection of the spot on which to sample within the rock was guided by the location of patches of cells as, owing to irregularities in pore spaces, they are not homogeneously distributed throughout the rock. For samples which were highly fluorescent at this level, the laser power

was reduced to 1% to ensure that the signal was not hidden by the fluorescence generated. Control spectra were also obtained from a segment of rock on which there were no cells and from dried cells of *Chroococcidiopsis* sp.029 on BG-11 agar.

4.3.4 Scanning Electron Microscopy

Both rock discs and glass discs were imaged using scanning electron microscopy. The rock discs were coated in gold before imaging using a Philips XL30CP scanning electron microscope (SEM) (Philips, UK) operated at 1 mbar pressure. Images were obtained using the absorbed current detector (AEI) at a voltage of 20 kV. Observations on the glass discs were carried out using a CamScan MX2500 SEM (CamScan, UK) operated in controlled pressure mode (Envac, 30 Pa). Images were recorded at a working distance of 20mm using the AEI at a voltage of 20 kV. Gold coating was carried out by the Scanning Electron Microscope Technician, School of Geosciences, University of Edinburgh.

4.4 Results

4.4.1 Post-flight Culturing

Within 4 weeks of inoculation of the fragments of rock discs, numerous 0.5-1mm green specks were observed on the rock fragments suggesting viable cells within the rock had begun to expand into larger colonies. After 2 months, growth was clearly observed on the rock and in the growth medium of all experimental samples (Figure 4.5). *Chroococcidiopsis* cells were confirmed under bright field microscopy. It was found that no samples on glass discs, whether in in low Earth orbit or stored in the lab, had remained viable.

Figure 4.5 Growth of *Chroococcidiopsis* in BG-11 medium inoculated with rock discs from all conditions. Left to right: stored in lab, dark in low Earth orbit and UV exposed in low Earth orbit. Growth is observed in all flasks. Picture taken after 2.5 months of incubation

4.4.2 Raman Spectroscopy

Carotenoid Detection on Glass Discs

Glass discs which had been inoculated with cells of *Chroococcidiopsis* and either stored under laboratory conditions or kept dark whilst in the EXPOSE-R facility clearly exhibited the characteristic carotenoid bands shown in Figure 4.4. This indicates that despite the complete loss of viability of the cells during the period of desiccation, the carotenoids had not undergone degradation.

In the UV-exposed samples on glass discs the carotenoid peaks were only detectable at a very low level in one sample which had been exposed to 0.01% of the incoming radiation greater than 110nm in a vented container (Table 4.2). All other UV-exposed samples tested exhibited no spectral peaks. Variations in the background fluorescence emission intensity were observed in several of these

Table 4.2 Detection of carotenoids on glass discs using Raman spectroscopy. + refers to a positive identification, − indicates no detection

Exposure	Sealed >110nm	Sealed >200nm	Vented >110nm	Vented >200nm
Dark	+	+	+	+
100%	-	-	-	-
1%	-	-	-	-
0.01%	-	-	+	-

UV-exposed samples.

Carotenoid Detection on Rock Discs

Rock discs which had been exposed to UV in low Earth orbit exhibited a browning of the surface which was not observed in rock discs which had been kept dark (Figure 4.6).

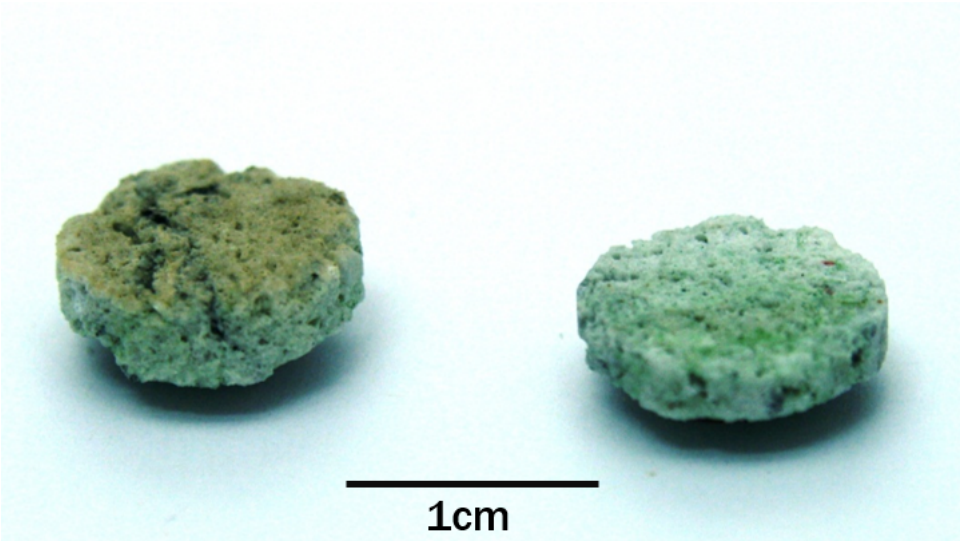

Figure 4.6 Examples of rock discs after return from the ISS. Browning of cells observed on rock discs exposed to UV radiation in low Earth orbit (left) and not on those kept dark in low Earth orbit (right)

The spectra obtained from cells in the rock discs are displayed in Figure 4.7. For cells on rock discs stored in the lab or kept dark in low Earth orbit, the carotenoid

signal was detected both on the surface and in the subsurface (Figure 4.7a and 4.7b).

In the rock discs it was found that cells on the UV-exposed surfaces of the rocks had experienced similar destruction to carotenoids as that exhibited by cells on glass UV-exposed discs (Figure 4.7c). When imaged through the Raman microscope, these cells had turned brown during exposure and they did not exhibit any characteristic Raman peaks when probed (Figure 4.7c).

However, below the surface in the cleaved samples, green flecks were observed which, when probed at 514nm, exhibited the typical carotenoid Raman spectral signals (Figure 4.7c). This demonstrates that the rocks were effective in adequately protecting the cells housed internally from 100% exposure to the full extraterrestrial radiation dose at wavelengths greater than 110 nm.

By probing rock which had not been inoculated with cells it was determined that, whilst some fluorescence contribution from glassy minerals in the rocks is present, there is no interference that would confuse the interpretation of these characteristic carotenoid spectral signals.

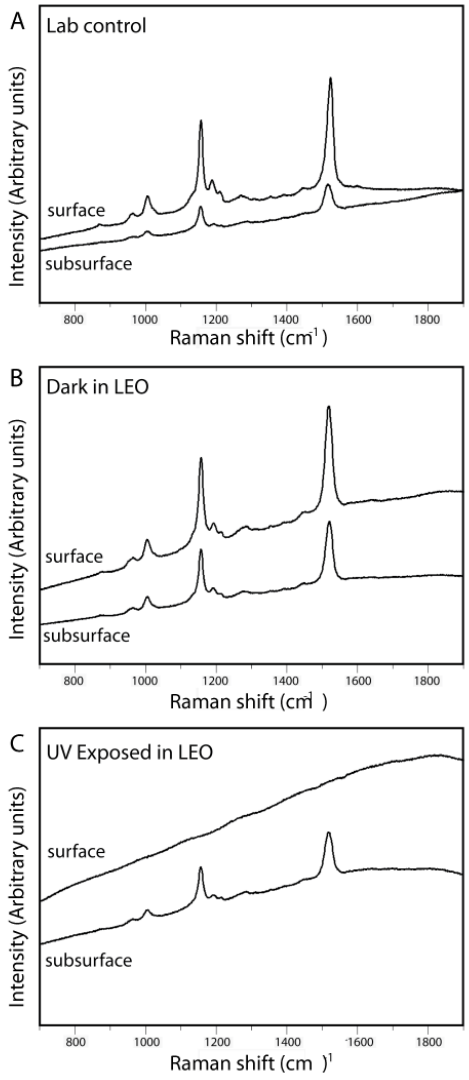

Figure 4.7 Raman spectra obtained from the surface and sub–surface of rock discs from each exposure condition

4.4.3 Microscopy

SEM images of cells in the pore space of the rocks in the control, dark and UV exposed samples are shown in Figure 4.8. Morphologically intact cells were observed in the UV-exposed rocks, even in pores directly exposed to the surface. This could suggest that UV bleaching of the cells had occurred and the biomolecules destroyed whilst the cells still maintained their shape.

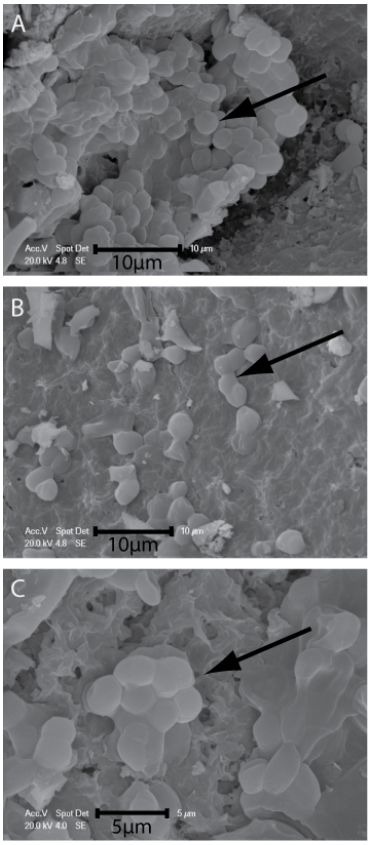

Figure 4.8 Scanning electron microscope images of *Chroococcidiopsis* cells inside the rock discs. A) Laboratory control B) Dark in low Earth orbit C) UV exposed in low Earth orbit. Shows morphology is preserved in all samples.

SEM images of the glass discs confirm that this is possible with the distinctive spherical shape of *Chroococcidiopsis* being observed on glass discs which had been kept dark and on discs exposed to UV radiation within vented containers (Figure 4.9). The latter of these received no shielding from the incident UV radiation.

However, intact cells were not observed on glass discs which had been kept sealed (data not shown).

No quantification of cell numbers was carried out as the cells were not homogeneously distributed throughout the substrate, making quantification unreliable.

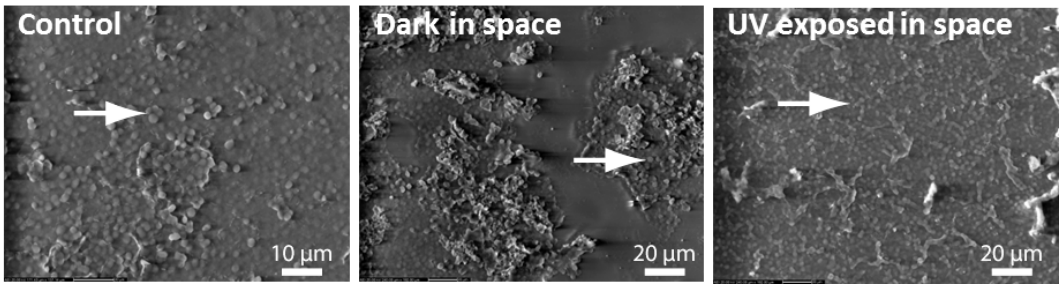

Figure 4.9 Scanning electron microscopy images of *Chroococcidiopsis* cells on the glass discs from each condition. From left to right: laboratory control, kept dark in low Earth orbit (vented), UV exposed in low Earth orbit (vented)

4.5 Discussion

In this chapter cyanobacteria inside rocks were exposed to the UV radiation conditions found in low Earth orbit to determine if an endolithic lifestyle could provide suitable micro-habitats for phototrophs on the pre-ozone early Earth. Impact shocked gneiss from the Haughton Impact Crater was chosen as it is known to support endolithic phototrophs in the extreme environment of the Canadian High Arctic.

Phototrophs have the requirement for photosynthetically active radiation (PAR) for growth, meaning that they must be exposed to sunlight with the concomitant exposure to UV radiation. Therefore, growing at a depth where UV radiation is completely extinguished is not an option. It is shown here that organisms within impact-shocked gneiss exposed to the intense UV radiation environment in low Earth orbit for 833 days were viable on their return to Earth. No viable cells remained on any of the glass discs regardless of exposure conditions (and

in controls). This could be a result of extreme desiccation of the thin layer of cells, as cells which were clumped inside the rocks due to the necessary space constraints might have been shielded by other cells as has been observed with other cyanobacteria [186].

It is also observed that essential biomolecules, carotenoids, are destroyed during long-term exposure to the UV radiation environment in low Earth orbit and that these are unaffected by the other space parameters. However, the positive detection of carotenoid signatures by Raman spectroscopy in cells exposed to 0.01% of the UV radiation of wavelengths greater than 110nm in vented containers suggests that the radiation dose received at this level may be close to a threshold level at which biological molecules can survive.

Carotenoids were detected in all samples (rock and glass) which had been kept dark, supporting earlier observations that UV radiation exposure is the most destructive aspect of exposure to space conditions [100].

Results on the UV-exposed glass and surface of the rock discs show that direct exposure to the worst case early Earth UV radiation conditions over a long period will have a destructive effect on biomolecules, destroying essential pigments even when this was attenuated to only 0.01% of the incoming UV. These results emphasize the low survivability of photosynthetic life on the surface of the early Earth in the absence of shielding or active repair.

However, carotenoids were detected in the subsurface of the rock discs exposed to UV radiation in low Earth orbit for 22 months. These results indicate that it would be possible for cyanobacteria to persist in a desiccated state for at least this long under the worst-case UV radiation conditions predicted for the early Earth. Indeed, this estimate should be considered conservative as the samples were exposed to shorter wavelengths of UV radiation (thus more damaging radiation) than is predicted from the carbon dioxide and nitrogen atmosphere on the early Earth.

This work provides strong evidence that endolithic phototrophs, such as those sheltering in the rocks at the Haughton Impact Crater, could have survived

long periods of time under early Earth-like UV fluxes. Since impact cratering is ubiquitous in the universe, this work also demonstrates the general principle that impact shocked rocks can provide protection against the worst-case UV radiation fluxes on any anoxic planet, including planets such as Mars.

4.6 Limitations and Future Directions

There are a number of limitations to this study which should be addressed in future work. Firstly, as with all space experiments, there is limited sample numbers so some of the analyses could not be conducted with replicates. Further samples would be required for SEM analysis on glass discs to compare whether morphological preservation was higher in vented containers compared to sealed containers.

Linked to this, it is unclear if the presence of an atmosphere would have a detrimental effect on cyanobacterial survivability under high UV radiation stress and further ground-based studies should focus on testing this. Preliminary work on this topic in the Cockell Lab has suggested higher moisture content may negatively influence survivability during UV exposure in this organism (Charles Cockell/Sarah Brown, Unpublished).

In this experiment it was only possible to test desiccated cells therefore all viability is maintained in the absence of active repair. Future work should focus on studying actively growing cells during the period of UV exposure. Additionally, protection afforded to cyanobacteria from other substrates such as quartz or gypsum in the space environment would be interesting to test as these also provide endolithic habitats in high UV environments on Earth [80, 187].

Protection afforded by Mars-like soil to cyanobacteria, including *Chroococcidiopsis*, is the subject of one EXPOSE-R2 experiment (follow up to EXPOSE-R) which was launched in May 2014 [188].

4.7 Conclusions

In conclusion, the protection afforded to organisms within impact-shocked rocks is adequate to preserve viable cyanobacterial cells in a desiccated state for at least 833 days under a UV flux at least equal to the worst-case scenario on the early Earth. This result could extend to other terrestrial-type rocky planets lacking a sufficient atmospheric UV radiation shield. Cells actively growing, unlike the desiccated cells studied here, would have the potential to actively repair UV radiation-induced damage (assuming the dose is sublethal), suggesting that these results are conservative. This work highlights the potential of impact craters and endolithic habitats as protective habitats on rocky planets with a high UV radiation flux and it empirically demonstrates that phototrophic microorganisms could have colonized early land masses under a worst-case UV radiation flux, even without active repair or protection under thick layers of cells.

Chapter 5

Rock-induced Changes in the Bacterial Proteome

5.1 Introduction

As described in Chapter 2, numerous studies describe the microbial release of bioessential elements from rocks [63, 67] and microbially induced changes in rock redox chemistry [56]. However, even in the absence of active microbial weathering, rock geochemistry can affect the structure, composition and metabolic activities of rock-dwelling microbial communities [94, 96, 189]. Rocks will release elements and alter surrounding fluid chemistry which can have stressful effects on the microbial community [117]. This chapter aims to investigate a highly simplified microbe-rock interaction by exposing one model organism in a well-defined growth medium to one rock type. The chemical and microbial processes involved in even such a highly simplified experiment are very complex but allow us to begin to build up a picture of mechanisms required by micro-organisms to live in a rock environment.

This chapter explores two hypotheses:

1. Changes associated with the release of elements from rock, whilst potentially providing nutrients, would also introduce physiological stresses in individual cells.

2. Micro-organisms will alter protein expression to respond to these stresses.

This is investigated by the quantification of changes in protein expression in the presence of rock using the bacterium *Cupriavidus metallidurans* CH34 as a model strain.
These data show that specific chemical changes occur because of the presence of the rocks and that these can be correlated with changes in the proteome expression profiles. These are primarily associated with nutrient limitation and stress responses despite the fact that the rock can act as an alternative source of important elements.
The work presented in this chapter is currently under review at The ISME Journal.

5.2 Methods

5.2.1 Experimental Overview

The experiments described in this chapter proceeded in three broad phases:

1. Comparison of growth, chemical changes and protein expression with and without basaltic rock added to optimal growth media.

2. Investigation of the effect of increased pH (pH 8) and high calcium in isolation, as both are observed to occur in these experiments when basalt is added.

3. Comparison of growth, chemical changes and protein expression with basalt added to nutrient-limited growth media, to assess the ability of *C. metallidurans* to use basalt as an alternative nutrient source.

5.2.2 Organism Selection

The Gram-negative Beta-proteobacterium *Cupriavidus metallidurans* CH34 (formerly *Wautersia*, *Ralstonia*, *Alcaligenes* [190]) is the model organism for this study. *Cupriavidus metallidurans* CH34 is a motile, non-spore forming, rod-shaped bacteria which is commonly used as a model organism for studying bacterial resistance to heavy metal contaminated environments [191–193]. This organism is capable of utilising a diverse suite of carbon and energy sources which make it well-suited to stressful environments. It can respire aerobically via oxidative phosphorylation but will reduce nitrate under low oxygen conditions [154, 172]. It also has the ability to oxidise sulfur and hydrogen [172]. It can metabolise heterotrophically but, in low carbon environments, it will adopt an autotrophic lifestyle, fixing CO_2 to synthesise organic molecules. It can also obtain organic compounds and energy from alcohols (e.g propanol, butanol and acetone) or monoaromatic hydrocarbons such as benzene [172].

This huge versatility can be explained by the genetic flexibility of *C. metallidurans* CH34 which has picked up many new capabilities via horizontal gene transfer. Indeed, Janssen *et al.* (2010) [172] describe the strain's 2nd chromosome as a "patchwork of gene clusters and sub-clusters generated by multiple integration events and subsequent gain (or loss) of acquired genes".

With these capabilities it is unsurprising that *C. metallidurans* has been isolated from a great diversity of extreme environments including heavy-metal contaminated sludge [194], spent nuclear fuel pools [195], spacecraft clean rooms [196, 197] and even the human body in the lungs of a patient with cystic fibrosis [198].

After the isolation of two related *Cupriavidus* species (*C. pinatubonesis* and *C. laharis*) from volcanic rocks in Mt. Pinatubo, Sato *et al.* (2006) suggested that volcanic environments which experience temperature fluctuations, desiccation cycles, scarce organic material and nutrient limitation could be the first natural habitats for *Cupriavidus* species. Adapting to life in a rocky environment would leave these species well placed to colonise industrial, contaminated habitats when they appeared. This has since been echoed in Diels *et al.* (2009) [192] and Olsson-Francis *et al.* (2010) [117]. Olsson-Francis *et al.* conducted a microarray study to determine the mechanisms of iron uptake from rock by *C. metallidurans* CH34 and concluded that the efflux mechanisms useful for heavy metal resistance were also employed during exposure to basalt [117].
The full genome is sequenced and gene functions well-annotated which makes *C. metallidurans* CH34 an excellent model organism for proteomics studies [172].

5.2.3 Substrate Selection

A poorly crystalline basaltic rock was used as the substrate. Basalt is a common igneous rock and the dominant rock type in oceanic crust. By selecting a poorly crystalline rock it can be assumed that the elements of interest are more homogeneously distributed throughout the substrate which could aid in making the experiments more controlled and reproducible.
The basalt used was collected from Skaptafell, Iceland (64°45'58"N 23°38'59"W). The rock composition, as determined by X-Ray Fluorescence (PANalytical PW2404, PANalytical, UK), was 44% SiO_2, 15% Al_2O_3, 11% Fe_2O_3, 7% MgO, 12% CaO, 1% Na_2O, 1% K_2O, 3% TiO_2, 0.2% MnO, 0.4% P_2O_5 with 5.6% lost on ignition. The rock also contained trace elements in the following concentrations: 111ppm Zn, 139ppm Cu, 98ppm Ni, 303ppm Cr, 353ppm V, 284ppm Ba, 45ppm Sc, 22ppm La, 55ppm Ce, 29ppm Nd, 1.5ppm Th, 1.2ppm Pb, 36ppm Nb, 128ppm Zr, 19ppm Y, 426ppm Sr and 17ppm Rb. The basalt was crushed and sieved to

isolate the 1 - 2.5 mm size fraction. This was rinsed thoroughly in ultrapure H_2O and dried overnight at room temperature before autoclaving at 121°C for 20 minutes.

5.2.4 Culturing and Growth

C. metallidurans was routinely cultured at 30°C in Tris salts minimal medium at pH 7 with 0.2% (w/v) sodium gluconate and ferric ammonium citrate as the iron source, as described previously [154] (See Chapter 3 for media composition). Reagent grade chemicals were used for media preparation (Sigma Aldrich, UK). Previously described MM284 has only enough phosphorus (as $Na_2HPO_4.2H_2O$) for complete consumption of the carbon source. The onset of the stationary phase is triggered when the carbon source is exhausted but phosphorus is also low by this time point. The medium is not supplemented with an excess of additional phosphorus.

In order to assess stresses induced by the presence of rock, cells were cultured (starting cell concentration = 2 x 10^4 CFU ml^{-1}) in 50 ml of "optimal growth medium" (i.e. MM284 + gluconate) with 5 g of sterile basalt added. All cultures were grown in acid-washed, sterile 100 ml Nalgene polymethylpentene flasks as in Olsson-Francis *et al.*, (2010) [117]. Cultures were capped with sterile foam bungs to allow gas exchange with the atmosphere. Each test condition was run in triplicate ($n = 3$). As it was unclear whether the presence of rock would subject the cells to physical shear stress during continuous shaking, experiments were conducted under static conditions with manual mixing at 24-hour intervals. Optical density was measured daily by visible spectrometry (absorbance at 600 nm, FLUOstar Optima, BMG Labtech, UK) as a proxy for cell growth. Optical density was measured on 200 μl of culture in a 96 well microplate (path length = 6.31mm). The experiment was conducted for 260 hours after which cells from all flasks were harvested and all following analysis conducted.

A complete set of abiotic controls were run in tandem by adding 50 ml of medium to 5 g sterile basalt in triplicate. These were not inoculated with cells and were kept at 30°C alongside the biotic replicates and also shaken every 24 hours. The control samples were used to quantify abiotic leaching from the rocks and to ensure that no particulate material interfered with optical density measurements. To isolate effects related to pH changes and changes in calcium concentration induced by the rocks, the proteomes of cells grown in the same medium with the pH altered to pH 8 (with NaOH) and with the addition of 10 mM of calcium chloride were investigated.

The high calcium experiments were conducted to follow up on observations from the initial experiments. As no rocks were involved, these cells were cultured at 30°C in a shaking incubator at 90 rpm. The proteome of cells in this condition were compared to cultures in optimal medium which were also shaken. This shortens the length of the experiment but will not affect the interpretation of results as the calcium effect is considered in comparison to the proteome of shaken control treatments (optimal medium + gluconate).

To compare the proteomes of cells initially limited of a specific element, and thus required to obtain that element from the rock, media with the iron or magnesium source omitted and basalt added as before was used. These elements were selected as they are two of the main inorganic cations required for bacterial growth and are major constituents of basaltic rocks [58]. Optical density was also monitored in the iron or magnesium limited media alone (no rock) to establish if the basalt was providing elements essential to growth. Abiotic triplicates of iron- and magnesium-limited media with rock were conducted as before.

The experimental protocol is summarised in Figure 5.1.

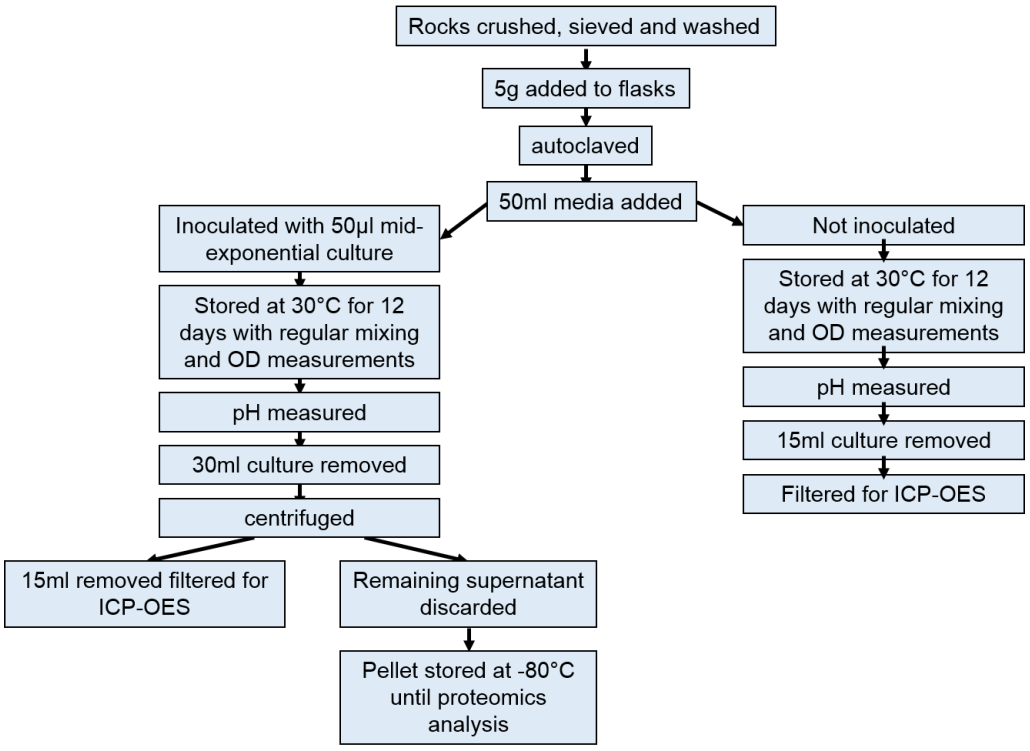

Figure 5.1 Summary of experimental protocol

5.2.5 Quantifying Chemical Changes

Inductively Couple Plasma - Optical Emission Spectroscopy was used to monitor chemical changes in the presence of rock and was conducted in collaboration with Dr Lorna Eades, School of Chemistry, University of Edinburgh.

Fifteen millilitres of supernatant were removed from the flasks at the time of cell harvest and passed through a 0.22 μm syringe filter. The filtered supernatant was acidified with 15 μl 70% nitric acid solution.

The samples were analysed using a Perkin Elmer Optima 5300 DV. Using a peristaltic pump, sample solutions were taken up into a Gem Tip cross-flow nebuliser and Scotts spray chamber at a rate of 1.5 mL min^{-1}.

The instrument was operated in axial mode for Fe and radial mode for all others. A range of calibration standards were prepared using single element 1000 mg l^{-1} stock solutions (Fisher Scientific, UK), diluted with deionised water (18Ω,

Table 5.1 Wavelengths used to report results for ICP-OES

Element	Wavelength
Fe	259.945nm
P	214.914nm
Al	396.153nm
Ca	317.933nm
Mg	280.271nm
Si	288.158nm
Zn	206.205nm
Mn	257.613nm

Elga USF). A multi element standard (ICP Multi element standard solution VI CertiPUR, Merk, UK) was used as a reference standard for Fe.

The selected wavelengths for each element were analysed in fully quantifiable mode (three points per unit wavelength). Three replicate runs per sample were employed. Initially 4 wavelengths were selected for each element and three replicate runs per sample were employed. The wavelengths used to report results are shown in Table 5.1. Standards of 0, 0.01, 0.1, 1, 2, 5, 10, 20, 50 and 100 mg l^{-1} were prepared for each element. Al, Co, Cr, Cu, Fe, Mn, Ni, P, Ti and Zn were calibrated using standards 0-1 mg l^{-1} whereas Ca, Mg and Si were calibrated using the full range of standards. With all of the calibration lines the correlation coefficients for the linear regression were 0.999 or better.

5.2.6 Protein Quantification

Cells were harvested at the time of the last optical density measurement for each condition (ie. after 260 hours) except in the high calcium condition where cells were harvested in the early stationary phase (approx. 40 hours). Thirty millilitres of culture was transferred to 50 ml falcon tubes and centrifuged for 10 minutes at 13,000 g. The supernatants were discarded and 10 ml phosphate buffered saline (PBS) solution added to the pellet before re–centrifuging. The supernatant was discarded and pellets stored at –80°C.

Amount of protein in each sample was determined by a Bradford protein assay [199] and proteins were broken down into their constituent peptides using a trypsin digest [161]. For the extraction and digest, 250μl 8M urea was added to each pellet and left to stand for 1 hour with regular vortexing. Fifty microlitres 1M ammonium bicarbonate, 50 μl 200nM dithiothreitol (DTT) and 50 μl iodoacetamide was then added. The digest was made up to 1 ml with sterile H_2O. After 1 hour, trypsin was added to a concentration of 1 μg per 40 μg protein and the digest left overnight. Ten micrograms of protein was purified using C18 Millipore Ziptips (Sigma-Aldrich, UK; See Chapter 3). Purified peptides were vacuum dried and stored at –20°C.

Peptides were analysed on a reverse phase microcolumn using a 140 minute gradient (controlled by a binary HPLC system 1200, Agilent, UK) coupled to a hybrid LTQ-Orbitrap XL mass spectrometer (Thermo-Fisher, UK) in data dependent mode, controlled through Xcalibur 2.0.7 as described previously [161]. Eight microliters of sample in loading buffer was injected.

Peak selection, normalisation and quantification were performed using Progenesis LC-MS (version 4.0, Nonlinear Dynamics, UK). Peptides (charges 2^+, 3^+ and 4^+) were identified by MASCOT (Matrix sciences, UK, version 2.3) searches of MS/MS data against the NCBI protein database subset [169] for *Cupriavidus metallidurans* (6766 sequences), using a trypsin/p enzyme restriction with a maximum missed-cut value of 2 i.e. the protease failed to cut the peptide where expected at one or two points. Variable methionine oxidation and fixed cysteine carbamidomethylation were used in all searches. Precursor mass tolerance was set to 7 ppm and MS/MS tolerance to 0.4 amu.

P-values on fold changes between experimental condition and control (optimal media without rock) were determined by one-way ANOVA on arcsinh-transformed protein intensities in Progenesis LC-MS [161]. Differentially expressed proteins were considered significant with an average intensity ratio of at least two-fold and a *P*-value less than 0.05 if detected with two or more peptides per protein with a MASCOT identification score greater than 20 (although greater than 40 is ideal).

Protein functions were assigned using expert manual annotation of the Cupriavidu2Scope Project on the MaGe platform [172] (Chapter 3).

5.2.7 Comparison of Protein Profiles

A Bray-Curtis similarity matrix based on the protein expression data was analysed using the PRIMER statistical package (version 6.1.13) with the PERMANOVA+ add-on (version 1.0.3) [200, 201] with assistance from Dr. J. Harrison, University of Edinburgh. Following non-parametric multidimensional scaling ordination (nMDS), a 2-way nested permutational analysis of variance (PERMANOVA; [171]) was performed with 'Medium type' and 'Presence of rock' as the factors (Type III sums of squares, 9999 unrestricted permutations of the raw data). Since different sets of growth media were used in the presence and absence of rock, the factor Medium type was nested under the factor Presence of rock. Post-hoc pairwise comparisons were performed using the same PERMANOVA settings, with the exception of P-values being derived by a Monte Carlo approach due to low numbers of permutations [201]. Variation in within-group dispersion was assessed using a test for the homogeneity of multivariate dispersions (PERMDISP, 9999 permutations) [202].

5.2.8 Phosphorus Partitioning Assays

To better understand phosphorus chemistry in the experiments, phosphorus partitioning assays were conducted by collaborators Dr Bryan Spears and Dr Alanna Moore at the Centre for Ecology and Hydrology, Edinburgh to complement the ICP-OES analysis. The ICP-OES phosphorus analysis indicates only the phosphorus concentrations after the sample has been filtered and does not indicate what form of phosphorus is present. This analysis quantifies the concentration of phosphorus which is partitioned into Soluble Reactive

Phosphorus (SRP), Total Soluble Phosphorus (TSP) and Total Phosphorus (TP). Abiotic and biotic treatments were prepared as before and optimal media was used for all phosphorus partitioning experiments. The four conditions tested were: inoculated optimal media with and without rocks and non-inoculated optimal media with and without rocks. The Soluble Reactive Phosphorus (SRP) fraction is largely comprised of the inorganic orthophosphate (PO_4) form of phosphorus. Soluble reactive phosphorus concentrations were determined following the method of Murphy and Riley (1962) [203]. This method uses a reagent of ammonium molybdate, potassium antimony tartrate, and L-ascorbic acid in 1 M of sulfuric acid, which reacts with the phosphate ion to form a phospho-molybdenum blue complex. Concentrations were determined by measuring absorbance at 882 nm in relation to known standards.

Total phosphorus (TP) is the sum of all of the phosphorus components. TP concentrations were determined on unfiltered samples, which were digested using a solution of sulphuric acid and potassium persulphate to convert all forms of phosphorus to soluble reactive phosphorus, which was then measured in a similar way to that described above. The method used was as described for total phosphorus by Wetzel and Likens (2000) [204], with an added acidification step (0.1 ml of 30% H_2SO_4 was added to the samples before addition of persulfate).

Total Soluble Phosphorus (TSP) is the total of all of the phosphorus forms which passed though the filter. TSP was determined in the same way as described for Total Phosphorus, but using a filtered sample. By subtracting TSP from TP, the amount of particulate phosphorus is calculated.

5.3 Results

5.3.1 Changes in Chemistry and Cell Division

Elemental Changes

Addition of rock was associated with several chemical changes in both *Cupriavidus*-inoculated (biotic) and non-inoculated (abiotic) experiments. The simplest way to view chemical forcing from the rock is to compare abiotic conditions with and without rock. At the end of the experiment (after 260 hours), phosphorus concentrations in the media had decreased when rock was added compared to media without rock (two-way t-test P = 0.0002, t = 73.2, df = 2, Figure 5.2d). All abiotic conditions involving the presence of rock resulted in increased iron, calcium, aluminium and silicon concentrations in relation to control samples (two way t-test P-value for Fe = 0.0004, Ca = 0.0006, Si = 0.0001, Al = 0.0002; Figure 5.2a, b, e, f). Zinc and manganese concentrations in the supernatant of all rock-amended growth media were consistently lower than in the non-inoculated, non-rock control medium (two-way t-test P-value for Mn = 0.007, Zn = 0.002); Figure 5.2g and h). *Cupriavidus*-inoculated cultures had approximately the same concentration of phosphorus with rock as without rock, both of which were much lower than in the original medium (Figure 5.2d). Co, Cr, Cu, Ni and Ti are not reported in Figure 5.2 as they were either not detected or unchanged.

Aluminium and silicon are not typically taken up by micro-organisms and thus are sometimes used to assess whether the organisms increase elemental release from the rock. In these experiments, aluminium and silicon concentrations are in fact lower in biotic treatments than in abiotic treatments.

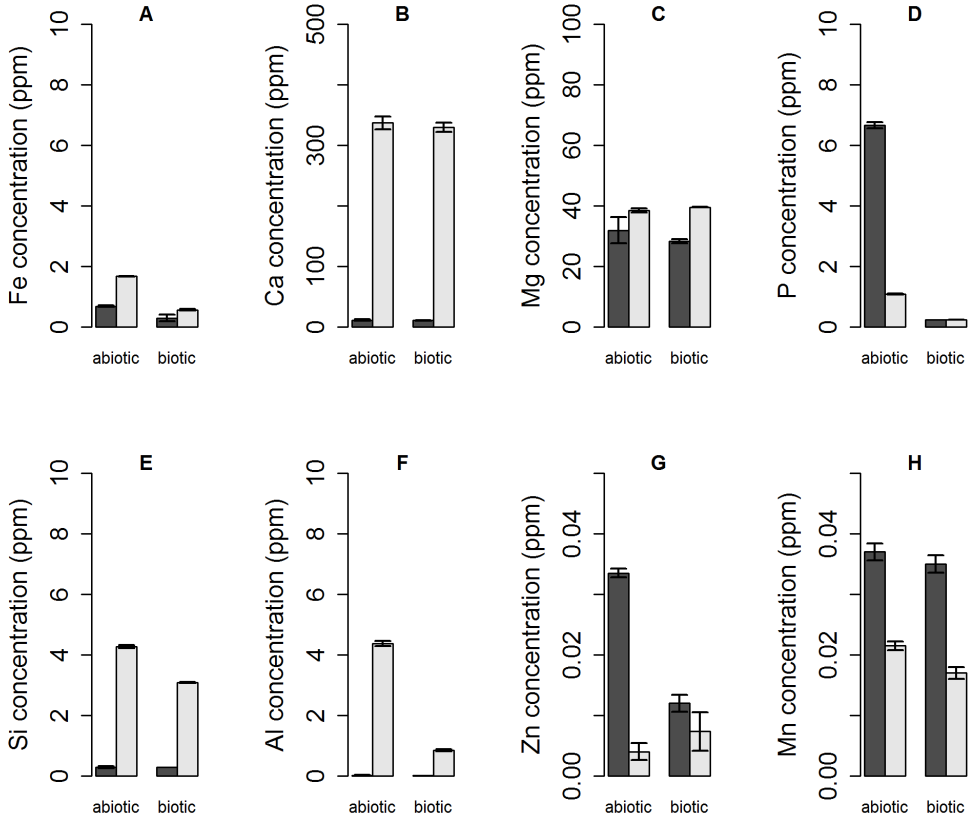

Figure 5.2 Comparison of final inorganic ion concentrations in culture supernatant of optimal media condition and optimal media with rock added (biotic and abiotic) at the end of the experiment as analysed by ICP-OES. Light grey = rock added, Dark grey = no rock. A) Iron B) Calcium C) Magnesium D) Phosphorus E) Silicon F) Aluminium G) Zinc H) Manganese. Abiotic = non-inoculated treatments, Biotic = inoculated treatments. Data shown are means ± SD (n=3).

pH Changes

In both *Cupriavidus*-inoculated and non-inoculated treatments, an increase from pH 7 to approximately pH 8 in the presence of rock was observed, regardless of initial media composition. In abiotic conditions without rock, the pH remained stable at pH 7 but rose to approximately pH 7.5 in biotic treatments without rocks.

Microbial Growth

Cultures grown in optimal media in the presence of rock, or in medium without rock but at higher pH, showed lower growth rates and lower final cell densities than cultures grown in optimal media (pH 7) without rocks (Figure 5.3). No growth was observed in non-inoculated experiments, indicating successful sterilisation of the basalt.

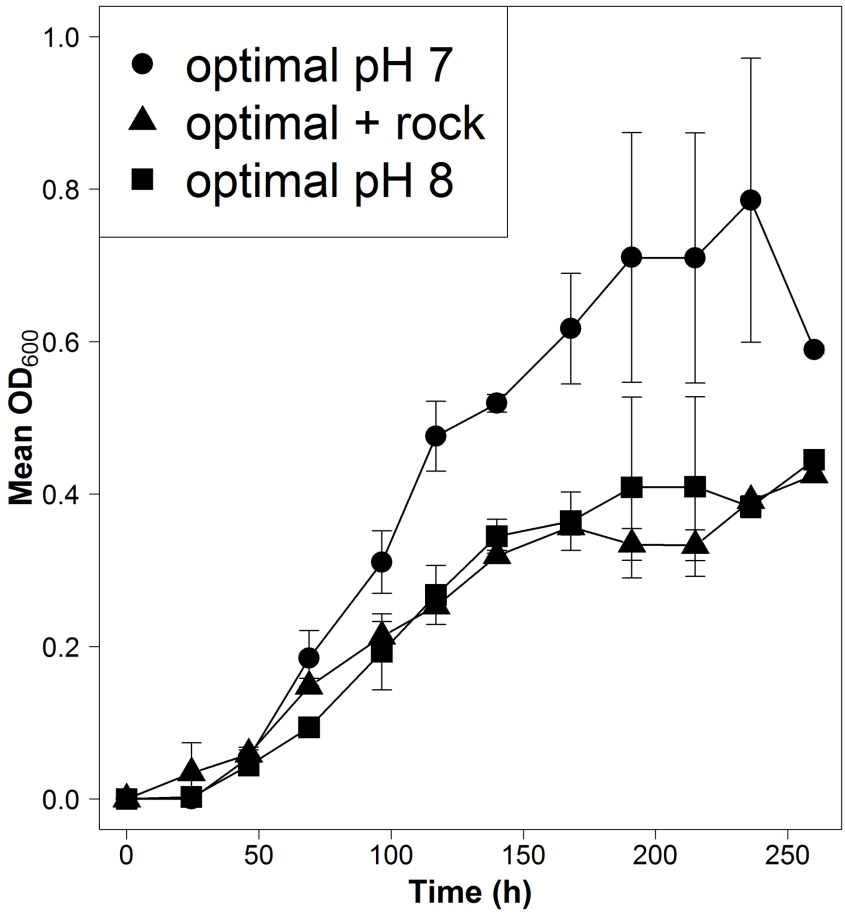

Figure 5.3 Growth curves of *Cupriavidus metallidurans* CH34 in optimal medium at pH 7, at pH 8 and with basaltic rock. The data shown are means ± SD (n=3). Uninoculated flasks were also measured, and optical density in all cases was very close to that of the blank (data not shown).

Phosphorus Partitioning Assays

Despite loss of phosphorus in abiotic treatments with rock added, the ICP-OES results displayed no difference in phosphorus concentrations between biotic treatments with rock and without. However, the ICP-OES phosphorus analysis can determine only the phosphorus concentrations after the sample has been filtered and does not indicate what form of phosphorus is present. To address this, phosphorus partitioning assays were conducted to gain a more detailed understanding of the changes in phosphorus chemistry. These assays can indicate the concentration of phosphorus which is: soluble and reactive, soluble and unreactive and in a particulate form, whereas ICP-OES only indicates total soluble phosphorus. The cause of phosphorus loss was assessed by determining the concentrations of soluble reactive phosphorus, total soluble phosphorus, total phosphorus and, by inference, particulate phosphorus (see Methods).

As a large amount of calcium was measured to have leached from the rocks (Figure 5.2), we may have expected calcium phosphate minerals to precipitate and thus, the assays to show higher particulate phosphorus in the presence of rock. However, no significant difference was observed in the particulate phosphorus concentrations between abiotic treatments with and without rock at the end of the experiment (two-way t-test: $P = 0.28$; Figure 5.4C) showing no precipitate had formed due to calcium leaching. The majority of total phosphorus in non-inoculated treatments with and without rock was present as soluble reactive phosphorus (Figure 5.4D). However, the total concentration of phosphorus in the presence of rock was lower than total phosphorus without rock (two-way t-test: $P = <0.001$; Figure 5.4A). This indicated a loss of phosphorus, but rules out loss through precipitate formation. In *Cupriavidus*-inoculated cultures, although the particulate phosphorus fraction was much higher (as available phosphorus was partitioned into cells), the total phosphorus was lower in the presence of rock, compared with conditions where rock was absent (two-way t-test: $P = <0.001$,

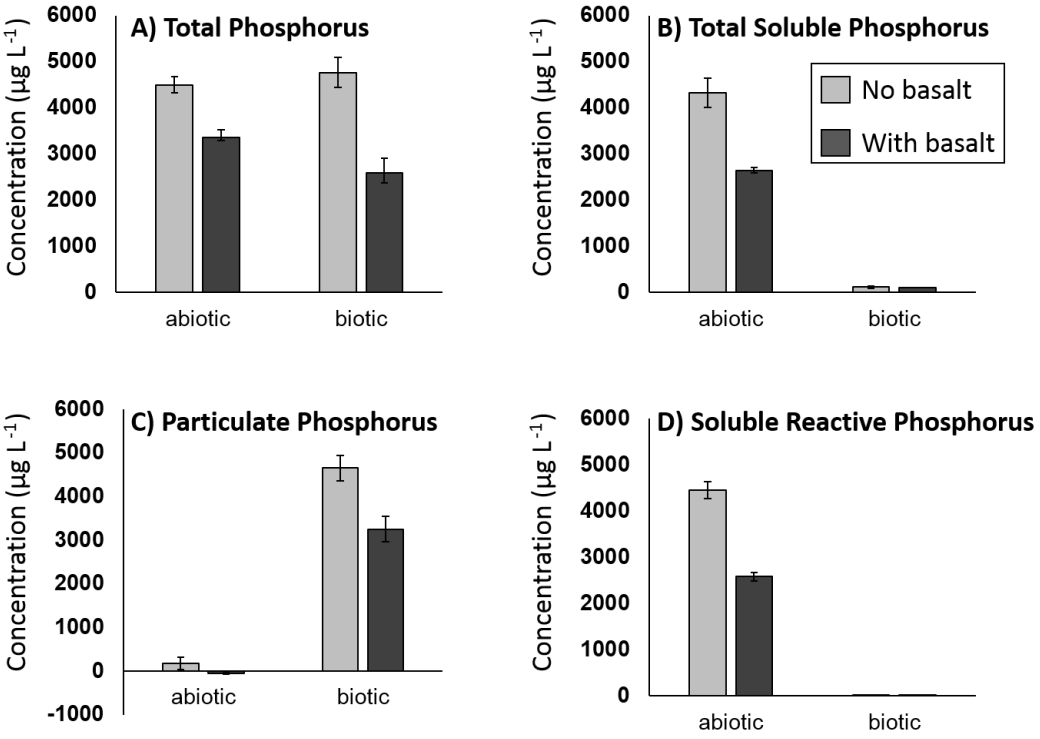

Figure 5.4 Comparison of concentrations of total phosphorus (A), total soluble phosphorus (B), particulate phosphorus (C) and soluble reactive phosphorus (D) measured with and without basalt present in inoculated and non-inoculated cultures. Data are shown as means ± SD (n = 3).

Figure 5.4A). This shows that there is a difference in phosphorus availability in biotic cultures in the presence of rock and explains why this was not picked up by the ICP-OES analysis.

5.3.2 Proteome Changes in Optimal Media with Basalt

A total of 1685 proteins were identified and quantified across all experimental treatments. This represents nearly 25% of all of the protein-coding genes in the *C. metallidurans* CH34 genome. Good technical reproducibility across triplicates was observed with each triplicate having a correlation coefficient of >0.99 when compared to the mean of the triplicates.

Proteome Response to Phosphate Removal

When the proteomes of cultures grown in optimal medium with and without rock were compared, fifty-two proteins are up-regulated (3% of the detected proteins). Table 5.2 lists the proteins which were up-regulated in cells grown in the presence of rock compared to cells grown in optimal media without rock. Most of these were from genes located on chromosome 1 (38) with fourteen on chromosome 2. These included a diverse suite of proteins associated with low levels of phosphorus (Table 5.2). This is in agreement with the chemical results which show phosphorus concentrations in abiotic cultures was lower in the presence of rock (See Figure 5.2). Up-regulated proteins were associated with two phosphate limitation-related strategies: increase of phosphate uptake from outside of the cell and scavenging of phosphate from intracellular reserves.

Table 5.2 – *Proteins up-regulated in optimal media with rock added compared to optimal media with no rock*

Common?	Protein description	Protein name	Locus Tag	MASCOT Score	No. peptides	FC	P value
Phosphorus limitation							
-	Periplasmic phosphate binding protein	PstS	Rmet_2185	2864	36	+2.2	1.8E-03
x	Phosphonate C-P lyase system	PhnL	Rmet_0761	27	5	+2.7	7.8E-03
-	Phosphonate-binding periplasmic protein	PhnD	Rmet_0774	2128	32	+2.0	5.5E-04
-	Phosphonate-binding periplasmic protein	PtxB	Rmet_2994	2675	27	+2.0	6.8E-03
x	Putative Patatin-like phospholipase	PatD	Rmet_0151	152	3	+2.1	2.4E-04
x	Phospholipase C	PlcN	Rmet_4192	1464	31	+3.0	3.5E-03
x	Phosphoglycolate phosphatase	CbbZ1	Rmet_1514	44	2	+3.5	6.7E-03
x	Alkaline phosphatase	PhoD	Rmet_2583	298	9	+5.8	1.7E-04
x	Putative polyphosphate kinase	Ppk	Rmet_0550	114	7	+2.6	3.2E-02
Alternative energy metabolisms							
x	Membrane-bound [NiFe]-hydrogenase formation protein	HoxQ	Rmet_1290	132	4	+2.4	7.9E-03
-	Sulfite:cytochrome c oxidoreductase molybdenum subunit	SorA	Rmet_4891	141	5	+2.3	2.8E-03
x	Formate dehydrogenase, gamma subunit	FdhC	Rmet_2758	132	4	+4.2	4.5E-03
x	Conserved hypothetical protein; putative exported lipoprotein	-	Rmet_2759	102	3	+7.4	6.6E-05
x	Formate dehydrogenase, beta subunit	FdhB	Rmet_2760	299	7	+10.8	6.5E-05
x	Formate dehydrogenase, alpha subunit	FdhA	Rmet_2761	1109	24	+4.2	1.1E-04
-	Disulfide oxidoreductase	-	Rmet_0109	109	4	+2.1	2.4E-03
-	Aldo/keto reductase	-	Rmet_3081	69	5	+3.0	5.7E-03
Membrane & periplasm proteins							
-	Colicin transporter of the tol-pal system, periplasmic component	TolB	Rmet_2675	799	15	+2.1	5.0E-03
-	Taurine ABC-type transporter, periplasmic component	TauA	Rmet_2859	109	8	+2.1	2.2E-02

Continued on next page

Table 5.2 – *Proteins up-regulated in optimal media with rock added compared to optimal media with no rock*

Common?	Protein description	Protein name	Locus Tag	MASCOT Score	No. peptides	FC	P value
-	DL-methionine ABC-type transporter, periplasmic substrate-binding component	MetQ	Rmet_4988	526	8	+2.5	6.9E-04
-	ABC-type transporter involved in toluene tolerance, periplasmic component	Ttg2	Rmet_4167	424	10	+2.1	3.0E-05
-	ABC-type transporter, solute-binding periplasmic component	-	Rmet_2122	265	10	+2.3	3.8E-03
x	ABC-type transporter, periplasmic component*	-	Rmet_5638	456	7	+3.0	2.5E-04
x	Metal cation RND-type transporter, membrane protein	HmyB	Rmet_4121	404	8	+7.9	5.0E-06
-	Putative lipoprotein	-	Rmet_3083	190	6	+2.6	5.3E-03
x	Putative lipoprotein precursor	-	Rmet_0997	33	3	+4.6	1.2E-03
x	Beta N-acetyl-glucosaminidase	NagZ	Rmet_2413	163	6	+5.7	5.1E-04
-	Phosphotransferase involved in extracellular matrix synthesis	EplL	Rmet_2726	47	2	+2.4	4.9E-02
x	Surface antigen-like outer membrane lipoprotein	-	Rmet_0849	99	3	+2.6	2.4E-04
x	Extra-cytoplasmic solute receptor, periplasmic protein	Bug	Rmet_5294	50	5	+4.8	2.5E-03
-	Extra-cytoplasmic solute receptor, periplasmic protein	Bug	Rmet_5869	51	2	+2.8	4.9E-04
-	Extra-cytoplasmic solute receptor, periplasmic protein	Bug	Rmet_0982	199	7	+2.3	9.4E-05
-	Extra-cytoplasmic solute receptor, periplasmic protein	Bug	Rmet_1184	481	11	+2.1	1.5E-03
Replication & Transcription & Translation							
-	DNA polymerase III subunit	HolC	Rmet_2806	20	2	+2.0	5.7E-04
-	Ribonucleotide-diphosphate reductase, subunit beta	NrdB	Rmet_3087	217	4	+2.0	7.2E-03
-	Cell division protein	ZapD	Rmet_3112	214	5	+2.5	1.8E-02
x	LysR family transcriptional regulator		Rmet_3446	34	3	+2.5	3.4E-04
x	GntR family transcriptional regulator	-	Rmet_5631	28	5	+9.0	2.5E-03
x	BolA family transcriptional regulator	BolA	Rmet_3251	29	3	+5.1	1.8E-03
-	Cold-shock responsive transcriptional repressor	Csp	Rmet_5818	257	3	+2.4	1.0E-02
x	50S ribosomal protein L28	RpmB	Rmet_2870	137	3	+2.0	3.7E-02

Continued on next page

Table 5.2 – *Proteins up-regulated in optimal media with rock added compared to optimal media with no rock*

Common?	Protein description	Protein name	Locus Tag	MASCOT Score	No. peptides	FC	P value
Other							
-	Sulfate/thiosulfate import ATP-binding protein	CysA	Rmet_1378	62	2	+2.6	3.4E-03
x	Sulphate adenylyltransferase subunit 1	CysN	Rmet_2812	852	14	+2.8	8.8E-04
-	Diguanylate cyclase*[1]	PleD	Rmet_0867	66	5	+3.2	4.7E-02
-	Short-chain dehydrogenase/reductase SDR	FabG	Rmet_4414	39	3	+2.5	8.5E-03
-	Methylmalonate-semialdehyde dehydrogenase	MmsA	Rmet_0206	361	9	+2.0	1.5E-03
-	Acyl-CoA-binding protein	-	Rmet_1394	184	7	+2.0	6.6E-04
-	Hemolysin-like Acyl-CoA N-acyltransferase	-	Rmet_2176	29	2	+2.5	8.8E-03
x	GCN5-related N-acetyltransferase	-	Rmet_5884	58	4	+4.3	2.4E-04
x	Homogentisate 1,2-dioxygenase, involved in phenylalanine & tyrosine degradation	HmgA	Rmet_4374	54	2	+4.7	4.5E-04
x	Putative glyoxalase or dioxygenase	-	Rmet_4030	71	2	+3.1	1.0E-03
-	Conserved hypothetical protein	-	Rmet_2632	183	5	+2.3	5.7E-03

Table 5.2 – *Proteins up-regulated in optimal media with rock added compared to optimal media with no rock*

Differentially expressed proteins were considered biologically significant with an average intensity ratio of at least two-fold and a p-value less than 0.05 if detected with two or more peptides per protein with a MASCOT identification score greater than 20. Bold locus tags highlight proteins in which more than one gene from the operon is differentially regulated. *[1] Also observed to be up-regulated in MM284 at pH 8. Column "Common?" indicates whether this protein was also up-regulated in the other media types with rock added i.e. minus Fe + rock and minus Mg + rock (discussed later in text).

Proteins involved in increased import of phosphorus represent pathways for transport of phosphorus in four forms: phosphate, phosphonate, organophosphate and phosphite. These include the PstS protein from the phosphate specific transport system which is involved in free phosphate import, the high affinity phosphate uptake system protein PhnD which transports phosphonate and organophosphate esters [205] and PtxB which is involved in transport of phosphonate or phosphite.

Proteins associated with intracellular scavenging typically do so by degrading larger phosphate–containing compounds. The up-regulated patatin (PatD) and phospholipase C (PlcN) enzymes, for example, release phosphorus from phospholipids [206, 207]. The high affinity phosphate uptake system protein PhnL is a component of the C-P lyase system which generates free phosphate groups by the degradation of organophosphates [208–210].

Phosphoglycolate phosphatase (CbbZ1) metabolises the phosphate-containing molecule 2-phosphoglycolate, typically produced during the repair of DNA damage caused by oxidative stress [211]. PhoD is an alkaline phosphatase enzyme thought to be a scavenging mechanism by which bacteria generate free phosphate groups from many types of molecule. Whilst Rmet_0550 is annotated as a hypothetical protein in the *C. metallidurans* CH34 genome, a BLAST search revealed that this protein shares an 81% similarity to polyphosphate kinase 2 in *Herbaspirillum sp.* YR522. Polyphosphate kinase is a membrane protein which catalyses the formation of polyphosphate from ATP and participates in oxidative phosphorylation.

Other Proteins Up-regulated in the Presence of Rock

In addition to the low phosphorus response, an up-regulation of proteins involved in alternative energy generating pathways in the membrane, and cellular redox homeostasis are observed (Table 5.2). These included proteins associated with hydrogen oxidation (i.e. hydrogenotrophy) (oxygen-tolerant membrane-bound

hydrogenase formation protein HoxQ) and an enzyme involved in sulphite oxidation (sulfite:cytochrome c oxidoreductase SorA). Also observed is an up-regulation of the entire set of proteins involved in formate oxidation (FdhA, FdhB, Rmet_2759, FdhC). These Fdh enzymes catalyse the oxidation of formate to CO_2 and H^+ and have been associated with stress responses in *Desulfovibrio vulgaris* [212].

The remaining up-regulated proteins were primarily associated with diverse membrane and periplasmic transport processes, and regulatory processes such as signalling and transcription regulation (Table 5.2).

Proteins Down-regulated in the Presence of Rock

Forty-five proteins are significantly down-regulated in the presence of rock and are shown in Table 5.3. These represent 2.7% of the detected proteins. Twenty-eight of these are from genes located on chromosome 1, fourteen from chromosome 2 and one each from plasmid pMOL28 and pMOL30. Down–regulation of metal cation responses and efflux systems was observed with rock present and included ZniA, ZniB and ZntA proteins which have a specific affinity for zinc and cadmium. Also down-regulated was the HmzP two-component transcriptional regulator, a metal cation resistance protein, and a ferric reductase (Rmet_3017) which is downstream of *hmzP*.

Table 5.3 – *Proteins down-regulated in optimal media with rock added compared to optimal media with no rock*

Common?	Protein description	Protein name	Locus Tag	MASCOT Score	No. peptides	FC	P value
Metal homeostasis							
-	Transcriptional regulator, part of two component system with HmzS	HmzR	Rmet_3016	64	6	$->500^{*1}$	2.80E-04
x	Ferric reductase, FAD/NAD(P)-binding	-	Rmet_3017	71	4	−15.1	2.60E-03
x	P-type ATPase involved in Zn(II), Cd(II), Ti(I) and Pb(II) resistance	ZntA	Rmet_4594	190	8	−4.4	1.10E-02
x	RND metal efflux pump, part B	ZniB	Rmet_5320	198	7	−2.3	8.60E-03
-	RND metal efflux pump, part A	ZniA	Rmet_5319	73	8	−2.9	2.70E-02
Transport over membrane							
x	Glycine betain/carnitine/choline ABC-type transporter, periplasmic component	-	Rmet_0799	45	6	−2.7	1.20E-02
-	ABC-type transporter, periplasmic component: HAAT family	-	Rmet_0920	67	5	−2.3	3.10E-02
x	ABC-type transporter, periplasmic component: HAAT family	-	Rmet_2820	51	3	−2.8	1.10E-02
-	ABC-type transporter subunit, ATP-binding component	YadG	Rmet_3253	136	7	−2.4	2.90E-03
x	ABC-type transporter, ATP-binding and membrane component	VcaM	Rmet_2516	87	5	−7.1	2.00E-02
-	TRAP-type mannitol/chloroaromatic compound transporter, periplasmic	-	Rmet_3543	873	16	−2.1	1.50E-04
-	Putative oligoketide cyclase/lipid transport protein	YfjG	Rmet_1457	51	2	−30.5	1.30E-02
x	Import inner membrane translocase	-	Rmet_0372	491	9	−2.2	1.10E-04
-	Extra-cytoplasmic solute receptor protein	Bug	Rmet_5038	23	3	−3.3	1.50E-03
Transcription							
-	XRE family transcriptional regulator	-	Rmet_4373	47	2	−2.3	2.60E-02
x	TetR family transcriptional regulator	-	Rmet_4909	48	4	−4.5	3.60E-02

Continued on next page

Table 5.3 – *Proteins down-regulated in optimal media with rock added compared to optimal media with no rock*

Common?	Protein description	Protein name	Locus Tag	MASCOT Score	No. peptides	FC	P value
-	LysR family transcriptional regulator	YcaN	Rmet_1897	11	6	−2.5	5.40E-03
x	Transcription termination factor	Rho	Rmet_2135	499	13	−2.7	7.90E-04
-	Purine-binding chemotaxis regulator	CheW	Rmet_3681	164	8	−2.3	2.50E-03
-	Histone-like bacterial DNA-binding protein	HupB	Rmet_6397	263	6	−4.2	1.80E-02
Biotin synthesis							
x	Adenosylmethionine-8-amino-7-oxononanoate transaminase	BioA	Rmet_0114	389	8	−2.8	1.20E-03
-	Amino-7-oxononanoate synthase	BioF	Rmet_0115	22	4	−>600	1.30E-04
Oxidoreductases							
x	NADH dehydrogenase, subunit J	NuoJ	Rmet_0936	79	5	−2.9	4.40E-03
-	Thiosulphate-binding sulfur oxidation protein	SoxZ	Rmet_3422	35	2	−2.5	1.30E-02
x	Short-chain dehydrogenase/reductase SDR	-	Rmet_4614	79	6	−2.4	2.20E-02
x	2-dehydropantoate 2-reductase	PanE	Rmet_5770	125	6	−2.2	1.30E-03
-	NAD-dependent formate dehydrogenase alpha subunit	FdsA	Rmet_0555	47	8	−2	7.70E-03
Other							
-	Chromosome segregation ATPase	Smc	Rmet_1426	187	14	−2.1	3.90E-02
-	General stress response protein	CsbD	Rmet_5008	34	2	−2.1	3.30E-02
x	Putative type-4 fimbrial biogenesis protein*2	PilY1	Rmet_0192	241	5	−3.1	8.10E-04
x	Isocitrate lyase*2	AceA	Rmet_1385	113	5	−4.6	8.50E-04
x	Alkaline phosphatase*2	PhoA1	Rmet_4084	1062	19	−3.1	3.10E-03
x	Acid phosphatase*2	AcpA	Rmet_4809	69	3	9.1	1.80E-03
x	KAP P-loop containing ATPase protein	-	Rmet_2164	85	13	−2.1	7.70E-03
x	ATPase-like protein	-	Rmet_3356	43	7	−4.6	1.10E-02
-	P-loop-containing ATPase protein	-	Rmet_0297	79	3	−10.1	3.90E-03
-	D-tyrosyl-tRNA(Tyr) deacylase	Dtd	Rmet_0418	25	2	−4.5	3.10E-02
-	Putative metallo-dependent amidohydrolase*2	-	Rmet_5313	91	4	−2.1	1.60E-03

Continued on next page

Table 5.3 – *Proteins down-regulated in optimal media with rock added compared to optimal media with no rock*

Common?	**Protein description**	**Protein name**	**Locus Tag**	**MASCOT Score**	**No. peptides**	**FC**	**P value**
-	4-hydroxybenzoate 3-monooxygenase	PobA	Rmet_4018	18	3	−2.7	4.50E-02
-	Acyl-CoA synthetase (AMP-dpendent)	-	Rmet_1061	56	6	−2.4	4.90E-04
-	Acyl carrier protein	AcpP	Rmet_4378	70	9	−2	3.80E-02
-	Fatty acid desaturase	-	Rmet_0888	53	6	−9.7	2.20E-02
x	Insertion element protein	TnpA	Rmet_5954	73	10	−2.9	3.80E-03
-	Carboxypeptidase G2 precursor	-	Rmet_0024	42	4	−>900	4.80E-03
-	Conserved hypothetical protein	-	Rmet_5391	41	2	−2.1	1.60E-02
x	Conserved hypothetical protein						

Table 5.3 – *Proteins down-regulated in optimal media with rock added compared to optimal media with no rock*

Differentially expressed proteins were considered biologically significant with an average intensity ratio of at least two-fold and a p-value less than 0.05 if detected with two or more peptides per protein with a MASCOT identification score greater than 20. *1 Fold changes >500 result from lack of detection in one condition. *2 Also observed to be down-regulated in MM284 at pH 8. Column "Common?" indicates whether this protein was also down-regulated in the other media types with rock added i.e. minus Fe + rock and minus Mg + rock (discussed later in text).

A down-regulation of proteins associated with consumption of high energy, phosphorus-containing compounds such as ATP and NADPH are observed. For example, three ATPases are down-regulated (Rmet_0297, Rmet_2164 and Rmet_3358) as are oxidoreductase enzymes associated with energy metabolism. Other down-regulated proteins included those involved in transcription, biotin synthesis, oxidoreductase reactions, transport and signalling (Table 5.3). Although typically associated with phosphorus homeostasis, alkaline phosphatase and the phosphoesterase down-regulated in the presence of rock were also down-regulated in the proteome of cells grown at pH 8. All proteins also down-regulated in cells cultured at pH 8 are highlighted in Table 5.3.

5.3.3 Proteome Changes at pH 8 and with 10mM Additional Calcium

Across all experimental treatments, rock-induced variation in protein expression was accompanied by increased pH and calcium concentrations in the growth media. Proteome responses to these conditions in isolation were characterised.

Proteome Changes at pH 8

Growth at pH 8 (Figure 5.3) was reduced in comparison with cells at pH 7. Growth at pH 8 was indistinguishable, with reference to both mean growth rates and final optical densities, from those observed in the presence of rock.
Cells grown in medium at pH 8 up-regulated 21 proteins and down-regulated 25 proteins compared with cells grown in medium at pH 7, 5 of which were also down-regulated in the proteome of cells grown in rock-amended media (Appendix Table A.1). These proteins are not functionally related to one another and no overall pattern is observed.

Proteome Changes at High Calcium Concentrations

At high calcium concentrations, increased expression of phosphate-related proteins was observed. Figure 5.5, shows the fold change of proteins up-regulated in cells grown in medium with an additional 10 mM of calcium chloride compared with cells grown in optimal medium. Whilst rates of cell division were unchanged by the addition of calcium (data not shown), the up-regulation of a similar suite of proteins related to phosphate uptake was observed at 10 mM of calcium chloride, as seen in the presence of rock. These proteins represent processes such as phosphate transport (PhoB and PhoU), phosphonate metabolism (PhnD and PhnM), phosphite transport (PtxB and PtxD) and the phosphate specific transport system (PstS). Proteins related to intracellular phosphate scavenging were not up-regulated in the presence of high calcium.

Despite the association between high calcium and the up-regulation of phosphate-limitation related proteins, ICP-OES analysis showed no decrease in phosphorus concentrations between optimal media and media with 10mM additional calcium (data not shown).

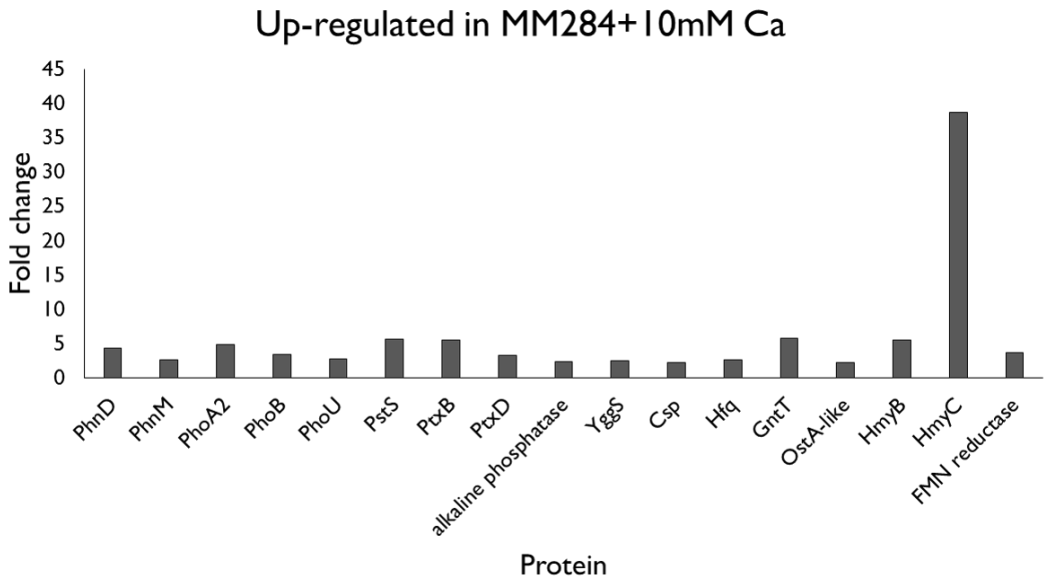

Figure 5.5 Fold change of proteins up-regulated with additional 10 mM of calcium compared to optimal medium shows up-regulation of phosphate-limitation proteins. High calcium also causes up-regulation of a small number of transmembrane transport proteins such as the Hmy heavy metal transmembrane transport system (HmyB and HmyC), a gluconate transporter (GntT), a cold shock regulatory response protein (Csp) and an RNA chaperone (Hfq) which binds sRNAs and mRNAs to facilitate mRNA translational regulation in response to envelope stress, environmental stress and changes in metabolite concentration. All P-values less than 0.05 and proteins identified by 2 or more peptides.

5.3.4 Effect of Initial Element Limitation

Experimental Set Up

To assess the importance of the rocks as providers of elements, experiments were conducted with basalt added to growth media deprived of iron or magnesium. These experiments were conducted at the same time, and under the same conditions, as those with optimal media and rock. Again, abiotic triplicates were conducted in tandem.

Changes in Chemistry and Growth

Figure 5.6 shows that, when iron or magnesium are omitted from the medium, they are re–supplied by the rock.

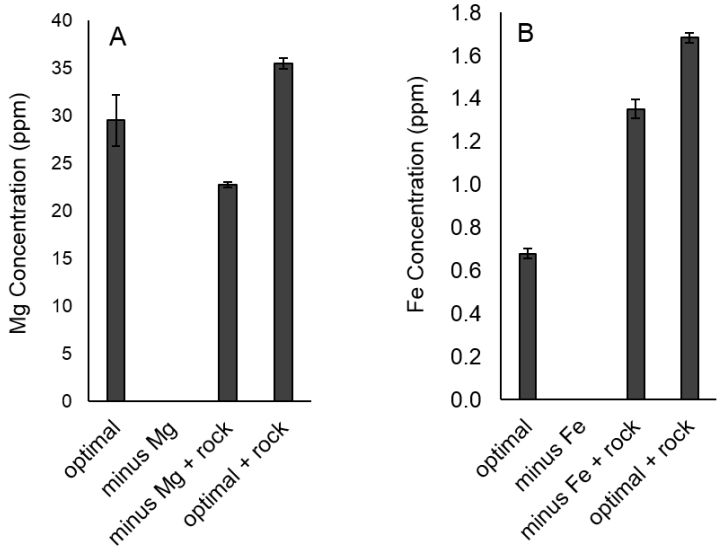

Figure 5.6 Bar graph showing rock supplies iron and magnesium to culture medium which can replace artificial sources omitted from the optimal media. A) Comparison of final magnesium concentrations in culture supernatant of optimal medium, no magnesium medium, no magnesium medium with rock and optimal media with rocks. B) Comparison of final iron concentrations in culture supernatant of optimal medium, no iron medium, no iron medium with rock and optimal media with rock. All conditions are abiotic. Data shown are means ± SD (n=3).

A greater than two fold decrease in cell density relative to the control was observed in medium without iron and no growth was observed in medium without magnesium (Figure 5.7). The addition of rock to all of these media resulted in almost identical growth curves across all conditions, with these data being indistinguishable from the growth curves obtained for optimal medium with rock (Figure 5.7).

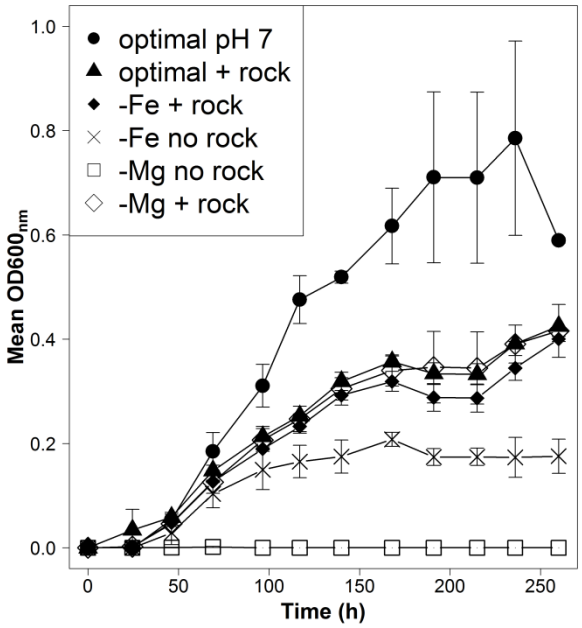

Figure 5.7 Comparison of growth of *Cupriavidus metallidurans* CH34 in different nutrient availability conditions. Shows improvement in growth compared to magnesium and iron starved cultures when rock is added. Rock curves fall within a similar range regardless of initial nutrient conditions. Data are shown as means ± SD (n = 3). Labels: optimal pH7 = optimal media at pH 7 with no rock, optimal + rock = optimal media with rock present, - Fe + rock = media with no iron added but rock present, - Fe no rock = media with no iron added and no rock present, - Mg no rock = media with no magnesium added and no rock present, - Mg + rock = media with no magnesium added but rock present.

Comparison of Proteome

Multivariate analysis of the protein expression data was performed for cultures incubated in optimal medium in the absence of rock, and three types of growth media in the presence of rock (see Methods). This identified two main clusters defined by the presence or absence of rocks (Figure 5.8). While these clusters were only 20% dissimilar (based on a group-average clustering of Bray-Curtis similarity values), the observed difference was highly significant (2-way nested PERMANOVA: pseudo-$F_{1,10}$ = 19.552, P = < 0.001). A significant effect of

medium type was also observed (2-way nested PERMANOVA: pseudo-$F_{3,10}$ = 4.060, P = 0.002). No significant variation in multivariate dispersion was observed between samples incubated in the presence or absence of rock (PERMDISP: $F_{1,10}$ < 0.001, P = 0.983), or in different types of media (PERMDISP: $F_{4,10}$ = 0.440, P = 0.916). These results give confidence that the differences shown by PERMANOVA are real and not just due to differences in multivariate dispersion (which can also influence *P*-values).

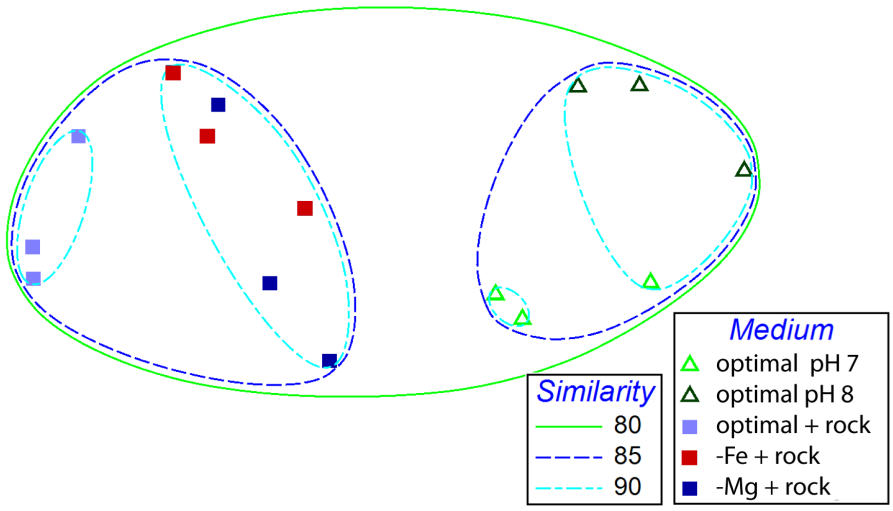

Figure 5.8 Non-metric multidimensional scaling (nMDS) ordination of *Cupriavidus metallidurans* CH34 cultures incubated in different types of growth media in the presence or absence of basalt. The ordination (stress = 0.07) was derived from a Bray-Curtis similarity matrix calculated from normalised protein expression data (see Methods). Similarity thresholds (%) are based on group-average clustering. See Figure 5.7 for label descriptions.

All of the media types in the presence of rock were 85% similar regardless of initial element limitation (Figure 5.8). However, cultures which were limited by magnesium or iron in the original medium before rocks were added were more similar to one another than to optimal media in the presence of rock (Monte Carlo P = optimal + rock vs no Fe + rock: 0.0327; optimal + rock vs no Mg + rock: 0.0228; no Mg + rock vs no Fe + rock: 0.209). In the absence of rock,

cultures at pH 8 showed a higher similarity to cultures at pH 7 than they did to any of the culture conditions involving the presence of rock (Figure 5.8).

Global test results for 2-way nested PERMANOVA with factor Medium type nested within factor Presence of rock are shown in Table 5.4. PERMANOVA pair-wise comparisons are shown in Table 5.5.

Table 5.4 Global test results (2-way nested PERMANOVA with factor Medium type nested within factor Presence of rock)

Factor	df	SS	Pseudo-F	P(perm)	Unique perms
Presence of rock	1	545.8	19.552	0.0001	9912
Medium type	3	339.99	4.0598	0.0019	9927

Table 5.5 PERMANOVA pairwise comparisons of proteome profiles between different medium types (nested within factor Presence of rock)

Groups	Average similarity (%)	t	P(perm)	Unique perms	P (MC)
pH 7 vs. pH 8	89	2.0657	0.101	10	0.0401
optimal + rock vs. -Fe + rock	89.9	2.1679	0.0982	10	0.0327
optimal + rock vs. -Mg + rock	88.1	2.3978	0.1005	10	0.0228
-Fe + rock vs. -Mg + rock	91.7	1.3272	0.1964	10	0.209

df = degrees of freedom, SS = Type III Sums of Squares, P(perm)= PERMANOVA P-value, Unique perms = No. of unique permutations, P(MC) = Monte Carlo P-value

Overlapping sets of up- and down-regulated proteins were identified in each of the experimental conditions (Figure 5.9). These data showed that a core set of proteins was always up-or down-regulated in the presence of rock, regardless of whether the cultures were starved of a specific element (Fe or Mg) or not. This observation is consistent with the results shown in Figure 5.8, supporting our finding that differences in protein expression were primarily attributable to the presence or absence of rock, as opposed to elemental starvation.

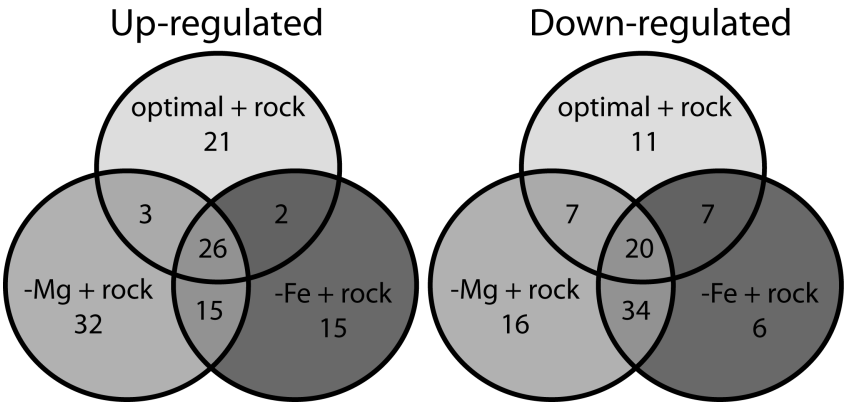

Figure 5.9 Venn diagrams displaying up- and down-regulated proteins common to different experimental groups.

Proteins differentially regulated in all conditions are marked with an "x" in the "Common?" column of Tables 5.2 and 5.3. The up-regulation of phosphate limitation proteins, the formate dehydrogenase regulon and proteins also differentially regulated at pH 8 dominated this group of common proteins.

5.4 Discussion

5.4.1 Microbial Response to Presence of Rock

Motivated by a desire to better understand the mechanisms micro-organisms require to inhabit a rock environment, this chapter investigated whether rocks induce specific microbial responses that are directly linked to chemical changes

induced by the presence of rock.

The first experiments used quantitative label-free proteomics to explore the molecular adaptations used by a model micro-organism (*Cupriavidus metalliduran*s CH34) grown in the presence of basalt. Two observed chemical changes in the growth media, increased pH and high calcium concentrations, were then investigated in isolation to unravel the driving factors behind the proteome changes. The use of elements leaching from the rock as alternative sources of iron or magnesium for the microbial population was then investigated.

These results show that, whilst the rock did provide an alternative source of iron and magnesium, growth was reduced compared to that in optimal (pH 7) media without rock (Figure 5.7). This reduced growth is not a result of lack of iron or magnesium, but is caused by the presence of rock in general, as it is also observed when rock is added to optimal media.

Slow cell division and reduced final optical density in the presence of rock are, most likely, the result of increased pH as growth profiles at pH 8 without rock were almost identical to growth in optimal media with rock (Figure 5.7). An increase in pH in the presence of rock is consistent with current knowledge on basalt glass dissolution, which begins with the release of monovalent and divalent cations via metal-proton exchange which consumes protons and could increase fluid pH [213]. Decreased growth in the presence of rock, driven by abiotic rock-water interactions is a good example of rock-induced stress. However, whilst rock-induced shifts in pH appeared to drive the decrease in growth rate, multivariate analysis of the proteome data (Figure 5.8) revealed that increased pH is not the main factor influencing protein expression.

A common factor in the proteome of all conditions with rocks present was the up-regulation of proteins associated with phosphate limitation. Phosphorus is partitioned differently in biotic and abiotic treatments ie. biotic treatments have high particulate phosphorus concentrations (as phosphorus is partitioned into cells) and abiotic treatments have the highest concentration partitioned into soluble phosphorus. However, the key finding is that regardless of partitioning

effects, the total phosphorus concentration in the system is lower in the presence of rock in both abiotic and biotic treatments. As there is a substantial amount of calcium leaching in the presence of rock, the loss of phosphorus could, theoretically, have been driven by calcium phosphate precipitation. However, the lack of particulate phosphorus in the abiotic partitioning assays with rock rules out abiotic precipitate formation (Figure 5.4c). Particulate phosphorus is high in biotic cultures and soluble (total and reactive) phosphorus is low but this is a result of soluble phosphorus uptake by cells and not mineral precipitation. Together, the low abiotic precipitate abundance and low total phosphorus concentrations when rock is added, are consistent with phosphate sorption onto the rock surface rather than phosphate mineral formation. This would completely remove it from the phosphorus speciation assays and lead to low total phosphorus concentrations as observed.

Investigation of increased calcium in isolation also showed that no phosphorus loss occurred at these calcium concentrations. However, despite phosphorus concentrations being unchanged by the addition of 10mM calcium, the proteomes of cells cultured in high calcium media displayed a similar up-regulation of phosphorus uptake proteins as was observed in the presence of rock. This demonstrated a previously unknown link between extracellular calcium concentrations and phosphorus homeostasis which should be further investigated.

The sorption of phosphates to mineral surfaces has been studied extensively and occurs when phosphates sorb to metal oxyhydroxides via ligand exchange, an OH^- or an H_2O molecule is released from the surface and a phosphate surface complex forms [214]. It is likely that this phosphorus sequestration results in exhaustion of available phosphorus before all the carbon source has been used and drives cells into an early, phosphorus limitation-induced stationary phase in the presence of rock as well as acting to limit biomass yield and drive protein expression.

It is unclear whether *C. metallidurans* CH34 has the ability to solubilise mineral phosphates, facilitating the direct scavenging of phosphorus from a rock surface,

or whether the up-regulated proteins assist in accumulation of phosphates from organic sources. However, the genetic capabilities that *C. metallidurans* possesses to overcome phosphorus sequestration within natural environments could confer a key advantage in the colonisation of rock habitats characterised by numerous pathways for phosphate removal.

Additionally, an up-regulation of proteins involved in alternative metabolisms such as hydrogen and sulphite oxidation was observed. This may result from a need to utilise a diverse range of energy-producing processes because of the lack of phosphorus and the need to respond to a stressful environment. In particular, the up-regulation of the formate dehydrogenase operon (observed here in all conditions in the presence of rocks) has been linked to stress responses by previous studies. For example, in *Desulfovibrio vulgaris*, the expression of the *fdhBAC* genes is associated with diverse stress responses [212] where all stress responses which down-regulate energy metabolism see a concomitant increase in the expression of one or more *fdh* genes. Consistent with this is the down-regulation of proteins associated with high energy phosphorus-containing compounds such as ATP which probably act to limit the consumption of these molecules due to their low availability.

The down-regulation of various zinc efflux proteins are also linked to the changing chemistry. It is unclear why the zinc and manganese concentrations are lower with rock present in both biotic and abiotic treatments but the lower concentrations cause the cells to limit efflux of zinc, presumably retaining higher intracellular stocks.

From both the element and proteome analysis, there is no evidence that *C. metallidurans* CH34 has an active role in rock weathering in this case. These data are more consistent with passive uptake of abiotically leached elements, and cellular responses to abiotic surface reactions induced by the fluid-rock interaction.

5.4.2 Significance

These results highlight the importance of proteomics in understanding the complex interaction between micro-organisms and their environment. Feedbacks between micro-organisms and geochemistry are poorly understood because environmental studies generally focus on the abundances of different taxa or functional genes, ignoring the fact that microbes are highly versatile, and thus will respond to environmental changes by altering which genes they express. The proteome of a micro-organism encompasses these highly complex responses and is therefore an essential tool if we are to understand the role of microbial life in shaping the geochemistry of the Earth, and concurrently, how microbial life responds to chemical changes.

As far as I am aware, this is the first time a label—free proteomics approach has been adopted to investigate microbe – rock interactions in laboratory microcosms. The only similar study which exists is that by Olsson-Francis *et al.*, (2010) [117] which used DNA microarrays to investigate iron uptake from basalt by *Cupriavidus metallidurans* CH34, the same organism adopted in this study. These authors observed an up-regulation of metal efflux genes which they attributed to leaching of toxic trace metals such as copper. The data presented in this chapter does not observe this phenomenon. Indeed, a down-regulation of zinc efflux proteins was observed and correlated with decreased zinc concentrations in the presence of rock as measured by ICP-OES. Whilst Olsson–Francis *et al.*, included trace element concentrations in the rock they failed to publish any elemental changes in the culture media. The observed decrease in phosphorus, zinc and managanese in the experiments discussed in this chapter shows that the influence of rock on growth conditions is complex and not readily predicted by rock compositon. Thus, studies which investigate molecular responses to the presence of rock yet do not conduct detailed chemical analysis of the growth media are limited at best.

However, if we were to speculate on the differences between this study and the

previous microarray study, it is most likely that these differences are attributable to differences in rock geochemistry and subsequent effect on growth media. It is also known that transcriptomics data is typically poorly correlated with protein expression data [149].

In addition to being the first study to use label–free proteomics to investigate microbe–rock interactions, this study has also yielded new insights into the links between extracellular calcium concentrations and regulation of phosphorus homeostasis which should be further investigated.

5.4.3 Future Work

Complete interpretation of these data would be aided by better fundamental understanding of elemental controls on protein expression. It is relatively easy to identify driving factors behind well-characterised responses such as phosphorus uptake. However, the global proteome response to such a stress in this organism is not well-known and likely to involve differential regulation of secondary targets, not directly associated with phosphorus homeostasis. This is particularly complicated in this case as the concentrations of several elements are altered at once. Included in this are some very poorly characterised elements such as magnesium, the effects of which have been the subject of few proteomics studies. Future studies should focus on characterising responses to relevant elements. Additionally, it is unclear how differing concentrations of multiple elements at once will will influence the proteome. This is essential if we are to unravel responses to elemental changes in complex, natural environments.

Whilst gaining more fundamental understanding of elemental controls on protein expression would aid in interpreting laboratory data, proteomics studies of rock-dwelling communities *in situ* would be the most effective way to unravel microbe-rock interactions in the natural environment. This field of metaproteomics is extremely new with the first ever MS-based metaproteomics study conducted in

2005 [215].

5.5 Conclusions

In conclusion, by modifying the ambient pH, releasing elements and sequestering phosphorus, rocks impose upon cells a multiple stress extreme environment that influences cell growth and requires the up and down-regulation of a diverse suite of proteins. The use of label-free quantitative proteomics has helped capture the diversity of this response and highlights the complex array of physiological responses that micro-organisms elicit in response to rock environments. It also demonstrates that a comprehensive understanding of the chemistry of the environment must be coupled with detailed knowledge of microbial nutrient and stress responses, if we are to truly understand the factors that drive the ability of micro-organisms to colonise and actively persist within rock environments. More broadly, this study highlights the need to quantify the subtle complexities of microbial interactions with their environment. This cannot be achieved on a taxa or genome level alone but must also look to the proteome to gain a complete picture of microbial responses to environmental changes.

Chapter 6

Proteome Response to Single and Multiple Nutrient Deficiency

6.1 Introduction

The previous chapter described how rocks can act as an alternative source of nutrients for bacteria. However it also shows that rocks themselves can induce nutrient stress. Nutrient limitation is an important stress in the biosphere and influences processes as diverse as crop yield [216], bioremediation efficiency [113] and ocean primary productivity [118]. Furthermore, rock habitats are typically nutrient limited and thus the micro-organisms rely heavily on the leaching of elements from the rocks themselves [74, 112].

Almost all proteomics studies on nutrient limitation in micro-organisms focus on limitation by a single nutrient [122–124]. This is despite studies showing that, in the natural environment, multiple nutrients are often limiting (See Chapter 2, e.g. [111, 114–116]. In the mathematical modelling community, debate has existed for many years on the most accurate way to represent multiple limiting substrates when modelling microbial nutrient limitation. Some argue that the

effect of multiple limiting substrates will be multiplicative, where the limitation of two elements is worse than the additive effect of each element on growth. Others argue that growth with multiple limiting substrates follows "Liebig's law of the minimum" and only the most limiting nutrient will influence the growth rate. Indeed, to this day, the approach adopted in models of microbial growth is simply related to which side of the debate the researcher falls on. For example, Huisman *et al.,* [217] follow Liebig's law in their model of primary productivity in the oceans and Bethke *et al.,* [218] use multiplicative growth kinetics in their model of microbial zoning in groundwater. Therefore, an experiment which could demonstrate that growth under multiple limiting substrates followed either of these approaches would be very valuable to modelling efforts.

By understanding the cellular response to multiple limiting nutrients we can gain some fresh insight into this problem, as we will be able to observe directly which stresses the organism is responding to, and the relative severity of each element stress. This chapter characterises the changes in the proteome of *C. metallidurans* CH34 (discussed in Chapter 5) in response to dual limitation by iron-phosphorus, iron-magnesium and magnesium-iron, and compares this to the proteome of cells grown under single limitation. These are three key elements for microbial growth and are discussed later in this section.

These experiments reveal the complex influence dual limitation of these elements has on the physiology of microbial cells. In doing so, we gain fresh insight into the old problem of multiple nutrient limitation and expand our understanding of microbial nutrient stress response capabilities in the environment.

The three elements chosen for this study are particularly interesting with regards to their environmental and microbial importance. Below, each element is discussed in turn.

Iron

Iron is the fourth most abundant element in the Earth's crust and is essential for almost all micro-organisms [42, 59]. Many enzymes contain iron in their redox centres making iron a key element in a vast array of metabolic processes such as respiration, DNA synthesis and the synthesis of metabolites [59].
Despite this importance, iron demand is typically higher than available supply in aerobic environments [42]. Indeed, iron is a key limiting nutrient in most of the world's oceans [116, 219, 220]. One of the main reasons for this is that micro-organisms evolved to use iron early in Earth history when the atmosphere was anoxic. The anoxic Earth contained abundant iron in its soluble, reduced Fe^{2+} redox state which can be readily taken up by cells. The atmosphere became oxygenated around 2.4 billion years ago, after which iron was mostly available in its oxidised, insoluble Fe^{3+} state [221].

Phosphorus

Phosphorus is a constituent of key cellular components such as membrane lipids and nucleic acids, making it essential for the fundamental structure of cells. Additionally, phosphorus is required for phosphorylation, one of the primary methods of cell signalling, and for production of ATP, the energy storage molecule of all life [130]. The high requirement for phosphorus combines with low environmental availability to make phosphorus deficiency an important environmental stress [222].
Low terrestrial environmental concentrations of phosphorus are caused, in part, by the reaction of phosphorus with mineral surfaces as observed in the previous chapter. However, phosphorus in terrestrial environments is supplied primarily from rock weathering, and thus phosphorus bioavailability is closely tied to this process [222, 223]. This also means that an environment starts with a fixed complement of phosphorus which is difficult to replace if even small amounts are

lost e.g. from run-off [223]. Phosphorus limitation is also a key factor limiting ocean primary productivity [224–228].

Magnesium

Magnesium stress is less well studied than iron or phosphorus stress. However, magnesium is the second most abundant cation in prokaryotic cells [229] and is essential for numerous key cellular processes such as ATP utilisation, genome stability and maintenance of membranes and ribosomes [60]. Furthermore, an estimated 16% of all microbial enzymes use magnesium as a cofactor [61]. This importance is reflected in experiments in the previous chapter which show complete growth inhibition of *C. metallidurans* when no magnesium is added to the medium.

6.2 Methods

6.2.1 Experimental Overview

This section presents a broad overview of the experimental strategy, before going on to discuss the methods in more detail in the rest of the section. The aim of this chapter is to understand the differences between the microbial response to single and multiple nutrient limitation. First, growth experiments were conducted to identify concentrations of nutrients which limit bacterial growth rate, on their own and in combination with another nutrient. Proteomics analysis was then conducted on sets of experiments consisting of: cells limited by nutrient A only, cells limited by nutrient B only and cells simultaneously limited by nutrients A and B. An overview of the experimental strategy is provided in Figure 6.1

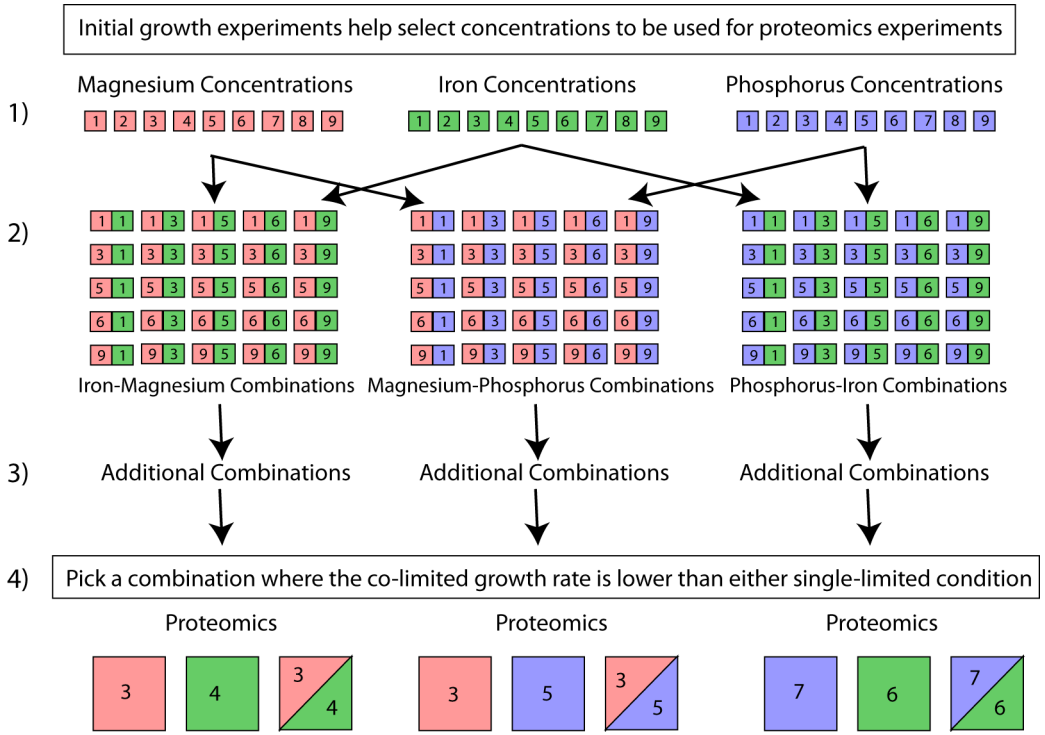

Figure 6.1 Overview of experiments. 1) Growth experiments conducted in which the concentration of magnesium, iron or phosphorus in the growth medium was varied and the subsequent differences in growth measured. 2) Informed from step 1, 5 concentrations were chosen for multiple limitation growth experiments. Selected such that no nutrient was added in the lowest concentration, optimal concentrations were added in the highest concentration, and the three concentrations in between were seen to be limiting in step 1. All possible combinations of concentrations were measured. 3) Some additional combinations tested as step 2 did not identify a concentration in which both elements clearly influenced the growth of the co-limited culture. 4) Proteomics analysis was conducted on three sets of experiments. Each set included: one limited of element A, one limited of element B and one limited of A and B. Numbers are representative and do not represent actual element concentrations used.

Preliminary growth experiments were required because, in order to investigate limitation by combinations of nutrients, it is important to first ensure that the individual nutrient concentrations we are going to test are in fact, limiting. By limiting, I mean that the concentration chosen results in a growth rate that is lower than the growth rate in optimal media. In the optimal media, the concentration of all nutrients is in the "saturated" range i.e. any further increase in nutrient will not result in further increase in growth rate. In order to determine limiting concentration ranges for each element, simple growth experiments were first conducted by testing 9 concentrations of nutrient, for iron, phosphorus and magnesium, ranging from none to the concentration in the optimal media.

For reasons of cost, only one set of experiments for each combination (phosphorus/iron, magnesium/phosphorus or iron/magnesium) could be analysed with proteomics. Therefore, it was decided that priority should be given to combinations of concentrations in which both elements had an influence on growth rate i.e. where the growth rate in the co-limited culture was lower than in either of the single-limited cultures.

A large number of growth experiments had to be run to identify suitable concentrations for each combination. Firstly, five (of the original nine) concentrations of each nutrient tested in the first experiment were chosen for multiple stress growth experiments. Each of the five concentrations of one element were combined with each of the five concentrations of the other element. For example, magnesium concentration 1 was paired with phosphorus 1 and phosphorus 2 and phosphorus 3, and so on, such that all possible combinations were tested. However, these initial experiments did not identify any combination in which the growth rate was lower in the co-limited condition than both of the single limitation conditions.

Additional combinations were tested and, eventually, suitable concentration combinations for proteomics were identified.

For the multiple limitation proteomics experiments three treatments were prepared for each combination: one limited by nutrient A, one limited by nutrient B and one where both nutrients were in the limiting range (the co-limited

treatment). Additionally, cells grown in optimal media were used as a control for all of the experiments. Cells were harvested and the proteome was analysed for each treatment.

In the results section later in this chapter, I present the results of the proteome analysis of the single-limited treatments before presenting the co-limited treatments so as to provide a good base understanding of the effect of each element on the proteome. The single-limitation descriptions are expanded to include comparisons of different severities of phosphorus and iron stress. This is made possible because the concentrations of phosphorus chosen for proteomics analysis for the iron–phosphorus and magnesium–phosphorus combinations were different, thus the phosphorus-limited treatment from the Fe–P set and phosphorus-limited treatment from the P–Mg set can be compared to each other in order to assess the effect of different severities of phosphorus stress on the proteome. Comparison between different severities of iron-limited conditions is also conducted for iron for the same reason.

In each of the sets which included magnesium (iron–magnesium and phosphorus–magnesium), the concentration of magnesium deemed most suitable (i.e. which resulted in a co-limited culture when used in combination with the other element) was the same for both experiments. Therefore, it was not possible to analyse different severities of magnesium stress.

Finally, in the second results section of this chapter, I compare the proteome profile of the co-limited treatment to its corresponding single-limited treatments via a combination of statistical and functional analysis.

6.2.2 Growth Under Single Nutrient Stress

This section describes the methods used for the single nutrient stress growth experiments (Figure 6.1). As discussed in Chapter 3, *C. metallidurans* is routinely cultured in Tris Salts Minimal Medium with 0.2% w/v sodium gluconate [154].

Table 6.1 Concentrations used for single element depletion experiments

Nutrient	**Concentration**								
P	450 μM	225 μM	112 μM	56 μM	28 μM	14 μM	7 μM	3.5 μM	0 μM
Mg	1.97 mM	984 μM	492 μM	246 μM	123 μM	61 μM	31 μM	15 μM	0 μM
Fe	31 μM	15 μM	8 μM	4 μM	2 μM	969 nM	434 nM	242 nM	0 nM

For nutrient stress experiments, medium without added phosphorus, iron or magnesium was used as the base medium. The pH of this base medium was adjusted to pH 7 with 1M NaOH and autoclaved at 121°C for 20 minutes. Thirty millilitres of sterile base medium was added to acid–washed, sterile, polymethylpentene flasks.

Separately, stocks of 2% w/v sodium phosphate dibasic dihydrate, 0.0502% w/v iron (III) chloride and 4% w/v magnesium chloride hexahydrate were filter sterilised. A concentration range was generated by creating a 2-fold dilution series of these stock solutions. These diluted stocks were added to each flask to the concentrations displayed in Table 6.1. The maximum concentrations were: 450 μM $Na_2HPO_4.2H_2O$, 1.97 mM $MgCl_2.6H_2O$ and 31 μM $FeCl_3$. These maximum concentrations are double those suggested for the standard MM284 growth medium to ensure growth rate saturation at the maximum concentration (see Chapter 3).

Before the experiment, cells were rejuvenated from frozen stocks in optimal medium at 30°C and shaken at 90 rpm for 3 days. Thirty microlitres of culture was transferred to fresh medium and grown in the same conditions until cells reached the early stationary phase ($OD_{600nm} > 1.1$, approximately 46 hours), 10 ml of culture was transferred to a fresh tube, centrifuged and re-suspended in the base (no P/Mg/Fe) medium. Thirty microlitres of washed cells were then transferred to each experimental flask (starting cell concentration approximately $1x10^6$ CFU $ml^{-}1$).

Each nutrient concentration was tested in duplicate. This resulted in 72 concurrent experiments. Triplicate experiments were out with the culturing capabilities of the lab as large (mimimum 10 ml) culture volumes were required for proteomics analysis and thus running automated experiments in 96 well microplates was not feasible.

Growth rates were monitored by optical density (absorbance at OD 600 nm) by transfer of 100 μl culture from the culture flasks to a 96 well microplate. The path length (the distance through which the optical density is measured i.e. from the top to the bottom of the liquid) was automatically corrected to 1 cm by the plate reader software.

Growth rates in each experiment were calculated by Timothy Bush (PhD student, School of Physics and Astronomy, University of Edinburgh) by performing a linear regression on the natural logarithm of the average optical density measurements taken in the exponential growth phase.

6.2.3 Growth Under Multiple Nutrient Stresses

Initial Experiments

Growth experiments were conducted to assess the effect of multiple nutrient stress on the growth of *C. metallidurans* and explore the best parameters to use for the proteomics experiments. The nutrient combinations tested were: iron and phosphorus, magnesium and phosphorus, magnesium and iron. Five concentrations for each element were selected for multiple deficiency experiments, based on the results of the single nutrient deficiency experiments and with the aim of sampling growth profiles for each element from no growth to optimal growth rate. Tables 6.2, 6.3 and 6.4 show the combinations of concentrations used in each experiment. For these experiments I have returned to using the element concentration in the original media recipe for iron and magnesium (see Chapter

3) as this concentration was found to be adequate for optimal growth rate in the single-limitation growth experiments. For phosphorus I continued to use double the concentration in the original media recipe.

Table 6.2 Concentration combinations used for magnesium and phosphorus stress experiments. The five different phosphorus concentrations used are listed along the top and labelled P1 to P5. The five different magnesium concentrations used are listed along the side and labelled Mg1 to Mg5. Every possible combination of phosphorus and magnesium concentration was tested. Each cell represents the magnesium and phosphorus concentrations of each of the 25 experiments. None of these combinations yielded results that indicated both nutrients had an effect on growth therefore additonal combinations had to be tested.

		P concentrations				
		P1: 450 μM	P2: 112 μM	P3: 28 μM	P4: 3.5 μM	P5: 0 μM
Mg concentrations	Mg1: 984 μM	Mg1 P1	Mg1 P2	Mg1 P3	Mg1 P4	Mg1 P5
	Mg2: 61 μM	Mg2 P1	Mg2 P2	Mg2 P3	Mg2 P4	Mg2 P5
	Mg3: 15 μM	Mg3 P1	Mg3 P2	Mg3 P3	Mg3 P4	Mg3 P5
	Mg4: 7.7 μM	Mg4 P1	Mg4 P2	Mg4 P3	Mg4 P4	Mg4 P5
	Mg5: 0 μM	Mg5 P1	Mg5 P2	Mg5 P3	Mg5 P4	Mg5 P5

Table 6.3 Concentration combinations used for iron and phosphorus stress experiments. The five different phosphorus concentrations used are listed along the top and labelled P1 to P5. The five different iron concentrations used are listed along the side and labelled Fe1 to Fe5. Every possible combination of phosphorus and iron concentration was tested. Each cell represents the iron and phosphorus concentrations of each of the 25 experiments. None of these combinations yielded results that indicated both nutrients had an effect on growth therefore additonal combinations had to be tested.

		P concentrations				
		P1: 450 μM	P2: 112 μM	P3: 28 μM	P4: 3.5 μM	P5: 0 μM
Fe concentration	Fe1: 15 μM	Fe1 P1	Fe1 P2	Fe1 P3	Fe1 P4	Fe1 P5
	Fe2: 2 μM	Fe2 P1	Fe2 P2	Fe2 P3	Fe2 P4	Fe2 P5
	Fe3: 242 nM	Fe3 P1	Fe3 P2	Fe3 P3	Fe3 P4	Fe3 P5
	Fe4: 121 nM	Fe4 P1	Fe4 P2	Fe4 P3	Fe4 P4	Fe4 P5
	Fe5: 0 nM	Fe5 P1	Fe5 P2	Fe5 P3	Fe5 P4	Fe5 P5

Table 6.4 Concentration combinations used for iron and magnesium stress experiments. The five different iron concentrations used are listed along the top and labelled Fe1 to Fe5. The five different magnesium concentrations used are listed along the side and labelled Mg1 to Mg5. Every possible combination of magnesium and iron concentration was tested. Each cell represents the magnesium and iron concentrations of each of the 25 experiments. None of these combinations yielded results that indicated both nutrients had an effect on growth therefore additonal combinations had to be tested.

	Fe concentrations					
	Fe1: 15 μM	Fe2: 2 μM	Fe3: 242 nM	Fe4: 121 nM	Fe5: 0 nM	
Mg concentrations	Mg1: 984 μM	Mg1 Fe1	Mg1 Fe2	Mg1 Fe3	Mg1 Fe4	Mg1 Fe5
	Mg2: 61 μM	Mg2 Fe1	Mg2 Fe2	Mg2 Fe3	Mg2 Fe4	Mg2 Fe5
	Mg3: 15 μM	Mg3 Fe1	Mg3 Fe2	Mg3 Fe3	Mg3 Fe4	Mg3 Fe5
	Mg4: 7.7 μM	Mg4 Fe1	Mg4 Fe2	Mg4 Fe3	Mg4 Fe4	Mg4 Fe5
	Mg4: 0 μM	Mg5 Fe1	Mg5 Fe2	Mg5 Fe3	Mg5 Fe4	Mg5 Fe5

Additional Concentrations

Despite testing a large number of concentrations, these initial experiments did not yield any combinations where low levels of two nutrients reduced the growth-rate more than low levels of one nutrient alone, as was required for proteomics analysis. The was true for all of the co-limiting conditions tested (ie. Fe-Mg, P-Mg or Fe-P). Therefore, a small number of additional combinations were tested separately to attempt to find combinations where both elements had an effect on the growth rate. The additional concentrations for iron and phosphorus are listed in Table 6.5. Additional concentrations for iron and magnesium are listed in Table 6.6. Additional concentrations for magnesium and phosphorus are listed in Table 6.7.

Based on these additional experiments, one combination was selected for proteomics analysis. These were: 56 μM phosphorus and 15 μM magnesium, 434 nM iron and 15 μM magnesium, 969 nM iron and 112 μM phosphorus.

Table 6.5 Additional iron and phosphorus combinations tested for multiple element stress experiments. Concentrations of all other elements was optimal.

P	Fe
450 μM	969 nM
225 μM	969 nM
112 μM	969 nM
56 μM	969 nM
450 μM	434 nM
225 μM	434 nM
112 μM	434 nM
56 μM	434 nM

Table 6.6 Additional iron and magnesium combinations used for multiple element stress experiments. Concentrations of all other elements was optimal.

Fe	Mg
61 μM	969 nM
15 μM	969 nM
61 μM	434 nM
15 μM	434 nM

Table 6.7 Additional phosphorus and magnesium combinations used for multiple element stress experiments. Concentrations of all other elements was optimal.

P	Mg
225 μM	984 μM
225 μM	61 μM
225 μM	15 μM
56 μM	984 μM
56 μM	61 μM
56 μM	15 μM

6.2.4 Protein Expression

Culturing and Cell Harvest

Protein abundances were determined for cells grown under different single and multiple nutrient stress conditions. Three experiments were conducted for each set of elements: low concentrations of each of the two elements separately (e.g iron alone; phosphorus alone) and deficiency of both elements simultaneously (e.g. low concentrations of both iron and phosphorus). Concentrations were chosen for proteomics based on the results of the additional growth experiments to select the condition where the co-limited culture had less growth than either single limited culture. Each experiment was prepared as before (Section 2.1) and treatments were tested in triplicate. Growth was monitored by optical density. When cultures reached mid-exponential phase, 5 ml culture was transferred to a 15 ml falcon tube and centrifuged. The supernatant was discarded and the cell pellet frozen at –80°C. Cells were not washed as there is no interference of the medium with the protein analysis and this allows minimal disruption to the cells. As the same concentration of magnesium was used in both the P–Mg and Fe–Mg sets, the same low magnesium–only triplicate was used as the "low magnesium" condition in both sets (see Figure 6.1).

Protein Extraction and Peptide Digest

To extract proteins, 200 μl 8M filter sterilised Urea was added to the cell pellet and left for 1 hour with regular vortexing and sonicating until particulate material was dissolved. Protein concentration was measured by Bradford assay [199]. One hundred micrograms of protein was transferred from each sample to a fresh tube for protease digestion. This was made up to 250 μl with 8 M Urea. Twenty five microlitres of 1M ammonium bicarbonate and 25 μl DTT were added and the solution left to stand for 30 minutes. Twenty five microlitres 500 mM

iodoacetamide and 670 μl H_2O was then added. Five micrograms (5 μl of 1 μg μl^{-1}) trypsin was added and the digest left to stand overnight.
Peptides were purified using Bond Elut C18 columns (Agilent, UK). Purified peptides were vacuum dried and stored at –20°C until analysis.

Mass Spectrometry

Peptides were analysed, as in Chapter 5, on a reverse phase microcolumn using a 140 minute gradient (controlled by a binary HPLC system 1200, Agilent, UK) coupled to a hybrid LTQ-Orbitrap XL mass spectrometer (Thermo-Fisher, UK) in data dependent mode, controlled through Xcalibur 2.0.7 software. Eight microliters of sample in loading buffer was injected.

Data Analysis

Peak picking and quantification were performed using Progenesis LC-MS (version 4.0, Nonlinear Dynamics, UK). Peptides (charges 2^+, 3^+ and 4^+) were identified by MASCOT (Matrix sciences, UK, version 2.3) searches of MS/MS data against the NCBI protein database subset [169] for *Cupriavidus metallidurans* (6766 sequences), using a trypsin/p enzyme restriction with a maximum missed-cut value of 2. Variable methionine oxidation and fixed cysteine carbamidomethylation were used in all searches.
Progenesis LC–MS normalisation used in the previous chapter was found to be inadequate and a more stringent manual normalisation was conducted. Each raw protein intensity was multiplied by 1 x 10^8 and divided by the sum of the total raw protein intensities. P-values on fold changes between experimental condition and control were determined by one-way ANOVA on arcsinh-transformed protein intensities. The arcsinh transformation is not linear at the low original abundances hence the multiplication of all raw intensities by 1 x 10^8. Differentially expressed proteins were considered significant with an average

intensity ratio of at least two-fold and a P-value less than 0.05 if detected with two or more peptides per protein with a MASCOT identification score greater than 20.

Comparison of protein profiles

A Bray-Curtis similarity matrix (see Chapter 3) based on the protein expression data was analysed using the PRIMER statistical package (version 6.1.13) with the PERMANOVA+ add-on (version 1.0.3) [200, 201] by Dr. J. Harrison. Following non-metric multidimensional scaling ordination, post-hoc pairwise comparisons were performed by 2-way nested permutational analysis of variance (PERMANOVA; [171]) with "type of deficiency" as the factor. P values were derived by a Monte Carlo approach due to low numbers of permutations [201].

Functional annotation

Once identification and quantification has been conducted and differentially regulated proteins highlighted, the biological function of proteins can then be identified. Annotation of function, and hence identification of important cellular responses, relies on previous annotation efforts from other authors. Protein functions in this thesis were primarily assigned using expert manual annotation of the *C. metallidurans* CH34 genome, available on the MaGe platform [172]. This database contains information on the protein name, description and protein functions.

This chapter relies heavily on the hierarchical approach to functional annotation adopted by the authors of the MaGe database [172]. In their annotation, specific processes are nested under high level processes e.g the high-level "Cellular process" group contains numerous sub-functions such as motility and adaptation to stress. Table 6.8 lists the high-level biological functions used in this chapter and gives examples of sub-functions contained within them.

Table 6.8 Groups of biological functions assigned to each protein and examples of sub-functions contained within that group

Functional group	**Sub-functions**
Amino acid biosynthesis and metabolism	synthesis, catabolism, degradation and utilization of amino acids
Purine, pyrimidines, nucleosides and nucleotides	proteins involved in synthesis of ribonucleotides, nulceotide and nucleoside salvage and interconversions, sugar-nucleotide synthesis and conversion
Fatty acid and phospholipid metabolism	biosynthesis and degradation of fatty acids and phospholipids
Biosynthesis of cofactors, prosthetic groups and carriers	biosynthesis of e.g. biotin, folic acid, heme, molybdopterin, glutathione or siderophores
Central intermediary metabolism	metabolism of phosphorus compounds, sulfur and nitrogen, one-carbon metabolism, electron carrier regeneration, nitrogen fixation
Energy metabolism	aerobic/anaerobic respiration, electron transport, glycolysis/gluconeogenesis, TCA cycle, synthesis and degradation of polysaccharides, pentose phosphate pathway, Entner-Doudoroff pathway
Transport and binding proteins	proteins which transport any substance across the membrane e.g cations, amino acids, peptides, carbohydrates etc
DNA metabolism	DNA replication, recombination, repair, degradation and chromosome-associated proteins
Transcription	degradation of RNA, DNA-dependent RNA polymerase, transcription factors and RNA processing
Protein synthesis	tRNA aminoacylation, ribosomal proteins, translation factors, tRNA/rRNA base modifications
Protein fate	protein/peptide secretion, trafficking and degradation; protein modification, repair, folding and stabilisation
Regulation	regulation of gene expression at transcription-, post-transcriptional- or DNA-level
Signal transduction	proteins which translate extracellular signal to cell response, e.g two-component systems
Cell envelope	surface structures, biosynthesis and degradation of peptidoglycan, polysaccharides and lipopolysaccharides
Cellular processes	cell division, motility, detoxification, adhesion, adaptation to stress
Biological process	construction of biomass, control, energy management, replication, respiration, scavenging, shape, storage
Mobile and extrachromosomal element functions	plasmid, prophage or transposon functions
Unassigned	function unknown

For ease of representation, high level functional associations are used for the plots used in this chapter and further detail provided in the text. In the MaGe database, 2 lines of evidence can be used to assign function: biological function and role. The biological function and role of a protein in a cell are manually assigned by the authors of the MaGe project based on both experimental evidence and similarity to genes with known functions in other organisms.
Here the biological function is presented where available. If no biological function is available I have assigned it to a functional category based on the available role assignment. These are assigned manually by the person annotating the genome and, at the high levels, are very similar. The functional role assignments are typically more specific than the biological function assignments. Proteins missing all of this information are categorised as "Unassigned".

6.3 Results: Proteome Changes Under Single Nutrient Stress

Before understanding how dual limitation influences the proteome, we must first characterise the effects of each element individually. In this section I separately discuss the response of *C. metallidurans* CH34 to iron, phosphorus and magnesium stress. For each element, I first provide a brief overview of the capabilities *C. metallidurans* CH34 is known to possess to cope with this stress, in order to predict what we might expect to observe. The changes in growth which occur as a result of varying concentrations of the element of interest is then shown. I then outline the differences in the proteome between limited and non-limited cells. For iron and phosphorus, two different concentrations were tested which also allows comparison of the proteome at two different severities of iron or phosphorus limitation.
These results form the basis of the analysis in the next section where I will then

compare the proteome of cells grown under dual limitation to the proteome of cells grown under single limitation. Full lists of proteins differentially regulated under each condition can be found in Appendix B.

6.3.1 Response to Iron Stress

Known Capabilities for Response to Iron Stress

Iron exists in a huge variety of mineral forms in nature but it is taken up directly in two forms: Fe^{2+} ions or heme. Heme is an organic compound, consisting of an Fe^{2+} ion in the centre of a porphyrin ring. In cells, heme is typically contained within hemoproteins. The most well-known hemoprotein is hemoglobin which is what forms the red pigment in blood. In micro-organisms, heme proteins are typically associated with redox enzymes such as cytochromes. Fe^{3+} is highly insoluble at circum-neutral pH and can only be taken up into cells after being bound to organic compounds called siderophores (discussed below).
C. metallidurans CH34 has a number of tools for coping with iron stress which have been elucidated from the genome sequence [172]:

1) Production of siderophores The *C. metallidurans* genome contains a set of genes for synthesis and uptake of siderophores. These are small iron-binding molecules, secreted by bacteria, to bind insoluble Fe^{3+} and allow uptake into the cell. *C. metallidurans* produces an uncommon siderophore, staphyloferrin B, that was first identified in this organism [230].

2) Uptake of Fe^{2+} and heme This organism also possesses genes for the uptake of Fe^{2+} and heme [172]. The heme uptake proteins utilise free heme from the extracellular environment which is released when dead cells degrade [231, 232].

3) Regulation by Fur Expression of the siderophore and iron uptake response

is tightly regulated by the Fur (ferric uptake regulation) protein. This is a "negative transcription factor regulator". When iron concentrations are high, the Fur protein is expressed and represses transcription of genes for siderophore production. When iron concentrations are low, Fur is not expressed and siderophore production proceeds [172, 230]. In bacteria, Fur regulation of siderophore synthesis is common and the protein may also be involved in wider regulation in the cell [59, 233].

Based on the known capabilities of *C. metallidurans* CH34 with regards to responses to iron stress, it could be expected that abundance of siderophores and iron transporters would increase in response to low iron conditions and that this will be Fur–regulated. Decreased abundance of Fur proteins would be expected at low iron.

Growth Response to Variations in Iron Concentration

Figure 6.2 shows the growth curves for *C. metallidurans* with different concentrations of iron ($FeCl_3$). This shows that growth limitation does not occur at iron concentrations above 969 nM. Even when no iron is added, some growth is still observed. This is consistent with observations in the previous chapter which showed some growth in medium with no iron added, or detected by ICP-OES.

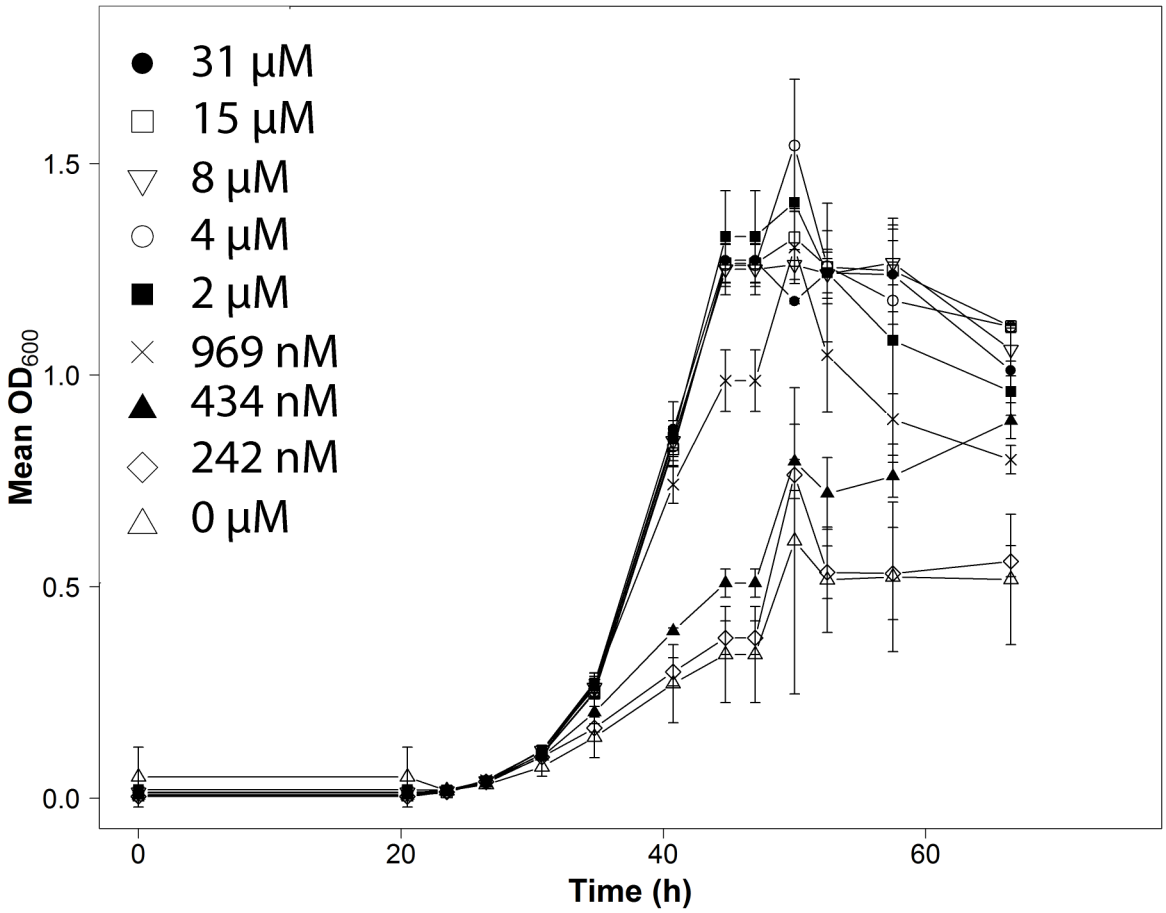

Figure 6.2 Growth of *C. metallidurans* CH34 with varying concentrations of iron

Protein Expression Under Iron Stress

Proteome changes in response to two different severities of iron stress were investigated: 969 nM and 434 nM. This section compares the protein abundances in each of these two iron-limited concentrations to the protein abundances in cells grown with optimal iron (15 μM). For simplicity, the 969 nM iron condition will be subsequently referred to as "low iron" and the 434 nM iron condition as "lowest iron".

Each condition had a similar number of up-regulated proteins: 68 for "low iron", 74 for "lowest iron". However, the "lowest iron" condition had more down-

regulated proteins: 103 compared to 68 for "low iron". Forty-three proteins were up-regulated in both conditions and forty-one down-regulated in both conditions, relative to the control.

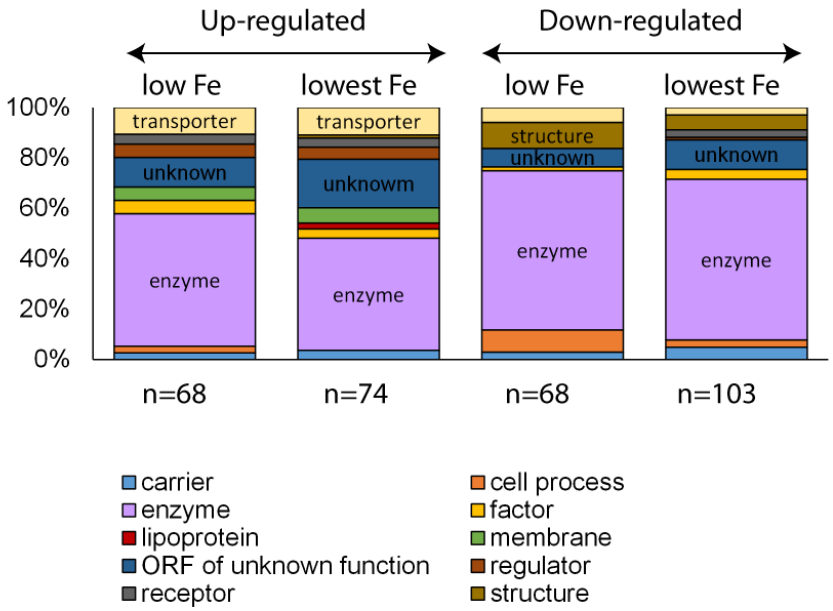

Figure 6.3 Type of proteins differentially regulated under "low" and "lowest" iron concentrations reveals coarse grain changes in abundance of transporters and cell structures under both severities of iron limitation. See Chapter 3 for description of classes.

Figure 6.3 shows the types of proteins which are differentially regulated in each condition. In addition to differential regulation of numerous enzymes in both conditions, an up-regulation of transporters and down-regulation of structural proteins is observed to be a key feature of this type of limitation. Despite different numbers of differentially regulated proteins, the proportion of each type of protein is very similar in both conditions. Descriptions of each type class can be found in Chapter 3.

Figure 6.4 Biological functions of proteins differentially regulated in the "low iron" and "lowest iron" conditions showing up-regulation of transport proteins and cofactor/carrier proteins. Transport proteins, protein synthesis, energy metabolism and cellular processes are down-regulated in "low" and "lowest" iron conditions.

Figure 6.4 shows the biological functions of proteins up- and down-regulated in both iron concentrations. A group of proteins classified to be involved in the "biosynthesis of cofactors, prosthetic groups and carriers" are up-regulated in both conditions as are proteins involved in "transport". Within these groups are proteins for siderophore synthesis, siderophore uptake, heme uptake and Fe^{2+} transport. One Fur-like ferric uptake regulator is also up-regulated.

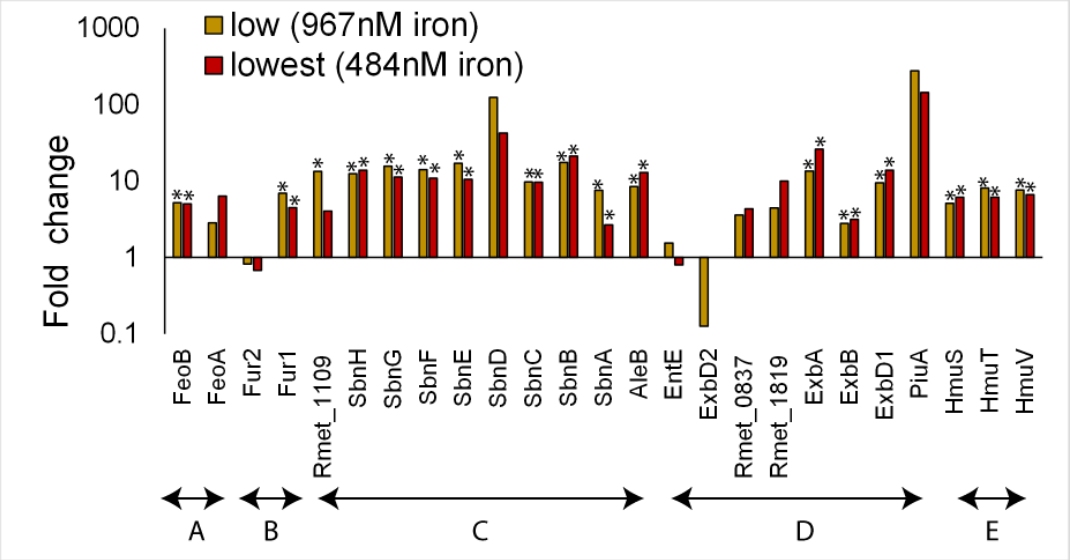

Figure 6.5 Fold change of siderophore synthesis/uptake and iron uptake proteins in "low iron" and "lowest iron" conditions. A) Fe^{2+} uptake. B) Regulation. C) Siderophore synthesis. D) Siderophore uptake. E) Heme uptake. * indicates proteins which meet strict significance criteria outlined in Chapter 3 and can be considered differentially regulated compared to the optimal control cultures. Fold change greater than 1 is up-regulated, less than 1 is down-regulated.

Fold change of proteins known to be associated with iron uptake are shown in Figure 6.5. This emphasises that the typical iron uptake response (increase in siderophore synthesis/uptake, Fe^{2+} uptake and heme uptake) has been induced in both conditions. Siderophore synthesis proteins are slightly more abundant in "low iron" conditions than in "lowest iron". However, SbnA is the only protein which would meet the criteria for significant up-regulation in "low iron" compared to "lowest iron" (2.8 fold higher at "low iron" compared to "lowest iron", $P = 0.018$). Therefore, expression of proteins for iron uptake is not higher at the

"lowest iron" concentration compared to "low iron" as might be expected.

Compared to the control, 68 proteins were down-regulated in the "low iron" concentration whereas 103 were down-regulated in the "lowest iron" condition. Forty-one of these down-regulated proteins are common to both of the conditions. The largest commonly down-regulated functional groups are associated with transport and energy metabolism (Figure 6.4). Most of these are iron–binding enzymes involved in electron transport and are listed in Table 6.9. The "lowest iron" condition contains an additional 14 down-regulated iron-binding proteins which are not down-regulated in the "low iron" condition (Table 6.10).

Table 6.9 Iron-containing enzymes down–regulated under both severities of iron deficiency

			"Low Iron"		"Lowest Iron"	
Locus Tag	Protein	Description	Fold change	P-value	Fold change	P-value
Rmet_0117	BioB	Biotin synthase	0.2	8.30E-07	0.13	9.60E-06
Rmet_0162	ThiC	Thiamin biosynthesis protein	0.4	7.80E-04	0.31	2.20E-03
Rmet_0367		Putative Fe-S oxidoreductase FAD/FMN-containing dehydrogenase oxidoreductase protein	0.49	2.60E-03	0.35	1.50E-03
Rmet_0928	NuoB	NADH dehydrogenase chain B	0.41	4.70E-02	0.17	2.40E-03
Rmet_0932	NuoF	NADH:ubiquinone oxidoreductase, chain F	0.39	1.30E-02	0.32	1.50E-03
Rmet_0933	NuoG	NADH dehydrogenase chain G	0.46	3.00E-04	0.38	3.10E-05
Rmet_0987		Cytochrome c, class IC 1	0.29	2.70E-03	0.13	1.30E-04
Rmet_0988		Cytochrome c553	0.29	3.90E-02	0.16	1.70E-02
Rmet_1087	AccA	Acetyl-CoA carboxylase, carboxytransferase, alpha subunit	0.34	1.30E-03	0.40	1.40E-03
Rmet_1522	HoxF	NAD-reducing hydrogenase diaphorase moiety large subunit	0.37	2.70E-02	0.25	2.10E-03
Rmet_2041	CcoP	Cbb3-type cytochrome oxidase, diheme subunit IV	0.43	2.20E-02	0.25	1.80E-04
Rmet_2043	CcoO	Cbb3-type cytochrome oxidase, monoheme subunit II	0.4	2.50E-02	0.21	2.50E-04
Rmet_2106	IspG	1-hydroxy-2-methyl-2-(E)-butenyl 4-diphosphate synthase	0.3	1.40E-03	0.26	1.50E-03
Rmet_2815	CysO	Protein involved in cysteine metabolism	0.24	1.10E-02	0.20	5.20E-03
Rmet_2868	IspH	1-hydroxy-2-methyl-2-(E)-butenyl 4-diphosphate reductase, 4Fe-4S protein	0.2	3.20E-04	0.11	5.60E-05
Rmet_3226	SspB	Protease specificity-enhancing factor	0.48	2.20E-02	0.39	7.10E-05
Rmet_3230	PetA	Ubiquinol-cytochrome c reductase, iron-sulfur subunit (Rieske Fe-S protein)	0.49	6.70E-04	0.39	1.30E-03
Rmet_3321		Dienelactone hydrolase	0.41	1.70E-02	0.29	5.60E-04
Rmet_3424		Cytochrome c551/c552 h16_A3570	0.36	8.00E-03	0.26	6.60E-04
Rmet_6339		Conserved barrel domain protein	0.40	1.70E-03	0.24	4.00E-04

Table 6.10 Iron-containing enzymes down–regulated only in the "lowest iron" condition

Locus Tag	Protein	Description	Fold change	P-value
Rmet_0061	LipA	Lipoate synthase	0.45	6.7E-03
Rmet_0931	NuoE	NADH dehydrogenase chain E	0.21	5.0E-03
Rmet_1146	EtfD	Electron transfer flavoprotein-ubiquinone oxidoreductase	0.43	4.0E-05
Rmet_1206	YkgE	Putative hydroxyacid oxidoreductase (Fe-S centre)	0.09	6.4E-03
Rmet_1297	HoxG	HoxG hydrogenase 1, large subunit	0.37	7.9E-05
Rmet_1524	HoxY	NAD-reducing hydrogenase delta subunit	0.47	2.3E-02
Rmet_2475	LeuC	3-isopropylmalate isomerase subunit, dehydratase component	0.36	2.1E-04
Rmet_2483	SdhB	Succinate dehydrogenase, FeS subunit	0.43	1.3E-03
Rmet_2747	HemY	Uncharacterized enzyme of heme biosynthesis	0.10	1.4E-04
Rmet_3228	PetC	Cytochrome c1 precursor (transmembrane protein)	0.48	2.2E-04
Rmet_3284		Cytochrome c4	0.35	6.5E-03
Rmet_3419	SoxX	Sulfur oxidation protein	0.19	6.1E-03
Rmet_3420	SoxA	Sulfur oxidation protein	0.50	2.5E-03
Rmet_4943		Putative iron-containing alcohol dehydrogenase	0.47	2.8E-02

Summary and Interpretation of Iron Stress Response

Three main observations about the response of *C. metallidurans* to iron stress have been highlighted in these experiments:

1) Up-regulation of iron uptake proteins Firstly, the comparison of two severities of iron deficiency indicate that induction of siderophore synthesis and uptake, heme uptake and Fe^{2+} uptake occurs at both of the iron concentrations tested ("lowest iron" = 434 nM, "low iron" = 969 nM). However, the abundance of these proteins was slightly higher in the "low iron" condition (Figure 6.5), despite a lower growth rate at the "lowest iron" (Figure 6.2). This suggests that, below 969 nM, the siderophore/iron uptake response has reached a maximum abundance and cannot be further up-regulated in response to reduced iron availability. Indeed, the "lowest iron" condition had slightly less siderophore proteins. Although the difference

in abundance in not significantly higher in the "low iron" conditions, this small difference between the "low" and "lowest" iron condition could be a result of a general lack of energy available to form siderophores at the "lowest iron".

2) Induction of an iron-sparing response If it is the case that the iron uptake response cannot be further up-regulated to respond to lower concentrations of iron, an alternative response is required. The results presented here show decreased abundance of iron-containing enzymes in response to iron stress. These are mostly related to electron transport and energy metabolism. Furthermore, the "lowest iron" condition shows down-regulation of an additional fourteen iron-binding proteins which are not differentially regulated in the "low iron" condition. This suggests that there may be a hierarchical down-regulation of iron-binding enzymes depending on the severity of iron stress. This iron sparing response is typical of that described for *E. coli* and *Bacillus subtilis* where small regulatory RNAs (controlled by Fur) enhance degradation of iron-containing proteins [234] in response to iron stress. Together these results suggest iron-sparing can be increased in response to increasing severity of iron deficiency even if iron uptake cannot. The mechanisms which facilitate iron-sparing in this organism should be further investigated.

3) Suggestion of opposite roles for different Fur proteins Two copies of the *fur* (ferric uptake regulator) gene exist in the *C. metallidurans* genome, annotated as *fur1* and *fur2*. These results strongly suggest the two copies of this gene have different functions (Figure 6.5). Expression of Fur2 is consistent with a typical ferric uptake regulator (decreased expression as siderophore expression is increased). However, Fur1 shows increased expression at low iron. This suggests that Fur2 acts as a typical negative regulator of siderophore synthesis and Fur1 may have a positive role in siderophore regulation. This information could be used to update the

genome information for these genes.

The proteins up-regulated in response to iron stress are consistent with the known capabilities of *C. metallidurans* CH34 discussed at the beginning of this section. However, the down-regulation of numerous iron-binding enzymes in response to iron-limitation has not been predicted for this organism before. The down-regulation of iron-binding proteins is consistent with mechanisms of "iron-sparing" only reported in other organisms e.g. *B. subtilis* [234].

6.3.2 Response to Phosphorus Stress

Known Capabilities for Response to Phosphorus Stress

The response of the *C. metallidurans* proteome to phosphorus deficiency has not been tested. However, the genome of the organism is very well understood. By understanding the genes possessed by this organism to tolerate phosphorus stress, we can predict what we might expect to happen to the proteome under phosphorus limitation [172]. The genome study suggests that *C. metallidurans* has the capability to uptake phosphorus in diverse forms. Phosphates (PO_4^{3-}) are used directly in cellular processes and are taken up via the phosphate specific transport system (*pstSCAB-phoU*). Alternatively *C. metallidurans* can uptake and degrade organo–phosphonate compounds via the *phn* system. Organo–phosphonates are a diverse group of organic compounds which contain a C-P bond. *C. metallidurans* can also oxidise reduced phosphite compounds to phosphate, the latter of which is used as a phosphorus source. This is done via the *ptxABCDE* genes [235].

The alkaline phosphatase genes *phoA1, phoA2* and *phoD* are also present in the genome. These remove phosphate groups from molecules and can aid in intracellular phosphate scavenging and enabling access to the extracellular dissolved organic phosphorus pool [236]. These are often observed to be up-

regulated under phosphorus stress [130].

In this organism, as in more well-characterised organisms such as *E.coli* [130], extracellular phosphate concentrations are sensed by a two-component regulator consisting of components PhoB and PhoR. PhoR is an inner membrane histidine kinase and PhoB is a DNA-binding response regulator [141]. When PhoR senses low phosphorus, it phosphorylates (adds a phosphate, PO_4^{3-}, group to) PhoB. When PhoB is phosphorylated, genes related to uptake and metabolism of various phosphorus compounds are transcribed. At high phosphorus concentrations, PhoR controls the activity of PhoB by prevention of phosphorylation (inhibition) or dephosphorylation of Phospho–PhoB (deactivation) [130].

Growth Response to Variations in Phosphorus Concentrations

Figure 6.6 shows the growth curves for *C. metallidurans* grown with different concentrations of phosphorus ($Na_2HPO_4.2H_2O$). These experiments achieved good coverage of different growth ranges from maximal to almost zero at the lowest phosphorus concentration.

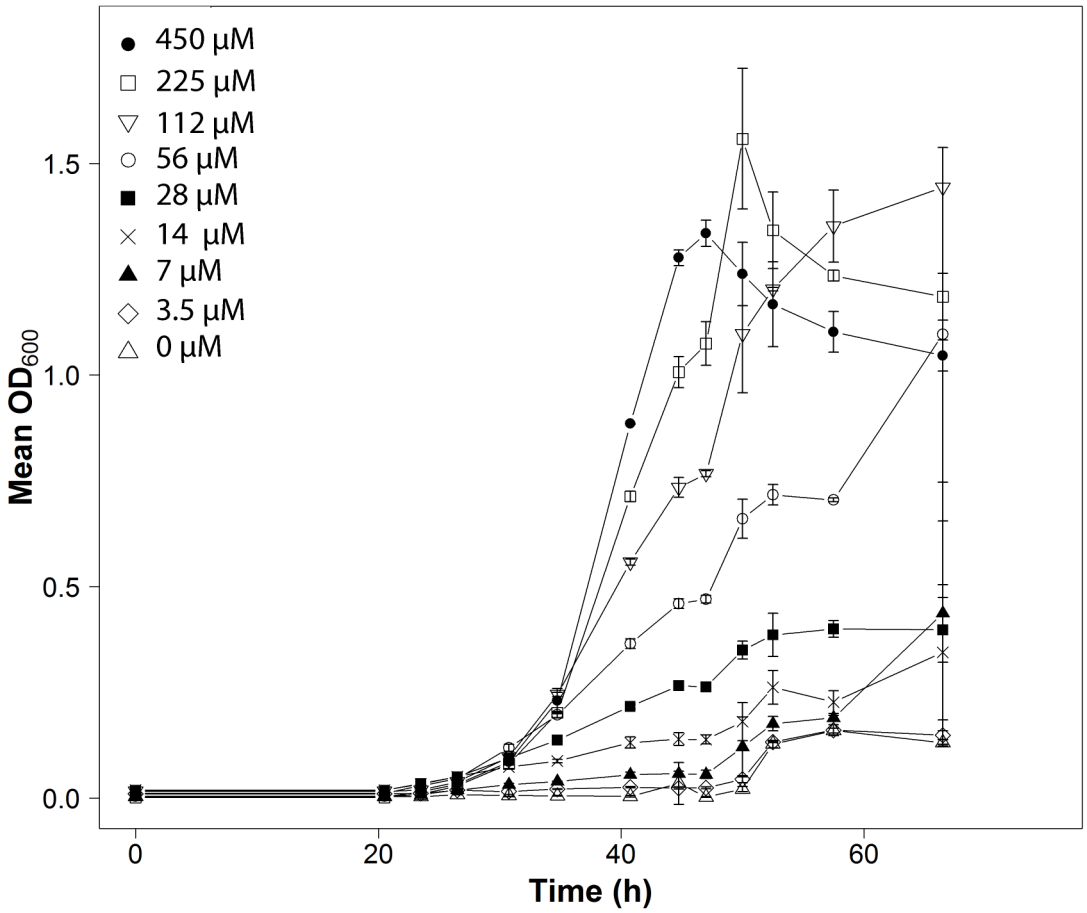

Figure 6.6 Growth of *C. metallidurans* CH34 with varying concentrations of phosphorus

Protein Expression Under Phosphorus Stress

The two phosphorus concentrations tested were 56 μM and 112 μM. This section compares the protein abundances of these two concentrations to the protein abundances of cells grown under phosphorus replete conditions (450 μM). For simplicity, the 112 μM condition will be subsequently referred to as "low phosphorus" and the 56 μM phosphorus condition as "lowest phosphorus".

Compared to the phosphorus-replete control, cells grown in the "low phosphorus" condition had 115 up-regulated and 86 down-regulated proteins whilst cells grown in the "lowest phosphorus" condition had 165 up-regulated proteins and

209 down-regulated proteins. Many of the proteins differentially regulated are common to both phosphorus-limited conditions. This includes ninety-one proteins up-regulated across both conditions and 61 down-regulated in both conditions.

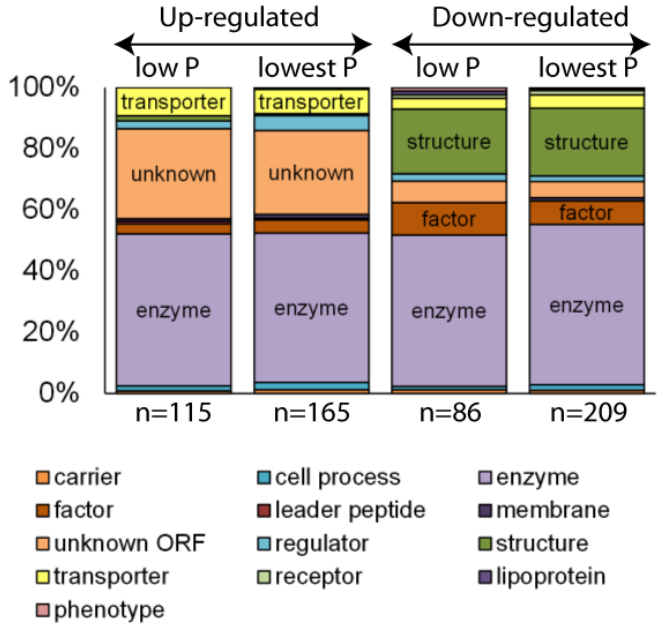

Figure 6.7 Types of proteins up- or down-regulated under "low" or "lowest" phosphorus concentrations

Overall patterns in the types of proteins differentially expressed is shown in Figure 6.7. The profiles of each phosphorus deficient condition are very similar despite different absolute protein numbers. Both show a high proportion of enzymes and unknown products. Transporters form the third largest group of up-regulated proteins (9% of "low" phosphorus and 8% of "lowest" phosphorus). Structural components and factors comprise a large proportion of the down-regulated response.

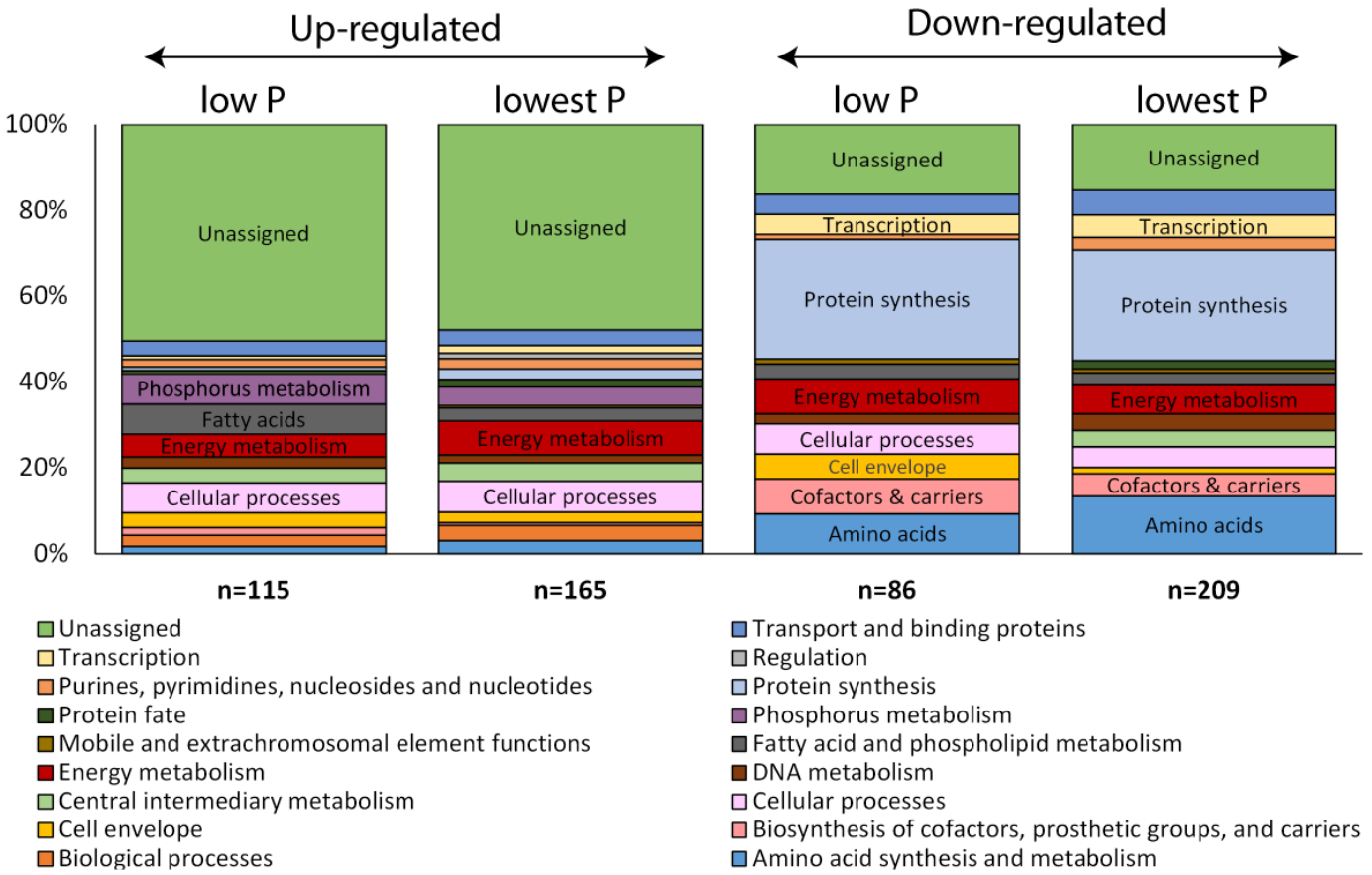

Figure 6.8 Functions of proteins up- and down-regulated in the "low phosphorus" and "lowest phosphorus" conditions. Very similar proteome profiles characterise both conditions however the "lowest phosphorus" condition has more differentially regulated proteins. Both conditions show an up-regulation of proteins for phosphorus metabolism, cellular processes and fatty acid/phospholiipid metabolism. Down-regulation of proteins for protein synthesis, transcription, energy metabolism, synthesis of cofactors/carriers/prosthetic groups and synthesis of amino acids are down-regulated.

Figure 6.8 displays the functions of proteins up/down-regulated at both phosphorus concentrations. This plot displays that a diverse array of protein functions were changed in response to phosphorus limitation in both conditions. Key features of this response are:

1) Up-regulation of phosphorus metabolism: The "Phosphorus metabolism" functional group contains proteins which facilitate transport of phosphates and phosphonate from the extracellular environment into the cell. The fold change of all detected phosphorus-related proteins in each condition is shown in Figure 6.9.

2) Up-regulation of oxidative stress responses: Proteins from the "cellular processes" function are observed in both up- and down-regulated groups. The up-regulated cellular process proteins are associated with stress responses. Four of these proteins are associated specifically with oxidative stress. Oxidative stress occurs when there are more reactive oxygen species (e.g. hydrogen peroxide) than the cell can adequately detoxify, ultimately disrupting the redox balance in the cell. Up-regulated proteins include KatA and KatG oxidative stress response proteins, and two proteins associated with glutathione metabolism (Gst and GshB). Glutathione is involved in detoxification during oxidative stress.

3) Down-regulation of protein synthesis: In the "low phosphorus" conditions, 24 proteins associated with protein synthesis were down-regulated and in the "lowest phosphorus", 54 were down-regulated. Nineteen of these were common to both conditions. This shows that down-regulation of protein synthesis is a key feature of phosphorus deficiency. Many of the proteins in this group are structural components of ribosomes, the protein-making machines of the cell.

4) Down-regulation of biosynthesis and energy functions: Down-regulation of proteins for synthesis of various biomolecules is particularly strong

in the "lowest phosphorus" conditions. Down-regulated is observed in proteins for: amino acid synthesis and metabolism (28), energy metabolism (14), transcription (11), biosynthesis of cofactors, prosthetic groups and carriers (11), and proteins for cell division (3). This is characteristic of an extreme shut down of high energy consuming processes in the most severe phosphorus-limiting condition such that, in simple terms, the cell makes less and uses less energy.

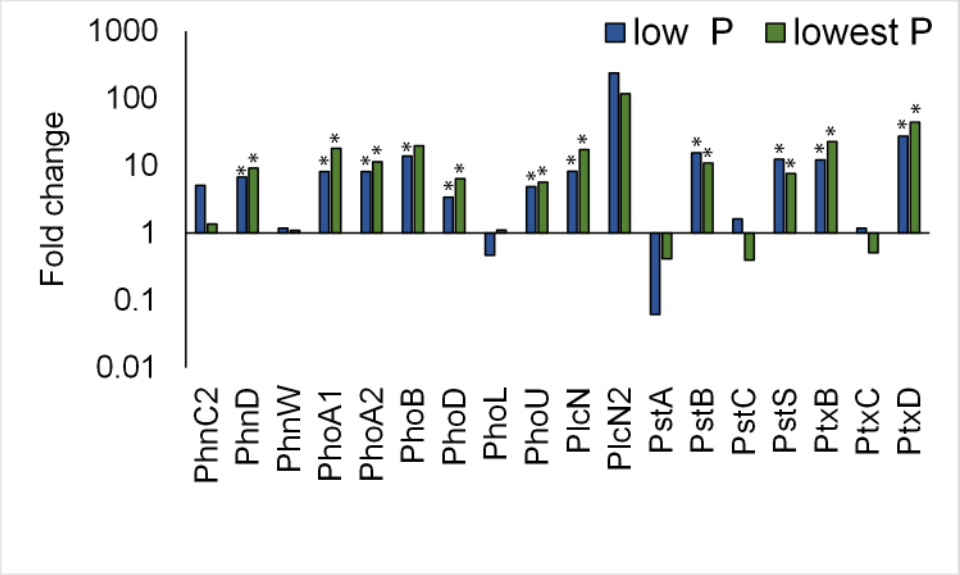

Figure 6.9 Fold change of known phosphorus–regulated proteins in cultures grown in "low phosphorus" and "lowest phosphorus" compared to cultures grown in optimal medium. Fold change greater than 1 is up-regulated, less than 1 is down-regulated.

Summary and Interpretation of Phosphorus Stress Response

The proteins differentially regulated under phosphorus stress are consistent with what we would expect from the known capabilities of *C. metallidurans* CH34 discussed at the beginning of this section. Low levels of phosphorus correlate with increased expression of the phosphate specific transport system, phosphonate and phosphite transport as well as phospholipases and phosphatases, representing an

attempt by the cells to increase intracellular phosphorus supply.

At the most severe phosphorus limitation tested ("lowest phosphorus"), an extreme shut-down of many cellular processes was observed, particularly proteins associated with protein synthesis, energy metabolism and synthesis of amino acids. The re-organisation of translational machinery under nutrient deficiency is typical of that associated with the Stringent Response (see Chapter 2). Particularly when the concomitant increase in proteins related to oxidative stress responses is considered.

6.3.3 Response to Magnesium Stress

Known Capabilities for Response to Magnesium Stress

The *C. metallidurans* genome encodes a modest inventory of mechanisms to transport magnesium into the cell. Magnesium is transported via three CorA family proteins: CorA1, CorA2 and CorA3. CorA proteins probably regulate intracellular magnesium concentrations via cytoplasmic gating domains which cause the channel to open when magnesium is low [237]. Kirsten *et al.,* (2011) found that only CorA1 was differentially regulated with varying magnesium concentrations and suggest this is the primary protein used for magnesium uptake in this organism. CorA2 and CorA3 are thought to be back up transporters [142]. It has been suggested that divalent metal deficiency in this organism may lead to non-specific uptake of divalent metal ions [142] (Figure 6.10). Some organisms co-ordinate uptake systems with efflux systems to form a "shunt" which is specific for that metal. Divalent metal uptake in *C. metallidurans* is very non-specific, occurring through non-specific channel proteins, and there is no evidence for metal shunts. Thus, during divalent metal ion deficiency, increases in intracellular concentrations of other metals may occur [142].

Other magnesium uptake proteins exist in other bacterial species but, as these

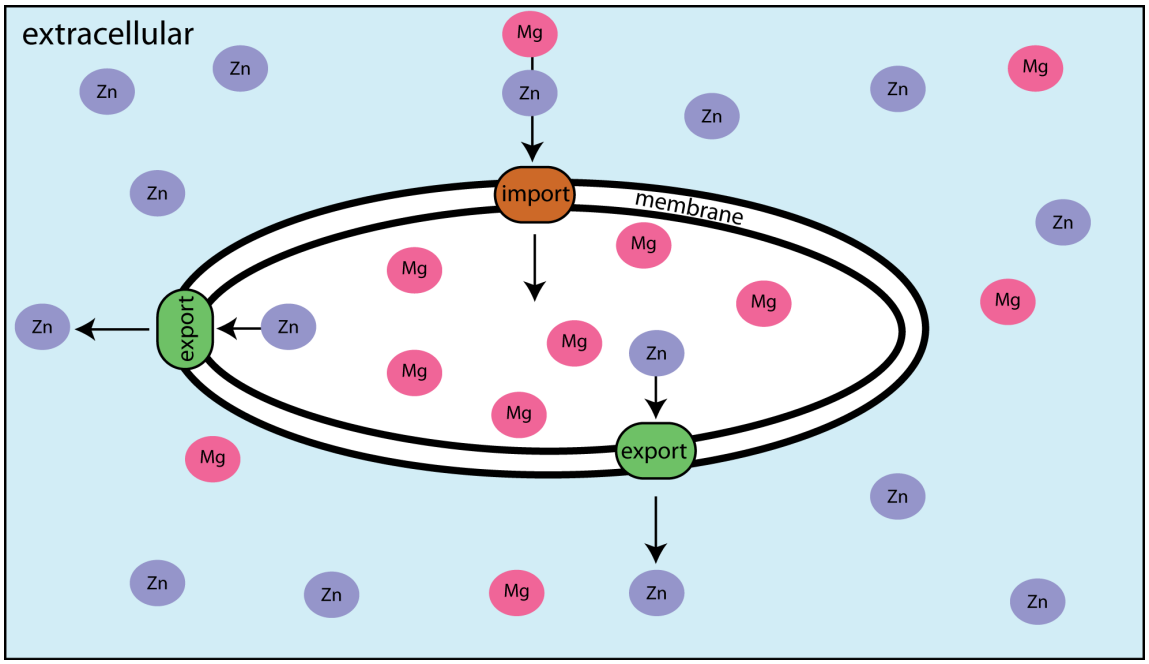

Figure 6.10 Schematic of the hypothesis of Kirsten *et al.*, (2011). Magnesium deficiency results in divalent metal efflux because magnesium transport proteins (orange) are not specific to magnesium (pink). During uptake of magnesium, these transporters also allow other divalent cations into the cell e.g. zinc (purple) which may be toxic. Efflux proteins (green) are thus required to export unwanted ions back out of the cell to avoid toxic effects.

are not present in *C. metallidurans* they will not be discussed here.

Based on the known capabilities of *C. metallidurans* we may expect magnesium deficiency to lead to changes in the abundance of CorA family proteins and changes in metal transport.

Growth Response to Variations in Magnesium Concentrations

Figure 6.11 shows the growth curves for *C. metallidurans* grown at different magnesium concentrations ($MgCl_2.6H_2O$). These curves indicate that the requirement for magnesium is very low and that additional, lower concentrations will be required to cover the full range of growth profiles between optimum magnesium and no added magnesium. Very little growth was observed under no added

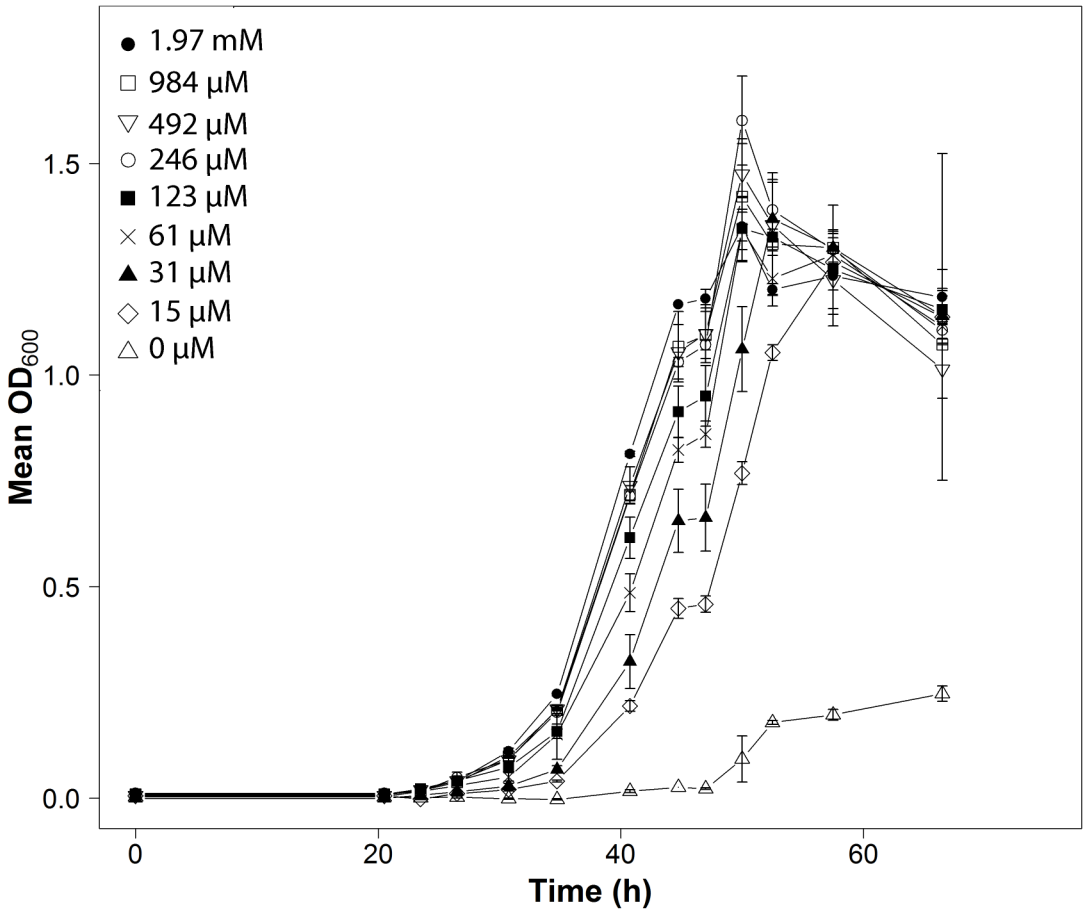

Figure 6.11 Growth of *C. metallidurans* CH34 with varying concentrations of magnesium

magnesium, consistent with the previous chapter.

Protein Expression Under Magnesium Stress

Only one concentration of magnesium is tested in these experiments. In cells grown at 15 μM magnesium, 47 proteins were up-regulated and 147 down-regulated compared to the control (1.97 mM Mg).

The type of proteins up- and down-regulated at low magnesium are shown in Figure 6.12. Aside from the differential regulation of enzymes in both groups, transporters are a key part of the up-regulated response.

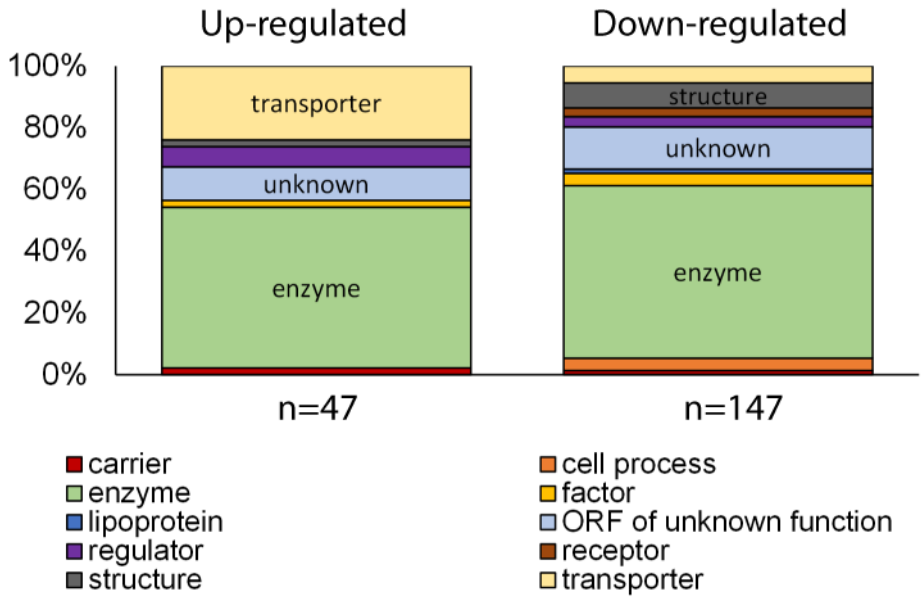

Figure 6.12 Types of proteins up- or down-regulated under magnesium limited conditions. Reveals differential regulation of transporters and structural proteins as well as numerous enzymes.

Figure 6.13 shows the biological functions differentially regulated under magnesium stress.

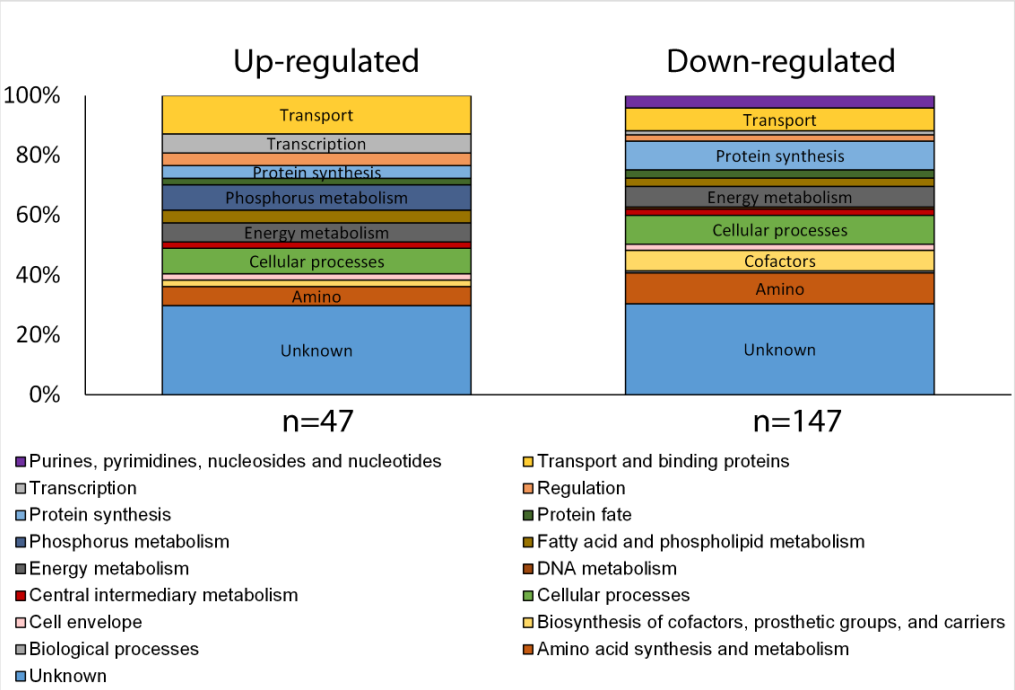

Figure 6.13 Functions of proteins differentially regulated under magnesium stress

A number of key features of can be highlighted from Figure 6.13:

1) Magnesium transporters not detected: Surprisingly, none of the known magnesium transporters in *C. metallidurans* were detected in this analysis. Therefore, it is not possible to compare the abundances of magnesium uptake proteins in each condition directly.

2) Divalent metal transporters up-regulated: Up-regulated transport proteins in Figure 6.13 were observed and were primarily associated with divalent metal cation efflux. These proteins are listed in Table 6.11. These proteins facilitate transport of metals such as nickel, cobalt, zinc and cadmium. Also up-regulated is the sigma factor RpoE, known to be up-regulated in response to divalent metal ion stress in this organism [238].

3)Up-regulated phosphorus uptake: Another group of up-regulated proteins are those involved in phosphorus uptake. These proteins are responsible for

the transport of phosphate and phosphite.

4)**Up-regulated stress response:** Proteins representative of stress are up-regulated. These include three proteins for detoxification, and regulation of cell redox homeostasis. Also up-regulated is CstA, a known starvation–induced protein [239] and PhcB required for synthesis of a cell to cell communication molecule (3-OH-PAME) in a closely related organism [172, 240].

5)**Down-regulation of protein synthesis:** The down-regulated proteins included proteins associated with protein synthesis. These included 11 ribosomal proteins and ribosome maturation factor RimP involved in ribosome biogenesis. Down-regulation of the house-keeping sigma factor RpoD1, the primary sigma factor used during exponential growth, and sigma factor RpoZ was also observed.

Table 6.11 Membrane transport proteins up-regulated under magnesium deficiency

Label	Gene	Product	Fold change	P-value
Rmet_1121	AcrD	Aminoglycoside/multidrug efflux system	7.0	1.5E-04
Rmet_5329	ZneA	Heavy metal cation tricomponent efflux pump	11.3	1.1E-04
Rmet_5330	ZneB	Membrane fusion protein heavy metal cation tricomponent efflux	20.6	4.3E-05
Rmet_5408		Putative efflux outer membrane protein	55.7	2.2E-02
Rmet_5682	NimB	Heavy metal cation tricomponent efflux membrane fusion protein	5.3	3.0E-05
Rmet_5981	CzcB	Cation proton antiporter efflux system involved in Cd(II), Zn(II), Co(II) resistance	5.3	3.5E-04
Rmet_6209	CnrB	Cation proton antiporter efflux system, involved in Co(II)/Ni(II) resistance	4.4	4.0E-04

Summary and Interpretation of Magnesium Stress Response

The up-regulation of divalent metal efflux under magnesium deficiency observed here supports observations made by Kirsten *et al.,* (2011). These authors

measured increased intracellular zinc concentrations under conditions of magnesium deficiency which led them to suggest a new hypothesis for how *C. metallidurans* manages metal stress that they term the "worry-later approach" (Figure 6.10). This suggests that, when uptake of one metal is increased, the cell will inadvertently uptake similar metal cations which may be toxic. This is a result of the fact that most metal uptake proteins have the ability to transport numerous types of element. These unwanted metals must then be transported back out of the cell. The up-regulation of divalent metal efflux proteins observed here could be explained by such a mechanism.

The lack of detection of any of the known magnesium uptake proteins is unfortunate and highlights an important limitation of proteomics approaches. Whilst proteomics is excellent at capturing the complexity of a response, it favours detection of the most abundant proteins because the most abundant ions are selected for fragmentation. This means that low abundance features will sometimes be missed. It is not clear from these results if magnesium uptake proteins were not expressed in any condition, or if they were simply not detected in all experiments.

6.4 Results: Proteome Changes Under Multiple Nutrient Stress

The previous section showed that the limitation of one nutrient alone caused very complex changes to the physiology of the cell. The following sections now investigate the changes in the proteome when cells are exposed to deficiency of two of these elements simultaneously. In each of these sections, I first compare the growth rates of cells grown under single- and dual-limitation which were gained from the "Additional experiments" described in the Methods section. These concentrations were chosen for the proteome analysis as single limitation caused

some decrease in growth rate, whilst co-limitation by both elements resulted in further decreases in growth rate.

I then compare the proteome profiles in the co-limited treatment to the single-limited treatments through a combination of multivariate statistical analysis and identification of proteins which are commonly regulated between conditions.

I then explore the functions of the proteins differentially regulated under nutrient co-limitation in order to identify the influence exerted on the co-limited treatment from each of the elements of interest. Lists of all of the proteins which were differentially regulated in each treatment can be found in Appendix B.

6.4.1 Simultaneous Iron and Phosphorus Stress

To assess the effect of low concentrations of both iron and phosphorus simultaneously, the proteome was characterised for cells grown in 969 nM iron and 112 μM phosphorus. This is equivalent to the "low phosphorus" and "low iron" described in the previous sections.

Comparison of growth rate under both single nutrient stress, multiple nutrient stress and optimal conditions is found in Figure 6.14. Iron deficiency and phosphorus deficiency alone result in a similar reduction in growth rate from the optimal. The multiple limited growth rate is slightly lower than the single limited conditions.

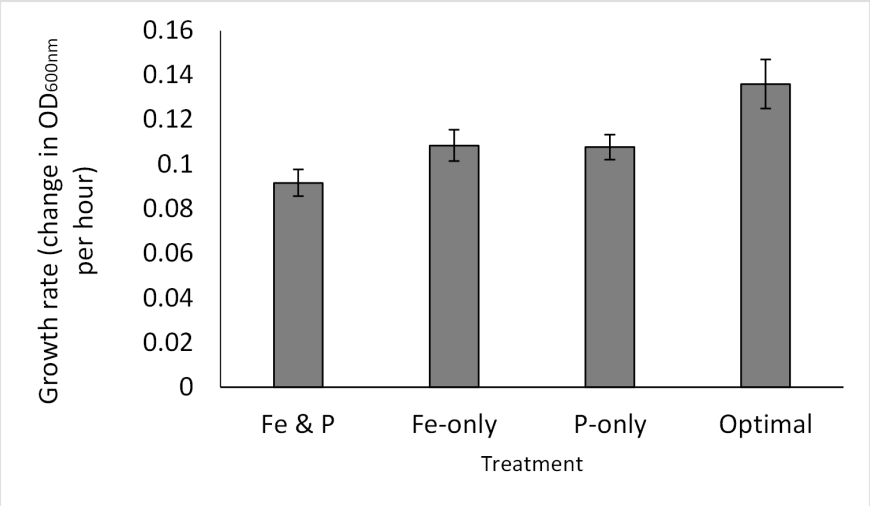

Figure 6.14 Comparison of average growth rate under single nutrient stress (Fe, P), under multiple nutrient stress (Fe & P) and optimal growth conditions.

As discussed in the last section, single deficiency of phosphorus increased expression of 115 proteins and single deficiency of iron increased expression of 68 proteins. Single deficiency of each element caused down-regulation of 86 proteins for phosphorus and 68 for iron. Under deficiency of both phosphorus and iron, 95 proteins were up-regulated and 58 proteins were down-regulated compared to the replete control.

Comparison of Multiple Stress Profile to Single Stress Profile

The nMDS plot in Figure 6.15 displays the similarity in the proteome profiles for each condition. The closer the points are to one another, the more similar they are. Statistics for this analysis are found in Table 6.12. The co-limited treatment is most similar to the phosphorus-limited treatment (87%). Indeed, the Monte Carlo P value for the comparison between the P-limited and the Fe-P co-limited treatment shows that there is no significant difference in expression profiles between these treatments (MC P = 0.1353). Similarity between the iron-limited and Fe-P co-limited treatments is lower (79%).

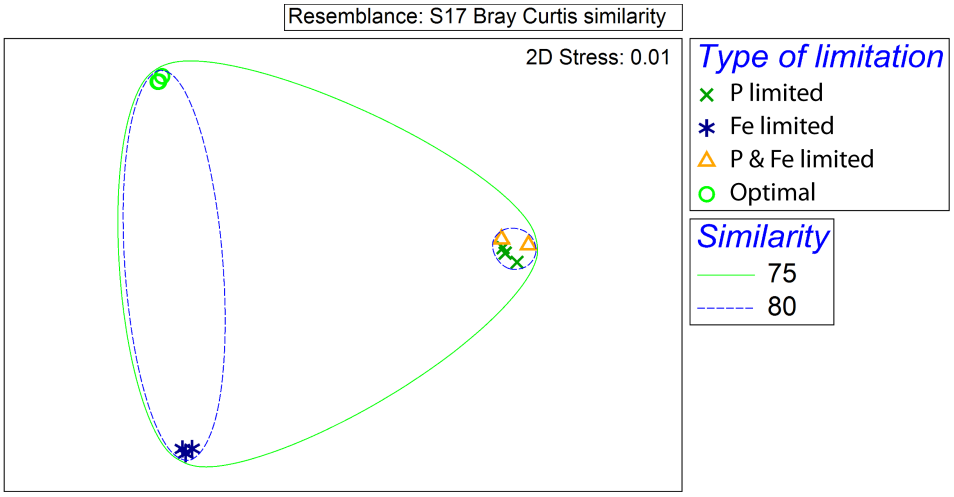

Figure 6.15 Non-metric multidimensional scaling ordination showing similarity of the proteome of cells only limited of iron or phosphorus to cells limited of both and to the optimal control. Ordination derived from a Bray-Curtis similarity matrix calculated from normalised protein expression data. Similarity thresholds based on group–average clustering. (See Chapter 3 for details on production of nMDS plots.)

Table 6.12 Pairwise PERMANOVA results for iron-phosphorus co-limitation experiments

Groups	Similarity	t	Unique permutations	P(MC)
Optimal vs. P limited	77%	4.5225	10	0.002
Optimal vs. Fe limited	82%	3.7227	10	0.0036
Optimal vs. Fe & P limited	75%	3.8763	10	0.0033
P limited vs. Fe limited	79%	3.8639	10	0.0039
P limited and Fe & P limited	87%	1.4934	10	0.1353
Fe limited and Fe & P limited	79%	3.1126	10	0.0092

Figure 6.16 shows the number of proteins differentially regulated in the co-limited condition which are also differentially regulated in one of the single limited conditions. The majority of both up- and down-regulated proteins in the co-limited condition are shared with the phosphorus-limited treatment. Only ten up-regulated proteins and five down-regulated proteins are shared with the iron-limited treatment.

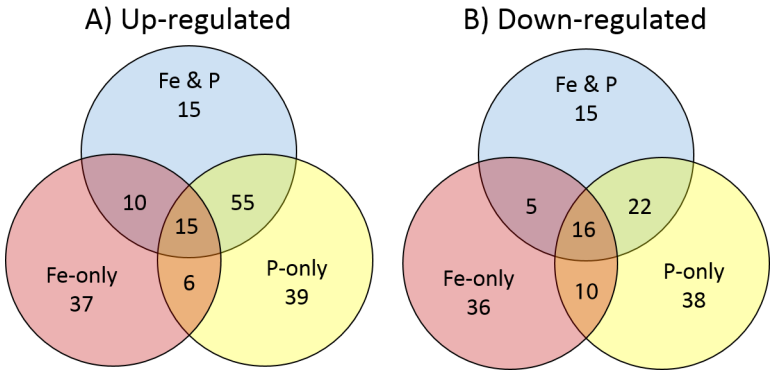

Figure 6.16 Venn diagram indicating the number of proteins differentially regulated in more than one treatment

Function of Proteins Differentially Regulated Under Dual Iron and Phosphorus Stress

Figure 6.17 shows the functional profiles of proteins up- or down-regulated under phosphorus limitation, iron limitation, and iron–phosphorus co-limitation. The co-limited condition, as might be expected from Figures 6.16 and 6.15, shares a lot of similar functions to the phosphorus-limited culture such as up-regulation of phosphorus metabolism and cellular processes, and down-regulation of protein synthesis. However the co-limited condition also shares a small number of key features with the iron-limited culture such as up-regulation of proteins for synthesis of cofactors, prosthetic groups and carriers.

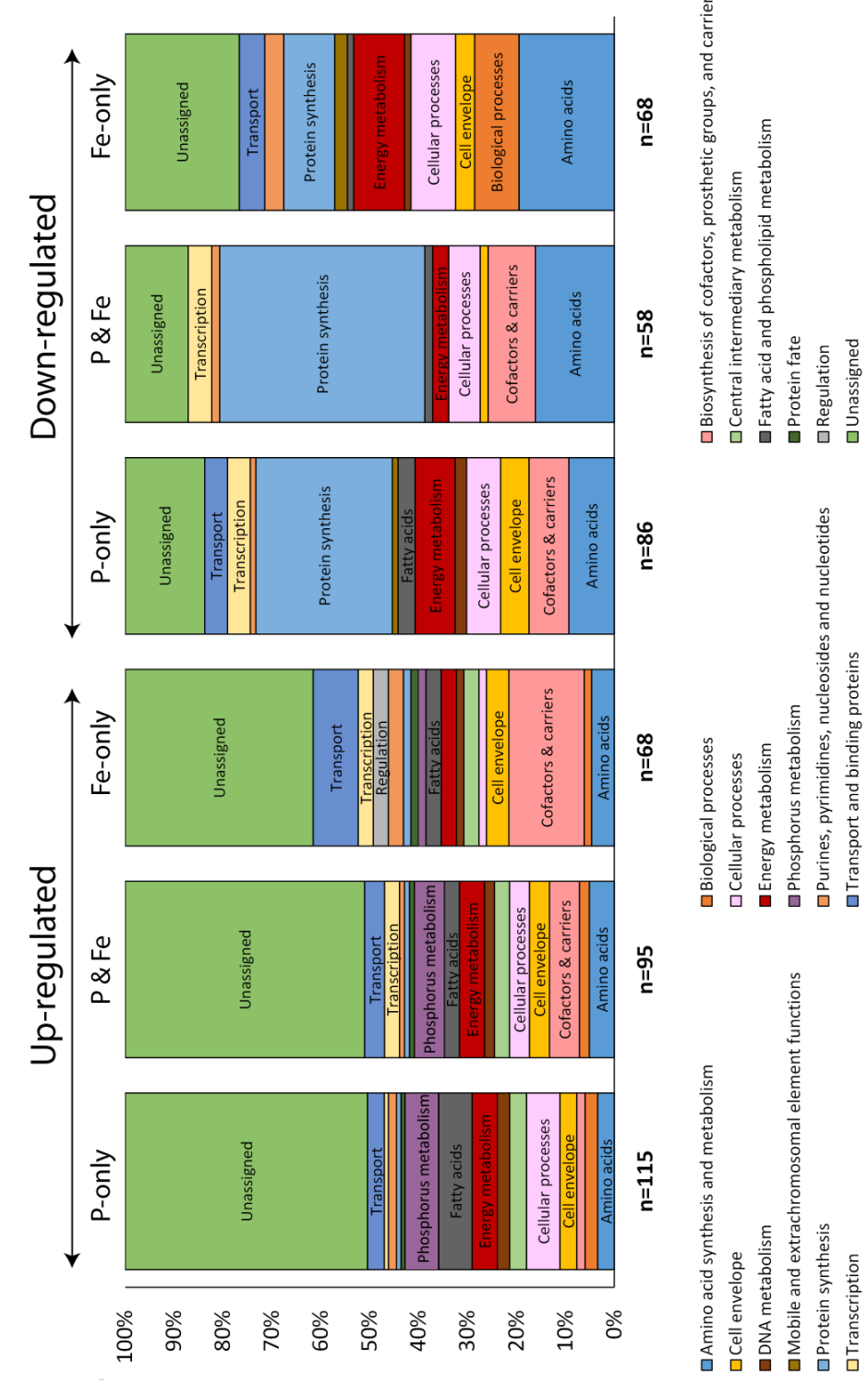

Figure 6.17 Functions of proteins up- or down-regulated in (from left to right) P-limited only treatment, Fe & P co-limited treatment and Fe-limited treatment.

The proteins shared between phosphorus limited and co-limited treatments have similar features to those differentially regulated under phosphorus deficiency alone. Three main functional groups are shared between these treatments:

1) Up-regulated phosphorus metabolism Proteins associated with phosphorus uptake and metabolism are up-regulated in both conditions (Figure 6.17). These are listed in Table 6.13 and the fold change of phosphorus-related proteins is shown in Figure 6.18.

2) Up-regulation of cellular processes This group represents a small number of stress-related proteins common to both Fe-P co-limited and P-limited conditions. These include the universal stress protein UspA8, hydroperoxidase KatG and an osmotically induced protein.

3) Down-regulation of protein synthesis Proteins associated with protein synthesis are down-regulated in both Fe–P co–limited and P–limited conditions as are proteins associated with transcription. This indicates a common down-regulation of high energy protein-making processes.

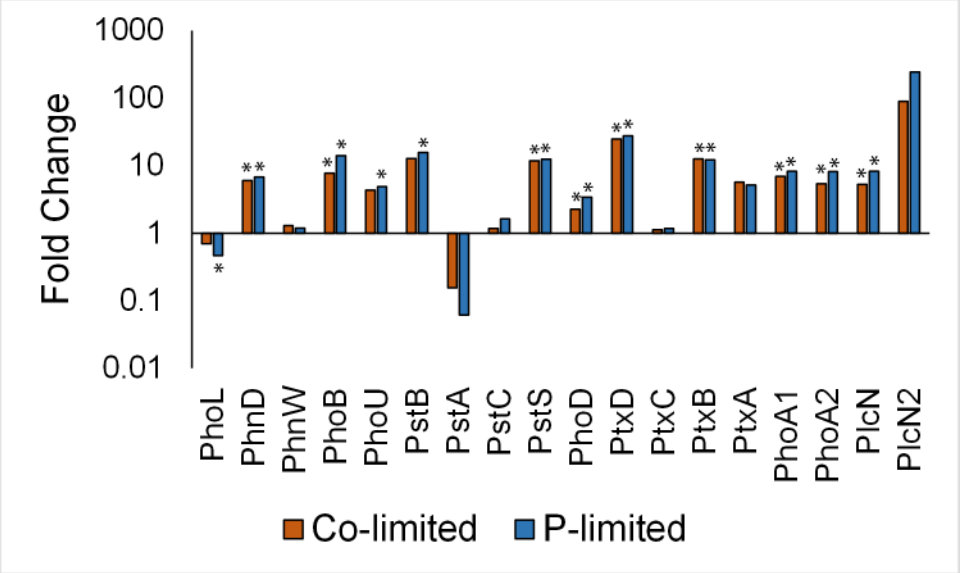

Figure 6.18 Fold change of known phosphorus-related proteins in the co-limited and phosphorus-limited treatments compared to the optimal control media. Less than one is down-regulated and greater than one is up-regulated. * indicates protein meets stringent significance criteria for differential regulation outlined in Chapter 3.

Table 6.13 List of proteins associated with phosphorus metabolism up-regulated in both the phoshorus-limited and Fe–P co-limited cultures.

			P & Fe limited		P-limited	
Locus Tag	**Protein Name**	**Description**	**Fold change**	**P value**	**Fold change**	**P value**
Rmet_0774	PhnD	Phosphonate/organophosphate ester transporter subunit	6	3.2E-03	6.8	2.1E-04
Rmet_2177	Ppx	exopolyphosphatase	3.3	1.9E-03	3.8	8.1E-03
Rmet_2178	Ppk	polyphosphate kinase, component of RNA degradosome	9.2	3.1E-03	8	1.5E-03
Rmet_2180	PhoB	DNA-binding response regulator in two-component regulatory system with PhoR	7.8	3.8E-04	14	2.5E-04
Rmet_2181	PhoU	negative regulator of PhoR/PhoB two-component regulator	4.3	6.3E-04	4.9	2.4E-05
Rmet_2182	PstB	phosphate transporter subunit	12.7	2.7E-04	15.7	9.6E-05
Rmet_2185	PstS	phosphate transporter subunit	11.8	2.1E-06	12.5	8.2E-05
Rmet_2583	PhoD	Phosphodiesterase/alkaline phosphatase D	2.3	3.2E-02	3.4	2.7E-03
Rmet_2994	PtxB	putative phosphonate ABC transporter	12.6	5.8E-06	12.2	2.4E-05
Rmet_4084	PhoA1	alkaline phosphatase	6.9	2.1E-03	8.2	1.6E-03
Rmet_4085	PhoA2	alkaline phosphatase	5.4	4.9E-04	8.2	1.2E-04
Rmet_4192	PlcN	phospholipase C signal peptide protein	5.3	3.1E-03	8.2	1.1E-04
Rmet_4809	AcpA	putative acid phosphatase protein	21.6	1.6E-02	31.9	1.8E-02

Only ten proteins were commonly up-regulated in both co-limited and iron-only limited treatments (Figure 6.16) but almost all were related to iron metabolism. Five of these up-regulated proteins (SbnH, SbnG, SbnC, SbnB and SbnA) are known to be responsible for the synthesis of siderophores. Additionally, the one up-regulated transport-related protein is HmuV, a heme transport protein.

Figure 6.19 compares the fold change of known iron-related proteins in the co-limited and iron-only limited conditions. This shows that whilst there is some common up-regulation of siderophores, the response is not as strong as under iron deficiency alone.

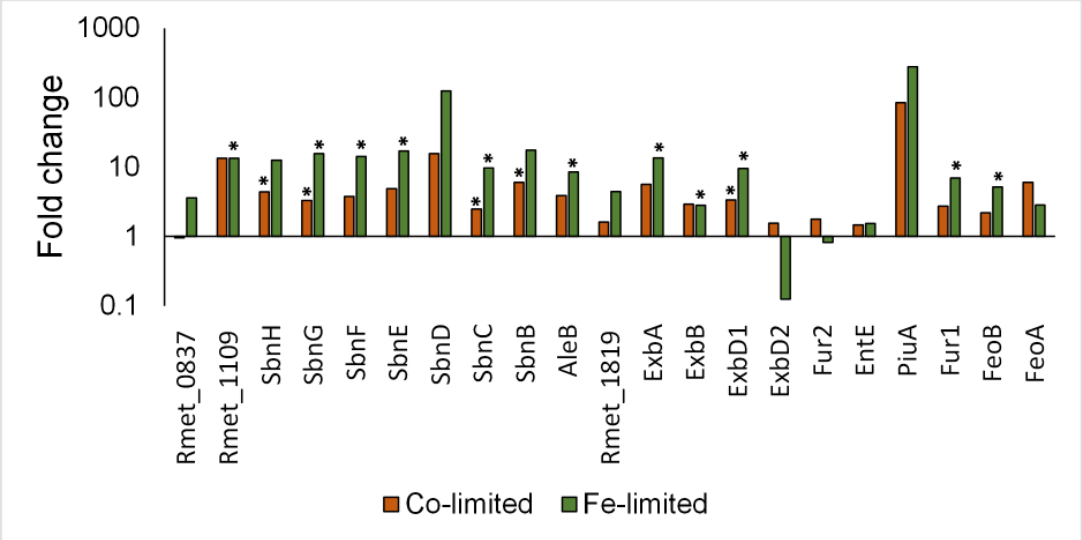

Figure 6.19 Fold change of known iron-regulated proteins in the Fe-P co-limited treatment and the iron-limited only treatment compared to the optimal control. Less than one is down-regulated and greater than one is up-regulated. * indicates protein meets stringent significance criteria for differential regulation outlined in Chapter 3.

Summary

In summary, these results show that phosphorus stress is the dominant influence on the proteome of cells exposed to both iron and phosphorus deficiency. However, some very specific aspects of the iron stress response are still observed in the

multiple stress cultures.

6.4.2 Simultaneous Phosphorus and Magnesium Stress

To assess the effect of simultaneous phosphorus and magnesium-deficiency, the proteome was characterised for cells grown in 15 μM magnesium and 56 μM phosphorus. This is equivalent to the "lowest phosphorus" treatment described in the single element deficiency section. Growth rates at the chosen conditions are shown in Figure 6.20. Both magnesium deficient and phosphorus deficient conditions show decreased growth rate from the control which is slightly lower in the phosphorus-deficient condition. The magnesium and phosphorus depleted condition (P & Mg) has a lower growth rate than the treatments with only one deficient nutrient.

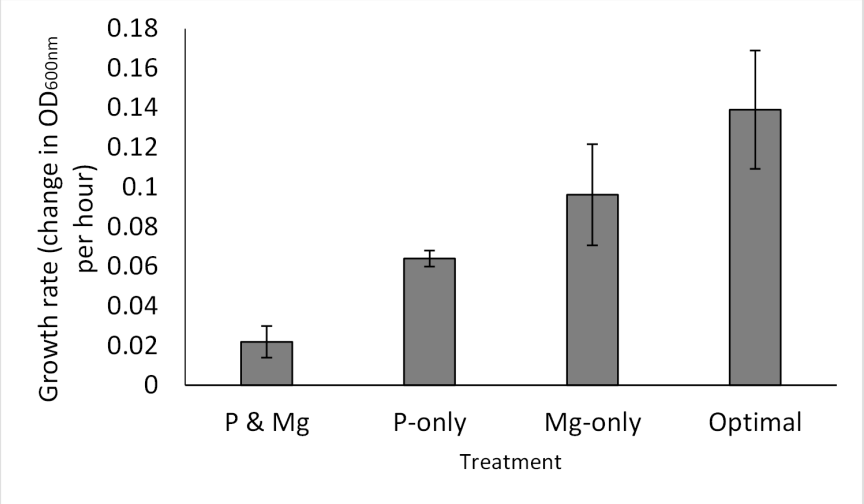

Figure 6.20 Comparison of average growth rate under single nutrient stress (Mg, P), under multiple nutrient stress (Mg & P) and optimal growth conditions.

Comparison of Multiple Stress Profile to Single Stress Profiles

Cells grown at this concentration of phosphorus (56 μM) showed up-regulation of 165 proteins and down-regulation of 209 proteins (see previous sections). Cells grown at this concentration of magnesium (15 μM) showed up-regulation of 47 proteins and down-regulation of 147 proteins. Simultaneous deficiency of both phosphorus and magnesium resulted in 157 up-regulated proteins and 106 down-regulated proteins. Figure 6.21 demonstrates that the proteome profile of the co-limited condition is much more similar to the phosphorus-limited condition (81%) than to the magnesium-limited condition (76%). Statistics of this analysis are shown in Table 6.14).

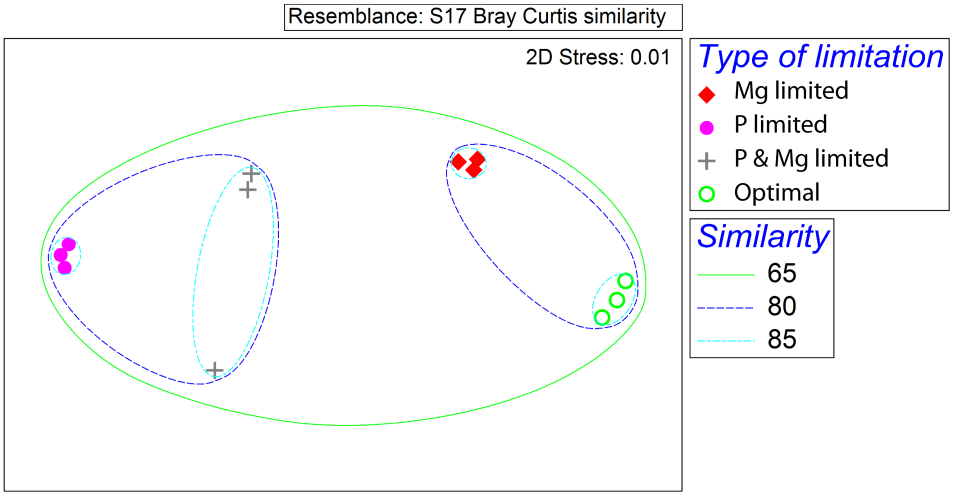

Figure 6.21 Non-metric multidimensional scaling ordination showing similarity of the proteome of cells only limited of magnesium or phosphorus to cells limited of both and to the optimal control. Ordination derived from a Bray-Curtis similarity matrix calculated from normalised protein expression data. Similarity thresholds based on group–average clustering. (See Chapter 3 for details on production of nMDS plots.)

Table 6.14 Pairwise PERMANOVA results for phosphorus-magnesium co-limitation experiments

Groups	Similarity	t	Unique permutations	P (MC)
Optimal vs. Mg limited	82%	4.4871	10	0.0021
Optimal vs. P-limited	65%	7.9381	10	0.0004
Optimal vs. P & Mg limited	70%	4.7969	10	0.0018
Mg limited vs. P limited	69%	7.5705	10	0.0003
Mg limited vs. Mg & P limited	76%	3.8779	10	0.0036
P limited vs. P & Mg limited	81%	2.7042	10	0.0122

The high similarity between the P-limited and the P-Mg co-limited condition is reflected in the high number of commonly regulated proteins in these conditions (Figure 6.22). In the P–Mg co-limited and phosphorus-limited treatments, 103 proteins were commonly up-regulated in both conditions compared to the control, and 61 were commonly down-regulated. Only five proteins were commonly up-regulated in the magnesium-limited and P–Mg co-limited treatment, and 7 were down-regulated.

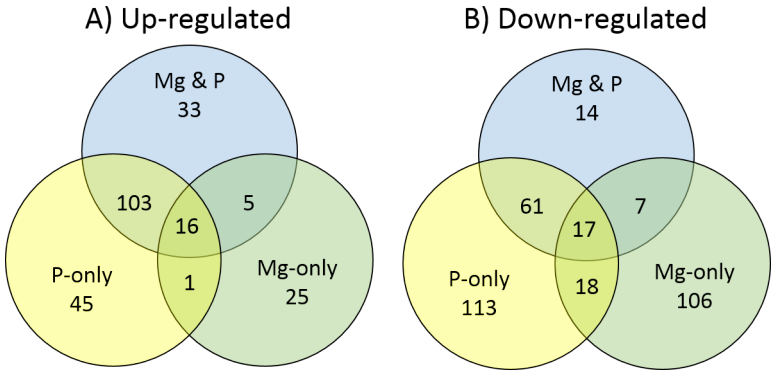

Figure 6.22 Venn diagram showing the number of proteins differentially regulated in more than one condition

Function of Proteins Differentially Regulated Under Dual Magnesium and Phosphorus Stress

The functions of proteins differentially regulated in phosphorus-limited, magnesium-limited and phosphorus-magnesium co-limited tratements are shown in Figure

6.23. A number of key features can be highlighted from these results:

1) Up-regulation of phosphorus metabolism in all conditions Consistent with the results from single deficiency of both magnesium and phosphorus, numerous proteins associated with phosphorus metabolism are up-regulated in all three treatments. It is not clear why magnesium stress induces an increase in phosphorus-related proteins.

2) Divalent metal uptake in Mg-limited and co-limited condition The very small number of up-regulated proteins common to both magnesium-limited and co-limited treatments are metal efflux proteins, consistent with the results for deficiency of magnesium alone.

3) Stress response in co-limited and phosphorus-limited A large number of proteins associated with protein synthesis were down-regulated in both the co-limited and P-limited treatments.

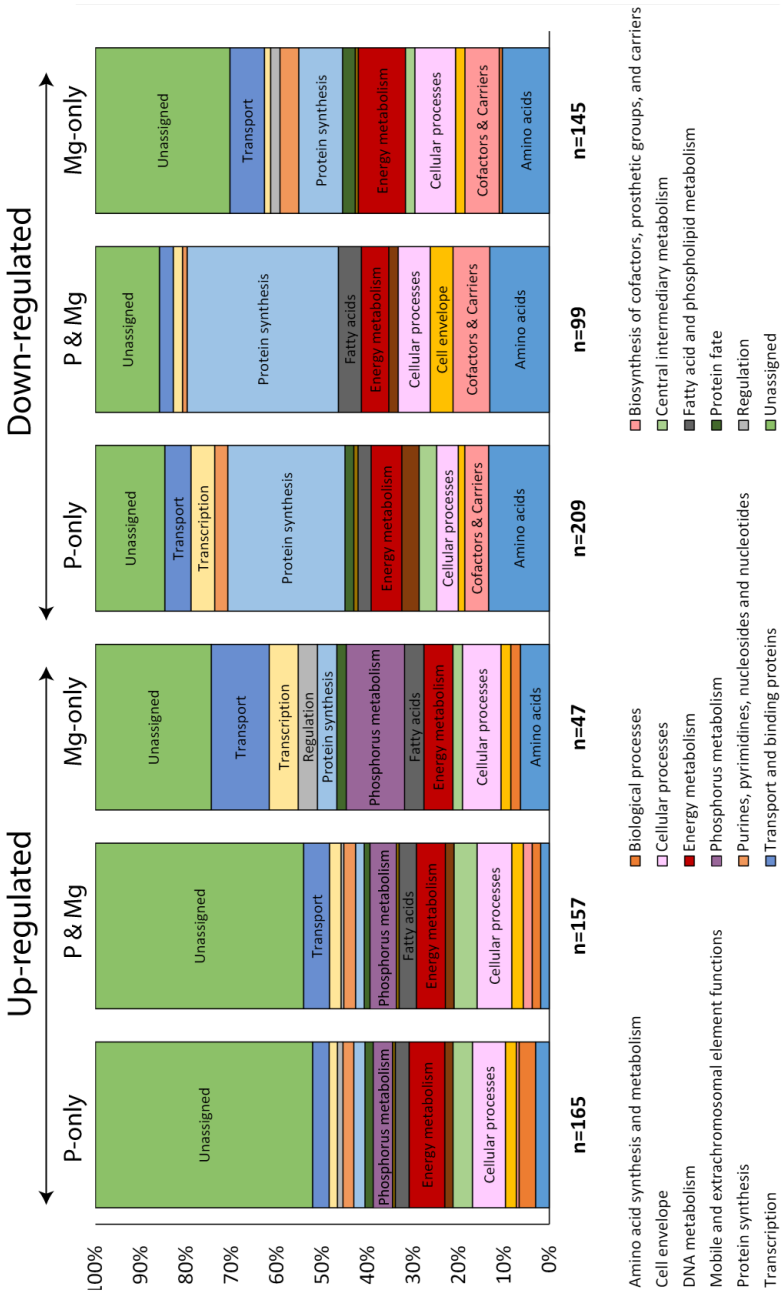

Figure 6.23 Proteins up- and down-regulated in (from left to right) P-limited, P & Mg limited and Mg-limited treatments. Differentially regulated protein profiles in P & Mg limited culture are very similar to those observed for the P-limited only treatment and show up-regulation of phosphorus metabolism and cellular processes, and down-regulation of protein synthesis and energy metabolism.

Summary

In summary, these results show that phosphorus stress is the dominant influence on the proteome of cells exposed to both magnesium and phosphorus deficiency. However, the up-regulation of divalent metal efflux proteins, a key feature of the magnesium response, is still observed in the multiple stress cultures.

6.4.3 Simultaneous Iron and Magnesium Stress

This section describes the proteome response of cells grown in low concentrations of iron and magnesium simultaneously. The magnesium concentration used was 15 μM magnesium and the iron concentration used was 434 nM iron. This correlates with the "lowest iron" condition discussed previously. Treatments deficient in iron only and magnesium only, showed similar decreases in growth rate compared to the control. The iron and magnesium deficient treatment showed decreased growth rate relative to the single limitation treatments.

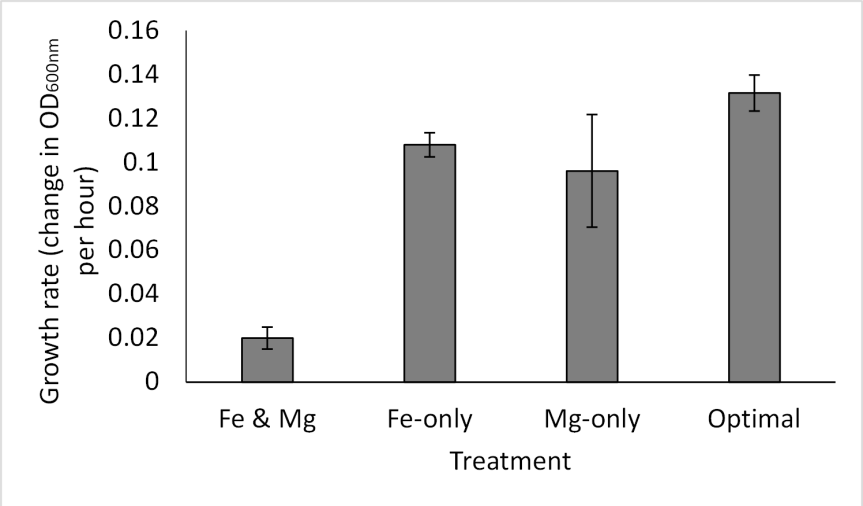

Figure 6.24 Comparison of average growth rate in iron–magnesium co-limited, iron–limited, magnesium–limited and optimal media.

Comparison of Multiple Stress Profile to Single Stress Profile

Cells grown at this concentration of magnesium showed 47 up- and 148 down-regulated proteins. Cells grown at this concentration of iron showed 74 up-regulated proteins and 103 down-regulated proteins compared to the control. Simultaneously low concentrations of both nutrients resulted in and 107 up- and 83 down-regulated proteins. Figure 6.25 reveals that the co-limited treatments show more similarity to cultures only limited of iron (87%) than to cultures only limited of magnesium (77%). PERMANOVA statistics for this analysis are shown in Table 6.15.

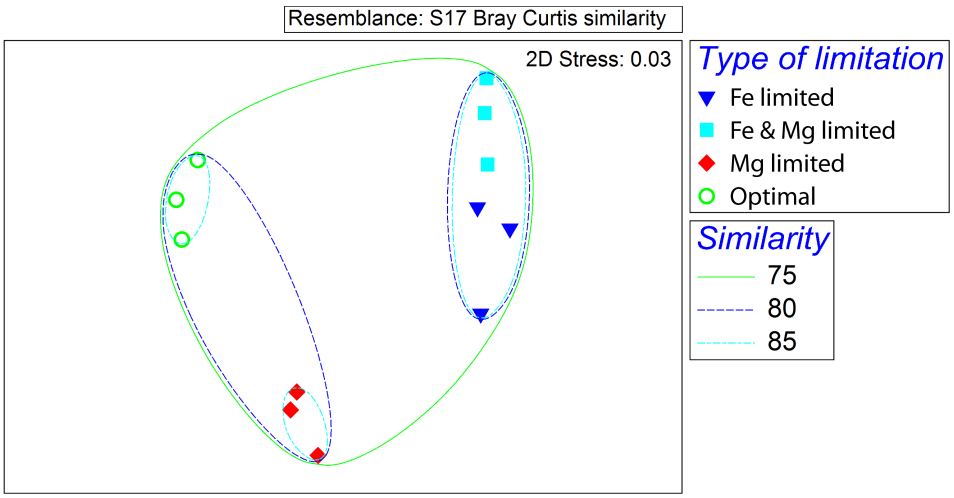

Figure 6.25 Non-metric multidimensional scaling ordination showing similarity of the proteome of cells only limited of iron or magnesium to cells limited of both and to the optimal control. Ordination derived from a Bray-Curtis similarity matrix calculated from normalised protein expression data. Similarity thresholds based on group–average clustering. (See Chapter 3 for details on production of nMDS plots.)

Table 6.15 Pairwise PERMANOVA results for iron–magnesium co-limitation experiments.

Groups	Similarity	t	Unique permutations	P (MC)
Optimal vs. Fe limited	79%	4.1594	10	0.0029
Optimal vs. Fe & Mg limited	78%	4.6997	10	0.0014
Optimal vs. Mg limited	82%	4.4871	10	0.0022
Fe limited vs. Fe & Mg limited	87%	2.2569	10	0.0316
Fe limited vs. Mg limited	81%	3.9258	10	0.0022
Mg limited vs. Fe & Mg limited	77%	5.3906	10	0.0013

The high similarity of the proteomes of cells grown in Fe-only limited media and Fe-Mg co-limited media is emphasised in Figure 6.26. Fe & Mg co-limited cultures shared 40 up-regulated proteins and 22 down-regulated proteins with the Fe-limited condition. Only 9 up-regulated and 7 down-regulated proteins were shared between co-limited and magnesium-limited cultures.

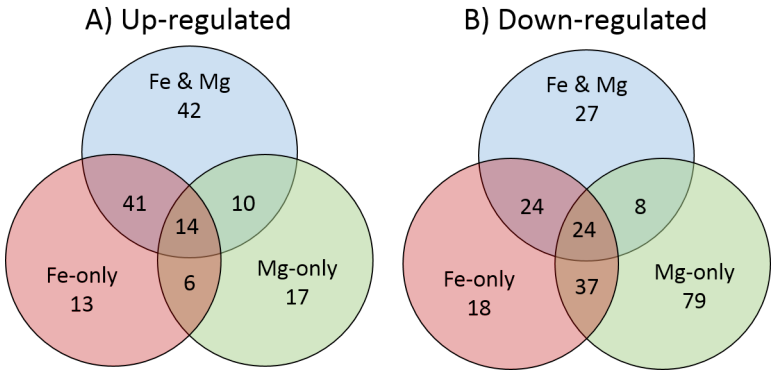

Figure 6.26 Venn diagram indicating the number of proteins differentially regulated in more than one treatment

Function of Proteins Differentially Regulated Under Dual Iron and Magnesium Stress

Functions of proteins differentially regulated in Fe & Mg co-limited cultures, and proteins differentially regulated with limitation of each individual element are shown in Figure 6.27. Both co-limited and iron-limited treatments show large proportions of up-regulated proteins in the"Transport and binding proteins" and

"Biosynthesis of cofactors, prosthetic groups and carriers" groups. Proteins in these groups were associated with siderophore synthesis, siderophore uptake and heme uptake.

Similar levels of abundance were observed in siderophore/iron metabolism proteins in both Fe-limited and Fe–Mg co-limited treatments and none of these proteins were significantly differentially regulated compared to the other. Proteins down-regulated in both co-limited and iron-limited treatments were in the "Energy metabolism" group. Most of these proteins were iron-binding enzymes associated with the electron transport chain.

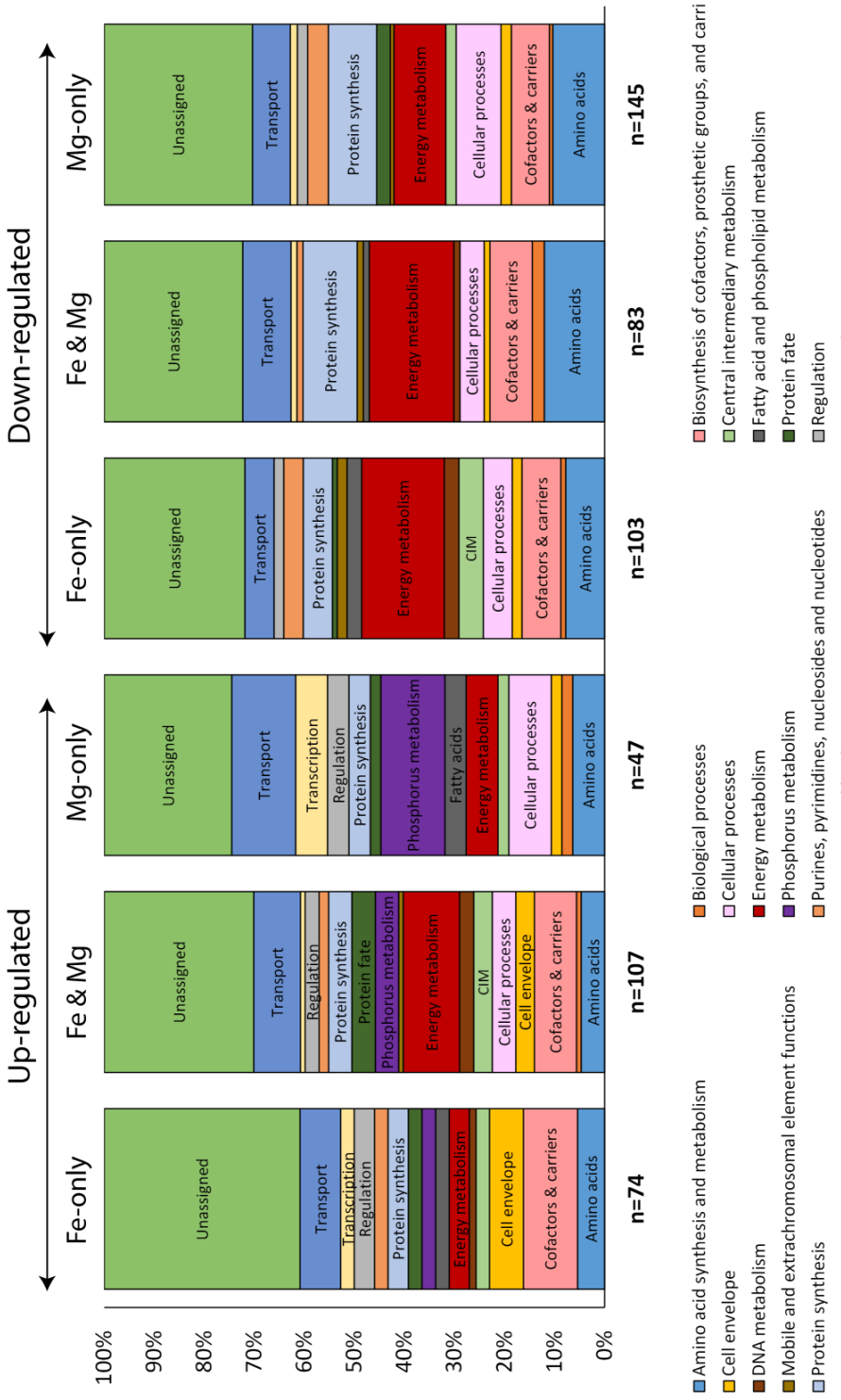

Figure 6.27 Functions of proteins differentially regulated in (from left to right) Fe-limited only, Fe & Mg limited, and Mg-limited only treatments.

Three of the nine proteins up-regulated in both co-limited and magnesium-limited treatments were associated with efflux of metal ions. These include CnrB (Co(II) and Ni(II) resistance), CzcB (Zn(II), Cd(II) and Co(II) resistance) and ZneB (Zn(II) resistance) which is consistent with our observations of up-regulation of metal efflux during deficiency of magnesium alone. Additionally, three proteins related to phosphorus metabolism are up-regulated in both of these conditions. These are PstB and PstS associated with phosphate uptake and PtxD associated with phosphonate uptake.

Summary

In summary, these results show that iron stress is the dominant influence on the proteome of cells exposed to both iron and magnesium deficiency. However, again, the up-regulation of divalent metal efflux proteins is still in the multiple stress cultures, indicating a small but specific contribution from magnesium deficiency.

6.4.4 Is a unique response to co-limitation exhibited?

The venn diagrams in Figures 6.26, 6.16 and 6.22 show that, in each of the pairwise experiments, there are some proteins which are only significantly differentially regulated in the co-limited treatment and not in either of the treatments limited by only one nutrient. This section explores the function of these proteins with a view to understanding whether the cells adopt unique responses to cope with limitation of multiple nutrients.

Lists of proteins differentially regulated only in the co-limited treatments are shown in Appendix tables B.9, B.10 and B.11. In the iron-phosphorus co-limited treatment, 15 proteins were uniquely up-regulated and 15 proteins uniquely down-regulated. In the magnesium-phosphorus co-limited treatment, 33 proteins were uniquely up-regulated and 14 down-regulated. In the magnesium-iron co-limited

treatment, 42 proteins were up-regulated and 27 proteins were down-regulated only in the co-limited condition. There is very little overlap in the proteins contained in each of the groups, suggesting there is not a general "co-limited" response. Rather the response appears to be dependent on which nutrients are co-limiting.

In the phosphorus-iron co-limited treatment, the main group of down-regulated proteins were associated with protein synthesis. There does not appear to be a strong up-regulation of any particular functional group. Indeed, the majority of up-regulated proteins (8 out of 15) are of unknown function.

In the iron-magnesium co-limited treatment, proteins down-regulated only in iron or magnesium limited treatments alone include proteins associated with protein synthesis. Additionally, six proteins associated with the transport and binding proteins functional group are down-regulated, three of which are Bug proteins. These are a family of extra-cytoplasmic solute receptors of which *C.metallidurans* has an unusually large number [172]. The over-representation of these proteins in *C. metallidurans* is speculated to assist in the uptake of carboxylated compounds from the environment [172]. Two other proteins in this group (NuoC and NuoD) are associated with aerobic respiration. Proteins associated with central intermediary metabolism, energy metabolism and stress are up-regulated. In particularly, six Cbb proteins associated with autotrophic metabolism [172] are up-regulated.

There does not appear to be strong up- or down-regulation of any particular functional group unique to the P-Mg co-limited condition. Interestingly, the Fur2 ferric uptake regulator is up-regulated in this treatment, as well as heme uptake protein HemY. More than half of the uniquely up-regulated proteins are of unknown function.

Although we do not observe a general response to co-limitation, each of the treatments discussed above appear to suggest co-limitation induces changes in energy metabolism, protein synthesis and stress responses which are not observed under limitation of only one element. This is possibly a result of the slower growth

rates observed under co-limitation.

6.5 Discussion

In each of the conditions with two deficient nutrients, the proteome profiles share a lot of similarities with single limitation of one of the nutrients and not with the other. This suggests that one of the elements has a much more significant effect on the processes occurring in the cell than the other element. This result has implications for the modelling of microbial growth limited by multiple nutrients. Two approaches to this problem exist. The first modelling approach assumes that, under limitation by multiple nutrients, the most limiting nutrient will ultimately limit growth, with the concentration of the other nutrient having no effect. This is commonly referred to as "Liebig's law of the minimum" (see Chapter 2). The other approach predicts that both nutrients influence growth, with a combined multiplicative effect. The proteomics analysis presented here supports the "Liebig's law interpretation" because it shows that one of the multiple limiting nutrients dominates the cellular response. More detailed growth data and modelling would be required to definitely assess how these results fit models.

However, although the proteome of cells in multiple stress treatments is primarily driven by response to one of the elements, the multiple stress cultures exhibit very specific features related to the other element. For example, in simultaneous deficiency of phosphorus and iron, only 10 proteins are commonly up-regulated in both iron-deficient and iron-phosphorus deficient cultures. However, 6 of these proteins were specifically related to iron uptake. Additionally, when comparing magnesium-limited cultures to iron-magnesium or phosphorus-magnesium co-limited cultures, the only common up-regulated response across the conditions was the increase in divalent metal efflux proteins, a key feature of magnesium deficiency. This suggests that whilst one nutrient causes global re-structuring of

cellular processes, the other nutrient only induces an attempt to uptake more nutrient.

Furthermore, this analysis may have relevance to the detection of multiple nutrient limitation in the natural environment. For example, a recent, high profile study by Saito *et al.,* [116] used a small number of protein biomarkers to identify simultaneous iron and phosphorus limitation in the Pacific Ocean. In contradiction to this, the results presented here suggest that using only a small number of biomarkers to identify simultaneous multiple nutrient stress in the environment may lead to misleading results. For example, in the phosphorus and iron limited experiments shown here, markers for both iron and phosphorus stress are detected. However, the proteome profiles show that phosphorus controls almost all of the cellular response in the co-limited cultures whereas iron had a very minor role.

As well as having broad implications for microbial stress responses in the environment, these findings are specifically applicable to microbial life in the rock habitats discussed in this thesis. In terrestrial environments, nutrient availability is determined by a complex inter-play of geological processes. As observed in the previous chapter, micro-organisms require tightly regulated cellular responses to avoid starvation or toxicity during microbe-rock interactions as element leaching changes the concentrations of numerous elements simultaneously. By gaining some insight into the cellular response to multiple simultaneous nutrient stresses in a controlled fashion, we can begin to build up a picture of how complex nutrient stresses manifest in bacterial cells. Although these laboratory-based nutrient stress experiments are much less complex than those encountered in the natural environment, they allow us to better understand how micro-organisms respond to complex nutrient stresses which will aid in our appreciation of microbial survival in, often nutrient poor, rock habitats.

6.6 Conclusion

These experiments reveal complex adaptations to iron, phosphorus and magnesium deficiency where specific stress responses are layered upon more general responses. The multiple stress results show that, in all cases, the co-limited treatment shares most features with only one of the single-limited treatments. This supports the idea that, at the cellular level, one element will dominate the response to multiple nutrient stress, similar to the concept proposed by "Liebig's law of the minimum". This has important implications for modelling the growth of micro-organisms by multiple limiting nutrients. In particular, improving the representation of microbial growth in environmental models will require an understanding of how the growth dynamics of these micro-organisms is influenced by different nutrient regimes. The fact that our experiments suggest that "Liebig's law of the minimum" is a more realistic way to understand microbial growth limited by multiple nutrients could have implications in many areas, from global geochemical models, to our understanding of microbial life in the ocean.

It is likely that multiple nutrient stress is common in rock environments which are typically nutrient poor. This is a result of adsorption of elements to rock surfaces, slow release rates from rocks or low fluxes from external nutrient sources. These results demonstrate the need for tightly controlled regulation of cellular machinery in response multiple simultaneous nutrient stress. The ability to prioritise the response to deal with the most limiting element whilst partitioning only a small amount of energy into dealing with the other stress could be an important trade off in these environments.

Chapter 7

Conclusions

7.1 Contribution to the Field

Each study presented in this thesis represents a significant contribution to the understanding of the interaction between microbial life and geology. The first study (Chapter 4) provides an important advance in our understanding of the history of land mass colonisation on the Earth. Although it has been appreciated for at least the last 30 years that endolithic lifestyles could buffer microbial communities from harsh surface conditions [180], the suitability of this environment on the early Earth has not been tested over long periods of time. This work demonstrates that *Chroococcidiopsis* sp. (a primitive and extreme-tolerant cyanobacterium) and its biomolecules can survive under UV radiation conditions more severe than the predicted "worst-case" early Earth scenario when protected just millimetres below the surface in rocks. This demonstrates that sheltering within rocks is a plausible stress avoidance strategy for phototrophs on the early Earth and provides the first empirical refutation of the idea that high UV flux on the early Earth would have prevented early colonisation of the land masses before the oxygenation of the atmosphere. Endolithic rock habitats

would have allowed micro-organisms to survive far from any water body, without the matting habit and without active repair.

The results presented in Chapter 5 demonstrate that, whilst rocks can provide nutrients for microbial communities, they can alter local chemistry and bind elements such that other nutrients become deficient. In the study presented, the addition of rock induced phosphorus deficiency, altered pH and caused changes in energy metabolism. Further chemical analysis revealed that phosphorus adsorption to rock surfaces was the key driver of the microbial response. This work demonstrates that rock geochemistry alone can drive the regulation of microbial metabolism by changing local chemistry, showing a new route by which geology can influence microbial growth and metabolism.

Chapter 6 investigated the response of a model bacterium to multiple nutrient stress, a common yet poorly understood environmental stress. These experiments revealed complex adaptations to iron, phosphorus and magnesium deficiency where specific stress responses are layered upon more general responses. Multiple stress results presented in Chapter 6 reveal the complex dynamics of the nutrient limitation response. The experiments in this chapter support the idea that, at the cellular level, one element will dominate the response to multiple nutrient stress, similar to the concept proposed by "Liebig's law of the minimum". However, a small contribution from the other element is also observed. This provides a novel contribution to the long-running debate on the dynamics of microbial growth with multiple limiting substrates and provides insight into the complex regulatory controls on microbial nutrient stress responses in the environment.

Together these results demonstrate that numerous advantages could be conferred to micro-organisms in rock habitats including protection from UV radiation (Chapter 4) and provision of nutrients (Chapter 5). However, in addition to the external environmental stresses encountered by rock-dwelling micro-organisms, rock-induced changes in chemistry can also induce stress. Chapters 5 and 6 highlight the complexity of microbial responses to extra-cellular chemical stress and reveal that a broad arsenal of tightly regulated stress responses are required

to cope with changing chemistry in the environment.

7.2 Future Work

There are numerous new research directions opened by each of the studies presented here. Work expanding on that presented in Chapter 4 could investigate how the presence of a primitive atmosphere would influence survival in high UV conditions. We may expect this to have an influence on survivability as, in the limited number of samples available for SEM analysis, it appeared that preservation of cell morphology was improved in samples exposed to space vacuum compared to those housed in an argon atmosphere. Future work should aim to elucidate the influence of atmospheric components on cell viability and biomarker preservation under extended periods of high UV exposure.

It would also be interesting to test UV survival of endoliths in other rock types such as gypsum. Gypsum, a calcium sulfate mineral, often houses phototrophic endolithic communities in deserts [187]. It is moderately water soluble at room temperature and will experience changes in chemistry in the temperature fluctuations observed during space exposure. Potentially, changes to a gypsum substrate would create an additional stress for micro-organisms. Gypsum deposits are known far back in Earth history and are therefore relevant for studies into early Earth endoliths and gypsum dunes are thought to exist on Mars (e.g. [241, 242]).

Work expanding on that presented in Chapter 5 could identify the dependence of these results on rock type. The rocks used here are a glass with very reactive surfaces, which resulted in phosphate adsorption and starvation. A previous study of microbe-rock interactions with *Cupriavidus metallidurans* suggested metal leaching was the key stress [117]. Disparity between these data suggest small differences in substrate could have a big effect on microbial responses. Future experiments could also aim to investigate the proteome under conditions

of active weathering. No active weathering occurs in Chapter 5. Therefore, it would be useful to repeat these experiments either under conditions where *C. metallidurans* actively contributes to rock weathering or with an organism which has a very strong effect on weathering.

Work expanding on that presented in Chapter 6 could map the experimental growth data on to popular mathematical models of double substrate-limited growth. The proteomics data suggest that the results are likely to mostly follow Liebig's law of the minimum where one nutrient dominates the effect on growth limitation but modelling would be required to confirm this. It would also be interesting to investigate the response to deficiency of nutrients which are dependent on each other (ie. one required for uptake of the other) or substituting (ie. one can be substituted for the other). It would also be interesting to more clearly establish the importance of multiple nutrient stress in rock environments. Numerous studies have focussed on identifying conditions for multiple nutrient stress in oceans and lakes. It is likely that multiple nutrient stress is also a terrestrial problem but this has not been extensively investigated. This analysis could be done via traditional nutrient addition experiments or *in situ* analysis of gene or protein expression in rock habitats.

More generally, future work which aims to better understand interactions between microbial life and geological processes should focus more attention on understanding multiple simultaneous stresses. For example, it has recently been shown that iron limitation combined with microaerobic conditions can reduce temperature sensitivity in some organisms [144]. It is likely that many of these co-dependencies exist and will be common in diverse rock habitats. However, a systematic characterisation of these dependencies, and a biochemical understanding of what drives them, is lacking.

Appendix A

Chapter 5 Tables

Appendix A contains a list of proteins differentially regulated in *C. metallidurans* CH34 when grown in media at pH 8 compared to media at pH 7, as discussed in Chapter 5.

A.1 Proteins differentially regulated at pH 8

Table A.1 – Proteins differentially regulated in optimal media at pH 8 compared to at pH 7

Protein description	Protein name	Locus tag	No. peptides	Score	FC	P value
Up-regulated vs. pH 7						
Type IV pilus structural subunit	PilA	Rmet_0697	2	134	+2.1	5.2E-04
dITP/XTP pyrophosphatase	YggV	Rmet_0851	4	91	+2.4	4.3E-02
GGDEF family protein		Rmet_0867	5	66	+5.1	1.5E-02
Transcriptional regulator, TetR/AcrR-family		Rmet_0901	4	19	+2.0	6.8E-04
Putative branched-chain amino acid permease protein		Rmet_0953	4	31	+2.3	4.0E-02
Acyl-CoA dehydrogenase		Rmet_1852	6	79	+2.1	2.1E-02
Beta N-acetyl-glucosaminidase	NagZ	Rmet_2413	6	163	+8.7	4.5E-03
Tyrosine-based site-specific recombinase	Int	Rmet_2561	12	75	+2.0	2.4E-02
Acyl-CoA thioesterase	YbgC	Rmet_2679	2	64	+2.2	3.5E-02
Quinolinate synthase, subunit A	NadA	Rmet_2874	4	61	+2.4	3.2E-02
Heavy metal cation tricomponent efflux outer membrane porin	HmvC	Rmet_3836	6	24	+2.0	6.2E-03
Paraquat-inducible protein B	PqiB	Rmet_4088	5	26	+2.2	1.3E-02
ABC-type dipeptide/oligopeptide/nickel transport system, substrate binding protein	DppA	Rmet_4578	9	83	+2.3	9.6E-03
Undecaprenyl-phosphate 4-deoxy-4-formamido-L-arabinose transferase	ArnC	Rmet_4590	3	53	+2.2	2.6E-02
NAD-dependent epimerase/dehydratase		Rmet_4804	4	53	+2.5	2.4E-02
Conserved hypothetical protein		Rmet_5074	12	654	+2.2	1.5E-02
Transcriptional regulator, LysR family		Rmet_5106	6	34	+2.1	2.8E-03
Transcriptional regulator, LysR family		Rmet_5220	5	43	+4.6	4.2E-02
Flagellar filament structural protein	FliC2	Rmet_5252	14	1469	+4.8	3.2E-02
Putative glycerol-3-phosphate oxidase		Rmet_5444	8	38	+2.9	1.8E-02
P-type ATPase involved in Pb(II) resistance	PbrA	Rmet_5947	13	109	+4.3	7.9E-03
Down-regulated vs.pH 7						
Putative type-4 fimbrial biogenesis protein	PilY1	Rmet_0192	5	241	−2.0	3.8E-03
Tetratricopeptide TPR 2 repeat protein		Rmet_0292	8	134	−2.1	2.1E-03

Continued on next page

Table A.1 – Proteins differentially regulated in optimal media at pH 8 compared to at pH 7

Protein description	**Protein name**	**Locus tag**	**No. peptides**	**Score**	**FC**	**P value**
Putative glycine betaine/carnitine/choline ABC-type transporter		Rmet_0799	6	45	−3.4	3.2E-02
Peptidase S11		Rmet_1204	8	50	−2.1	4.5E-02
Sulfate transporter subunit	CysP	Rmet_1369	12	300	−3.4	4.0E-02
Isocitrate lyase	AceA	Rmet_1385	5	113	−4.3	2.9E-02
Pili assembly chaperone, required for type 1 fimbriae	FimC	Rmet_1666	4	218	−2.4	8.6E-03
Cytochrome d1, heme region	NirF	Rmet_2080	8	48	−2.7	8.0E-03
Conserved hypothetical protein		Rmet_2133	2	219	−2.2	7.4E-03
Hypothetical protein		Rmet_2170	2	19	−7.2	4.0E-02
50S ribosomal subunit protein L32	RpmF	Rmet_2432	7	164	−2.0	2.3E-02
DNA polymerase III chi subunit	HolC	Rmet_2806	2	20	−2.0	2.0E-02
Putative superfamily S-adenosyl-L-methionine-dependent methyl-transferase		Rmet_2828	5	57	−2.1	1.3E-02
Putative phosphonate ABC transporter, periplasmic phosphonate-binding protein	PtxB	Rmet_2994	27	2675	−2.0	1.1E-02
Conserved hypothetical protein		Rmet_3715	3	115	−3.1	4.1E-02
Alkaline phosphatase	PhoA1	Rmet_4084	19	1062	−2.6	5.0E-03
1-Cysteine peroxiredoxin		Rmet_4131	4	98	−2.7	4.1E-03
Amino acid processing enzyme		Rmet_4194	5	66	−2.0	3.6E-02
Transcriptional regulator, TraR/DksA family		Rmet_4453	2	16	−5.6	3.6E-03
Putative acid phosphatase protein	AcpA	Rmet_4809	3	69	−11.1	4.7E-04
Hypothetical protein		Rmet_4833	3	69	−3.2	2.4E-02
Acetoacetyl-CoA reductase	PhaB3	Rmet_5123	7	259	−2.1	1.6E-02
Extra-cytoplasmic solute receptor protein	Bug	Rmet_5294	5	50	−2.9	1.3E-02
Arylsulfatase-like enzyme	AslA	Rmet_5416	7	177	−2.2	1.7E-02
Conserved hypothetical protein						

Table A.1 – Proteins differentially regulated in optimal media at pH 8 compared to at pH 7

Appendix B

Chapter 6 Tables

The tables presented in Appendix B list the proteins which are differentially regulated in the various experimental treatments discussed in Chapter 6. Proteins are considered differentially regulated if they are 2-fold higher or lower than in the control i.e. the fold change (FC) is greater than 2 (up-regulated) or lower than 0.5 (down-regulated). Descriptions and functional annotations were derived from the MaGe database [172]. Proteins without a functional annotation in the MaGe database are classed as "unassigned".

B.1 Proteins differentially regulated in the "lowest iron" treatment

B.1.1 Up-regulated compared to the control

Table B.1 – Proteins up-regulated in "lowest iron" media compared to optimal media

Locus tag	Protein name	Description	No. peptides	Score	FC	P value
Amino acid synthesis and metabolism						
Rmet_2467	TrpB	Tryptophan synthase	4	377	3.4	4.8E-05
Rmet_5602		Putative threonine dehydratase	5	349	10.3	1.0E-04
Rmet_0398	GdhA	Glutamate dehydrogenase	11	979	3.0	5.8E-04
Rmet_4537	SerA2	D-3-phosphoglycerate dehydrogenase, NAD-binding	9	596	5.9	2.9E-07
Biosynthesis of cofactors, prosthetic groups, and carriers						
Rmet_1110	SbnH	Diaminopimelate decarboxylase implied in the biosynthesis of staphyloferrin B	9	695	13.8	7.9E-05
Rmet_1111	SbnG	2-dehydro-3-deoxyglucarate aldolase implied in the biosynthesis of staphyloferrin B	8	474	11.2	4.2E-04
Rmet_1112	SbnF	IucC-like protein implied in the biosynthesis of staphyloferrin B	17	1287	10.9	5.5E-06
Rmet_1113	SbnE	Siderophore synthetase component protein IucA-like implied in the biosynthesis of staphyloferrin B	15	994	10.5	6.6E-05
Rmet_1115	SbnC	IucC-like protein implied in the biosynthesis of staphyloferrin B	11	794	9.7	8.4E-06
Rmet_1116	SbnB	Ornithine cyclodeaminase implied in the biosynthesis of staphyloferrin B	26	2563	21.2	1.8E-06
Rmet_1117	SbnA	Cysteine synthase implied in the biosynthesis of staphyloferrin B	7	554	2.7	3.1E-03
Rmet_1118	AleB	Staphyloferrin B receptor	8	442	13.0	2.0E-04
Cell envelope						
Rmet_0712	OmpA	Outer membrane protein or related peptidoglycan-associated (lipo)protein	11	907	2.3	4.7E-04
Rmet_0917		Putative peptidoglycan binding protein containing LysM domain	9	769	3.0	2.2E-02
Rmet_1352	ComL	DNA uptake lipoprotein	4	214	2.0	1.4E-04

Continued on next page

Table B.1 – Proteins up-regulated in "lowest iron" media compared to optimal media

Locus tag	Protein name	Description	No. peptides	Score	FC	P value
Rmet_1455	YbbK	Putative protease, membrane anchored	11	982	4.1	1.5E-03
Rmet_4988	MetQ	DL-methionine ABC-type transporter	3	133	2.3	3.3E-04
Central intermediary metabolism						
Rmet_0967	GstI	Glutathione S-transferase	12	888	5.2	4.1E-05
Rmet_0992	Nit	Nitrilase	2	69	2.1	2.4E-02
DNA metabolism						
Rmet_6191	Bph2	Histone-like DNA-binding protein	2	94	2.2	2.7E-02
Energy metabolism						
Rmet_1093	Adh	Alcohol dehydrogenase, 1-propanol preferring	16	1304	2.2	5.4E-04
Rmet_1515	CbbG1	Glyceraldehyde-3-phosphate dehydrogenase A	8	585	3.3	1.3E-02
Rmet_2089	TalB	Transaldolase B	4	101	2.3	2.7E-03
Fatty acid and phospholipid metabolism						
Rmet_1200	PhaP	Phasin (PHA-granule associated protein)	27	3727	2.9	2.7E-05
Rmet_2643	Cfa	Cyclopropane-fatty-acyl-phospholipid synthase	5	258	6.4	3.7E-05
Phosphorus metabolism						
Rmet_2182	PstB	Phosphate transporter subunit	5	218	3.7	7.4E-03
Rmet_2992	PtxD	Phosphonate dehydrogenase (NAD-dependent phosphite dehydrogenase)	12	859	2.4	9.5E-03
Protein fate						
Rmet_1026	IscU	FeS cluster assembly scaffold protein	9	570	2.2	4.7E-03
Rmet_1429	Dmf	Polypeptide or peptide deformylase	2	77	2.2	9.0E-03
Protein synthesis						
Rmet_0831	AlaS	Alanyl-tRNA synthetase	19	1089	2.4	1.5E-04
Rmet_1160	ThrS	Threonyl-tRNA synthetase	20	1366	4.0	1.1E-05
Rmet_5930	FusA2	Elongation factor G2	16	1795	3.3	2.5E-03
Purines, pyrimidines, nucleosides and nucleotides						
Rmet_3087	NrdB	Ribonucleoside-diphosphate reductase beta subunit	6	263	2.5	1.8E-03
Rmet_3088	NrdA	Ribonucleoside-diphosphate reductase alpha subunit	31	2313	2.3	1.1E-04
Regulation						
Rmet_0001	DnaA	Chromosomal replication initiator protein DnaA	2	123	11.7	7.9E-03
Rmet_2425	RpoE	RNA polymerase sigma 24 (sigma E) factor	2	89	30.1	2.7E-02

Continued on next page

Table B.1 – Proteins up-regulated in "lowest iron" media compared to optimal media

Locus tag	Protein name	Description	No. peptides	Score	FC	P value
Rmet_5746	Fur1	Ferric uptake regulator	6	418	4.5	6.9E-05
Transcription						
Rmet_3564	Fmt	Methionyl-tRNA formyltransferase	3	123	4.9	4.9E-04
Rmet_4773		Putative endoribonuclease L-PSP	2	135	4.1	4.8E-05
Transport and binding proteins						
Rmet_1121	AcrD	Aminoglycoside/multidrug efflux system	4	209	9.4	3.5E-04
Rmet_2277	ExbA	TonB-like protein, membrane spanning	3	204	26.2	1.0E-05
Rmet_2279	ExbD1	Biopolymer transport protein	6	484	13.9	4.0E-05
Rmet_5376	HmuT	Hemin-binding periplasmic protein hmuT precursor	8	770	6.2	1.2E-04
Rmet_5378	HmuV	Putative Hemin ABC transport system, ATP-binding protein	7	371	6.6	7.2E-04
Rmet_5890	FeoB	Fe^{2+} transport system protein B	5	269	5.1	1.5E-03
Unassigned						
Rmet_0016		Conserved hypothetical protein	3	214	7.2	1.3E-03
Rmet_0310		Putative intracellular protease/amidase/DJ-1/PfpI family	11	1465	3.4	4.8E-04
Rmet_0421		Conserved hypothetical protein	12	1251	2.7	3.4E-03
Rmet_0534		Conserved hypothetical protein	3	97	2.8	7.2E-03
Rmet_0562	AckA2	Acetate kinase	8	440	2.8	1.5E-02
Rmet_0838	PiuC	PKHD-type hydroxylase (Iron-uptake factor)	6	379	5.1	3.2E-03
Rmet_1063	TrxB	Thioredoxin reductase	4	277	3.9	4.5E-03
Rmet_1518	CbbA2	Fructose-bisphosphate aldolase	6	506	2.7	1.3E-02
Rmet_1695		Conserved hypothetical protein; putative exported protein	3	257	4.8	3.6E-04
Rmet_1704		Conserved hypothetical protein; putative exported protein	8	754	2.2	8.4E-04
Rmet_1790	GlcD	Glycolate oxidase subunit	4	253	3.3	6.2E-04
Rmet_2278	ExbB	Biopolymer transport	7	543	3.2	1.7E-03
Rmet_2614		Putative GTP cyclohydrolase	5	411	3.1	3.0E-04
Rmet_2636		Thioredoxin domain-containing protein	5	286	2.2	3.0E-03
Rmet_2875	Scd	Fatty-acid desaturase	4	256	6.6	2.1E-03
Rmet_3358		Conserved hypothetical protein	2	86	8.0	1.1E-03
Rmet_3904	PrkA	Serine protein kinase	10	487	6.0	3.5E-04
Rmet_4200		Conserved hypothetical protein	3	200	5.3	2.3E-03
Rmet_4347		Alkylhydroperoxidase AhpD core	2	73	2.0	2.1E-02

Continued on next page

Table B.1 – Proteins up-regulated in "lowest iron" media compared to optimal media

Locus tag	Protein name	Description	No. peptides	Score	FC	P value
Rmet_4545		Conserved hypothetical protein	3	152	2.3	4.6E-03
Rmet_4679		Conserved hypothetical protein, Ycil-related domain	2	138	2.7	4.3E-02
Rmet_5374		Hypothetical protein	7	618	14.1	1.7E-05
Rmet_5375	HmuS	Hemin transport protein; putative Hemin-degrading	8	571	6.2	1.5E-04
Rmet_5405		Conserved hypothetical protein; putative periplasmic protein	8	703	3.8	1.0E-04
Rmet_5416	AslA	Arylsulfatase-like enzyme	18	1366	2.5	1.3E-04
Rmet_5578		Conserved hypothetical protein; putative signal peptide	11	733	10.5	1.2E-05
Rmet_5638		ABC-type transporter, periplasmic component	11	879	13.5	2.1E-05
Rmet_5639		Conserved hypothetical protein; putative exported protein	2	124	8.1	2.0E-04
Rmet_5753		Conserved hypothetical protein	7	430	2.8	2.2E-02

Table B.1 – Proteins up-regulated in "lowest iron" media compared to optimal media

B.1.2 Down-regulated compared to the control

Table B.2 – Proteins down-regulated in "lowest iron" media compared to optimal media

Locus tag	Protein name	Description	No. peptides	Score	FC	P value
Amino acid synthesis and metabolism						
Rmet_0140	ArgB	Acetylglutamate kinase	9	598	0.35	1.4E-02
Rmet_0911	IlvI	Acetolactate synthase III, large subunit	7	414	0.45	2.2E-03
Rmet_2815	CysO	Protein involved in cysteine metabolism	3	149	0.20	5.2E-03
Rmet_2473	LeuD	3-isopropylmalate isomerase subunit	7	357	0.24	4.0E-04
Rmet_2475	LeuC	3-isopropylmalate isomerase subunit, dehydratase component	8	630	0.36	2.1E-04
Rmet_3241	HisI	Phosphoribosyl-AMP cyclohydrolase	2	105	0.38	6.8E-03
Rmet_3262	GltD	Glutamate synthase, 4Fe-4S protein, small subunit	18	1298	0.33	2.1E-04
Rmet_3263	GltB	Glutamate synthase, large subunit	43	2962	0.27	8.5E-06
Biological processes						
Rmet_1206	YkgE	Putative hydroxyacid oxidoreductase (Fe-S centre)	2	120	0.09	6.4E-03
Biosynthesis of cofactors, prosthetic groups, and carriers						
Rmet_0061	LipA	Lipoate synthase	2	93	0.45	6.7E-03
Rmet_0114	BioA	7,8-diaminopelargonic acid synthase, PLP-dependent	6	351	0.43	1.5E-03
Rmet_0117	BioB	Biotin synthase	14	936	0.13	9.6E-06
Rmet_0162	ThiC	Thiamin (pyrimidine moiety) biosynthesis protein	13	866	0.31	2.2E-03
Rmet_1192	FolD	Bifunctional protein	4	200	0.29	3.0E-03
Rmet_2106	IspG	1-hydroxy-2-methyl-2-(E)-butenyl 4-diphosphate synthase	3	227	0.26	1.5E-03
Rmet_2785	CobT	Nicotinate-nucleotide dimethylbenzimidazole-P phophoribosyl transferase	2	118	0.49	3.3E-02
Rmet_2868	IspH	1-hydroxy-2-methyl-2-(E)-butenyl 4-diphosphate reductase, 4Fe-4S protein	3	145	0.11	5.6E-05
Cell envelope						
Rmet_0533	KdsB	3-deoxy-manno-octulosonate cytidylyltransferase	3	95	0.30	4.6E-02
Rmet_2186	GlmM	Phosphoglucosamine mutase	8	544	0.31	9.0E-03
Cellular process						
Rmet_0458	UspA1	Universal stress protein, UspA family	7	535	0.37	3.9E-04

Continued on next page

Table B.2 – Proteins down-regulated in "lowest iron" media compared to optimal media

Locus tag	Protein name	Description	No. peptides	Score	FC	P value
Rmet_3124	FtsA	ATP-binding cell division protein	5	356	0.30	6.2E-04
Rmet_3226	SspB	ClpXP protease specificity-enhancing factor	3	170	0.39	7.1E-05
Rmet_0034	MinD	Septum site-determining protein	5	255	0.43	3.3E-02
Rmet_4395	UspA9	Universal stress protein	7	557	0.36	2.8E-04
Rmet_4862		Conserved hypothetical protein	2	104	0.26	9.6E-03
Central intermediary metabolism						
Rmet_0172	MetF	5,10-methylenetetrahydrofolate reductase	2	66	0.38	3.4E-04
Rmet_2513		Aminotransferase family protein	7	289	0.47	6.4E-03
Rmet_3419	SoxX	Sulfur oxidation protein	2	218	0.19	6.1E-03
Rmet_3420	SoxA	Sulfur oxidation protein	5	262	0.50	2.5E-03
Rmet_4943		Putative iron-containing alcohol dehydrogenase	2	105	0.47	2.8E-02
DNA metabolism						
Rmet_1189	XthA2	Exodeoxyribonuclease III	2	129	0.01	2.2E-05
Rmet_1426	Smc	Chromosome segregation ATPase	5	339	0.47	4.1E-03
Rmet_2617	XseB	Exonuclease VII small subunit	2	99	0.50	7.9E-03
Energy metabolism						
Rmet_0222	NppD	2-nitropropane dioxygenase	2	154	0.36	3.9E-02
Rmet_0931	NuoE	NADH dehydrogenase, chain E	2	130	0.21	5.0E-03
Rmet_0932	NuoF	NADH:ubiquinone oxidoreductase, chain F	7	395	0.32	1.5E-03
Rmet_0933	NuoG	NADH dehydrogenase, chain G	22	1527	0.38	3.1E-05
Rmet_0987		Cytochrome c, class IC 1	4	317	0.13	1.3E-04
Rmet_0988		Cytochrome c553	6	401	0.16	1.7E-02
Rmet_1146	EtfD	Electron transfer flavoprotein-ubiquinone oxidoreductase	10	711	0.43	4.0E-05
Rmet_1285	HypB1	GTP hydrolase	2	74	0.43	1.7E-02
Rmet_1297	HoxG	Hydrogenase 1	24	1369	0.37	7.9E-05
Rmet_1522	HoxF	NAD-reducing hydrogenase diaphorase moiety large subunit	10	799	0.25	2.1E-03
Rmet_1524	HoxY	NAD-reducing hydrogenase	4	224	0.47	2.3E-02
Rmet_1539	HypD2	Protein required for maturation of hydrogenases	7	342	0.26	9.5E-04
Rmet_2273	FumA	Fumarate hydratase class I	18	1326	0.45	4.2E-04
Rmet_2483	SdhB	Succinate dehydrogenase, FeS subunit	15	996	0.43	1.3E-03
Rmet_2492	AcnA2	Aconitate hydratase 1	26	1915	0.47	3.9E-03

Continued on next page

Table B.2 – Proteins down-regulated in "lowest iron" media compared to optimal media

Locus tag	Protein name	Description	No. peptides	Score	FC	P value
Rmet_3228	PetC	Cytochrome c1 precursor	6	470	0.48	2.2E-04
Rmet_3230	PetA	Ubiquinol-cytochrome c reductase, iron-sulfur subunit	5	302	0.39	1.3E-03
Fatty acid and phospholipid metabolism						
Rmet_0106	AtoB	Acetyl-CoA acetyltransferase	5	320	0.37	4.1E-02
Rmet_1087	AccA	Acetyl-CoA carboxylase, carboxytransferase, alpha subunit	5	355	0.40	1.4E-03
Rmet_2429	FabD	Malonyl-CoA-acyl-carrier-protein transacylase	2	191	0.42	2.3E-02
Mobile and extrachromosomal element functions						
Rmet_1313	TmoD	Toluene-4-monooxygenase system protein D	3	241	0.43	3.4E-03
Rmet_6062	ParB	Plasmid replication partition related protein	2	163	0.16	2.8E-02
Protein fate						
Rmet_5411		Putative membrane Zinc metallopeptidase	3	129	0.08	2.7E-03
Protein synthesis						
Rmet_0411	RpsI	30S ribosomal subunit protein S9	7	610	0.37	3.5E-03
Rmet_0748	RpsP	30S ribosomal subunit protein S16	2	155	0.44	8.9E-03
Rmet_1162	RpmI	50S ribosomal subunit protein L35	2	86	0.34	3.2E-02
Rmet_1163	RplT	50S ribosomal subunit protein L20	2	176	0.38	7.9E-03
Rmet_2870	RpmB	50S ribosomal subunit protein L28	4	279	0.16	2.1E-04
Rmet_3305	RplE	50S ribosomal subunit protein L5	8	476	0.45	1.3E-02
Purines, pyrimidines, nucleosides and nucleotides						
Rmet_0942		Putative ADP-ribose pyrophosphatase	2	123	0.13	2.2E-02
Rmet_2739	PyrX	Dihydroorotase	3	116	0.06	3.8E-02
Rmet_2741	PyrR	Pyrimidine operon regulatory protein	4	309	0.27	3.4E-02
Rmet_3238		Diadenosine tetraphosphate hydrolase	3	102	0.01	4.2E-02
Regulation						
Rmet_5816	CspA	Major cold shock protein	2	231	0.48	7.4E-03
Rmet_6162		Transcriptional regulator, XRE family	2	85	0.18	4.3E-02
Transport and binding proteins						
Rmet_0928	NuoB	NADH dehydrogenase chain B	3	278	0.17	2.4E-03
Rmet_1184	Bug	Extra-cytoplasmic Solute Receptor	4	353	0.47	6.9E-03
Rmet_3076	Bug	Extra-cytoplasmic Solute Receptor	2	178	0.49	2.2E-02
Rmet_3237	TatA	TatABCE protein translocation system subunit	2	160	0.02	2.1E-02

Continued on next page

Table B.2 – Proteins down-regulated in "lowest iron" media compared to optimal media

Locus tag	Protein name	Description	No. peptides	Score	FC	P value
Rmet_3671	Bug	Extra-cytoplasmic Solute Receptor	2	56	0.01	5.3E-03
Rmet_6339		Cupin 2 conserved barrel domain protein	2	82	0.24	4.0E-04
Unassigned						
Rmet_0086		Putative sulfurtransferase	2	74	0.50	1.6E-02
Rmet_0097		Conserved hypotethical protein	2	74	0.22	7.5E-04
Rmet_0367		Putative Fe-S oxidoreductase FAD/FMN-containing dehydrogenase oxidoreductase protein	5	353	0.35	1.5E-03
Rmet_0408		Conserved hypothetical protein	4	208	0.45	2.9E-04
Rmet_0492		Conserved hypothetical protein	3	210	0.11	6.7E-03
Rmet_0673	PilL2	Type IV pilus protein histidine kinase/response regulator	4	225	0.11	3.4E-05
Rmet_0825		Conserved hypothetical protein; putative membrane protein	2	111	0.46	8.3E-03
Rmet_0972		Putative aminoglycoside phosphotransferase	4	227	0.22	1.6E-02
Rmet_1368	SerB	Phosphoserine phosphatase	4	236	0.45	2.3E-03
Rmet_1452		Conserved hypothetical protein	2	106	0.07	3.7E-02
Rmet_2041	CcoP	cbb3-type cytochrome oxidase, diheme subunit IV	6	375	0.25	1.8E-04
Rmet_2043	CcoO	cbb3-type cytochrome oxidase, monoheme subunit II	4	203	0.21	2.5E-04
Rmet_2125		L-carnitine dehydratase/bile acid-inducible protein	2	126	0.41	5.0E-02
Rmet_2436	SohB	Peptidase S49, periplasmic serine protease	2	62	0.21	1.4E-03
Rmet_2494		Conserved hypothetical protein	5	262	0.41	6.3E-03
Rmet_2747	HemY	Uncharacterized enzyme of heme biosynthesis	2	63	0.10	1.4E-04
Rmet_2754	ldcC	Arginine/lysine/ornithine decarboxylase	8	396	0.27	1.9E-04
Rmet_2790		Conserved hypothetical protein	3	267	0.09	3.4E-04
Rmet_2890		Putative glyoxalase	2	87	0.05	1.5E-02
Rmet_3159	HipO	Hippurate hydrolase	2	134	0.40	1.9E-02
Rmet_3284		Cytochrome c4	5	425	0.35	6.5E-03
Rmet_3321		Dienelactone hydrolase	3	298	0.29	5.6E-04
Rmet_3424		Cytochrome c551/c552	4	358	0.26	6.6E-04
Rmet_3665		Hypothetical protein	8	604	0.48	4.8E-02
Rmet_4030		Putative glyoxalase or dioxygenase	2	69	0.42	9.5E-03
Rmet_4809	AcpA	Putative acid phosphatase protein	3	144	0.06	3.8E-02
Rmet_5074		Conserved hypothetical protein	7	363	0.32	1.0E-05

Continued on next page

Table B.2 – Proteins down-regulated in "lowest iron" media compared to optimal media

Locus tag	Protein name	Description	No. peptides	Score	FC	P value
Rmet_5645	Adh	Alcohol dehydrogenase, zinc-binding	6	291	0.20	1.0E-02

Table B.2 – Proteins down-regulated in "lowest iron" media compared to optimal media

B.2 Proteins differentially regulated in the "low iron" condition

B.2.1 Up-regulated compared to the control

Table B.3 – Proteins up-regulated in "low iron" media compared to optimal media

Locus tag	Protein name	Description	No. peptides	Score	FC	P value
Amino acid synthesis and metabolism						
Rmet_0398	GdhA	Glutamate dehydrogenase	11	979	2.3	8.5E-04
Rmet_0681	GlnB	Regulatory protein P-II for glutamine synthetase	5	362	2.7	1.9E-03
Rmet_2467	TrpB	Tryptophan synthase, beta subunit	4	377	2.1	1.8E-02
Rmet_3248	HisD	Bifunctional histidinal dehydrogenase and histidinol dehydrogenase	3	105	2.0	8.1E-03
Rmet_4537	SerA2	D-3-phosphoglycerate dehydrogenase, NAD-binding	9	596	3.3	3.8E-05
Rmet_5602		Putative threonine dehydratase	5	349	2.6	2.3E-03
Biological processes						
Rmet_1382	RraA	Ribonuclease E inhibitor protein	2	66	3.5	1.5E-03
Biosynthesis of cofactors, prosthetic groups, and carriers						
Rmet_0839		(S)-2-hydroxy-acid oxidase 1	6	410	2.6	3.6E-03
Rmet_1110	SbnH	Diaminopimelate decarboxylase implied in the biosynthesis of staphyloferrin B	9	695	12.6	2.7E-04
Rmet_1111	SbnG	2-dehydro-3-deoxyglucarate aldolase implied in the biosynthesis of staphyloferrin B	8	474	15.7	8.9E-05
Rmet_1112	SbnF	IucC-like protein implied in the biosynthesis of staphyloferrin B	17	1287	14.2	2.0E-05
Rmet_1113	SbnE	Siderophore synthetase component protein IucA-like implied in the biosynthesis of staphyloferrin B	15	994	17.1	3.2E-05
Rmet_1115	SbnC	IucC-like protein implied in the biosynthesis of staphyloferrin B	11	794	9.7	1.0E-04
Rmet_1116	SbnB	Ornithine cyclodeaminase implied in the biosynthesis of staphyloferrin B	26	2563	17.5	1.5E-06
Rmet_1117	SbnA	Cysteine synthase implied in the biosynthesis of staphyloferrin B	7	554	7.6	1.2E-03
Rmet_1118	AleB	Staphyloferrin B receptor	8	442	8.5	2.8E-04

Continued on next page

Table B.3 – Proteins up-regulated in "low iron" media compared to optimal media

Locus tag	Protein name	Description	No. peptides	Score	FC	P value
Rmet_2689	RibC	Riboflavin synthase alpha chain	3	221	2.2	8.1E-04
Cell envelope						
Rmet_0252	GrxC	Glutaredoxin 3	2	106	2.6	8.1E-03
Rmet_0917		Putative peptidoglycan binding protein containing LysM domain	9	769	2.0	2.9E-02
Rmet_1455	YbbK	Putative protease, membrane anchored	11	982	4.0	1.6E-03
Cellular process						
Rmet_2957	Gst-1	Glutathione S-transferase	2	99	2.9	1.3E-02
Central intermediary metabolism						
Rmet_0967	GstI	Glutathione S-transferase	12	888	4.2	1.4E-05
Rmet_1574	LdcA	L,D-carboxypeptidase A	2	80	3.0	7.4E-03
DNA metabolism						
Rmet_0315	Ssb1	Single-stranded DNA-binding protein (Helix-destabilizing protein)	3	348	2.7	2.1E-05
Energy metabolism						
Rmet_1515	CbbG1	Glyceraldehyde-3-phosphate dehydrogenase A	8	585	2.1	2.6E-02
Rmet_2089	TalB	Transaldolase B	4	101	3.1	2.9E-03
Fatty acid and phospholipid metabolism						
Rmet_1863		Acyl-CoA synthetase (AMP-forming)/AMP-acid ligase II	2	125	2.2	3.2E-02
Rmet_2643	Cfa	Cyclopropane-fatty-acyl-phospholipid synthase	5	258	4.5	7.0E-06
Phosphorus metabolism						
Rmet_2992	PtxD	Phosphonate dehydrogenase	12	859	2.4	3.8E-03
Protein fate						
Rmet_1026	IscU	FeS cluster assembly scaffold protein	9	570	2.2	1.5E-02
Protein synthesis						
Rmet_5930	FusA2	Elongation factor G 2	16	1795	2.1	5.3E-03
Purines, pyrimidines, nucleosides and nucleotides						
Rmet_3087	NrdB	Ribonucleoside-diphosphate reductase beta subunit	6	263	3.7	1.9E-04
Rmet_3088	NrdA	Ribonucleoside-diphosphate reductase alpha subunit	31	2313	2.9	4.0E-05
Regulation						
Rmet_2425	RpoE	RNA polymerase sigma 24 (sigma E) factor	2	89	31.1	6.0E-03
Rmet_5746	Fur1	Ferric uptake regulator	6	418	6.9	1.3E-06
Transcription						

Continued on next page

Table B.3 – Proteins up-regulated in "low iron" media compared to optimal media

Locus tag	Protein name	Description	No. peptides	Score	FC	P value
Rmet_2135	Rho	Transcription termination factor Rho	11	602	3.4	5.0E-03
Rmet_4773		Putative endoribonuclease L-PSP	2	135	3.7	1.2E-03
Transport and binding proteins						
Rmet_1121	AcrD	Aminoglycoside/multidrug efflux system	4	209	5.3	5.3E-03
Rmet_2277	ExbA	TonB-like protein, membrane spanning	3	204	13.5	3.5E-04
Rmet_2279	ExbD1	Biopolymer transport protein	6	484	9.5	9.1E-06
Rmet_5376	HmuT	Hemin-binding periplasmic protein	8	770	8.1	1.2E-05
Rmet_5378	HmuV	Putative Hemin ABC transport system, ATP-binding protein	7	371	7.6	1.7E-04
Rmet_5890	FeoB	Fe^{2+} transport system protein B	5	269	5.2	1.1E-04
Unassigned						
Rmet_0016		Conserved hypothetical protein	3	214	6.8	1.4E-02
Rmet_0186	GlmU	Fused N-acetyl glucosamine-1-phosphate uridyltransferase	4	145	3.8	4.8E-02
Rmet_0310		Putative intracellular protease/amidase/DJ-1/PfpI family	11	1465	4.4	9.2E-05
Rmet_0838	PiuC	PKHD-type hydroxylase (Iron-uptake factor)	6	379	4.6	2.7E-03
Rmet_1063	TrxB1	Thioredoxin reductase	4	277	3.0	1.1E-03
Rmet_1109		Conserved hypothetical protein	3	169	13.4	2.3E-03
Rmet_1157		Hydrolase, alpha/beta fold family	2	97	6.3	4.2E-02
Rmet_1696		Conserved hypothetical protein; putative exported protein	10	702	2.1	2.0E-02
Rmet_1790	GlcD	Glycolate oxidase subunit GlcD	4	253	2.2	1.0E-02
Rmet_2022		Enoyl-CoA hydratase/isomerase	4	160	2.2	6.6E-04
Rmet_2278	ExbB	Biopolymer transport protein	7	543	2.8	3.9E-03
Rmet_2632		Conserved hypothetical protein	2	105	2.9	1.6E-02
Rmet_2875	Scd	Fatty-acid desaturase	4	256	3.0	1.8E-03
Rmet_3904	PrkA	Serine protein kinase	10	487	3.4	2.9E-04
Rmet_4167	Ttg2	ABC-type transporter involved in toluene tolerance, periplasmic component	4	245	2.3	2.3E-03
Rmet_4200		Conserved hypothetical protein	3	200	4.1	1.6E-02
Rmet_5004		Antibiotic biosynthesis monooxygenase	2	78	2.3	1.9E-03
Rmet_5374		Hypothetical protein	7	618	12.7	5.3E-05
Rmet_5375	HmuS	Hemin transport protein	8	571	5.1	9.8E-05
Rmet_5562		Histone-like nucleoid-structuring protein H-NS	2	249	2.6	4.2E-02

Continued on next page

Table B.3 – Proteins up-regulated in "low iron" media compared to optimal media

Locus tag	Protein name	Description	No. peptides	Score	FC	P value
Rmet_5578		Conserved hypothetical protein; putative signal peptide	11	733	12.2	5.3E-07
Rmet_5638		ABC-type transporter, periplasmic component	11	879	8.5	7.8E-05
Rmet_5639		Conserved hypothetical protein; putative exported protein	2	124	7.5	4.8E-04
Rmet_5796		D-isomer specific 2-hydroxyacid dehydrogenase, NAD-binding	3	149	2.4	1.8E-03
Rmet_5936		Putative monooxygenase with luciferase-like ATPase activity	2	80	2.4	6.1E-03

Table B.3 – Proteins up-regulated in "low iron" media compared to optimal media

B.2.2 Down-regulated compared to the control

Table B.4 – Proteins down-regulated in "low iron" media compared to optimal media

Locus tag	Protein name	Description	No. peptides	Score	FC	P value
Amino acid synthesis and metabolism						
Rmet_1967	AatA	Aspartate aminotransferase	4	229	0.50	4.4E-02
Rmet_2195	CarA	Carbamoyl phosphate synthetase small subunit, glutamine amidotransferase	4	228	0.43	1.5E-02
Rmet_2816	CysI	Sulfite reductase, beta subunit (hemoprotein with two 4Fe-4S domains)	9	546	0.38	5.5E-03
Rmet_2815	CysO	Protein involved in cysteine metabolism	3	149	0.24	1.1E-02
Rmet_3241	HisI	Phosphoribosyl-AMP cyclohydrolase	2	105	0.49	3.6E-02
Rmet_3263	GltB	Glutamate synthase, large subunit	43	2962	0.43	6.2E-04
Biosynthesis of cofactors, prosthetic groups, and carriers						
Rmet_0114	BioA	7,8-diaminopelargonic acid synthase, PLP-dependent	6	351	0.48	4.4E-04
Rmet_0115	BioF	8-amino-7-oxononanoate synthase	2	128	0.22	4.3E-05
Rmet_0117	BioB	Biotin synthase	14	936	0.20	8.3E-07
Rmet_0162	ThiC	Thiamin biosynthesis protein	13	866	0.40	7.8E-04
Rmet_2106	IspG	1-hydroxy-2-methyl-2-(E)-butenyl 4-diphosphate synthase	3	227	0.30	1.4E-03
Rmet_2785	CobT	Nicotinate-nucleotide dimethylbenzimidazole-P phophoribosyl transferase	2	118	0.40	2.2E-02
Rmet_2868	IspH	1-hydroxy-2-methyl-2-(E)-butenyl 4-diphosphate reductase, 4Fe-4S protein	3	145	0.20	3.2E-04
Cell envelope						
Rmet_0533	KdsB	3-deoxy-manno-octulosonate cytidylyltransferase	3	95	0.45	9.8E-03
Rmet_0727	RfaE	Fused heptose 7-phosphate kinase; heptose 1-phosphate adenyltransferase	2	158	0.35	2.9E-03
Rmet_3250	MurA	UDP-N-acetylglucosamine 1-carboxyvinyltransferase	4	294	0.49	7.6E-03
Cellular process						
Rmet_0458	UspA1	Universal stress protein, UspA family	7	535	0.41	9.1E-04
Rmet_2935	PilU	Type IV pilus twitching motility protein	3	104	0.48	2.6E-02

Continued on next page

Table B.4 – Proteins down-regulated in "low iron" media compared to optimal media

Locus tag	Protein name	Description	No. peptides	Score	FC	P value
Rmet_3124	FtsA	ATP-binding cell division protein	5	356	0.47	1.6E-02
Rmet_3226	SspB	ClpXP protease specificity-enhancing factor	3	170	0.48	2.2E-02
Rmet_3272	PilM	Type IV pilus assembly protein PilM	2	101	0.42	1.8E-03
Rmet_3506	GidA	Glucose-inhibited cell-division protein	2	168	0.43	1.6E-02
Rmet_4395	UspA9	Universal stress protein	7	557	0.21	2.3E-05
DNA metabolism						
Rmet_0998	RecN	Recombination and repair protein	2	112	0.45	1.7E-02
Energy metabolism						
Rmet_0932	NuoF	NADH:ubiquinone oxidoreductase, chain F	7	395	0.39	1.3E-02
Rmet_0933	NuoG	NADH dehydrogenase chain G	22	1527	0.46	3.0E-04
Rmet_0987		Cytochrome c, class IC 1	4	317	0.29	2.7E-03
Rmet_0988		Cytochrome c553	6	401	0.29	3.9E-02
Rmet_1285	HypB1	GTP hydrolase	2	74	0.49	2.9E-02
Rmet_1522	HoxF	NAD-reducing hydrogenase diaphorase moiety large subunit	10	799	0.37	2.7E-02
Rmet_3230	PetA	Ubiquinol-cytochrome c reductase, iron-sulfur subunit	5	302	0.49	6.7E-04
Rmet_5312	Cpo	Non-heme chloroperoxidase	4	313	0.50	1.6E-02
Fatty acid and phospholipid metabolism						
Rmet_1087	AccA	Acetyl-CoA carboxylase, carboxytransferase, alpha subunit	5	355	0.34	1.3E-03
Mobile and extrachromosomal element functions						
Rmet_1313	TmoD	Toluene-4-monooxygenase system protein D	3	241	0.44	1.3E-02
Rmet_6316	ParB	ParB involved in chromosome partitioning	2	55	0.37	2.9E-02
Protein synthesis						
Rmet_0411	RpsI	30S ribosomal subunit protein S9	7	610	0.47	9.0E-03
Rmet_2455	RpsU1	30S ribosomal subunit protein S21	2	113	0.40	9.2E-03
Rmet_2869	FkpB	FKBP-type peptidyl-prolyl cis-trans isomerase	2	175	0.47	3.2E-03
Rmet_2870	RpmB	50S ribosomal subunit protein L28	4	279	0.41	3.3E-02
Rmet_3302	RplF	50S ribosomal subunit protein L6	14	1054	0.49	3.5E-03
Rmet_3308	RpsQ	30S ribosomal subunit protein S17	3	253	0.34	1.2E-02
Rmet_3335	RplL	50S ribosomal subunit protein L7/L12	11	980	0.40	1.9E-03
Rmet_5623		Peptidylprolyl isomerase, FKBP-type	3	216	0.47	3.3E-02
Purines, pyrimidines, nucleosides and nucleotides						

Continued on next page

Table B.4 – Proteins down-regulated in "low iron" media compared to optimal media

Locus tag	Protein name	Description	No. peptides	Score	FC	P value
Rmet_0150	PyrE	Orotate phosphoribosyltransferase	4	273	0.40	1.7E-02
Rmet_0942		Putative ADP-ribose pyrophosphatase	2	123	0.07	9.4E-03
Rmet_2739	PyrX	Dihydroorotase	3	116	0.07	3.8E-02
Transport and binding proteins						
Rmet_0928	NuoB	NADH dehydrogenase chain B	3	278	0.41	4.7E-02
Rmet_3237	TatA	TatABCE protein translocation system subunit	2	160	0.03	4.1E-02
Rmet_5682	NimB	Heavy metal cation tricomponent efflux membrane fusion protein	6	358	0.45	1.6E-04
Rmet_6339		Cupin 2 conserved barrel domain protein (0rf25)	2	82	0.40	1.7E-03
Unassigned						
Rmet_0097		Conserved hypotethical protein	2	74	0.22	1.1E-02
Rmet_0367		Putative Fe-S oxidoreductase FAD/FMN-containing dehydrogenase oxidoreductase protein	5	353	0.49	2.6E-03
Rmet_0665	LemA	LemA like protein	2	67	0.11	3.6E-02
Rmet_0718	TyrA	Prephenate dehydrogenase	2	84	0.39	1.4E-02
Rmet_0904		Glycosyltransferase, group 1	8	421	0.48	7.2E-03
Rmet_1368	SerB	Phosphoserine phosphatase	4	236	0.48	4.2E-03
Rmet_1600		Conserved hypothetical protein; putative exported protein	4	224	0.25	5.1E-03
Rmet_2041	CcoP	cbb3-type cytochrome oxidase, diheme subunit IV	6	375	0.43	2.2E-02
Rmet_2043	CcoO	cbb3-type cytochrome oxidase, monoheme subunit II	4	203	0.40	2.5E-02
Rmet_2436	SohB	Peptidase S49, periplasmic serine protease (ClpP class)	2	62	0.24	2.2E-02
Rmet_2890		Putative glyoxalase	2	87	0.11	2.9E-02
Rmet_3075		Conserved hypothetical protein; putative exported protein	2	72	0.46	4.5E-03
Rmet_3321		Dienelactone hydrolase	3	298	0.41	1.7E-02
Rmet_3424		cytochrome c551/c552	4	358	0.36	8.0E-03
Rmet_3473		Cytochrome c family protein	7	420	0.49	1.4E-03
Rmet_4584		Conserved hypothetical protein	2	162	0.26	2.4E-02
Rmet_5074		Conserved hypothetical protein	7	363	0.44	1.3E-04
Rmet_5645	Adh	Alcohol dehydrogenase, zinc-binding	6	291	0.28	8.6E-03

Table B.4 – Proteins down-regulated in "low iron" media compared to optimal media

B.3 Proteins differentially regulated in the "lowest phosphorus" treatment

B.3.1 Up-regulated compared to the control

Table B.5 – Proteins up-regulated in "lowest phosphorus" media compared to optimal media

Locus tag	Protein name	Description	Score	No. peptides	FC	P value
Amino acid synthesis and metabolism						
Rmet_0242	GshA	Glutamate-cysteine ligase	7	384	2.3	6.7E-03
Rmet_0398	GdhA	Glutamate dehydrogenase	11	979	2.0	6.9E-04
Rmet_0681	GlnB	Regulatory protein P-II for glutamine synthetase	5	362	3.2	7.8E-05
Rmet_1766	GadB	Glutamate decarboxylase B, PLP-dependent	16	1343	3.2	1.1E-04
Rmet_2862	ArgD	Bifunctional N-succinyldiaminopimelate-aminotransferase/acetylornithine transaminase protein	12	753	2.3	4.2E-03
Biological processes						
Rmet_1009	RutE	Oxidoreductase subunit of the alternative pyrimidine degradation pathway	4	277	2.3	1.7E-02
Rmet_1382	RraA	Ribonuclease E inhibitor protein	2	66	2.4	4.8E-03
Rmet_3645		Carboxymethylenebutenolidase hydrolase	5	405	2.1	9.1E-03
Rmet_4084	PhoA1	Alkaline phosphatase	10	665	18.1	1.8E-04
Rmet_4085	PhoA2	Alkaline phosphatase	6	451	11.5	3.6E-06
Rmet_4131		1-Cysteine peroxiredoxin	2	223	9.6	4.2E-05
Biosynthesis of cofactors, prosthetic groups, and carriers						
Rmet_0127	YjiA	Cobalamin synthesis protein	9	585	4.5	1.1E-03
Cell envelope						
Rmet_0712	OmpA	Outer membrane protein or related peptidoglycan-associated (lipo)protein	11	907	2.7	3.6E-04
Rmet_1685		Putative HlyD family secretion protein	6	301	2.4	1.8E-03
Rmet_2732	RbfC	dTDP-4-deoxyrhamnose-3,5-epimerase	7	402	3.0	2.2E-03
Rmet_4192	PlcN	Phospholipase C	29	2461	17.5	1.8E-06

Continued on next page

Table B.5 – Proteins up-regulated in "lowest phosphorus" media compared to optimal media

Locus tag	Protein name	Description	No. peptides	Score	FC	P value
Cellular process						
Rmet_0035	MinC	Cell division inhibitor MinC	5	383	2.1	3.7E-02
Rmet_0243	GshB	Glutathione synthetase	6	463	3.7	5.8E-03
Rmet_1849		Putative oxidoreductase/alcolhol dehydrogenase	3	315	3.0	5.3E-03
Rmet_1950	AhpC	Alkyl hydroperoxide reductase	15	1584	2.5	1.3E-03
Rmet_1951	AhpD	Alkyl hydroperoxide reductase D	7	546	4.0	6.1E-03
Rmet_2791	ZapA	Cell division protein	5	373	3.1	5.2E-03
Rmet_2957	Gst-1	Glutathione S-transferase	2	99	2.9	5.8E-03
Rmet_3346	UspA8	Universal stress protein	4	371	11.6	1.6E-04
Rmet_3616		Osmotically inducible protein (OsmC-like)	3	218	6.4	5.1E-03
Rmet_4751	MscS	Mechanosensitive ion channel	4	395	4.0	1.4E-03
Rmet_5371	KatG	Catalase/hydroperoxidase	5	344	12.3	4.9E-07
Rmet_5599	KatA	Catalase	31	2585	4.3	1.3E-03
Central intermediary metabolism						
Rmet_0559	Ldh	L-Lactate dehydrogenase	4	161	26.9	2.1E-04
Rmet_0572	CpdB	2':3'-cyclic-nucleotide 2'-phosphodiesterase	7	411	6.0	2.9E-03
Rmet_0774	PhnD	Phosphonate/organophosphate ester transporter subunit	9	733	9.3	3.8E-05
Rmet_1498	CbbO	Rubisco activation protein	7	385	3.5	4.6E-03
Rmet_3419	SoxX	Sulfur oxidation protein	2	218	2.5	1.9E-02
Rmet_4929	Gst	Glutathione S-transferase enzyme with thioredoxin-like domain	4	272	2.1	1.0E-02
Rmet_5402		Putative alkyl sulfatase	15	987	2.8	7.4E-04
DNA metabolism						
Rmet_0315	Ssb1	Single-stranded DNA-binding protein (Helix-destabilizing protein)	3	348	5.0	8.9E-06
Rmet_2101	Hfq	Host factor I protein	4	189	8.4	4.1E-04
Rmet_3538	Hup	Histone-like DNA-binding protein	10	1221	2.8	1.1E-02
Energy metabolism						
Rmet_0197	Qor	Guinone oxidoreductase, NADPH-dependent	3	218	4.8	4.8E-03
Rmet_0386		Putative 3-hydroxyacyl-coa dehydrogenase oxidoreductase protein	4	237	2.3	7.4E-03
Rmet_0931	NuoE	NADH dehydrogenase chain E	2	130	4.2	4.6E-03
Rmet_0988		Cytochrome c553	6	401	2.3	4.9E-02
Rmet_1093	Adh	Alcohol dehydrogenase, 1-propanol preferring	16	1304	18.5	3.9E-06

Continued on next page

Table B.5 – Proteins up-regulated in "lowest phosphorus" media compared to optimal media

Locus tag	Protein name	Description	No. peptides	Score	FC	P value
Rmet_1515	CbbG1	Glyceraldehyde-3-phosphate dehydrogenase A	8	585	3.2	1.3E-03
Rmet_1523	HoxU	NAD-reducing hydrogenase diaphorase moiety small subunit	3	222	2.5	3.4E-02
Rmet_2089	TalB	Transaldolase B	4	101	4.2	2.3E-04
Rmet_2451	Fdx	Ferredoxin	2	112	12.9	4.8E-04
Rmet_2492	AcnA2	Aconitate hydratase 1	26	1915	3.1	4.9E-04
Rmet_4063	NapA	Periplasmic nitrate reductase, large subunit	8	510	17.4	5.7E-05
Rmet_5128	AldB	Aldehyde dehydrogenase 2	8	507	5.5	1.8E-04
Rmet_5312	Cpo	Non-heme chloroperoxidase	4	313	3.5	6.9E-05
Fatty acid and phospholipid metabolism						
Rmet_0113		Enoyl-CoA hydratase/carnithine racemase	2	140	7.4	3.6E-04
Rmet_0565	FabI	Enoyl-acyl-carrier-protein reductase, NADH-dependent	6	610	19.6	4.4E-05
Rmet_1200	PhaP	Phasin (PHA-granule associated protein)	27	3727	5.5	8.8E-06
Rmet_2643	Cfa	Cyclopropane-fatty-acyl-phospholipid synthase	5	258	5.5	4.6E-04
Rmet_4076		Putative short-chain dehydrogenase/reductase SDR	2	87	26.4	1.6E-04
Mobile and extrachromosomal element functions						
Rmet_6063	PaaY	ATPase involved in plasmid partitioning	2	79	217.1	7.5E-03
Phosphorus metabolism						
Rmet_2178	Ppk	Polyphosphate kinase, component of RNA degradosome	2	96	30.3	1.2E-04
Rmet_2180	PhoB	DNA-binding response regulator in two-component regulatory system with PhoR	2	179	19.9	2.6E-03
Rmet_2181	PhoU	Negative regulator of PhoR/PhoB two-component regulator	10	969	5.7	1.8E-04
Rmet_2182	PstB	Phosphate transporter subunit	5	218	10.9	2.1E-04
Rmet_2185	PstS	Phosphate transporter subunit	25	2142	7.6	8.7E-05
Rmet_2992	PtxD	Phosphonate dehydrogenase	12	859	44.4	7.8E-06
Rmet_2994	PtxB	Putative phosphonate ABC transporter	16	1495	22.9	3.2E-05
Protein fate						
Rmet_0283		Peptidase M16-like protein	4	283	2.5	5.6E-03
Rmet_1429	Dmf	Polypeptide or peptide deformylase	2	77	5.8	3.2E-04
Rmet_5411		Putative membrane Zinc metallopeptidase, M50 family	3	129	16.1	1.9E-03
Protein synthesis						
Rmet_0437	SurA	Peptidyl-prolyl cis-trans isomerase	8	548	2.3	4.8E-03

Continued on next page

Table B.5 – Proteins up-regulated in "lowest phosphorus" media compared to optimal media

Locus tag	Protein name	Description	No. peptides	Score	FC	P value
Rmet_0686	LolA	Outer membrane lipoprotein carrier protein	4	201	10.3	2.6E-04
Rmet_0852	Rph	Ribonuclease PH	2	188	2.8	1.9E-02
Rmet_2512		Putative endoribonuclease L-PSP (protein synthesis inhibitor)	4	312	2.3	4.0E-02
Purines, pyrimidines, nucleosides and nucleotides						
Rmet_0211		Diadenosine tetraphosphate hydrolase	2	182	3.1	7.2E-03
Rmet_2095		Phosphoribosyltransferase	2	177	2.6	2.7E-02
Rmet_2740	PyrB	Aspartate carbamoyltransferase, catalytic chain	5	294	3.5	6.2E-04
Rmet_2741	PyrR	Bifunctional protein: pyrimidine operon regulatory protein/uracil phosphoribosyltransferase	4	309	2.2	4.2E-02
Regulation						
Rmet_1194		Two component transcriptional regulator, LuxR family	4	409	2.7	3.6E-03
Rmet_2941	OxyR	Oxidative stress-inducible genes activator	2	92	2.3	2.9E-03
Transcription						
Rmet_1601		Regulatory protein, MarR family	4	188	2.1	3.8E-02
Rmet_2135	Rho	Transcription termination factor Rho	11	602	3.8	1.7E-03
Rmet_5818	Csp	Cold-shock responsive transcriptional repressor	4	264	3.7	5.1E-03
Transport and binding proteins						
Rmet_1408	DppA1	Putative peptide transporter subunit	7	434	2.3	2.7E-02
Rmet_1702	AcrF	Multidrug efflux system protein	15	1082	2.7	6.3E-04
Rmet_1985	YbjL	Putative transporter	8	668	3.3	8.6E-05
Rmet_3145	Bug	Extra-cytoplasmic Solute Receptor protein	3	301	2.3	3.1E-03
Rmet_4840		Putative ABC transporter, periplasmic binding component involved in Fe^{3+} transport	2	52	4.2	1.7E-05
Rmet_5408		Putative efflux outer membrane protein	2	142	45.5	2.7E-02
Unassigned						
Rmet_0016		Conserved hypothetical protein	3	214	64.3	1.3E-05
Rmet_0084		Predicted hydrolase or acyltransferase	2	111	14.6	3.3E-04
Rmet_0109		2-hydroxychromene-2-carboxylate isomerase	3	291	2.9	1.7E-02
Rmet_0152		Conserved hypothetical protein	4	227	2.3	1.8E-03
Rmet_0222	NppD	2-nitropropane dioxygenase	2	154	2.1	4.6E-02
Rmet_0298		Conserved hypothetical protein	3	242	4.4	7.3E-04

Continued on next page

Table B.5 – Proteins up-regulated in "lowest phosphorus" media compared to optimal media

Locus tag	Protein name	Description	No. peptides	Score	FC	P value
Rmet_0310		Putative intracellular protease/amidase	11	1465	4.5	4.1E-05
Rmet_0421		Conserved hypothetical protein	12	1251	4.9	2.4E-04
Rmet_0546	BdhA	D-beta-hydroxybutyrate dehydrogenase	2	55	2.5	1.3E-04
Rmet_0562	AckA2	Acetate kinase	8	440	7.9	5.6E-04
Rmet_0563	Ptb	Phosphate acetyltransferase	6	373	32.8	1.6E-04
Rmet_0564		Conserved hypothetical protein	16	1113	4.7	2.9E-05
Rmet_0673	PilL2	Type IV pilus protein histidine kinase/response regulator hybrid	4	225	2.1	7.6E-04
Rmet_0690		Putative amino-acid-binding periplasmic ABC transporter protein	5	426	7.0	5.8E-04
Rmet_0785		Conserved hypothetical protein	4	261	2.7	8.5E-03
Rmet_0862		Conserved hypothetical protein	6	402	7.4	3.7E-04
Rmet_0904		Glycosyltransferase	8	421	5.3	1.4E-05
Rmet_1017	Phaz1	Intracellular poly(3-hydroxybutyrate) depolymerase	6	305	2.6	3.9E-03
Rmet_1059	PaaY	Carbonic anhydrases/acetyltransferases, isoleucine patch superfamily	5	261	2.8	1.3E-02
Rmet_1084		Conserved hypothetical protein with TPR domain	3	153	3.3	2.8E-03
Rmet_1183		Conserved hypothetical signal peptide protein	7	579	12.4	1.3E-03
Rmet_1187		Hypothetical protein	4	447	2.8	4.6E-04
Rmet_1357	PhaA	Acetyl-CoA acetyltransferase	22	2097	2.2	5.7E-04
Rmet_1394		Acyl-CoA-binding protein	4	241	11.6	3.0E-03
Rmet_1418		Hypothetical protein	6	476	4.5	2.5E-04
Rmet_1452		Conserved hypothetical protein	2	106	6.3	2.7E-02
Rmet_1695		Conserved hypothetical protein; putative exported protein	3	257	3.6	7.5E-03
Rmet_1696		Conserved hypothetical protein; putative exported protein	10	702	17.9	1.5E-04
Rmet_1704		Conserved hypothetical protein; putative exported protein	8	754	3.1	4.3E-04
Rmet_1705		Conserved hypothetical protein; putative exported protein	14	1519	5.1	1.8E-05
Rmet_1706		Conserved hypothetical protein; putative exported protein	3	233	2.1	6.7E-03
Rmet_1830	GcvT	Putative glycine cleavage T protein	3	111	2.5	2.2E-03
Rmet_1971		Conserved hypothetical protein	2	98	6.3	4.7E-04
Rmet_1984	AsdA	L-Aspartate decarboxylase	25	1718	5.4	9.1E-05
Rmet_2041	CcoP	cbb3-type cytochrome oxidase, diheme subunit IV	6	375	2.0	1.3E-02
Rmet_2071	YggX	Fe(II) trafficking protein	2	83	2.7	1.6E-02
Rmet_2125		L-carnitine dehydratase/bile acid-inducible protein	2	126	4.0	8.1E-03

Continued on next page

Table B.5 – Proteins up-regulated in "lowest phosphorus" media compared to optimal media

Locus tag	Protein name	Description	No. peptides	Score	FC	P value
Rmet_2128		Conserved hypothetical protein	6	510	2.2	3.1E-03
Rmet_2133		Conserved hypothetical protein	3	457	3.5	1.7E-02
Rmet_2243		Conserved hypothetical protein	2	234	5.2	4.1E-05
Rmet_2281		Conserved hypothetical protein	5	282	5.0	2.6E-04
Rmet_2491		Conserved hypothetical protein; putative exported protein	6	343	2.5	7.0E-05
Rmet_2496		Putative extracellular solute-binding	3	134	22.3	4.0E-03
Rmet_2583	PhoD	Phosphodiesterase/alkaline phosphatase D	9	614	6.4	1.3E-04
Rmet_2608		Conserved hypothetical protein	4	308	3.0	1.8E-02
Rmet_2614		Putative GTP cyclohydrolase	5	411	2.5	2.7E-03
Rmet_2620	SseA	Rhodanese-related sulfurtransferase	2	144	2.5	2.5E-03
Rmet_2622		Putative carboxymethylenebutenolidase	4	283	2.2	4.7E-02
Rmet_2632		Conserved hypothetical protein	2	105	5.2	2.4E-03
Rmet_2668		Conserved hypothetical protein	4	245	4.6	1.9E-02
Rmet_2968		2-Hydroxychromene-2-carboxylate isomerase	5	330	2.7	4.2E-03
Rmet_2984		Conserved hypothetical protein	3	304	6.6	2.0E-05
Rmet_3064	AccB	Acetyl CoA carboxylase, BCCP subunit	3	344	6.5	6.1E-04
Rmet_3358		Conserved hypothetical protein	2	86	14.4	4.5E-04
Rmet_3428		Conserved hypothetical protein; predicted periplasmic or secreted lipoprotein	7	525	2.2	6.2E-03
Rmet_3471		Conserved hypothetical protein	3	200	13.9	4.0E-03
Rmet_3826		Conserved hypothetical protein	6	367	10.7	3.4E-04
Rmet_3904	PrkA	Serine protein kinase	10	487	11.3	5.2E-06
Rmet_4030		Putative glyoxalase or dioxygenase	2	69	4.5	2.9E-04
Rmet_4140		Putative methyltransferase	3	180	3.0	6.3E-03
Rmet_4167	Ttg2	ABC-type transporter involved in toluene tolerance, periplasmic component	4	245	10.1	6.2E-03
Rmet_4200		Conserved hypothetical protein	3	200	12.0	5.6E-04
Rmet_4347		Alkylhydroperoxidase	2	73	3.3	2.0E-03
Rmet_4400		Conserved hypothetical protein	5	436	5.7	6.3E-03
Rmet_4584		Conserved hypothetical protein	2	162	9.5	1.7E-02
Rmet_4809	AcpA	Putative acid phosphatase protein	3	144	50.7	4.4E-03

Continued on next page

Table B.5 – Proteins up-regulated in "lowest phosphorus" media compared to optimal media

Locus tag	**Protein name**	**Description**	**No. peptides**	**Score**	**FC**	**P value**
Rmet_4999		Conserved hypothetical protein	8	472	5.1	7.7E-05
Rmet_5000		Conserved hypothetical protein	13	758	2.9	5.5E-04
Rmet_5043		Conserved hypothetical protein	10	801	4.7	9.8E-04
Rmet_5065		Conserved hypothetical protein	4	219	2.2	5.9E-04
Rmet_5124		Conserved hypothetical protein	2	141	4.7	6.9E-05
Rmet_5311		Isochorismatase hydrolase	4	347	4.2	6.7E-03
Rmet_5313		Putative metallo-dependent amidohydrolase	12	729	7.2	8.3E-04
Rmet_5405		Conserved hypothetical protein; putative periplasmic protein	8	703	15.2	1.0E-05
Rmet_5406		Conserved hypothetical protein	4	205	24.3	5.0E-05
Rmet_5600		Conserved hypothetical protein; ankyrin domain protein	4	384	5.8	9.4E-04
Rmet_5645	Adh	Alcohol dehydrogenase, zinc-binding	6	291	3.4	2.0E-02
Rmet_5753		Conserved hypothetical protein	7	430	22.8	3.4E-04
Rmet_5796		D-isomer specific 2-hydroxyacid dehydrogenase, NAD-binding	3	149	5.6	3.3E-04

Table B.5 – Proteins up-regulated in "lowest phosphorus" media compared to optimal media

B.3.2 Down-regulated compared to the control

Table B.6 – Proteins down-regulated in "lowest phosphorus" media compared to optimal media

Locus tag	Protein name	Description	No. peptides	Score	FC	P value
Amino acid synthesis and metabolism						
Rmet_0354	IlvA	Threonine deaminase	6	305	0.24	3.4E-03
Rmet_0715	SerC	3-phosphoserine/phosphohydroxythreonine aminotransferase	11	603	0.36	2.5E-03
Rmet_0716	PheA	Prephenate dehydratase, Chorismate mutase	3	267	0.31	1.4E-05
Rmet_0911	IlvI	Acetolactate synthase III, large subunit	7	414	0.33	5.2E-03
Rmet_0913	IlvC	Ketol-acid reductoisomerase	25	2316	0.47	1.2E-05
Rmet_1089	LysC	Aspartate kinase	6	366	0.40	2.1E-03
Rmet_1164	PheS	Phenylalanine tRNA synthetase, alpha subunit	6	368	0.45	2.3E-03
Rmet_1400	DadX	Alanine racemase 2, PLP-binding	2	52	0.06	7.3E-04
Rmet_1420	DapE	N-succinyl-diaminopimelate deacylase	5	263	0.32	1.0E-03
Rmet_1424	DapC	Probable succinyldiaminopimelate aminotransferase protein	4	202	0.49	8.6E-04
Rmet_1956	ArgE1	Acetylornithine deacetylase	3	147	0.17	6.9E-04
Rmet_2467	TrpB	Tryptophan synthase, beta subunit	4	377	0.44	3.5E-03
Rmet_2476	LivF1	Leucine/isoleucine/valine transporter subunit	2	163	0.48	3.2E-02
Rmet_2627	ThrB	Homoserine kinase	2	86	0.20	3.5E-04
Rmet_2696		Aspartate/tyrosine/aromatic aminotransferase	3	168	0.19	2.6E-02
Rmet_2812	CysN	Sulfate adenylyltransferase, subunit 1	4	320	0.12	4.7E-05
Rmet_2815	CysO	Protein involved in cysteine metabolism	3	149	0.15	5.8E-03
Rmet_2816	CysI	Sulfite reductase, beta subunit (hemoprotein with two 4Fe-4S domains)	9	546	0.21	4.3E-04
Rmet_2938	ProC	Pyrroline-5-carboxylate reductase	4	198	0.07	6.4E-04
Rmet_3181	TrpC	Indole-3-glycerol phosphate synthase	2	95	0.08	1.3E-03
Rmet_3241	HisI	Phosphoribosyl-AMP cyclohydrolase	2	105	0.26	1.8E-03
Rmet_3248	HisD	Bifunctional histidinal dehydrogenase and histidinol dehydrogenase	3	105	0.43	3.5E-02
Rmet_3249	HisG	ATP phosphoribosyltransferase	4	143	0.14	3.9E-03
Rmet_3262	GltD	Glutamate synthase, 4Fe-4S protein, small subunit	18	1298	0.42	2.1E-04
Rmet_3263	GltB	Glutamate synthase, large subunit	43	2962	0.34	1.2E-04

Continued on next page

Table B.6 – Proteins down-regulated in "lowest phosphorus" media compared to optimal media

Locus tag	Protein name	Description	No. peptides	Score	FC	P value
Rmet_4563		Transcriptional regulator, LysR family	8	377	0.29	2.8E-03
Rmet_4583	GltL	glutamate/aspartate transport protein	4	321	0.46	7.6E-05
Rmet_5602		Putative threonine dehydratase	5	349	0.16	2.7E-03
Biosynthesis of cofactors, prosthetic groups, and carriers						
Rmet_0061	LipA	Lipoate synthase	2	93	0.01	1.0E-02
Rmet_0114	BioA	7,8-diaminopelargonic acid synthase, PLP-dependent	6	351	0.22	2.5E-03
Rmet_0115	BioF	8-amino-7-oxononanoate synthase	2	128	0.13	3.8E-04
Rmet_0117	BioB	Biotin synthase	14	936	0.15	2.2E-03
Rmet_0162	ThiC	Thiamin biosynthesis protein	13	866	0.43	2.4E-05
Rmet_0486	MoaC	Molybdopterin biosynthesis, protein C	2	52	0.14	1.8E-04
Rmet_1441	Dxr	1-deoxy-D-xylulose 5-phosphate reductoisomerase	5	413	0.49	2.9E-02
Rmet_1964	MoeA	Molybdopterin biosynthesis protein	2	112	0.10	7.6E-04
Rmet_2463	FolC	Bifunctional folylpolyglutamate synthase and dihydrofolate synthase	4	263	0.29	2.2E-03
Rmet_2615	Dxs	1-deoxyxylulose-5-phosphate synthase	10	491	0.36	6.1E-04
Rmet_2868	IspH	1-hydroxy-2-methyl-2-(E)-butenyl 4-diphosphate reductase, 4Fe-4S protein	3	145	0.13	3.0E-05
Cell envelope						
Rmet_0187	GlmS	L-glutamine:D-fructose-6-phosphate aminotransferase	14	901	0.40	4.0E-04
Rmet_0533	KdsB	3-deoxy-manno-octulosonate cytidylyltransferase	3	95	0.38	1.4E-02
Rmet_1352	ComL	DNA uptake lipoprotein	4	214	0.45	1.0E-02
Cellular process						
Rmet_0034	MinD	Septum site-determining protein	5	255	0.48	2.3E-02
Rmet_0458	UspA1	Universal stress protein, UspA family	7	535	0.35	3.0E-04
Rmet_2417	Era	Membrane-associated, 16S rRNA-binding GTPase	2	108	0.21	1.3E-04
Rmet_3123	FtsZ	GTP-binding tubulin-like cell division protein	10	824	0.45	1.5E-03
Rmet_3124	FtsA	ATP-binding cell division protein	5	356	0.14	5.0E-05
Rmet_3226	SspB	ClpXP protease specificity-enhancing factor	3	170	0.16	1.3E-02
Rmet_3506	GidA	Glucose-inhibited cell-division protein	2	168	0.42	9.5E-03
Rmet_3574	CstA	Starvation-induced protein involved in peptide utilization during carbon starvation	3	172	0.09	7.3E-03
Rmet_5635		Penicillin amidase (peptidase S45)	2	116	0.25	3.9E-02

Continued on next page

Table B.6 – Proteins down-regulated in "lowest phosphorus" media compared to optimal media

Locus tag	Protein name	Description	No. peptides	Score	FC	P value
Rmet_5981	CzcB	Membrane fusion protein, three components cation proton antiporter efflux system involved in Cd(II), Zn(II), Co(II) resistance	4	232	0.21	5.6E-03
Central intermediary metabolism						
Rmet_0081	MhpD2	2-Oxopent-4-enoate hydratase	3	141	0.30	1.7E-02
Rmet_0170	AhcY	Adenosylhomocysteinase	9	543	0.45	5.2E-04
Rmet_0172	MetF	5,10-methylenetetrahydrofolate reductase	2	66	0.10	4.3E-03
Rmet_0378	AspS	Aspartyl-tRNA synthetase	16	976	0.47	5.4E-04
Rmet_2755	Dcd	2'-deoxycytidine 5'-triphosphate deaminase	2	99	0.30	2.2E-02
Rmet_3420	SoxA	Sulfur oxidation protein	5	262	0.25	4.3E-04
Rmet_3422	SoxZ	Thiosulphate-binding sulfur oxidation protein	5	378	0.29	1.6E-04
Rmet_3578	GyaR	Glyoxylate reductase	2	49	0.48	2.1E-02
DNA metabolism						
Rmet_0002	DnaN	DNA polymerase III, beta subunit	12	915	0.41	1.1E-03
Rmet_1189	XthA2	Exodeoxyribonuclease III	2	129	0.22	3.3E-02
Rmet_1428	LigA	DNA ligase	2	56	0.47	2.6E-02
Rmet_2129	DnaX	DNA polymerase III tau/gamma subunit	4	266	0.27	1.1E-03
Rmet_2914	PcnB	Poly(A) polymerase I polynucleotide adenylyltransferase	2	62	0.36	1.4E-02
Rmet_4742		Histone-like DNA-binding protein	13	1003	0.50	1.4E-03
Rmet_6191	Bph2	Histone-like DNA-binding protein	5	500	0.23	1.6E-05
Energy metabolism						
Rmet_0261	CoxB	Cytochrome c oxidase, subunit II	7	458	0.43	2.6E-05
Rmet_0470	SucD	Succinyl-CoA synthetase, NAD(P)-binding, alpha subunit	13	1096	0.45	4.6E-05
Rmet_0933	NuoG	NADH dehydrogenase chain G	22	1527	0.45	5.2E-05
Rmet_1045	Edd	6-phosphogluconate dehydratase	11	702	0.49	1.4E-03
Rmet_1146	EtfD	Electron transfer flavoprotein-ubiquinone oxidoreductase	10	711	0.39	1.1E-03
Rmet_1285	HypB1	HypB1 GTP hydrolase involved in nickel liganding into hydrogenases	2	74	0.09	1.8E-03
Rmet_1297	HoxG	Hydrogenase 1	24	1369	0.30	9.8E-05
Rmet_1536	HypB2	GTP hydrolase involved in nickel liganding into hydrogenases	16	1175	0.26	1.1E-02
Rmet_1539	HypD2	Protein required for maturation of hydrogenases	7	342	0.46	1.8E-02
Rmet_2273	FumA	Fumarate hydratase class I	18	1326	0.45	5.2E-04
Rmet_2750	Ppc	Phosphoenolpyruvate carboxylase	11	592	0.29	4.2E-03

Continued on next page

Table B.6 – Proteins down-regulated in "lowest phosphorus" media compared to optimal media

Locus tag	Protein name	Description	No. peptides	Score	FC	P value
Rmet_2980	CbbT2	Transketolase 1, thiamin-binding	10	843	0.43	2.1E-04
Rmet_3498	AtpF	F0 sector of membrane-bound ATP synthase, subunit b	7	505	0.48	1.6E-04
Rmet_3577	PckG	Phosphoenolpyruvate carboxykinase	14	727	0.36	5.8E-05
Fatty acid and phospholipid metabolism						
Rmet_0108		Acyl-CoA dehydrogenase, short-chain specific	3	88	0.39	1.4E-02
Rmet_0212	HbdA	3-hydroxybutyryl-CoA dehydrogenase	4	226	0.32	1.6E-03
Rmet_1087	AccA	Acetyl-CoA carboxylase, carboxytransferase, alpha subunit	5	355	0.46	3.7E-04
Rmet_1853	AtoB	Acetyl-CoA acetyltransferase / thiolase	7	400	0.38	1.1E-03
Rmet_2429	FabD	Malonyl-CoA-acyl-carrier-protein transacylase	2	191	0.44	9.6E-03
Rmet_2635	FadD	Long-chain-fatty-acid-CoA ligase	4	172	0.42	4.8E-02
Mobile and extrachromosomal element functions						
Rmet_6062	ParB	Plasmid replication- partition related protein	2	163	0.02	7.1E-03
Rmet_6316	ParB	ParB involved in chromosome partitioning	2	55	0.10	1.3E-02
Protein fate						
Rmet_0991	TldD	Peptidase	6	321	0.39	1.4E-02
Rmet_1026	IscU	FeS cluster assembly scaffold protein	9	570	0.47	2.9E-03
Rmet_2188	FtsH	Protease	13	915	0.46	2.4E-03
Rmet_2892	ClpA	ATPase and specificity subunit of ClpA-ClpP ATP-dependent serine protease	9	538	0.39	1.7E-03
Protein synthesis						
Rmet_0046	GatB	Glutamyl-tRNA amidotransferase subunit B	4	335	0.39	7.9E-05
Rmet_0288	RplY	50S ribosomal protein L25	9	692	0.18	2.7E-06
Rmet_0410	RplM	50S ribosomal subunit protein L13	8	586	0.44	2.9E-03
Rmet_0411	RpsI	30S ribosomal subunit protein S9	7	610	0.12	2.8E-05
Rmet_0695	SerS	Seryl-tRNA synthetase	10	701	0.45	1.2E-02
Rmet_0722	RpsA	30S ribosomal subunit protein S1	32	2781	0.37	4.8E-04
Rmet_0748	RpsP	30S ribosomal subunit protein S16	2	155	0.40	3.1E-04
Rmet_0751	RplS	50S ribosomal subunit protein L19	11	889	0.41	2.3E-03
Rmet_0921	RpsO	30S ribosomal subunit protein S15	5	392	0.31	5.0E-03
Rmet_1025	IscS	Cysteine desulfurase	11	798	0.37	4.5E-04
Rmet_1161	InfC	Protein chain initiation factor IF-3	4	241	0.20	1.3E-02

Continued on next page

Table B.6 – Proteins down-regulated in "lowest phosphorus" media compared to optimal media

Locus tag	Protein name	Description	No. peptides	Score	FC	P value
Rmet_1444	HlpA	Periplasmic chaperone	5	270	0.46	4.0E-05
Rmet_1976	RplI	50S ribosomal subunit protein L9	12	772	0.47	2.5E-04
Rmet_2031	InfB	Translation initiation factor 2	19	1855	0.44	2.6E-04
Rmet_2137		50S ribosomal protein L31 type B	4	297	0.30	1.1E-05
Rmet_2412	Efp	Translation elongation factor P	7	402	0.41	1.9E-04
Rmet_2432	RpmF	50S ribosomal subunit protein L32	2	296	0.13	2.1E-04
Rmet_2455	RpsU1	30S ribosomal subunit protein S21	2	113	0.14	2.1E-03
Rmet_2630	ValS	Valyl-tRNA synthetase	11	831	0.28	4.6E-05
Rmet_2870	RpmB	50S ribosomal subunit protein L28	4	279	0.26	3.8E-04
Rmet_2871	RpmG	50S ribosomal subunit protein L33	5	593	0.41	6.1E-04
Rmet_2904	RpsT	30S ribosomal subunit protein S20	6	466	0.12	4.7E-05
Rmet_2921	DnaJ	Chaperone Hsp40, co-chaperone with DnaK	2	57	0.03	1.5E-03
Rmet_3106	RplU	50S ribosomal subunit protein L21	3	200	0.26	1.4E-04
Rmet_3290	RplQ	50S ribosomal subunit protein L17	5	286	0.17	1.1E-03
Rmet_3292	RpsD	30S ribosomal subunit protein S4	12	988	0.32	7.3E-04
Rmet_3293	RpsK	30S ribosomal subunit protein S11	7	667	0.22	3.0E-06
Rmet_3294	RpsM	30S ribosomal subunit protein S13	9	503	0.34	1.9E-03
Rmet_3298	RplO	50S ribosomal subunit protein L15	8	544	0.36	3.9E-04
Rmet_3299	RpmD	50S ribosomal subunit protein L30	2	217	0.18	1.0E-05
Rmet_3300	RpsE	30S ribosomal subunit protein S5	11	957	0.43	3.2E-04
Rmet_3301	RplR	50S ribosomal subunit protein L18	7	631	0.25	1.1E-05
Rmet_3302	RplF	50S ribosomal subunit protein L6	14	1054	0.20	1.8E-04
Rmet_3304	RpsN	30S ribosomal subunit protein S14	4	297	0.21	1.2E-03
Rmet_3305	RplE	50S ribosomal subunit protein L5	8	476	0.44	1.2E-02
Rmet_3306	RplX	50S ribosomal subunit protein L24	11	1005	0.12	3.7E-05
Rmet_3307	RplN	50S ribosomal subunit protein L14	8	523	0.19	4.6E-04
Rmet_3308	RpsQ	30S ribosomal subunit protein S17	3	253	0.14	5.6E-04
Rmet_3310	RplP	50S ribosomal subunit protein L16	4	302	0.42	1.7E-04
Rmet_3311	RpsC	30S ribosomal subunit protein S3	14	1134	0.48	3.2E-03
Rmet_3312	RplV	50S ribosomal subunit protein L22	7	503	0.15	3.1E-04
Rmet_3313	RpsS	30S ribosomal subunit protein S19	5	470	0.23	4.8E-04

Continued on next page

Table B.6 – Proteins down-regulated in "lowest phosphorus" media compared to optimal media

Locus tag	Protein name	Description	No. peptides	Score	FC	P value
Rmet_3314	RplB	50S ribosomal subunit protein L2	16	1303	0.18	7.8E-05
Rmet_3315	RplW	50S ribosomal subunit protein L23	5	506	0.32	7.7E-04
Rmet_3316	RplD	50S ribosomal subunit protein L4	13	1027	0.26	1.3E-05
Rmet_3317	RplC	50S ribosomal subunit protein L3	13	1056	0.29	8.6E-05
Rmet_3323	RpsJ	30S ribosomal subunit protein S10	6	531	0.39	1.3E-04
Rmet_3326	RpsG	30S ribosomal subunit protein S7	8	480	0.33	3.4E-03
Rmet_3327	RpsL	30S ribosomal subunit protein S12	5	329	0.29	7.5E-04
Rmet_3336	RplJ	50S ribosomal subunit protein L10	12	938	0.28	1.0E-04
Rmet_3337	RplA	50S ribosomal subunit protein L1	18	1252	0.19	6.8E-06
Rmet_3338	RplK	50S ribosomal subunit protein L11	5	241	0.18	1.5E-04
Rmet_4357		Transcriptional regulator	2	56	0.43	2.9E-02
Rmet_5623		Peptidylprolyl isomerase	3	216	0.32	4.0E-04
Purines, pyrimidines, nucleosides and nucleotides						
Rmet_0506	PurK	Phosphoribosylaminoimidazole carboxylase ATPase subunit	7	578	0.41	1.3E-03
Rmet_0532	Adk	Adenylate kinase	7	294	0.33	6.7E-04
Rmet_0856	Gmk	Guanylate kinase	2	137	0.41	3.1E-02
Rmet_0890	Add	Adenosine deaminase	2	69	0.30	5.9E-05
Rmet_1461	GuaB	Inosine-5'-monophosphate dehydrogenase	19	1386	0.48	7.4E-04
Rmet_1820	PurT	Phosphoribosylglycinamide formyltransferase 2	5	229	0.33	3.0E-05
Transcription						
Rmet_0302	RpoX	Sigma 54 modulation protein, ribosome-associated	6	489	0.12	2.2E-04
Rmet_1044	YebK	Transcriptional regulator, RpiR family	2	271	0.19	2.1E-02
Rmet_1078	SuhB	Inositol monophosphatase	4	231	0.47	1.2E-03
Rmet_1232	YhgF	Putative RNA-binding transcription accessory protein	4	200	0.15	2.2E-04
Rmet_2034		Pseudouridine synthase	5	254	0.33	4.1E-04
Rmet_2037	FnrL	Transcriptional regulator	2	96	0.32	6.6E-04
Rmet_2092	Rnr	Exoribonuclease R, RNase R	4	180	0.33	1.4E-03
Rmet_2192	GreA	Transcription elongation factor	4	291	0.31	9.9E-03
Rmet_3333	RpoC	RNA polymerase, beta prime subunit	64	4280	0.43	5.9E-05
Rmet_3564	Fmt	Methionyl-tRNA formyltransferase	3	123	0.45	5.4E-03
Rmet_4773		Putative endoribonuclease L-PSP	2	135	0.31	1.5E-03

Continued on next page

Table B.6 – Proteins down-regulated in "lowest phosphorus" media compared to optimal media

Locus tag	Protein name	Description	No. peptides	Score	FC	P value
Transport and binding proteins						
Rmet_0070		ABC-type transporter, periplasmic component	2	71	0.20	2.3E-03
Rmet_0521	Bug	Extra-cytoplasmic Solute Receptor protein	31	2977	0.40	5.4E-03
Rmet_0802		Putative ABC-type transporter glycine betaine/L-proline transporter	7	410	0.37	1.1E-05
Rmet_0929	NuoC	NADH dehydrogenase chain C	4	185	0.38	9.1E-05
Rmet_1209		ABC transporter-related protein	6	276	0.36	1.1E-02
Rmet_2279	ExbD1	Biopolymer transport protein	6	484	0.43	7.5E-04
Rmet_2945	YajC	Preprotein translocase auxiliary subunit	6	435	0.34	5.8E-04
Rmet_3153		ABC-type branched-chain amino acid transport system, periplasmic component	3	182	0.24	1.1E-03
Rmet_3589	AcrB	Multidrug efflux system protein	7	505	0.47	5.0E-03
Rmet_3613	YidC	Inner membrane insertion protein YidC/OxaA	11	705	0.34	6.9E-05
Rmet_3671	Bug	Extra-cytoplasmic Solute Receptor	2	56	0.00	1.4E-03
Rmet_5616	Bug	Extra-cytoplasmic solute receptor protein	2	110	0.16	8.1E-04
Unassigned						
Rmet_0097		Conserved hypotethical protein	2	74	0.08	3.5E-04
Rmet_0305		Conserved hypothetical protein; OstA-like protein	2	173	0.44	8.7E-03
Rmet_0367		Putative Fe-S oxidoreductase FAD/FMN-containing dehydrogenase oxidoreductase protein	5	353	0.23	1.6E-03
Rmet_0408		Conserved hypothetical protein	4	208	0.44	8.1E-03
Rmet_0419	YbhB	Phospholipid-binding protein	3	211	0.25	1.3E-03
Rmet_0665	LemA	LemA like protein	2	67	0.02	1.8E-05
Rmet_0697	PilA	Type IV pilus structural subunit PilA	4	285	0.40	1.1E-03
Rmet_0718	TyrA	Prephenate dehydrogenase	2	84	0.24	2.5E-03
Rmet_0972		Putative aminoglycoside phosphotransferase	4	227	0.22	5.6E-05
Rmet_0986		Putative ATPase, AAA family	11	726	0.38	9.9E-04
Rmet_1443	YaeT	Outer membrane protein assembly factor	3	143	0.20	3.3E-03
Rmet_1600		Conserved hypothetical protein; putative exported protein	4	224	0.23	4.1E-03
Rmet_1808	PepM	Phosphoenolpyruvate phosphomutase	8	420	0.20	1.3E-05
Rmet_1851		Short-chain dehydrogenase/reductase SDR	2	86	0.10	1.4E-02
Rmet_1864		Conserved hypothetical protein	2	114	0.32	2.0E-02

Continued on next page

Table B.6 – Proteins down-regulated in "lowest phosphorus" media compared to optimal media

Locus tag	**Protein name**	**Description**	**No. peptides**	**Score**	**FC**	**P value**
Rmet_2024	BipA	GTP-binding protein	5	270	0.44	5.0E-03
Rmet_2061		Conserved hypothetical protein	3	115	0.40	2.8E-03
Rmet_2436	SohB	Peptidase S49, periplasmic serine protease (ClpP class)	2	62	0.39	6.7E-03
Rmet_2440	Rne	Fused ribonucleaseE: endoribonuclease, RNA-binding protein, RNA degradosome binding protein	21	1441	0.32	8.3E-04
Rmet_2452	TrxB2	Thioredoxin reductase	13	741	0.37	2.8E-04
Rmet_2470		Type IV-pili assembly fimV-related transmembrane protein	14	1017	0.38	4.2E-04
Rmet_2547		Conserved hypothetical protein	6	405	0.43	7.3E-04
Rmet_2737		Hypothetical protein	2	102	0.49	7.3E-04
Rmet_2861		Ferredoxin	4	225	0.31	1.1E-02
Rmet_2934	Gpo	Glutathione peroxidase	3	150	0.27	2.0E-03
Rmet_3069		Carbohydrate kinase	5	404	0.33	1.1E-04
Rmet_3233		Trypsin-like serine protease	5	275	0.47	3.7E-03
Rmet_5004		Antibiotic biosynthesis monooxygenase	2	78	0.09	1.3E-02
Rmet_5074		Conserved hypothetical protein	7	363	0.21	1.8E-02
Rmet_6330		Hypothetical protein	2	111	0.41	9.0E-04
Rmet_6408		Putative rhodanese-related sulfurtransferase	2	145	0.11	9.7E-03
Rmet_6523		Conserved hypothetical protein	2	101	0.38	4.0E-02

Table B.6 – Proteins down-regulated in "lowest phosphorus" media compared to optimal media

B.4 Proteins differentially regulated in the "low phosphorus" treatment

B.4.1 Up-regulated compared to the control

Table B.7 – Proteins up-regulated in "low phosphorus" media compared to optimal media

Locus tag	Protein name	Description	No. peptides	Score	FC	P value
Amino acid synthesis and metabolism						
Rmet_0398	GdhA	Glutamate dehydrogenase	11	979	2.1	9.0E-04
Rmet_0681	GlnB	Regulatory protein P-II for glutamine synthetase	5	362	4.0	2.9E-04
Biological processes						
Rmet_1206	YkgE	Putative hydroxyacid oxidoreductase (Fe-S centre)	2	120	3.7	4.3E-02
Rmet_4084	PhoA1	Alkaline phosphatase	10	665	8.2	1.6E-03
Rmet_4085	PhoA2	Alkaline phosphatase	6	451	8.2	1.2E-04
Biosynthesis of cofactors, prosthetic groups, and carriers						
Rmet_0728	RfaD	ADP-L-glycero-D-mannoheptose-6-epimerase, NAD(P)-binding	2	152	2.1	4.5E-02
Rmet_2689	RibC	Riboflavin synthase alpha chain	3	221	2.3	8.3E-04
Cell envelope						
Rmet_0712	OmpA	Outer membrane protein or related peptidoglycan-associated (lipo)protein	11	907	2.0	5.3E-03
Rmet_1685		Putative HlyD family secretion protein	6	301	2.3	2.3E-03
Rmet_2732	RbfC	dTDP-4-deoxyrhamnose-3,5-epimerase	7	402	2.6	1.6E-02
Rmet_4192	PlcN	Phospholipase C	29	2461	8.2	1.1E-04
Cellular process						
Rmet_0243	GshB	Glutathione synthetase	6	463	2.2	1.4E-02
Rmet_2021		NADPH-dependent FMN reductase	5	359	2.3	3.0E-03
Rmet_2957	Gst-1	Glutathione S-transferase	2	99	3.7	1.1E-02
Rmet_3346	UspA8	Universal stress protein, UspA family	4	371	6.7	2.7E-03
Rmet_3616		Osmotically inducible protein (OsmC-like)	3	218	3.5	4.0E-02
Rmet_5252	FliC2	Flagellar filament structural protein (flagellin)	2	239	2.5	9.7E-03

Continued on next page

Table B.7 – Proteins up-regulated in "low phosphorus" media compared to optimal media

Locus tag	Protein name	Description	No. peptides	Score	FC	P value
Rmet_5371	KatG	Catalase/hydroperoxidase HPI(I)	5	344	2.3	2.2E-02
Rmet_5599	KatA	Catalase	31	2585	2.0	2.5E-02
Central intermediary metabolism						
Rmet_0559	Ldh	L-Lactate dehydrogenase	4	161	11.3	6.7E-03
Rmet_0774	PhnD	Phosphonate/organophosphate ester transporter subunit	9	733	6.8	2.1E-04
Rmet_1574	LdcA	L,D-carboxypeptidase A	2	80	2.7	2.4E-03
Rmet_5402		Putative alkyl sulfatase	15	987	2.6	1.5E-02
DNA metabolism						
Rmet_0315	Ssb1	Single-stranded DNA-binding protein (Helix-destabilizing protein)	3	348	3.1	1.5E-03
Rmet_1428	LigA	DNA ligase, NAD(+)-dependent	2	56	2.4	3.7E-02
Rmet_2101	Hfq	Host factor I protein	4	189	13.8	7.2E-04
Energy metabolism						
Rmet_1093	Adh	Alcohol dehydrogenase, 1-propanol preferring	16	1304	4.4	1.3E-04
Rmet_1515	CbbG1	Glyceraldehyde-3-phosphate dehydrogenase A	8	585	2.2	4.2E-03
Rmet_2089	TalB	Transaldolase B	4	101	2.5	5.3E-04
Rmet_4063	NapA	Periplasmic nitrate reductase, large subunit	8	510	5.5	9.0E-04
Rmet_5128	AldB	Aldehyde dehydrogenase 2	8	507	2.2	1.8E-02
Rmet_5312	Cpo	Non-heme chloroperoxidase	4	313	2.8	2.0E-02
Fatty acid and phospholipid metabolism						
Rmet_0113		Enoyl-CoA hydratase/carnithine racemase	2	140	5.1	1.9E-02
Rmet_0565	FabI	Enoyl-acyl-carrier-protein reductase, NADH-dependent	6	610	8.5	1.6E-04
Rmet_1200	PhaP	Phasin (PHA-granule associated protein)	27	3727	2.9	4.9E-04
Rmet_1446	FabZ	(3R)-hydroxymyristol acyl carrier protein dehydratase	3	204	2.5	1.7E-02
Rmet_2643	Cfa	Cyclopropane-fatty-acyl-phospholipid synthase	5	258	3.1	1.9E-03
Rmet_2850	HutG1	N-Formylglutamate amidohydrolase	2	65	3.0	1.9E-03
Rmet_4076		Putative short-chain dehydrogenase/reductase SDR	2	87	3.5	6.6E-03
Rmet_5601		Short-chain dehydrogenase/reductase SDR	3	121	5.3	4.8E-02
Phosphorus metabolism						
Rmet_2177	Ppx	Exopolyphosphatase	3	193	3.8	8.1E-03
Rmet_2178	Ppk	Polyphosphate kinase, component of RNA degradosome	2	96	8.0	1.5E-03

Continued on next page

Table B.7 – Proteins up-regulated in "low phosphorus" media compared to optimal media

Locus tag	Protein name	Description	No. peptides	Score	FC	P value
Rmet_2180	PhoB	DNA-binding response regulator in two-component regulatory system with PhoR	2	179	14.0	2.5E-04
Rmet_2181	PhoU	Negative regulator of PhoR/PhoB two-component regulator	10	969	4.9	2.4E-05
Rmet_2182	PstB	Phosphate transporter subunit	5	218	15.7	9.6E-05
Rmet_2185	PstS	Phosphate transporter subunit	25	2142	12.5	8.1E-05
Rmet_2992	PtxD	Phosphonate dehydrogenase	12	859	27.5	1.4E-06
Rmet_2994	PtxB	Putative phosphonate ABC transporter, periplasmic phosphonate-binding protein	16	1495	12.2	2.3E-05
Protein fate						
Rmet_0283		Peptidase M16-like protein	4	283	2.4	1.4E-02
Protein synthesis						
Rmet_3190	DsbC	Protein-disulfide isomerase	3	137	2.2	3.0E-03
Purines, pyrimidines, nucleosides and nucleotides						
Rmet_0211		Diadenosine tetraphosphate hydrolase	2	182	2.3	2.7E-02
Rmet_2740	PyrB	Aspartate carbamoyltransferase, catalytic chain	5	294	2.4	3.0E-03
Transcription						
Rmet_2135	Rho	Transcription termination factor Rho	11	602	6.5	3.6E-03
Transport and binding proteins						
Rmet_1121	AcrD	Aminoglycoside/multidrug efflux system	4	209	4.8	4.5E-03
Rmet_1985	YbjL	Putative transporter	8	668	2.1	5.9E-04
Rmet_4789	MetQ	DL-methionine transporter subunit	4	211	5.6	1.1E-02
Rmet_4840		Putative ABC transporter, periplasmic binding component involved in Fe^{3+} transport	2	52	2.5	5.6E-03
Unassigned						
Rmet_0016		Conserved hypothetical protein	3	214	8.7	2.1E-02
Rmet_0084		Predicted hydrolase or acyltransferase	2	111	3.0	3.2E-03
Rmet_0152		Conserved hypothetical protein	4	227	4.3	6.2E-04
Rmet_0186	GlmU	Fused N-acetyl glucosamine-1-phosphate uridyltransferase	4	145	3.8	4.4E-02
Rmet_0298		Conserved hypothetical protein	3	242	3.6	3.7E-03
Rmet_0310		Putative intracellular protease/amidase/DJ-1/PfpI family	11	1465	5.0	4.2E-06
Rmet_0421		Conserved hypothetical protein	12	1251	2.9	1.1E-03

Continued on next page

Table B.7 – Proteins up-regulated in "low phosphorus" media compared to optimal media

Locus tag	Protein name	Description	No. peptides	Score	FC	P value
Rmet_0546	BdhA	D-beta-hydroxybutyrate dehydrogenase	2	55	3.2	3.4E-03
Rmet_0562	AckA2	Acetate kinase	8	440	5.5	6.3E-04
Rmet_0563	Ptb	Phosphate acetyltransferase	6	373	9.3	2.1E-03
Rmet_0690		Putative amino-acid-binding periplasmic abc transporter protein	5	426	2.7	1.4E-02
Rmet_0785		Conserved hypothetical protein	4	261	2.8	1.5E-03
Rmet_0862		Conserved hypothetical protein	6	402	2.3	4.2E-03
Rmet_0904		Glycosyltransferase, group 1	8	421	5.9	7.6E-06
Rmet_1021		Conserved hypothetical protein	3	214	2.0	5.1E-03
Rmet_1059	PaaY	Carbonic anhydrases/acetyltransferases, isoleucine patch superfamily	5	261	2.1	3.2E-03
Rmet_1183		Conserved hypothetical signal peptide protein	7	579	3.0	1.5E-02
Rmet_1695		Conserved hypothetical protein; putative exported protein	3	257	3.2	1.8E-03
Rmet_1696		Conserved hypothetical protein; putative exported protein	10	702	5.8	1.9E-03
Rmet_1705		Conserved hypothetical protein; putative exported protein	14	1519	3.1	2.0E-04
Rmet_1706		Conserved hypothetical protein; putative exported protein	3	233	2.1	3.0E-03
Rmet_1714		Conserved hypothetical protein	3	108	2.7	4.1E-02
Rmet_1971		Conserved hypothetical protein	2	98	4.6	4.3E-04
Rmet_1984	AsdA	L-Aspartate decarboxylase	25	1718	2.6	1.7E-04
Rmet_2125		L-carnitine dehydratase/bile acid-inducible protein	2	126	3.2	1.1E-02
Rmet_2243		Conserved hypothetical protein	2	234	2.6	3.4E-03
Rmet_2281		Conserved hypothetical protein	5	282	4.0	2.9E-03
Rmet_2496		Putative extracellular solute-binding	3	134	8.7	1.1E-02
Rmet_2583	PhoD	Phosphodiesterase/alkaline phosphatase D	9	614	3.4	2.7E-03
Rmet_2587	GstN	Glutathione s-transferase protein	5	197	4.3	1.6E-02
Rmet_2620	SseA	Rhodanese-related sulfurtransferase	2	144	2.3	4.6E-02
Rmet_2632		Conserved hypothetical protein	2	105	7.1	2.0E-03
Rmet_2968		2-Hydroxychromene-2-carboxylate isomerase	5	330	3.7	2.2E-03
Rmet_2984		Conserved hypothetical protein	3	304	2.2	2.0E-02
Rmet_3064	AccB	Acetyl CoA carboxylase, BCCP subunit	3	344	5.4	3.1E-02
Rmet_3071		Histone H1-like protein HC2	3	211	3.1	8.0E-04
Rmet_3358		Conserved hypothetical protein	2	86	6.4	5.0E-02
Rmet_3579		Conserved hypothetical protein	4	268	2.8	3.1E-02

Continued on next page

Table B.7 – Proteins up-regulated in "low phosphorus" media compared to optimal media

Locus tag	Protein name	Description	No. peptides	Score	FC	P value
Rmet_3826		Conserved hypothetical protein	6	367	6.6	6.3E-04
Rmet_3904	PrkA	Serine protein kinase	10	487	4.4	1.6E-04
Rmet_4030		Putative glyoxalase or dioxygenase	2	69	3.3	5.4E-04
Rmet_4086		Conserved hypothetical protein (membrane)	5	243	6.4	5.3E-03
Rmet_4140		Putative methyltransferase	3	180	3.6	6.1E-04
Rmet_4167	Ttg2	ABC-type transporter involved in toluene tolerance, periplasmic component	4	245	8.7	2.2E-02
Rmet_4200		Conserved hypothetical protein	3	200	5.2	3.1E-03
Rmet_4347		Alkylhydroperoxidase AhpD core	2	73	2.1	6.0E-03
Rmet_4400		Conserved hypothetical protein	5	436	8.7	2.5E-03
Rmet_4809	AcpA	Putative acid phosphatase protein	3	144	31.9	1.8E-02
Rmet_4999		Conserved hypothetical protein	8	472	2.4	2.2E-03
Rmet_5000		Conserved hypothetical protein	13	758	2.6	1.8E-03
Rmet_5007		Conserved hypothetical protein	2	199	4.8	6.6E-03
Rmet_5043		Conserved hypothetical protein	10	801	3.3	1.0E-03
Rmet_5313		Putative metallo-dependent amidohydrolase	12	729	3.7	6.1E-04
Rmet_5405		Conserved hypothetical protein; putative periplasmic protein	8	703	3.4	1.6E-03
Rmet_5406		Conserved hypothetical protein	4	205	4.3	3.8E-03
Rmet_5600		Conserved hypothetical protein; ankyrin domain protein	4	384	3.5	6.2E-03
Rmet_5753		Conserved hypothetical protein	7	430	5.9	5.0E-05
Rmet_5796		D-isomer specific 2-hydroxyacid dehydrogenase, NAD-binding	3	149	4.0	1.9E-03

Table B.7 – Proteins up-regulated in "low phosphorus" media compared to optimal media

B.4.2 Down-regulated compared to the control

Table B.8 – Proteins down-regulated in "low phosphorus" media compared to optimal media

Locus tag	Protein name	Description	No. peptides	Score	FC	P value
Amino acid synthesis and metabolism						
Rmet_0716	PheA	Prephenate dehydratase, Chorismate mutase	3	267	0.32	3.8E-05
Rmet_0911	IlvI	Acetolactate synthase III, large subunit	7	414	0.38	2.0E-03
Rmet_2812	CysN	Sulfate adenylyltransferase, subunit 1	4	320	0.33	2.1E-04
Rmet_2813	CysD	Sulfate adenylyltransferase, subunit 2.	4	231	0.39	5.4E-03
Rmet_2815	CysO	Protein involved in cysteine metabolism	3	149	0.33	2.8E-02
Rmet_2816	CysI	Sulfite reductase, beta subunit (hemoprotein with two 4Fe-4S domains)	9	546	0.42	1.3E-03
Rmet_3181	TrpC	Indole-3-glycerol phosphate synthase	2	95	0.35	3.4E-02
Rmet_3241	HisI	Phosphoribosyl-AMP cyclohydrolase	2	105	0.39	1.2E-02
Biosynthesis of cofactors, prosthetic groups, and carriers						
Rmet_0061	LipA	Lipoate synthase	2	93	0.06	7.8E-04
Rmet_0114	BioA	7,8-diaminopelargonic acid synthase, PLP-dependent	6	351	0.44	5.7E-05
Rmet_0115	BioF	8-amino-7-oxononanoate synthase	2	128	0.11	1.2E-03
Rmet_0117	BioB	Biotin synthase	14	936	0.29	1.9E-03
Rmet_1964	MoeA	Molybdopterin biosynthesis protein (MoeA-like, domain I and II)	2	112	0.20	2.2E-02
Rmet_2615	Dxs	1-deoxyxylulose-5-phosphate synthase, thiamine-requiring, FAD-requiring	10	491	0.44	3.2E-04
Rmet_2868	IspH	1-hydroxy-2-methyl-2-(E)-butenyl 4-diphosphate reductase, 4Fe-4S protein	3	145	0.40	4.2E-04
Cell envelope						
Rmet_0533	KdsB	3-deoxy-manno-octulosonate cytidylyltransferase	3	95	0.41	1.3E-02
Rmet_0727	RfaE	Fused heptose 7-phosphate kinase; heptose 1-phosphate adenyltransferase	2	158	0.35	4.7E-03
Rmet_2674	Pal	Peptidoglycan-associated outer membrane lipoprotein	12	832	0.43	1.0E-02
Rmet_2733	RfbA	Glucose-1-phosphate thymidylyltransferase	6	346	0.47	1.0E-03
Rmet_3133	MurE	UDP-N-acetylmuramoyl-L-alanyl-D-glutamate:meso-diaminopimelate ligase	2	77	0.46	2.0E-02

Continued on next page

Table B.8 – Proteins down-regulated in "low phosphorus" media compared to optimal media

Locus tag	Protein name	Description	No. peptides	Score	FC	P value
Cellular process						
Rmet_0034	MinD	Septum site-determining protein minD	5	255	0.41	9.4E-04
Rmet_0458	UspA1	Universal stress protein, UspA family	7	535	0.42	6.8E-04
Rmet_2417	Era	Membrane-associated, 16S rRNA-binding GTPase	2	108	0.38	1.1E-02
Rmet_3226	SspB	ClpXP protease specificity-enhancing factor	3	170	0.32	3.2E-02
Rmet_3272	PilM	Type IV pilus assembly protein PilM	2	101	0.41	4.6E-04
Rmet_3574	CstA	Starvation-induced protein involved in peptide utilization during carbon starvation	3	172	0.39	4.6E-02
DNA metabolism						
Rmet_2914	PcnB	Poly(A) polymerase I polynucleotide adenylyltransferase	2	62	0.38	1.1E-02
Rmet_6191	Bph2	Histone-like DNA-binding protein	3	279	0.24	5.3E-03
Energy metabolism						
Rmet_1285	HypB1	GTP hydrolase involved in nickel liganding into hydrogenases	2	74	0.37	3.8E-02
Rmet_1297	HoxG	Hydrogenase 1	24	1369	0.42	1.4E-03
Rmet_1522	HoxF	NAD-reducing hydrogenase diaphorase moiety large subunit	10	799	0.48	4.2E-03
Rmet_1523	HoxU	NAD-reducing hydrogenase diaphorase moiety small subunit	3	222	0.48	3.1E-02
Rmet_1524	HoxY	NAD-reducing hydrogenase hoxS delta subunit	4	224	0.39	1.0E-04
Rmet_2048	OdhL	Dihydrolipoamide dehydrogenase	18	1484	0.43	6.4E-03
Rmet_2980	CbbT2	Transketolase 1, thiamin-binding	10	843	0.49	4.3E-04
Fatty acid and phospholipid metabolism						
Rmet_0108		Acyl-CoA dehydrogenase, short-chain specific	3	88	0.49	1.4E-02
Rmet_1853	AtoB	Acetyl-CoA acetyltransferase/thiolase	7	400	0.41	1.4E-03
Rmet_2055	UgpB	Glycerol-3-phosphate transporter subunit	4	172	0.46	7.2E-04
Mobile and extrachromosomal element functions						
Rmet_6316	ParB	ParB involved in chromosome partitioning	2	55	0.40	3.6E-02
Protein synthesis						
Rmet_0288	RplY	50S ribosomal protein L25 (General stress protein CTC)	9	692	0.34	1.7E-04
Rmet_0411	RspI	30S ribosomal subunit protein S9	7	610	0.35	1.1E-02
Rmet_0818	GlnS	Glutamyl-tRNA synthetase	6	260	0.47	2.4E-02
Rmet_1161	InfC	Protein chain initiation factor IF-3	4	241	0.36	6.2E-05
Rmet_1163	RplT	50S ribosomal subunit protein L20	2	176	0.43	2.2E-02

Continued on next page

Table B.8 – Proteins down-regulated in "low phosphorus" media compared to optimal media

Locus tag	Protein name	Description	No. peptides	Score	FC	P value
Rmet_1979	RpsF	30S ribosomal subunit protein S6	8	694	0.42	1.2E-03
Rmet_2031	InfB	Translation initiation factor 2	19	1855	0.46	3.1E-03
Rmet_2412	Efp	Translation elongation factor P	7	402	0.43	8.9E-05
Rmet_2432	RpmF	50S ribosomal subunit protein L32	2	296	0.36	7.6E-04
Rmet_2455	RpsU1	30S ribosomal subunit protein S21	2	113	0.30	4.3E-03
Rmet_2630	ValS	Valyl-tRNA synthetase	11	831	0.42	8.7E-04
Rmet_2885	IleS	Isoleucyl-tRNA synthetase	15	1072	0.50	2.4E-02
Rmet_2904	RpsT	30S ribosomal subunit protein S20	6	466	0.32	3.9E-03
Rmet_2921	DnaJ	Chaperone Hsp40, co-chaperone with DnaK	2	57	0.29	4.3E-02
Rmet_3290	RplQ	50S ribosomal subunit protein L17	5	286	0.48	3.7E-03
Rmet_3293	RpsK	30S ribosomal subunit protein S11	7	667	0.48	1.1E-04
Rmet_3302	RplF	50S ribosomal subunit protein L6	14	1054	0.43	1.9E-03
Rmet_3306	RplX	50S ribosomal subunit protein L24	11	1005	0.45	1.3E-02
Rmet_3307	RplN	50S ribosomal subunit protein L14	8	523	0.49	1.4E-03
Rmet_3308	RpsQ	30S ribosomal subunit protein S17	3	253	0.32	1.3E-03
Rmet_3313	RpsS	30S ribosomal subunit protein S19	5	470	0.50	8.3E-03
Rmet_3314	RplB	50S ribosomal subunit protein L2	16	1303	0.44	4.2E-04
Rmet_3335	RplL	50S ribosomal subunit protein L7/L12	11	980	0.34	7.8E-04
Rmet_3338	RplK	50S ribosomal subunit protein L11	5	241	0.43	1.9E-04
Purines, pyrimidines, nucleosides and nucleotides						
Rmet_0856	Gmk	Guanylate kinase	2	137	0.35	8.7E-03
Transcription						
Rmet_0302	RpoX	Sigma 54 modulation protein, ribosome-associated	6	489	0.31	1.4E-02
Rmet_1044	YebK	Transcriptional regulator, RpiR family	2	271	0.20	4.8E-02
Rmet_1232	YhgF	Putative RNA-binding transcription accessory protein	4	200	0.31	1.0E-03
Rmet_2037	FnrL	Transcriptional regulator	2	96	0.47	3.1E-02
Transport and binding proteins						
Rmet_0452	PhoL	Putative enzyme with nucleoside triphosphate hydrolase domain	2	73	0.47	4.8E-04
Rmet_3153		ABC-type branched-chain amino acid transport system, periplasmic component	3	182	0.40	3.9E-02
Rmet_5616	Bug	Extra-cytoplasmic solute receptor protein	2	110	0.36	4.2E-04

Continued on next page

Table B.8 – Proteins down-regulated in "low phosphorus" media compared to optimal media

Locus tag	Protein name	Description	No. peptides	Score	FC	P value
Rmet_6209	CnrB	Membrane fusion protein, three components cation proton antiporter efflux system, involved in Co(II), Ni(II) resistance	4	238	0.41	3.0E-02
Unassigned						
Rmet_0095		Conserved hypothetical protein	3	165	0.31	3.2E-03
Rmet_0097		Conserved hypotethical protein	2	74	0.17	2.9E-03
Rmet_0367		Putative Fe-S oxidoreductase	5	353	0.46	3.5E-02
Rmet_0665	LemA	LemA like protein	2	67	0.04	6.5E-05
Rmet_0718	TyrA	Prephenate dehydrogenase	2	84	0.49	1.5E-02
Rmet_1600		Conserved hypothetical protein; putative exported protein	4	224	0.27	2.1E-03
Rmet_1808	PepM	Phosphoenolpyruvate phosphomutase	8	420	0.45	1.7E-04
Rmet_2033		Conserved hypothetical protein	2	163	0.43	2.6E-02
Rmet_2747	HemY	Uncharacterized enzyme of heme biosynthesis	2	63	0.03	1.3E-03
Rmet_2875	Scd	Fatty-acid desaturase	4	256	0.33	6.3E-04
Rmet_3075		Conserved hypothetical protein; putative exported protein	2	72	0.49	8.2E-04
Rmet_3380		Ca^{2+} sensor (EF-Hand superfamily)	2	134	0.32	2.5E-02
Rmet_5074		Conserved hypothetical protein	7	363	0.23	2.4E-06
Rmet_6408		Putative rhodanese-related sulfurtransferase	2	145	0.22	1.5E-02

Table B.8 – Proteins down-regulated in "low phosphorus" media compared to optimal media

B.5 Proteins differentially regulated in the low magnesium treatment

B.5.1 Up-regulated compared to the control

Table B.9 – Proteins up-regulated in magnesium-limited media compared to optimal media

Locus tag	Protein name	Description	Score	No. peptides	FC	P value
Amino acid synthesis and metabolism						
Rmet_1956	ArgE1	Acetylornithine deacetylase	147	3	2.1	4.8E-05
Rmet_2467	TrpB	Tryptophan synthase beta chain	377	4	2.6	4.0E-05
Rmet_4537	SerA2	D-3-phosphoglycerate dehydrogenase, NAD-binding	596	9	2.0	1.3E-04
Biosynthesis of cofactors, prosthetic groups, and carriers						
Rmet_2688	RibD	Riboflavin biosynthesis protein RibD	85	3	2.3	2.8E-02
Cell envelope						
Rmet_2936	PilT	Type IV pilus twitching motility protein	130	2	3.1	1.9E-03
Rmet_2957	Gst-1	Glutathione S-transferase	99	2	2.0	1.3E-02
Rmet_3574	CstA	Starvation-induced protein involved in peptide utilization during carbon starvation	172	3	2.6	2.2E-03
Rmet_5981	CzcB	Cobalt-zinc-cadmium resistance protein CzcB	232	4	5.3	3.5E-04
Central intermediary metabolism						
Rmet_5402		Putative alkyl sulfatase	987	15	2.1	1.0E-03
Energy metabolism						
Rmet_1515	CbbG1	Glyceraldehyde-3-phosphate dehydrogenase	585	8	2.5	1.2E-03
Rmet_1535	HypA2	Probable hydrogenase nickel incorporation protein	113	2	3.0	3.6E-04
Rmet_2134	TrxA	Thioredoxin	816	10	2.6	9.8E-03
Fatty acid and phospholipid metabolism						
Rmet_1200	PhaP	Phasin (PHA-granule associated protein)	3727	27	2.8	1.7E-04
Rmet_2643	Cfa	Cyclopropane-fatty-acyl-phospholipid synthase	258	5	2.4	1.2E-04
Phosphorus metabolism						

Continued on next page

Table B.9 – Proteins up-regulated in magnesium-limited media compared to optimal media

Locus tag	Protein name	Description	Score	No. peptides	FC	P value
Rmet_2180	PhoB	DNA-binding response regulator in two-component regulatory system with PhoR	179	2	5.4	3.7E-03
Rmet_2181	PhoU	Phosphate-specific transport system accessory protein	969	10	4.4	4.4E-05
Rmet_2182	PstB	Phosphate import ATP-binding protein	218	5	8.9	1.7E-04
Rmet_2185	PstS	Phosphate-binding protein	2142	25	15.8	4.5E-06
Rmet_2992	PtxD	Phosphonate dehydrogenase	859	12	4.3	4.0E-05
Rmet_2994	PtxB	Phosphite transport system-binding protein	1495	16	3.1	5.3E-03
Protein fate						
Rmet_1026	IscU	FeS cluster assembly scaffold protein	570	9	2.4	1.2E-04
Protein synthesis						
Rmet_0448	GlyQ	Glycine-tRNA ligase alpha subunit	132	3	4.5	1.5E-02
Rmet_0831	AlaS	Alanine–tRNA ligase	1089	19	2.4	5.3E-04
Regulation						
Rmet_0001	DnaA	Chromosomal replication initiator protein DnaA	123	2	9.2	1.9E-02
Rmet_2952	PhcB	Enzyme required for production of 3-OH PAME	290	5	3.8	3.1E-03
Transcription						
Rmet_2034		Pseudouridine synthase	254	5	3.3	3.2E-03
Rmet_3564	Fmt	Methionyl-tRNA formyltransferase	123	3	6.1	3.7E-04
Rmet_4773		Putative endoribonuclease L-PSP	135	2	2.1	6.9E-04
Transport and binding proteins						
Rmet_1121	AcrD	Aminoglycoside/multidrug efflux system	209	4	7.0	1.5E-04
Rmet_5329	ZneA	Heavy metal cation tricomponent efflux pump ZneA	279	4	11.3	1.1E-04
Rmet_5330	ZneB	Membrane fusion protein heavy metal cation tricomponent efflux	559	9	20.6	4.3E-05
Rmet_5408		Putative efflux outer membrane protein	142	2	55.7	2.2E-02
Rmet_5682	NimB	Heavy metal cation tricomponent efflux membrane fusion protein	358	6	5.3	3.0E-05
Rmet_6209	CnrB	Nickel and cobalt resistance protein	238	4	4.4	4.0E-04
Unassigned						
Rmet_0310		Putative intracellular protease/amidase/DJ-1/PfpI family	1465	11	4.1	9.3E-06
Rmet_0421		Uncharacterised protein	1251	12	2.3	1.4E-02
Rmet_1157		Hydrolase, alpha/beta fold family	97	2	4.4	2.1E-02
Rmet_1695		Uncharacterised protein	257	3	4.0	5.0E-04

Continued on next page

Table B.9 – Proteins up-regulated in magnesium-limited media compared to optimal media

Locus tag	Protein name	Description	Score	No. peptides	FC	P value
Rmet_2435		RNA polymerase sigma factor	89	2	60.5	2.5E-03
Rmet_2636		Thioredoxin domain-containing protein	286	5	4.2	1.4E-04
Rmet_3202		Uncharacterised protein	138	2	3.8	4.4E-02
Rmet_3566		Uncharacterised protein	442	5	2.1	4.7E-03
Rmet_3904	PrkA	Putative serine protein kinase	487	10	3.0	5.2E-04
Rmet_4545		Uncharacterised protein	152	3	2.9	1.4E-03
Rmet_5311		Isochorismatase hydrolase	347	4	2.3	3.8E-02
Rmet_5936		Putative monooxygenase with luciferase-like ATPase activity conserved hypothetical protein	80	2	2.2	1.8E-02

Table B.9 – Proteins up-regulated in magnesium-limited media compared to optimal media

B.5.2 Down-regulated compared to the control

Table B.10 – Proteins down-regulated in magnesium-limited media compared to optimal media

Locus tag	Protein name	Description	Score	No. peptides	FC	P value
Amino acid synthesis and metabolism						
Rmet_0049	GatA1	Glutamyl/Aspartyl-tRNA amidotransferase subunit A	491	9	0.49	6.7E-04
Rmet_0140	ArgB	Acetylglutamate kinase	598	9	0.37	9.4E-03
Rmet_0911	IlvI	Acetolactate synthase III, large subunit	414	7	0.37	2.6E-04
Rmet_1164	PheS	Phenylalanine tRNA synthetase, alpha subunit	368	6	0.48	6.8E-03
Rmet_1966	ThrA	Homoserine dehydrogenase	591	7	0.43	1.3E-02
Rmet_1967	AatA	Aspartate aminotransferase	229	4	0.49	1.6E-03
Rmet_2812	CysN	Sulfate adenylyltransferase, subunit 1	320	4	0.31	1.8E-04
Rmet_2815	CysO	Protein involved in cysteine metabolism	149	3	0.31	1.5E-02
Rmet_0681	GlnB	Regulatory protein P-II for glutamine synthetase	362	5	0.48	1.5E-02
Rmet_2473	LeuD	3-isopropylmalate isomerase subunit	357	7	0.38	4.0E-03
Rmet_2751	ArgH	Argininosuccinate lyase	512	7	0.44	5.0E-03
Rmet_3242	HisF	Imidazole glycerol phosphate synthase	120	2	0.29	2.3E-02
Rmet_3247	HisC	Histidinol-phosphate aminotransferase	209	4	0.38	9.6E-03
Rmet_3263	GltB	Glutamate synthase, large subunit	2962	43	0.42	1.8E-04
Rmet_4564	MetE	5-methyltetrahydropteroyltriglutamate– homocysteine methyltransferase	2408	34	0.50	1.6E-05
Biological processes						
Rmet_1009	RutE	Oxidoreductase subunit of the alternative pyrimidine degradation pathway	277	4	0.24	4.9E-03
Biosynthesis of cofactors, prosthetic groups, and carriers						
Rmet_0115	BioF	8-amino-7-oxononanoate synthase	128	2	0.39	2.2E-02
Rmet_0117	BioB	Biotin synthase	936	14	0.26	8.4E-05
Rmet_0486	MoaC	Molybdopterin biosynthesis, protein C	52	2	0.34	1.4E-02
Rmet_0839		(S)-2-hydroxy-acid oxidase 1	410	6	0.45	3.2E-03
Rmet_1192	FolD	Bifunctional protein	200	4	0.40	6.7E-03
Rmet_1441	Dxr	1-deoxy-D-xylulose 5-phosphate reductoisomerase	413	5	0.42	1.4E-02

Continued on next page

Table B.10 – Proteins down-regulated in magnesium-limited media compared to optimal media

Locus tag	Protein name	Description	Score	No. peptides	FC	P value
Rmet_2642	PdxH	Pyridoxine 5'-phosphate oxidase	185	4	0.47	4.4E-03
Rmet_2774	PanC	Pantothenate synthetase	90	2	0.32	1.7E-02
Rmet_2785	CobT	Nicotinate-nucleotide dimethylbenzimidazole-P phophoribosyl transferase	118	2	0.43	4.9E-02
Rmet_2868	IspH	1-hydroxy-2-methyl-2-(E)-butenyl 4-diphosphate reductase, 4Fe-4S protein	145	3	0.26	1.2E-04
Rmet_2873	NadC	Nicotinate-nucleotide pyrophosphorylase	87	2	0.42	3.0E-02
Cell envelope						
Rmet_0533	KdsB	3-deoxy-manno-octulosonate cytidylyltransferase	95	3	0.42	6.7E-03
Rmet_2186	GlmM	Phosphoglucosamine mutase	544	8	0.31	3.1E-02
Rmet_5339		CsgG family protein; Curli production assembly/transport component	106	2	0.29	1.0E-02
Cellular process						
Rmet_1849		Putative oxidoreductase/alcolhol dehydrogenase	315	3	0.50	3.5E-02
Rmet_3123	FtsZ	GTP-binding tubulin-like cell division protein	824	10	0.31	1.1E-03
Rmet_3124	FtsA	ATP-binding cell division protein	356	5	0.27	3.6E-04
Rmet_3226	SspB	Protease specificity-enhancing factor	170	3	0.31	3.3E-03
Rmet_3272	PilM	Type IV pilus assembly protein	101	2	0.46	1.1E-02
Rmet_3346	UspA8	Universal stress protein	371	4	0.30	1.5E-02
Rmet_3506	GidA	Glucose-inhibited cell-division protein	168	2	0.32	1.1E-02
Rmet_0035	MinC	Cell division inhibitor	383	5	0.44	2.6E-02
Rmet_1951	AhpD	Alkyl hydroperoxide reductase D	546	7	0.22	7.1E-03
Rmet_2935	PilU	Type IV pilus twitching motility protein	104	3	0.27	2.6E-02
Rmet_4019	SurE	5'-nucleotidase; stationary-phase survival protein	83	2	0.31	5.4E-03
Rmet_4395	UspA9	Universal stress protein	557	7	0.47	2.8E-04
Rmet_4862		Conserved hypothetical protein	104	2	0.28	3.4E-02
Rmet_5669	CopC2	Copper resistance C protein precursor	170	2	0.11	8.0E-03
Central intermediary metabolism						
Rmet_2513		Aminotransferase family protein	289	7	0.49	1.1E-04
Rmet_3419	SoxX	Sulfur oxidation protein	218	2	0.28	1.3E-02
Rmet_4943		Putative iron-containing alcohol dehydrogenase	105	2	0.36	1.0E-02
DNA metabolism						

Continued on next page

Table B.10 – Proteins down-regulated in magnesium-limited media compared to optimal media

Locus tag	Protein name	Description	Score	No. peptides	FC	P value
Rmet_1189	XthA2	Exodeoxyribonuclease III	129	2	0.01	7.1E-07
Energy metabolism						
Rmet_0197	Qor	Quinone oxidoreductase, NADPH-dependent	218	3	0.46	7.6E-03
Rmet_0222	NppD	2-nitropropane dioxygenase	154	2	0.04	6.6E-04
Rmet_0931	NuoE	NADH dehydrogenase chain E	130	2	0.19	3.4E-03
Rmet_0932	NuoF	NADH:ubiquinone oxidoreductase, chain F	395	7	0.40	1.5E-03
Rmet_0974	PaaH	3-hydroxybutyryl-CoA dehydrogenase	326	4	0.24	3.7E-03
Rmet_0975	Gst-1	Glutathione S-transferase	184	4	0.44	1.8E-02
Rmet_0987		Cytochrome c, class IC 1	317	4	0.40	3.8E-03
Rmet_1522	HoxF	NAD-reducing hydrogenase diaphorase moiety large subunit	799	10	0.40	5.1E-03
Rmet_1536	HypB2	GTP hydrolase involved in nickel liganding into hydrogenases	1175	16	0.32	4.8E-02
Rmet_1539	HypD2	Protein required for maturation of hydrogenases	342	7	0.35	2.4E-03
Rmet_2895	Icd	Isocitrate dehydrogenase	171	4	0.45	2.1E-04
Rmet_0106	AtoB	Acetyl-CoA acetyltransferase	320	5	0.47	1.3E-02
Rmet_1087	AccA	Acetyl-CoA carboxylase, carboxytransferase, alpha subunit	355	5	0.44	2.1E-04
Rmet_1153	AtoD	Acetyl-CoA:acetoacetyl-CoA transferase, alpha subunit	316	6	0.46	6.4E-03
Rmet_2147	FabI	Enoyl-acyl-carrier-protein reductase, NADH-dependent	624	8	0.50	4.0E-04
Mobile and extrachromosomal element functions						
Rmet_6062	ParB	Plasmid replication- partition related protein	163	2	0.14	2.0E-02
Protein fate						
Rmet_1028	HscB	DnaJ-like molecular chaperone specific for IscU	163	3	0.22	7.2E-03
Rmet_1434	Map	Methionine aminopeptidase	172	4	0.49	1.9E-02
Rmet_1884	ClpX	ATPase and specificity subunit of ClpX-ClpP ATP-dependent serine protease	543	7	0.44	7.5E-03
Rmet_5411		Putative membrane Zinc metallopeptidase, M50 family	129	3	0.07	9.1E-03
Protein synthesis						
Rmet_0410	RplM	50S ribosomal subunit protein L13	586	8	0.44	6.7E-04
Rmet_0411	RpsI	30S ribosomal subunit protein S9	610	7	0.49	6.1E-04
Rmet_0440	TrpS	Tryptophanyl-tRNA synthetase	476	8	0.45	1.4E-02
Rmet_0686	LolA	Outer membrane lipoprotein carrier protein	201	4	0.27	1.1E-02
Rmet_0748	RpsP	30S ribosomal subunit protein S16	155	2	0.31	3.8E-03

Continued on next page

Table B.10 – Proteins down-regulated in magnesium-limited media compared to optimal media

Locus tag	Protein name	Description	Score	No. peptides	FC	P value
Rmet_1163	RplT	50S ribosomal subunit protein L20	176	2	0.40	2.7E-02
Rmet_1979	RpsF	30S ribosomal subunit protein S6	694	8	0.44	3.8E-03
Rmet_2103	YfgL	Outer membrane protein assembly complex subunit	313	5	0.41	2.3E-03
Rmet_2432	RpmF	50S ribosomal subunit protein L32	296	2	0.39	4.9E-03
Rmet_2870	RpmB	50S ribosomal subunit protein L28	279	4	0.20	2.4E-04
Rmet_3305	RplE	50S ribosomal subunit protein L5	476	8	0.38	8.5E-04
Rmet_3309	RpmC	50S ribosomal subunit protein L29	237	3	0.49	6.1E-03
Rmet_3326	RpsG	30S ribosomal subunit protein S7	480	8	0.49	1.5E-02
Rmet_3327	RplL	30S ribosomal subunit protein S12	329	5	0.38	2.4E-03
Purines, pyrimidines, nucleosides and nucleotides						
Rmet_0150	PyrE	Orotate phosphoribosyltransferase	273	4	0.37	1.2E-02
Rmet_0942		Putative ADP-ribose pyrophosphatase	123	2	0.15	1.3E-02
Rmet_1870	PurL	Phosphoribosylformyl-glycineamide synthetase	988	13	0.45	1.5E-04
Rmet_2739	PyrX	Dihydroorotase	116	3	0.08	3.6E-02
Rmet_2740	PyrB	Aspartate carbamoyltransferase	294	5	0.33	1.2E-03
Rmet_2741	PyrR	Bifunctional protein: pyrimidine operon regulatory protein/uracil phosphoribosyltransferase	309	4	0.34	4.8E-02
Regulation						
Rmet_1194		Two component transcriptional regulator, LuxR family	409	4	0.49	1.2E-02
Rmet_2941	OxyR	Oxidative stress-inducible genes activator	92	2	0.42	1.3E-03
Rmet_6162		Transcriptional regulator, XRE family	85	2	0.10	4.7E-05
Transcription						
Rmet_0857	RpoZ	DNA-directed RNA polymerase omega subunit	200	5	0.46	8.7E-03
Rmet_2606	RpoD1	RNA polymerase sigma D factor (housekeeping sigma factor)	753	13	0.49	2.6E-05
Transport and binding proteins						
Rmet_0372	Tim44	Import inner membrane translocase	544	9	0.47	9.8E-04
Rmet_1209		ABC transporter-related protein	276	6	0.46	2.3E-04
Rmet_1404	YheS	Putative fused transporter subunits of ABC superfamily	143	2	0.08	1.1E-03
Rmet_2891	Bug	Extra-cytoplasmic Solute Receptor	108	2	0.50	3.3E-02
Rmet_3076	Bug	Extra-cytoplasmic Solute Receptor	178	2	0.50	2.8E-02
Rmet_3237	TatA	TatABCE protein translocation system subunit	160	2	0.01	1.8E-02

Continued on next page

Table B.10 – Proteins down-regulated in magnesium-limited media compared to optimal media

Locus tag	Protein name	Description	Score	No. peptides	FC	P value
Rmet_3543		TRAP-type mannitol/chloroaromatic compound transporter	473	8	0.49	8.6E-03
Rmet_3671	Bug	Extra-cytoplasmic solute Receptor	56	2	0.00	1.4E-03
Rmet_4286	Bug	Extra-cytoplasmatic solute receptor	341	6	0.39	4.0E-04
Rmet_5378	HmuV	Putative Hemin ABC transport system, ATP-binding protein	371	7	0.29	6.0E-03
Rmet_6339		Cupin 2 conserved barrel domain protein	82	2	0.39	9.3E-03
Unassigned						
Rmet_0024		Carboxypeptidase G2 precursor	227	4	0.47	3.4E-03
Rmet_0086		Putative sulfurtransferase	74	2	0.22	7.4E-04
Rmet_0087	BhmT	Homocysteine S-methyltransferase	107	2	0.48	3.8E-02
Rmet_0097		Conserved hypothetical protein	74	2	0.15	7.5E-04
Rmet_0152		Conserved hypothetical protein	227	4	0.34	1.5E-02
Rmet_0492		Conserved hypothetical protein	210	3	0.27	4.1E-02
Rmet_0563	Ptb	Phosphate acetyltransferase	373	6	0.35	2.5E-02
Rmet_0673	PilL2	Type IV pilus protein histidine kinase/response regulator	225	4	0.26	7.2E-06
Rmet_0718	TyrA	Prephenate dehydrogenase	84	2	0.44	1.1E-02
Rmet_1368	SerB	Phosphoserine phosphatase	236	4	0.29	4.0E-04
Rmet_1452		Conserved hypothetical protein	106	2	0.07	3.6E-02
Rmet_1600		Conserved hypothetical protein; putative exported protein	224	4	0.33	5.2E-04
Rmet_1974		Conserved hypothetical protein	149	2	0.24	1.0E-02
Rmet_2033		Conserved hypothetical protein	163	2	0.29	2.4E-02
Rmet_2043	CcoO	Cbb3-type cytochrome oxidase, monoheme subunit II	203	4	0.32	6.6E-04
Rmet_2094		NAD-dependent epimerase/dehydratase	117	2	0.31	6.9E-03
Rmet_2125		L-carnitine dehydratase/bile acid-inducible protein	126	2	0.12	6.5E-03
Rmet_2436	SohB	Peptidase S49, periplasmic serine protease (ClpP class)	62	2	0.13	8.5E-03
Rmet_2452	TrxB2	Thioredoxin reductase	741	13	0.38	3.1E-03
Rmet_2494		Conserved hypothetical protein	262	5	0.40	4.6E-03
Rmet_2620	SseA	Rhodanese-related sulfurtransferase	144	2	0.37	1.7E-03
Rmet_2632		Conserved hypothetical protein	105	2	0.18	6.8E-03
Rmet_2657		Conserved hypothetical protein	84	2	0.20	8.6E-03
Rmet_2668		Conserved hypothetical protein	245	4	0.26	4.6E-02
Rmet_2747	HemY	Uncharacterized enzyme of heme biosynthesis	63	2	0.12	3.9E-03

Continued on next page

Table B.10 – Proteins down-regulated in magnesium-limited media compared to optimal media

Locus tag	Protein name	Description	Score	No. peptides	FC	P value
Rmet_2790		Conserved hypothetical protein	267	3	0.09	1.4E-04
Rmet_2890		Putative glyoxalase	87	2	0.06	1.1E-02
Rmet_3071		Histone H1-like protein HC2	211	3	0.44	1.5E-03
Rmet_3116		Conserved hypothetical protein	326	5	0.27	1.1E-02
Rmet_3159	HipO	Hippurate hydrolase	134	2	0.34	1.1E-04
Rmet_3188		Unassigned peptidase	250	4	0.35	4.1E-02
Rmet_3321		Dienelactone hydrolase	298	3	0.46	3.2E-03
Rmet_3424		Cytochrome c551/c552	358	4	0.47	1.3E-03
Rmet_3471		Conserved hypothetical protein	200	3	0.18	2.4E-02
Rmet_3665		Hypothetical protein	604	8	0.31	7.9E-03
Rmet_3697		Conserved hypothetical protein	163	3	0.49	9.1E-03
Rmet_3896		Thiamine pyrophosphate-requiring enzyme	110	2	0.08	7.9E-04
Rmet_4584		Conserved hypothetical protein	162	2	0.19	1.7E-02
Rmet_5267		Putative alpha/beta hydrolase	119	2	0.40	3.8E-02
Rmet_5600		Conserved hypothetical protein	384	4	0.42	2.3E-02
Rmet_5645	Adh	Alcohol dehydrogenase, zinc-binding	291	6	0.35	1.4E-03
Rmet_5796		D-isomer specific 2-hydroxyacid dehydrogenase, NAD-binding	149	3	0.19	1.2E-03
Rmet_6558		Putative hypothetical protein	137	2	0.01	3.2E-02

Table B.10 – Proteins down-regulated in magnesium-limited media compared to optimal media

B.6 Proteins differentially regulated in the phosphorus and iron co-limited treatment

B.6.1 Up-regulated compared to the control

Table B.11 – Proteins up-regulated in Fe-P co-limited media compared to optimal media

Locus tag	Protein name	Description	No. peptides	Score	FC	P value
Amino acid synthesis and metabolism						
Rmet_0398	GdhA	Glutamate dehydrogenase	11	979	2.2	5.2E-04
Rmet_0681	GlnB	Regulatory protein P-II for glutamine synthetase	5	362	2.5	7.0E-03
Biological Process						
Rmet_4084	Phoa1	Alkaline phosphatase	10	665	6.9	2.1E-03
Rmet_4085	Phoa2	Alkaline phosphatase	6	451	5.4	4.9E-04
Biosynthesis of cofactors, prosthetic groups, and carriers						
Rmet_1110	SbnH	Diaminopimelate decarboxylase implied in the biosynthesis of staphyloferrin B	9	695	4.4	1.2E-02
Rmet_1111	SbnG	2-dehydro-3-deoxyglucarate aldolase implied in the biosynthesis of staphyloferrin B	8	474	3.3	2.0E-02
Rmet_1115	SbnC	IucC-like protein implied in the biosynthesis of staphyloferrin B	11	794	2.5	5.7E-03
Rmet_1116	SbnB	Ornithine cyclodeaminase implied in the biosynthesis of staphyloferrin B	26	2563	6.0	3.3E-02
Rmet_1117	SbnA	Cysteine synthase implied in the biosynthesis of staphyloferrin B	7	554	3.0	2.4E-02
Rmet_2689	RibC	Riboflavin synthase alpha chain	3	221	2.4	4.8E-02
Cell envelope						
Rmet_0712	OmpA	Outer membrane protein or related peptidoglycan-associated (lipo)protein	11	907	2.2	2.4E-02
Rmet_1455	YbbK	Putative protease, membrane anchored	11	982	2.8	1.3E-02
Rmet_1685		Putative HlyD family secretion protein	6	301	2.6	8.7E-04

Continued on next page

Table B.11 – Proteins up-regulated in Fe-P co-limited media compared to optimal media

Locus tag	Protein name	Description	No. peptides	Score	FC	P value
Rmet_4192	PlcN	Phospholipase C signal peptide protein	29	2461	5.3	3.1E-03
Cellular process						
Rmet_3346	UspA8	Universal stress protein, UspA family	4	371	6.9	3.0E-03
Rmet_3616		Osmotically inducible protein (OsmC-like)	3	218	2.2	4.7E-03
Rmet_4751	MscS	Mechanosensitive ion channel	4	395	2.1	1.3E-02
Rmet_5371	KatG	Catalase/hydroperoxidase HPI(I)	5	344	5.3	2.4E-03
Central intermediary metabolism						
Rmet_0572	CpdB	2':3'-cyclic-nucleotide 2'-phosphodiesterase	7	411	2.3	5.1E-03
Rmet_0774	PhnD	Phosphonate/organophosphate ester transporter subunit	9	733	6.0	3.2E-03
Rmet_5402		Putative alkyl sulfatase	15	987	2.9	1.4E-03
DNA metabolism						
Rmet_0315	Ssb1	Single-stranded DNA-binding protein (Helix-destabilizing protein)	3	348	2.3	3.6E-03
Rmet_2101	Hfq	Host factor I protein	4	189	12.0	4.5E-02
Energy metabolism						
Rmet_1093	Adh	Alcohol dehydrogenase, 1-propanol preferring	16	1304	6.2	8.9E-05
Rmet_1511	CbbF2	Fructose-1,6-bisphosphatase I	6	419	3.1	2.2E-02
Rmet_1515	CbbG1	Glyceraldehyde-3-phosphate dehydrogenase A	8	585	2.1	3.4E-03
Rmet_4063	NapA	Periplasmic nitrate reductase, large subunit	8	510	4.1	7.8E-03
Rmet_5927	MocA	Aldo/keto oxidoreductase, NADP-binding	6	307	2.3	2.7E-03
Fatty acid and phospholipid metabolism						
Rmet_0565	FabI	Enoyl-acyl-carrier-protein reductase, NADH-dependent	6	610	9.5	2.8E-04
Rmet_1200	PhaP	Phasin (PHA-granule associated protein)	27	3727	3.5	1.3E-05
Rmet_2643	Cfa	Cyclopropane-fatty-acyl-phospholipid synthase	5	258	5.0	5.8E-03
Phosphorus metabolism						
Rmet_2177	Ppx	Exopolyphosphatase	3	193	3.3	1.9E-03
Rmet_2178	Ppk	Polyphosphate kinase, component of RNA degradosome	2	96	9.2	3.1E-03
Rmet_2180	PhoB	DNA-binding response regulator in two-component regulatory system with PhoR	2	179	7.8	3.8E-04
Rmet_2181	PhoU	Negative regulator of PhoR/PhoB two-component regulator	10	969	4.3	6.3E-04
Rmet_2182	PstB	Phosphate transporter subunit	5	218	12.7	2.7E-04
Rmet_2185	PstS	Phosphate transporter subunit	25	2142	11.8	2.1E-06

Continued on next page

Table B.11 – Proteins up-regulated in Fe-P co-limited media compared to optimal media

Locus tag	Protein name	Description	No. peptides	Score	FC	P value
Rmet_2992	PtxD	Phosphonate dehydrogenase	12	859	24.7	1.1E-05
Rmet_2994	PtxB	Putative phosphonate ABC transporter	16	1495	12.6	5.8E-06
Protein fate						
Rmet_0283		Peptidase M16-like protein (Probable peptidase signal peptide protein)	4	283	2.6	2.9E-03
Protein synthesis						
Rmet_5930	FusA2	Elongation factor G2	16	1795	2.1	1.2E-02
Purines, pyrimidines, nucleosides and nucleotides						
Rmet_2740	PyrB	Aspartate carbamoyltransferase, catalytic chain	5	294	2.1	7.9E-03
Transcription						
Rmet_1601		Regulatory protein, MarR family	4	188	2.6	2.5E-02
Rmet_2135	Rho	Transcription termination factor Rho	11	602	2.0	1.4E-03
Rmet_5818	Csp	Cold-shock responsive transcriptional repressor	4	264	4.0	8.1E-04
Transport and binding proteins						
Rmet_1121	AcrD	Aminoglycoside/multidrug efflux system	4	209	4.6	3.0E-02
Rmet_1702	AcrF	Multidrug efflux system protein	15	1082	2.1	6.3E-03
Rmet_1985	YbjL	Putative transporter	8	668	2.5	3.6E-03
Rmet_5378	HmuV	Putative Hemin ABC transport system, ATP-binding protein	7	371	4.3	1.4E-02
Unassigned						
Rmet_0084		Predicted hydrolase or acyltransferase	2	111	4.1	2.1E-03
Rmet_0310		Putative intracellular protease/amidase/DJ-1/PfpI family	11	1465	6.2	1.3E-03
Rmet_0421		Conserved hypothetical protein	12	1251	3.1	1.3E-03
Rmet_0562	AckA2	Acetate kinase	8	440	3.8	9.6E-03
Rmet_0563	Ptb	Phosphate acetyltransferase	6	373	10.0	1.4E-03
Rmet_0564		Conserved hypothetical protein	16	1113	2.1	1.7E-02
Rmet_0862		Conserved hypothetical protein	6	402	3.1	1.8E-02
Rmet_0904		Glycosyltransferase, group 1	8	421	4.4	7.1E-03
Rmet_1183		Conserved hypothetical signal peptide protein	7	579	3.2	2.2E-02
Rmet_1394		Acyl-CoA-binding protein	4	241	4.9	2.5E-02
Rmet_1418		Hypothetical protein	6	476	2.8	6.3E-03
Rmet_1695		Conserved hypothetical protein; putative exported protein	3	257	5.0	3.5E-04

Continued on next page

Table B.11 – Proteins up-regulated in Fe-P co-limited media compared to optimal media

Locus tag	Protein name	Description	No. peptides	Score	FC	P value
Rmet_1696		Conserved hypothetical protein; putative exported protein	10	702	5.8	1.5E-03
Rmet_1704		Conserved hypothetical protein; putative exported protein	8	754	3.1	6.4E-04
Rmet_1705		Conserved hypothetical protein; putative exported protein	14	1519	3.4	1.8E-04
Rmet_1706		Conserved hypothetical protein; putative exported protein	3	233	2.1	4.2E-03
Rmet_1830	GcvT	Putative glycine cleavage T protein (aminomethyl transferase)	3	111	2.1	1.2E-02
Rmet_1971		Conserved hypothetical protein	2	98	3.5	3.7E-02
Rmet_1984	AsdA	L-Aspartate decarboxylase	25	1718	2.9	1.3E-04
Rmet_2243		Conserved hypothetical protein	2	234	2.9	3.3E-04
Rmet_2281		Conserved hypothetical protein	5	282	3.0	3.4E-02
Rmet_2583	PhoD	Phosphodiesterase/alkaline phosphatase D	9	614	2.3	3.2E-02
Rmet_2632		Conserved hypothetical protein	2	105	3.5	5.0E-02
Rmet_2968		2-Hydroxychromene-2-carboxylate isomerase	5	330	2.6	6.5E-03
Rmet_2984		Conserved hypothetical protein	3	304	4.2	2.9E-04
Rmet_3826		Conserved hypothetical protein	6	367	3.7	3.4E-04
Rmet_3904	PrkA	Serine protein kinase	10	487	8.6	2.6E-03
Rmet_4030		Putative glyoxalase or dioxygenase	2	69	2.4	7.5E-03
Rmet_4140		Putative methyltransferase	3	180	3.4	2.3E-03
Rmet_4200		Conserved hypothetical protein	3	200	6.8	2.3E-03
Rmet_4347		Alkylhydroperoxidase AhpD core	2	73	2.9	4.0E-02
Rmet_4584		Conserved hypothetical protein	2	162	3.3	1.3E-02
Rmet_4809	AcpA	Putative acid phosphatase protein	3	144	21.6	1.6E-02
Rmet_5000		Conserved hypothetical protein	13	758	3.9	2.1E-02
Rmet_5007		Conserved hypothetical protein	2	199	6.6	2.5E-02
Rmet_5043		Conserved hypothetical protein	10	801	2.5	3.8E-03
Rmet_5311		Isochorismatase hydrolase	4	347	3.9	1.2E-02
Rmet_5313		Putative metallo-dependent amidohydrolase	12	729	4.4	9.2E-04
Rmet_5374		Hypothetical protein	7	618	6.9	3.3E-03
Rmet_5405		Conserved hypothetical protein; putative periplasmic protein	8	703	4.4	1.4E-04
Rmet_5406		Conserved hypothetical protein	4	205	4.0	1.8E-02
Rmet_5600		Conserved hypothetical protein; ankyrin domain protein	4	384	2.2	1.8E-02
Rmet_5638		ABC-type transporter, periplasmic component	11	879	4.7	2.6E-03

Continued on next page

Table B.11 – Proteins up-regulated in Fe-P co-limited media compared to optimal media

Locus tag	Protein name	Description	No. peptides	Score	FC	P value
Rmet_5753		Conserved hypothetical protein	7	430	11.7	5.7E-05
Rmet_5796		D-isomer specific 2-hydroxyacid dehydrogenase, NAD-binding	3	149	2.5	2.7E-02
Rmet_6396		Hypothetical protein	3	314	2.1	2.3E-02

Table B.11 – Proteins up-regulated in Fe-P co-limited media compared to optimal media

B.6.2 Down-regulated compared to the control

Table B.12 – Proteins down-regulated in Fe-P co-limited media compared to optimal media

Locus tag	Protein name	Description	No. peptides	Score	FC	P value
Amino acid synthesis and metabolism						
Rmet_0354	IlvA	Threonine deaminase	6	305	0.24	3.4E-03
Rmet_0715	SerC	3-phosphoserine/phosphohydroxythreonine aminotransferase	11	603	0.36	2.5E-03
Rmet_0716	PheA	Prephenate dehydratase, Chorismate mutase	3	267	0.31	1.4E-05
Rmet_0911	IlvI	Acetolactate synthase III, large subunit	7	414	0.33	5.2E-03
Rmet_0913	IlvC	Ketol-acid reductoisomerase	25	2316	0.47	1.2E-05
Rmet_1089	LysC	Aspartate kinase	6	366	0.40	2.1E-03
Rmet_1164	PheS	Phenylalanine tRNA synthetase, alpha subunit	6	368	0.45	2.3E-03
Rmet_1400	DadX	Alanine racemase 2, PLP-binding	2	52	0.06	7.3E-04
Rmet_1420	DapE	N-succinyl-diaminopimelate deacylase	5	263	0.32	1.0E-03
Rmet_1424	DapC	Probable succinyldiaminopimelate aminotransferase protein	4	202	0.49	8.6E-04
Rmet_1956	ArgE1	Acetylornithine deacetylase	3	147	0.17	6.9E-04
Rmet_2467	TrpB	Tryptophan synthase, beta subunit	4	377	0.44	3.5E-03
Rmet_2476	LivF1	Leucine/isoleucine/valine transporter subunit	2	163	0.48	3.2E-02
Rmet_2627	ThrB	Homoserine kinase	2	86	0.20	3.5E-04
Rmet_2696		Aspartate/tyrosine/aromatic aminotransferase	3	168	0.19	2.6E-02
Rmet_2812	CysN	Sulfate adenylyltransferase, subunit 1	4	320	0.12	4.7E-05
Rmet_2815	CysO	Protein involved in cysteine metabolism	3	149	0.15	5.8E-03
Rmet_2816	CysI	Sulfite reductase, beta subunit (hemoprotein with two 4Fe-4S domains)	9	546	0.21	4.3E-04
Rmet_2938	ProC	Pyrroline-5-carboxylate reductase	4	198	0.07	6.4E-04
Rmet_3181	TrpC	Indole-3-glycerol phosphate synthase	2	95	0.08	1.3E-03
Rmet_3241	HisI	Phosphoribosyl-AMP cyclohydrolase	2	105	0.26	1.8E-03
Rmet_3248	HisD	Bifunctional histidinal dehydrogenase and histidinol dehydrogenase	3	105	0.43	3.5E-02
Rmet_3249	HisG	ATP phosphoribosyltransferase	4	143	0.14	3.9E-03
Rmet_3262	GltD	Glutamate synthase, 4Fe-4S protein, small subunit	18	1298	0.42	2.1E-04
Rmet_3263	GltB	Glutamate synthase, large subunit	43	2962	0.34	1.2E-04

Continued on next page

Table B.12 – Proteins down-regulated in Fe-P co-limited media compared to optimal media

Locus tag	Protein name	Description	No. peptides	Score	FC	P value
Rmet_4563		Transcriptional regulator, LysR family, MetR-like	8	377	0.29	2.8E-03
Rmet_4583	GltL	Glutamate/aspartate transport protein	4	321	0.46	7.6E-05
Rmet_5602		Putative threonine dehydratase	5	349	0.16	2.7E-03
Biosynthesis of cofactors, prosthetic groups, and carriers						
Rmet_0061	LipA	Lipoate synthase	2	93	0.01	1.0E-02
Rmet_0114	BioA	7,8-diaminopelargonic acid synthase, PLP-dependent	6	351	0.22	2.5E-03
Rmet_0115	BioF	8-amino-7-oxononanoate synthase	2	128	0.13	3.8E-04
Rmet_0117	BioB	Biotin synthase	14	936	0.15	2.2E-03
Rmet_0162	ThiC	Thiamin (pyrimidine moiety) biosynthesis protein	13	866	0.43	2.4E-05
Rmet_0486	MoaC	Molybdopterin biosynthesis, protein C	2	52	0.14	1.8E-04
Rmet_1441	Dxr	1-deoxy-D-xylulose 5-phosphate reductoisomerase	5	413	0.49	2.9E-02
Rmet_1964	MoeA	Molybdopterin biosynthesis protein	2	112	0.10	7.6E-04
Rmet_2463	FolC	Bifunctional folylpolyglutamate synthase and dihydrofolate synthase	4	263	0.29	2.2E-03
Rmet_2615	Dxs	1-deoxyxylulose-5-phosphate synthase	10	491	0.36	6.1E-04
Rmet_2868	IspH	1-hydroxy-2-methyl-2-(E)-butenyl 4-diphosphate reductase, 4Fe-4S protein	3	145	0.13	3.0E-05
Cell envelope						
Rmet_0187	GlmS	L-glutamine:D-fructose-6-phosphate aminotransferase	14	901	0.40	4.0E-04
Rmet_0533	KdsB	3-deoxy-manno-octulosonate cytidylyltransferase	3	95	0.38	1.4E-02
Rmet_1352	ComL	DNA uptake lipoprotein	4	214	0.45	1.0E-02
Cellular process						
Rmet_0034	MinD	Septum site-determining protein minD	5	255	0.48	2.3E-02
Rmet_0458	UspA1	Universal stress protein, UspA family	7	535	0.35	3.0E-04
Rmet_2417	Era	Membrane-associated, 16S rRNA-binding GTPase	2	108	0.21	1.3E-04
Rmet_3123	FtsZ	GTP-binding tubulin-like cell division protein	10	824	0.45	1.5E-03
Rmet_3124	FtsA	ATP-binding cell division protein	5	356	0.14	5.0E-05
Rmet_3226	SspB	ClpXP protease specificity-enhancing factor	3	170	0.16	1.3E-02
Rmet_3506	GidA	Glucose-inhibited cell-division protein	2	168	0.42	9.5E-03
Rmet_3574	CstA	Starvation-induced protein involved in peptide utilization during carbon starvation	3	172	0.09	7.3E-03
Rmet_5635		Penicillin amidase (peptidase S45)	2	116	0.25	3.9E-02

Continued on next page

Table B.12 – Proteins down-regulated in Fe-P co-limited media compared to optimal media

Locus tag	Protein name	Description	No. peptides	Score	FC	P value
Rmet_5981	CzcB	Membrane fusion protein, three components cation proton antiporter efflux system involved in Cd(II), Zn(II), Co(II) resistance	4	232	0.21	5.6E-03
Central intermediary metabolism						
Rmet_0081	MhpD2	2-Oxopent-4-enoate hydratase	3	141	0.30	1.7E-02
Rmet_0170	AhcY	Adenosylhomocysteinase	9	543	0.45	5.2E-04
Rmet_0172	MetF	5,10-methylenetetrahydrofolate reductase	2	66	0.10	4.3E-03
Rmet_0378	AspS	Aspartyl-tRNA synthetase	16	976	0.47	5.4E-04
Rmet_2755	Dcd	2'-deoxycytidine 5'-triphosphate deaminase	2	99	0.30	2.2E-02
Rmet_3420	SoxA	Sulfur oxidation protein	5	262	0.25	4.3E-04
Rmet_3422	SoxZ	Thiosulphate-binding sulfur oxidation protein	5	378	0.29	1.6E-04
Rmet_3578	GyaR	Glyoxylate reductase	2	49	0.48	2.1E-02
DNA metabolism						
Rmet_0002	DnaN	DNA polymerase III, beta subunit	12	915	0.41	1.1E-03
Rmet_1189	XthA2	Exodeoxyribonuclease III	2	129	0.22	3.3E-02
Rmet_1428	LigA	DNA ligase, NAD(+)-dependent	2	56	0.47	2.6E-02
Rmet_2129	DnaX	DNA polymerase III tau/gamma subunit	4	266	0.27	1.1E-03
Rmet_2914	PcnB	Poly(A) polymerase I polynucleotide adenylyltransferase	2	62	0.36	1.4E-02
Rmet_4742		Histone-like DNA-binding protein	13	1003	0.50	1.4E-03
Rmet_6191	Bph2	Histone-like DNA-binding protein	5	500	0.23	1.6E-05
Energy metabolism						
Rmet_0261	CoxB	Cytochrome c oxidase, subunit II	7	458	0.43	2.6E-05
Rmet_0470	SucD	Succinyl-CoA synthetase, NAD(P)-binding, alpha subunit	13	1096	0.45	4.6E-05
Rmet_0933	NuoG	NADH dehydrogenase chain G	22	1527	0.45	5.2E-05
Rmet_1045	Edd	6-phosphogluconate dehydratase	11	702	0.49	1.4E-03
Rmet_1146	EtfD	Electron transfer flavoprotein-ubiquinone oxidoreductase	10	711	0.39	1.1E-03
Rmet_1285	HypB1	HypB1 GTP hydrolase involved in nickel liganding into hydrogenases	2	74	0.09	1.8E-03
Rmet_1297	HoxG	HoxG hydrogenase 1, large subunit Uptake hydrogenase large subunit	24	1369	0.30	9.8E-05
Rmet_1536	HypB2	GTP hydrolase involved in nickel liganding into hydrogenases	16	1175	0.26	1.1E-02
Rmet_1539	HypD2	Protein required for maturation of hydrogenases	7	342	0.46	1.8E-02
Rmet_2273	FumA	Fumarate hydratase class I	18	1326	0.45	5.2E-04
Rmet_2750	Ppc	Phosphoenolpyruvate carboxylase	11	592	0.29	4.2E-03

Continued on next page

Table B.12 – Proteins down-regulated in Fe-P co-limited media compared to optimal media

Locus tag	Protein name	Description	No. peptides	Score	FC	P value
Rmet_2980	CbbT2	Transketolase 1, thiamin-binding	10	843	0.43	2.1E-04
Rmet_3498	AtpF	F0 sector of membrane-bound ATP synthase, subunit b	7	505	0.48	1.6E-04
Rmet_3577	PckG	Phosphoenolpyruvate carboxykinase	14	727	0.36	5.8E-05
Fatty acid and phospholipid metabolism						
Rmet_0108		Acyl-CoA dehydrogenase, short-chain specific	3	88	0.39	1.4E-02
Rmet_0212	HbdA	3-hydroxybutyryl-CoA dehydrogenase	4	226	0.32	1.6E-03
Rmet_1087	AccA	Acetyl-CoA carboxylase, carboxytransferase, alpha subunit	5	355	0.46	3.7E-04
Rmet_1853	AtoB	Acetyl-CoA acetyltransferase/thiolase	7	400	0.38	1.1E-03
Rmet_2429	FabD	Malonyl-CoA-acyl-carrier-protein transacylase	2	191	0.44	9.6E-03
Rmet_2635	FadD	Long-chain-fatty-acid-CoA ligase	4	172	0.42	4.8E-02
Mobile and extrachromosomal element functions						
Rmet_6062	ParB	Plasmid replication- partition related protein	2	163	0.02	7.1E-03
Rmet_6316	ParB	Involved in chromosome partitioning	2	55	0.10	1.3E-02
Protein fate						
Rmet_0991	TldD	Peptidase	6	321	0.39	1.4E-02
Rmet_1026	IscU	FeS cluster assembly scaffold protein	9	570	0.47	2.9E-03
Rmet_2188	FtsH	Protease	13	915	0.46	2.4E-03
Rmet_2892	ClpA	ATPase and specificity subunit of ClpA-ClpP ATP-dependent serine protease	9	538	0.39	1.7E-03
Protein synthesis						
Rmet_0046	GatB	Glutamyl-tRNA amidotransferase subunit B	4	335	0.39	7.9E-05
Rmet_0288	RplY	50S ribosomal protein L25	9	692	0.18	2.7E-06
Rmet_0410	RplM	50S ribosomal subunit protein L13	8	586	0.44	2.9E-03
Rmet_0411	RpsI	30S ribosomal subunit protein S9	7	610	0.12	2.8E-05
Rmet_0695	SerS	Seryl-tRNA synthetase	10	701	0.45	1.2E-02
Rmet_0722	RpsA	30S ribosomal subunit protein S1	32	2781	0.37	4.8E-04
Rmet_0748	RpsP	30S ribosomal subunit protein S16	2	155	0.40	3.1E-04
Rmet_0751	RplS	50S ribosomal subunit protein L19	11	889	0.41	2.3E-03
Rmet_0921	RpsO	30S ribosomal subunit protein S15	5	392	0.31	5.0E-03
Rmet_1025	IscS	Cysteine desulfurase	11	798	0.37	4.5E-04
Rmet_1161	InfC	Protein chain initiation factor IF-3	4	241	0.20	1.3E-02

Continued on next page

Table B.12 – Proteins down-regulated in Fe-P co-limited media compared to optimal media

Locus tag	Protein name	Description	No. peptides	Score	FC	P value
Rmet_1444	HlpA	Periplasmic chaperone	5	270	0.46	4.0E-05
Rmet_1976	RplI	50S ribosomal subunit protein L9	12	772	0.47	2.5E-04
Rmet_2031	InfB	Translation initiation factor 2	19	1855	0.44	2.6E-04
Rmet_2137		50S ribosomal protein L31 type B	4	297	0.30	1.1E-05
Rmet_2412	Efp	Translation elongation factor P	7	402	0.41	1.9E-04
Rmet_2432	RpmF	50S ribosomal subunit protein L32	2	296	0.13	2.1E-04
Rmet_2455	RpsU1	30S ribosomal subunit protein S21	2	113	0.14	2.1E-03
Rmet_2630	ValS	Valyl-tRNA synthetase	11	831	0.28	4.6E-05
Rmet_2870	RpmB	50S ribosomal subunit protein L28	4	279	0.26	3.8E-04
Rmet_2871	RpmG	50S ribosomal subunit protein L33	5	593	0.41	6.1E-04
Rmet_2904	RpsT	30S ribosomal subunit protein S20	6	466	0.12	4.7E-05
Rmet_2921	DnaJ	chaperone Hsp40, co-chaperone with DnaK	2	57	0.03	1.5E-03
Rmet_3106	RplU	50S ribosomal subunit protein L21	3	200	0.26	1.4E-04
Rmet_3290	RplQ	50S ribosomal subunit protein L17	5	286	0.17	1.1E-03
Rmet_3292	RpsD	30S ribosomal subunit protein S4	12	988	0.32	7.3E-04
Rmet_3293	RpsK	30S ribosomal subunit protein S11	7	667	0.22	3.0E-06
Rmet_3294	RpsM	30S ribosomal subunit protein S13	9	503	0.34	1.9E-03
Rmet_3298	RplO	50S ribosomal subunit protein L15	8	544	0.36	3.9E-04
Rmet_3299	RpmD	50S ribosomal subunit protein L30	2	217	0.18	1.0E-05
Rmet_3300	RpsE	30S ribosomal subunit protein S5	11	957	0.43	3.2E-04
Rmet_3301	RplR	50S ribosomal subunit protein L18	7	631	0.25	1.1E-05
Rmet_3302	RplF	50S ribosomal subunit protein L6	14	1054	0.20	1.8E-04
Rmet_3304	RpsN	30S ribosomal subunit protein S14	4	297	0.21	1.2E-03
Rmet_3305	RplE	50S ribosomal subunit protein L5	8	476	0.44	1.2E-02
Rmet_3306	RplX	50S ribosomal subunit protein L24	11	1005	0.12	3.7E-05
Rmet_3307	RplN	50S ribosomal subunit protein L14	8	523	0.19	4.6E-04
Rmet_3308	RpsQ	30S ribosomal subunit protein S17	3	253	0.14	5.6E-04
Rmet_3310	RplP	50S ribosomal subunit protein L16	4	302	0.42	1.7E-04
Rmet_3311	RpsC	30S ribosomal subunit protein S3	14	1134	0.48	3.2E-03
Rmet_3312	RplV	50S ribosomal subunit protein L22	7	503	0.15	3.1E-04
Rmet_3313	RpsS	30S ribosomal subunit protein S19	5	470	0.23	4.8E-04

Continued on next page

Table B.12 – Proteins down-regulated in Fe-P co-limited media compared to optimal media

Locus tag	Protein name	Description	No. peptides	Score	FC	P value
Rmet_3314	RplB	50S ribosomal subunit protein L2	16	1303	0.18	7.8E-05
Rmet_3315	RplW	50S ribosomal subunit protein L23	5	506	0.32	7.7E-04
Rmet_3316	RplD	50S ribosomal subunit protein L4	13	1027	0.26	1.3E-05
Rmet_3317	RplC	50S ribosomal subunit protein L3	13	1056	0.29	8.6E-05
Rmet_3323	RpsJ	30S ribosomal subunit protein S10	6	531	0.39	1.3E-04
Rmet_3326	RpsG	30S ribosomal subunit protein S7	8	480	0.33	3.4E-03
Rmet_3327	RpsL	30S ribosomal subunit protein S12	5	329	0.29	7.5E-04
Rmet_3336	RplJ	50S ribosomal subunit protein L10	12	938	0.28	1.0E-04
Rmet_3337	RplA	50S ribosomal subunit protein L1	18	1252	0.19	6.8E-06
Rmet_3338	RplK	50S ribosomal subunit protein L11	5	241	0.18	1.5E-04
Rmet_4357	GntR	Transcriptional regulator,	2	56	0.43	2.9E-02
Rmet_5623		peptidylprolyl isomerase, FKBP-type	3	216	0.32	4.0E-04
Purines, pyrimidines, nucleosides and nucleotides						
Rmet_0506	PurK	Phosphoribosylaminoimidazole carboxylase ATPase subunit	7	578	0.41	1.3E-03
Rmet_0532	Adk	Adenylate kinase	7	294	0.33	6.7E-04
Rmet_0856	Gmk	Guanylate kinase	2	137	0.41	3.1E-02
Rmet_0890	Add	Adenosine deaminase	2	69	0.30	5.9E-05
Rmet_1461	GuaB	Inosine-5'-monophosphate dehydrogenase	19	1386	0.48	7.4E-04
Rmet_1820	PurT	Phosphoribosylglycinamide formyltransferase 2	5	229	0.33	3.0E-05
Transcription						
Rmet_0302	RpoX	Sigma 54 modulation protein, ribosome-associated	6	489	0.12	2.2E-04
Rmet_1044	YebK	Transcriptional regulator	2	271	0.19	2.1E-02
Rmet_1078	SuhB	Inositol monophosphatase	4	231	0.47	1.2E-03
Rmet_1232	YhgF	Putative RNA-binding transcription accessory protein	4	200	0.15	2.2E-04
Rmet_2034		Pseudouridine synthase	5	254	0.33	4.1E-04
Rmet_2037	FnrL	Transcriptional regulator	2	96	0.32	6.6E-04
Rmet_2092	Rnr	Exoribonuclease R, RNase R	4	180	0.33	1.4E-03
Rmet_2192	GreA	Transcription elongation factor	4	291	0.31	9.9E-03
Rmet_3333	RpoC	RNA polymerase, beta prime subunit	64	4280	0.43	5.9E-05
Rmet_3564	Fmt	Methionyl-tRNA formyltransferase	3	123	0.45	5.4E-03
Rmet_4773		Putative endoribonuclease L-PSP	2	135	0.31	1.5E-03

Continued on next page

Table B.12 – Proteins down-regulated in Fe-P co-limited media compared to optimal media

Locus tag	Protein name	Description	No. peptides	Score	FC	P value
Transport and binding proteins						
Rmet_0070		ABC-type transporter, periplasmic component	2	71	0.20	2.3E-03
Rmet_0521	Bug	Extra-cytoplasmic Solute Receptor protein	31	2977	0.40	5.4E-03
Rmet_0802		Putative ABC-type transporter glycine betaine/L-proline transporter	7	410	0.37	1.1E-05
Rmet_0929	NuoC	NADH dehydrogenase chain C	4	185	0.38	9.1E-05
Rmet_1209		ABC transporter-related protein	6	276	0.36	1.1E-02
Rmet_2279	ExbD1	Biopolymer transport protein	6	484	0.43	7.5E-04
Rmet_2945	YajC	Preprotein translocase auxiliary subunit	6	435	0.34	5.8E-04
Rmet_3153		ABC-type branched-chain amino acid transport system	3	182	0.24	1.1E-03
Rmet_3589	AcrB	Multidrug efflux system protein	7	505	0.47	5.0E-03
Rmet_3613	YidC	Inner membrane insertion protei	11	705	0.34	6.9E-05
Rmet_3671	Bug	Extra-cytoplasmic Solute Receptor	2	56	0.00	1.4E-03
Rmet_5616	Bug	Extra-cytoplasmic solute receptor protein	2	110	0.16	8.1E-04
Unassigned						
Rmet_0097		Conserved hypothetical protein	2	74	0.08	3.5E-04
Rmet_0305		Conserved hypothetical protein; OstA-like protein	2	173	0.44	8.7E-03
Rmet_0367		Putative Fe-S oxidoreductase FAD/FMN-containing dehydrogenase oxidoreductase protein	5	353	0.23	1.6E-03
Rmet_0408		Conserved hypothetical protein	4	208	0.44	8.1E-03
Rmet_0419	YbhB	Phospholipid-binding protein	3	211	0.25	1.3E-03
Rmet_0665	LemA	LemA like protein	2	67	0.02	1.8E-05
Rmet_0697	PilA	Type IV pilus structural subunit	4	285	0.40	1.1E-03
Rmet_0718	TyrA	Prephenate dehydrogenase	2	84	0.24	2.5E-03
Rmet_0972		Putative aminoglycoside phosphotransferase	4	227	0.22	5.6E-05
Rmet_0986		Putative ATPase, AAA family	11	726	0.38	9.9E-04
Rmet_1443	YaeT	Outer membrane protein assembly factor	3	143	0.20	3.3E-03
Rmet_1600		Conserved hypothetical protein; putative exported protein	4	224	0.23	4.1E-03
Rmet_1808	PepM	Phosphoenolpyruvate phosphomutase	8	420	0.20	1.3E-05
Rmet_1851		Short-chain dehydrogenase/reductase SDR	2	86	0.10	1.4E-02
Rmet_1864		Conserved hypothetical protein	2	114	0.32	2.0E-02
Rmet_2024	BipA	GTP-binding protein	5	270	0.44	5.0E-03

Continued on next page

Table B.12 – Proteins down-regulated in Fe-P co-limited media compared to optimal media

Locus tag	Protein name	Description	No. peptides	Score	FC	P value
Rmet_2061		Conserved hypothetical protein	3	115	0.40	2.8E-03
Rmet_2436	SohB	Peptidase S49, periplasmic serine protease	2	62	0.39	6.7E-03
Rmet_2440	Rne	Fused ribonucleaseE: endoribonuclease, RNA-binding protein, RNA degradosome binding protein	21	1441	0.32	8.3E-04
Rmet_2452	TrxB2	Thioredoxin reductase	13	741	0.37	2.8E-04
Rmet_2470		Type IV-pili assembly FimV-related transmembrane protein	14	1017	0.38	4.2E-04
Rmet_2547		Conserved hypothetical protein	6	405	0.43	7.3E-04
Rmet_2737		Hypothetical protein	2	102	0.49	7.3E-04
Rmet_2861		Ferredoxin	4	225	0.31	1.1E-02
Rmet_2934	Gpo	Glutathione peroxidase	3	150	0.27	2.0E-03
Rmet_3069		Carbohydrate kinase, PfkB family	5	404	0.33	1.1E-04
Rmet_3233		Trypsin-like serine protease	5	275	0.47	3.7E-03
Rmet_5004		Antibiotic biosynthesis monooxygenase	2	78	0.09	1.3E-02
Rmet_5074		Conserved hypothetical protein	7	363	0.21	1.8E-02
Rmet_6330		Hypothetical protein	2	111	0.41	9.0E-04
Rmet_6408		Putative rhodanese-related sulfurtransferase	2	145	0.11	9.7E-03
Rmet_6523		Conserved hypothetical protein	2	101	0.38	4.0E-02

Table B.12 – Proteins down-regulated in Fe-P co-limited media compared to optimal media

B.7 Proteins differentially regulated in the phosphorus and magnesium co-limited treatment

B.7.1 Up-regulated compared to the control

Table B.13 – Proteins up-regulated in P-Mg co-limited media compared to optimal media

Locus tag	Protein name	Description	No. peptides	Score	FC	P value
Amino acid synthesis and metabolism						
Rmet_2902	ArgF	Ornithine carbamoyltransferase	250	6	2.5	2.9E-03
Rmet_0398	GdhA	Glutamate dehydrogenase	979	11	2.6	8.3E-05
Rmet_0681	GlnB	Regulatory protein P-II for glutamine synthetase	362	5	3.8	1.5E-05
Biological processes						
Rmet_4084	PhoA1	Alkaline phosphatase	665	10	15.4	1.6E-03
Rmet_4085	PhoA2	Alkaline phosphatase	451	6	10.4	2.3E-05
Rmet_4131		1-Cysteine peroxiredoxin	223	2	4.6	3.0E-04
Biosynthesis of cofactors, prosthetic groups, and carriers						
Rmet_0728	RfaD	ADP-L-glycero-D-mannoheptose-6-epimerase, NAD(P)-binding	152	2	3.1	1.6E-04
Rmet_2689	RibC	Riboflavin synthase alpha chain	221	3	2.5	3.4E-02
Rmet_2976	Fur2	DNA-binding transcriptional dual regulator of siderophore biosynthesis and transport (Ferric uptake regulation protein)	389	5	2.4	1.3E-03
Cell envelope						
Rmet_0712	OmpA	Outer membrane protein or related peptidoglycan-associated (lipo)protein	907	11	3.2	1.3E-03
Rmet_1685		Putative HlyD family secretion protein	301	6	3.0	6.1E-03
Rmet_2732	RbfC	dTDP-4-deoxyrhamnose-3,5-epimerase	402	7	2.3	2.8E-03
Rmet_4192	PlcN	Phospholipase C signal peptide protein	2461	29	12.1	2.0E-05
Cellular process						
Rmet_1849		Putative oxidoreductase/alcolhol dehydrogenase	315	3	2.2	7.0E-05

Continued on next page

Table B.13 – Proteins up-regulated in P-Mg co-limited media compared to optimal media

Locus tag	Protein name	Description	No. peptides	Score	FC	P value
Rmet_2021		NADPH-dependent FMN reductase	359	5	2.5	1.1E-03
Rmet_3346	UspA8	Universal stress protein, UspA family	371	4	8.7	1.7E-04
Rmet_5371	KatG	Catalase/hydroperoxidase	344	5	3.9	4.1E-03
Rmet_5599	KatA	Catalase	2585	31	2.5	5.8E-03
Rmet_0243	GshB	Glutathione synthetase	463	6	2.5	1.0E-02
Rmet_1951	AhpD	Alkyl hydroperoxide reductase D	546	7	2.7	1.5E-03
Rmet_2791	ZapA	Cell division protein	373	5	2.6	1.1E-02
Rmet_2957	Gst-1	Glutathione S-transferase	99	2	3.3	2.0E-04
Rmet_3616		Osmotically inducible protein (OsmC-like)	218	3	5.4	1.1E-02
Rmet_3618	Ohr	Organic hydroperoxide resistance protein, 0smC family	453	6	2.1	2.3E-02
Rmet_4751	MscS	Mechanosensitive ion channel	395	4	2.4	1.8E-05
Central intermediary metabolism						
Rmet_0559	Ldh	L-Lactate dehydrogenase	161	4	11.7	2.5E-02
Rmet_0572	CpdB	2':3'-cyclic-nucleotide 2'-phosphodiesterase	411	7	4.6	5.4E-04
Rmet_0774	PhnD	Phosphonate/organophosphate ester transporter subunit	733	9	13.3	1.1E-04
Rmet_0992	Nit	Nitrilase	69	2	3.9	2.8E-05
Rmet_1498	CbbO	Rubisco activation protein	385	7	3.7	7.4E-04
Rmet_4929	Gst	Glutathione S-transferase enzyme with thioredoxin-like domain	272	4	2.2	2.8E-03
Rmet_4943		Putative iron-containing alcohol dehydrogenase	105	2	2.4	3.7E-02
Rmet_5402		Putative alkyl sulfatase	987	15	3.2	2.8E-02
DNA metabolism						
Rmet_0315	Ssb1	Single-stranded DNA-binding protein (Helix-destabilizing protein)	348	3	3.2	1.2E-04
Rmet_2101	Hfq	Host factor I protein	189	4	16.1	8.7E-05
Rmet_3538	Hup	Histone-like DNA-binding protein	1221	10	2.2	3.4E-02
Energy metabolism						
Rmet_0197	Qor	Quinone oxidoreductase, NADPH-dependent	218	3	2.6	3.6E-02
Rmet_0988		Cytochrome c553	401	6	2.7	4.5E-02
Rmet_1093	Adh	Alcohol dehydrogenase, 1-propanol preferring	1304	16	7.0	1.1E-09
Rmet_1511	CbbF2	Fructose-1,6-bisphosphatase I	419	6	3.0	5.6E-08
Rmet_1515	CbbG1	Glyceraldehyde-3-phosphate dehydrogenase A	585	8	3.0	2.8E-05
Rmet_1537	HypF2	Carbamoyl phosphate phosphatase	368	6	2.9	9.3E-04

Continued on next page

Table B.13 – Proteins up-regulated in P-Mg co-limited media compared to optimal media

Locus tag	Protein name	Description	No. peptides	Score	FC	P value
Rmet_2089	TalB	Transaldolase B	101	4	2.3	1.5E-06
Rmet_4063	NapA	Periplasmic nitrate reductase, large subunit	510	8	10.6	8.1E-08
Rmet_5128	AldB	Aldehyde dehydrogenase 2	507	8	4.8	2.9E-04
Rmet_5312	Cpo	Non-heme chloroperoxidase	313	4	2.6	1.3E-06
Fatty acid and phospholipid metabolism						
Rmet_0113		Enoyl-CoA hydratase/carnithine racemase	140	2	4.3	2.5E-03
Rmet_0565	FabI	Enoyl-acyl-carrier-protein reductase, NADH-dependent	610	6	12.7	1.3E-06
Rmet_1200	PhaP	Phasin (PHA-granule associated protein)	3727	27	3.9	1.1E-05
Rmet_2643	Cfa	Cyclopropane-fatty-acyl-phospholipid synthase	258	5	3.3	6.3E-03
Rmet_2850	HutG1	N-Formylglutamate amidohydrolase	65	2	4.6	3.6E-04
Rmet_4076		Putative short-chain dehydrogenase/reductase SDR	87	2	12.1	2.1E-08
Mobile and extrachromosomal element functions						
Rmet_6063	ParA	ATPase involved in plasmid partitioning	79	2	57.6	2.3E-02
Phosphorus metabolism						
Rmet_2177	Ppx	Exopolyphosphatase	193	3	5.1	1.1E-02
Rmet_2178	Ppk	Polyphosphate kinase, component of RNA degradosome	96	2	19.3	1.1E-04
Rmet_2180	PhoB	DNA-binding response regulator in two-component regulatory system with PhoR	179	2	5.9	1.1E-02
Rmet_2181	PhoU	Negative regulator of PhoR/PhoB two-component regulator	969	10	3.6	5.4E-05
Rmet_2182	PstB	Phosphate transporter subunit	218	5	15.8	2.1E-05
Rmet_2185	PstS	Phosphate transporter subunit	2142	25	13.8	1.3E-05
Rmet_2583	PhoD	Phosphodiesterase/alkaline phosphatase D	614	9	4.1	6.5E-05
Rmet_2992	PtxD	Phosphonate dehydrogenase	859	12	25.3	4.6E-05
Rmet_2994	PtxB	Putative phosphonate ABC transporter	1495	16	17.8	8.4E-07
Protein fate						
Rmet_0283		Peptidase M16-like protein (Probable peptidase signal peptide protein)	283	4	2.6	2.5E-03
Rmet_5411		Putative membrane Zinc metallopeptidase	129	3	5.9	4.9E-04
Protein synthesis						
Rmet_0831	AlaS	Alanyl-tRNA synthetase	1089	19	4.9	1.1E-02
Rmet_1085	CysS	Cysteinyl-tRNA synthetase	306	4	2.1	6.0E-03

Continued on next page

Table B.13 – Proteins up-regulated in P-Mg co-limited media compared to optimal media

Locus tag	Protein name	Description	No. peptides	Score	FC	P value
Rmet_3190	DsbC	Protein-disulfide isomerase	137	3	2.2	3.5E-02
Purines, pyrimidines, nucleosides and nucleotides						
Rmet_0211		Diadenosine tetraphosphate	182	2	2.4	2.0E-02
Rmet_2095		Phosphoribosyltransferase (PRTase)	177	2	2.2	1.5E-02
Rmet_2740	PyrB	Aspartate carbamoyltransferase	294	5	2.7	6.5E-03
Rmet_2741	PyrR	Bifunctional protein: pyrimidine operon regulatory protein	309	4	2.1	6.2E-04
Regulation						
Rmet_2941	OxyR	Oxidative stress-inducible genes activator	92	2	2.1	5.9E-03
Transcription						
Rmet_1601		Regulatory protein, MarR family	188	4	2.5	8.6E-03
Rmet_2135	Rho	Transcription termination factor Rho	602	11	2.3	2.2E-04
Rmet_4773		Putative endoribonuclease L-PSP	135	2	3.3	3.4E-02
Rmet_5818	Csp	Cold-shock responsive transcriptional repressor	264	4	15.8	1.3E-03
Transport and binding proteins						
Rmet_1701	AcrA	Cation/multidrug efflux system, mebrane-fusion component	206	3	2.1	4.8E-05
Rmet_1702	AcrF	Multidrug efflux system protein	1082	15	2.1	1.6E-03
Rmet_1985	YbjL	Putative transporter	668	8	2.4	9.1E-03
Rmet_4789	MetQ	DL-methionine transporter subunit	211	4	5.2	3.3E-02
Rmet_4840		Putative ABC transporter, periplasmic binding component involved in Fe^{3+} transport	52	2	3.5	2.5E-03
Rmet_5329	ZneA	Heavy metal cation tricomponent efflux pump	279	4	2.7	4.1E-03
Rmet_5330	ZneB	Membrane fusion protein heavy metal cation tricomponent efflux	559	9	2.3	2.9E-05
Rmet_5408		Putative efflux outer membrane protein	142	2	53.3	1.5E-04
Rmet_5682	NimB	Heavy metal cation tricomponent efflux membrane fusion protein	358	6	3.5	7.1E-06
Unassigned						
Rmet_0084		Predicted hydrolase	111	2	5.7	4.4E-03
Rmet_0137		Conserved hypothetical protein	368	7	2.1	1.8E-02
Rmet_0152		Conserved hypothetical protein	227	4	2.9	1.1E-03
Rmet_0186	GlmU	Fused N-acetyl glucosamine-1-phosphate uridyltransferase	145	4	2.9	2.7E-04
Rmet_0310		Putative intracellular protease/amidase/DJ-1/PfpI family	1465	11	4.1	5.8E-04
Rmet_0421		Conserved hypothetical protein	1251	12	3.3	1.6E-03

Continued on next page

Table B.13 – Proteins up-regulated in P-Mg co-limited media compared to optimal media

Locus tag	Protein name	Description	No. peptides	Score	FC	P value
Rmet_0546	BdhA	D-beta-hydroxybutyrate dehydrogenase	55	2	2.1	5.3E-04
Rmet_0562	AckA2	Acetate kinase	440	8	5.5	1.9E-04
Rmet_0563	Ptb	Phosphate acetyltransferase	373	6	14.6	1.5E-05
Rmet_0564		Conserved hypothetical protein	1113	16	2.1	5.2E-04
Rmet_0690		Putative amino-acid-binding periplasmic ABC transporter protein	426	5	4.3	4.5E-03
Rmet_0862		Conserved hypothetical protein	402	6	4.4	1.4E-03
Rmet_0904		Glycosyltransferase, group 1	421	8	5.7	9.4E-06
Rmet_1021		Conserved hypothetical protein	214	3	2.3	9.1E-04
Rmet_1059	PaaY	Carbonic anhydrases/acetyltransferases, isoleucine patch superfamily	261	5	2.8	1.0E-02
Rmet_1084		Conserved hypothetical protein with TPR domain	153	3	4.3	2.6E-02
Rmet_1183		Conserved hypothetical signal peptide protein	579	7	7.8	1.8E-03
Rmet_1187		Hypothetical protein	447	4	2.5	3.3E-04
Rmet_1394		Acyl-CoA-binding protein	241	4	17.6	1.3E-03
Rmet_1418		Hypothetical protein	476	6	4.7	5.6E-05
Rmet_1452		Conserved hypothetical protein	106	2	4.3	1.3E-03
Rmet_1646		Putative MscS Mechanosensitive ion channel	96	2	2.6	3.4E-02
Rmet_1695		Conserved hypothetical protein; putative exported protein	257	3	6.4	2.3E-05
Rmet_1696		Conserved hypothetical protein; putative exported protein	702	10	8.9	1.1E-04
Rmet_1704		Conserved hypothetical protein; putative exported protein	754	8	3.6	1.0E-03
Rmet_1705		Conserved hypothetical protein; putative exported protein	1519	14	2.9	2.1E-05
Rmet_1706		Conserved hypothetical protein; putative exported protein	233	3	2.4	5.5E-04
Rmet_1830	GcvT	Putative glycine cleavage T protein	111	3	2.4	1.1E-03
Rmet_1971		Conserved hypothetical protein	98	2	3.5	1.1E-02
Rmet_1984	AsdA	L-Aspartate decarboxylase	1718	25	3.0	2.5E-05
Rmet_2063		Rhodanese-related sulfurtransferase	210	4	2.1	1.3E-02
Rmet_2125		L-carnitine dehydratase/bile acid-inducible protein	126	2	3.4	8.1E-03
Rmet_2133		Conserved hypothetical protein	457	3	2.5	2.2E-02
Rmet_2243		Conserved hypothetical protein	234	2	3.9	5.5E-05
Rmet_2281		Conserved hypothetical protein	282	5	3.1	2.8E-03
Rmet_2491		Conserved hypothetical protein; putative exported protein	343	6	2.1	1.6E-03

Continued on next page

Table B.13 – Proteins up-regulated in P-Mg co-limited media compared to optimal media

Locus tag	Protein name	Description	No. peptides	Score	FC	P value
Rmet_2496		Putative extracellular solute-binding, family 5 ABC-type transporter protein	134	3	9.0	1.4E-02
Rmet_2587	GstN	Glutathione s-transferase protein	197	5	16.7	1.0E-03
Rmet_2668		Conserved hypothetical protein	245	4	2.4	2.3E-03
Rmet_2747	HemY	Uncharacterized enzyme of heme biosynthesis	63	2	3.1	8.3E-03
Rmet_2968		2-Hydroxychromene-2-carboxylate isomerase	330	5	3.6	2.8E-04
Rmet_2984		Conserved hypothetical protein	304	3	4.6	1.5E-04
Rmet_3071		Histone H1-like protein HC2	211	3	2.5	1.1E-04
Rmet_3358		Conserved hypothetical protein	86	2	6.8	1.4E-03
Rmet_3579		Conserved hypothetical protein	268	4	2.6	1.2E-04
Rmet_3826		Conserved hypothetical protein	367	6	3.8	7.5E-06
Rmet_3904	PrkA	Serine protein kinase	487	10	7.0	1.1E-03
Rmet_4030		Putative glyoxalase or dioxygenase	69	2	4.7	4.8E-05
Rmet_4086		Conserved hypothetical protein	243	5	7.4	1.5E-03
Rmet_4140		Putative methyltransferase	180	3	2.6	3.0E-04
Rmet_4167	Ttg2	ABC-type transporter involved in toluene tolerance, periplasmic component	245	4	14.8	2.4E-02
Rmet_4200		Conserved hypothetical protein	200	3	6.7	5.0E-04
Rmet_4347		Alkylhydroperoxidase AhpD core	73	2	2.4	7.4E-04
Rmet_4584		Conserved hypothetical protein	162	2	3.8	3.6E-02
Rmet_4809	AcpA	Putative acid phosphatase protein	144	3	37.8	3.1E-04
Rmet_4999		Conserved hypothetical protein	472	8	3.0	5.1E-05
Rmet_5000		Conserved hypothetical protein	758	13	5.8	5.8E-03
Rmet_5007		Conserved hypothetical protein	199	2	8.9	1.3E-03
Rmet_5043		Conserved hypothetical protein	801	10	3.0	1.3E-04
Rmet_5124		Conserved hypothetical protein	141	2	2.1	1.8E-03
Rmet_5267		Putative alpha/beta hydrolase; putative prolyl aminopeptidase	119	2	2.7	2.7E-03
Rmet_5313		Putative metallo-dependent amidohydrolase	729	12	6.1	4.2E-04
Rmet_5374		Hypothetical protein	618	7	2.4	1.4E-03
Rmet_5405		Conserved hypothetical protein; putative periplasmic protein	703	8	5.6	1.2E-04
Rmet_5406		Conserved hypothetical protein	205	4	8.3	3.8E-04

Continued on next page

Table B.13 – Proteins up-regulated in P-Mg co-limited media compared to optimal media

Locus tag	Protein name	Description	No. peptides	Score	FC	P value
Rmet_5600		Conserved hypothetical protein; ankyrin domain protein	384	4	3.6	5.4E-03
Rmet_5638		ABC-type transporter, periplasmic component	879	11	2.1	2.6E-02
Rmet_5753		Conserved hypothetical protein	430	7	13.6	1.4E-08
Rmet_5796		D-isomer specific 2-hydroxyacid dehydrogenase, NAD-binding	149	3	3.7	1.5E-04
Rmet_6330		Hypothetical protein (Orf16)	111	2	2.0	3.7E-04
Rmet_6396		Hypothetical protein	314	3	6.0	1.1E-02

Table B.13 – Proteins up-regulated in P-Mg co-limited media compared to optimal media

B.7.2 Down-regulated compared to the control

Table B.14 – Proteins down-regulated in P-Mg co-limited media compared to optimal media

Locus tag	Protein name	Description	No. peptides	Score	FC	P value
Amino acid synthesis and metabolism						
Rmet_0716	PheA	Prephenate dehydratase, Chorismate mutase	267	3	0.31	6.8E-04
Rmet_0911	IlvI	Acetolactate synthase III, large subunit	414	7	0.22	8.3E-04
Rmet_1134	MetY	O-Acetylhomoserine sulfhydrylase	219	3	0.42	2.2E-03
Rmet_2812	CysN	Sulfate adenylyltransferase, subunit 1	320	4	0.20	1.4E-03
Rmet_2813	CysD	Sulfate adenylyltransferase, subunit 2	231	4	0.46	4.3E-03
Rmet_2815	CysO	Protein involved in cysteine metabolism	149	3	0.35	2.3E-04
Rmet_2816	CysI	Sulfite reductase, beta subunit (hemoprotein with two 4Fe-4S domains)	546	9	0.47	1.0E-02
Rmet_5602		Putative threonine dehydratase	349	5	0.49	3.8E-02
Rmet_0402	GltL	Glutamate and aspartate transporter subunit	486	6	0.44	1.3E-02
Rmet_3241	HisI	Phosphoribosyl-AMP cyclohydrolase	105	2	0.40	2.6E-02
Rmet_3249	HisG	ATP phosphoribosyltransferase	143	4	0.45	5.1E-05
Rmet_3262	GltD	Glutamate synthase, 4Fe-4S protein, small subunit	1298	18	0.45	3.5E-05
Rmet_3263	GltB	Glutamate synthase, large subunit	2962	43	0.44	8.8E-03
Biosynthesis of cofactors, prosthetic groups, and carriers						
Rmet_0061	LipA	Lipoate synthase	93	2	0.18	2.4E-05
Rmet_0114	BioA	7,8-diaminopelargonic acid synthase, PLP-dependent	351	6	0.37	2.1E-04
Rmet_0117	BioB	Biotin synthase	936	14	0.20	2.9E-05
Rmet_0162	ThiC	Thiamin biosynthesis protein	866	13	0.42	5.1E-03
Rmet_1964	MoeA	Molybdopterin biosynthesis protein	112	2	0.26	8.5E-03
Rmet_2615	Dxs	1-deoxyxylulose-5-phosphate synthase	491	10	0.49	3.1E-04
Rmet_2688	RibD	Fused diaminohydroxyphosphoribosylaminopyrimidine deaminase	85	3	0.29	4.4E-02
Rmet_2868	IspH	1-hydroxy-2-methyl-2-(E)-butenyl 4-diphosphate reductase, 4Fe-4S protein	145	3	0.38	2.1E-03
Cell envelope						
Rmet_0533	KdsB	3-deoxy-manno-octulosonate cytidylyltransferase	95	3	0.31	1.1E-03

Continued on next page

Table B.14 – Proteins down-regulated in P-Mg co-limited media compared to optimal media

Locus tag	Protein name	Description	No. peptides	Score	FC	P value
Rmet_0727	RfaE	Fused heptose 7-phosphate kinase; heptose 1-phosphate adenyltransferase	158	2	0.42	8.2E-03
Rmet_2186	GlmM	Phosphoglucosamine mutase	544	8	0.49	4.2E-02
Rmet_2674	Pal	Peptidoglycan-associated outer membrane lipoprotein	832	12	0.44	2.3E-04
Rmet_2733	RbfA	Glucose-1-phosphate thymidylyltransferase	346	6	0.41	1.7E-02
Cellular process						
Rmet_0458	UspA1	Universal stress protein, UspA family	535	7	0.29	7.5E-05
Rmet_2417	Era	Membrane-associated, 16S rRNA-binding GTPase	108	2	0.41	2.4E-03
Rmet_3123	FtsZ	GTP-binding tubulin-like cell division protein	824	10	0.47	3.0E-03
Rmet_3124	FtsA	ATP-binding cell division protein	356	5	0.38	1.4E-06
Rmet_3226	SspB	ClpXP protease specificity-enhancing factor	170	3	0.32	5.8E-03
Rmet_0034	MinD	Septum site-determining protein	255	5	0.42	2.4E-03
Rmet_4862		Conserved hypothetical protein	104	2	0.16	3.9E-03
DNA metabolism						
Rmet_2129	DnaX	DNA polymerase III tau/gamma subunit	266	4	0.43	2.7E-05
Rmet_6191	Bph2	Histone-like DNA-binding protein (Orf41)	279	3	0.18	3.5E-02
Energy metabolism						
Rmet_0470	SucD	Succinyl-CoA synthetase, NAD(P)-binding, alpha subunit	1096	13	0.48	1.5E-04
Rmet_1297	HoxG	Hydrogenase 1	1369	24	0.40	1.5E-03
Rmet_1524	HoxY	NAD-reducing hydrogenase	224	4	0.46	2.9E-02
Rmet_1536	HypB2	GTP hydrolase involved in nickel liganding into hydrogenases	1175	16	0.33	2.0E-03
Rmet_2483	SdhB	Succinate dehydrogenase, FeS subunit	996	15	0.37	8.5E-04
Rmet_2980	CbbT2	Transketolase 1, thiamin-binding	843	10	0.41	2.3E-04
Fatty acid and phospholipid metabolism						
Rmet_1853	AtoB	Acetyl-CoA acetyltransferase / thiolase	400	7	0.46	2.6E-05
Rmet_2147	FabI	Enoyl-acyl-carrier-protein reductase, NADH-dependent	624	8	0.46	1.8E-03
Rmet_2428	FabG	3-oxoacyl-acyl-carrier-protein reductase	471	5	0.50	1.2E-04
Rmet_2429	FabD	Malonyl-CoA-acyl-carrier-protein transacylase	191	2	0.50	6.1E-03
Rmet_2464	AccD	Acetyl-CoA carboxylase, beta (carboxyltranferase) subunit	187	3	0.38	2.0E-05
Protein synthesis						
Rmet_0288	RplY	50S ribosomal protein L25 (General stress protein CTC)	692	9	0.29	1.1E-05

Continued on next page

Table B.14 – Proteins down-regulated in P-Mg co-limited media compared to optimal media

Locus tag	Protein name	Description	No. peptides	Score	FC	P value
Rmet_0411	RpsI	30S ribosomal subunit protein S9	610	7	0.42	1.2E-02
Rmet_1025	IscS	Cysteine desulfurase	798	11	0.48	4.5E-05
Rmet_1161	InfC	Protein chain initiation factor IF-3	241	4	0.18	3.3E-03
Rmet_1163	RplT	50S ribosomal subunit protein L20	176	2	0.18	4.3E-02
Rmet_1435	RpsB	30S ribosomal subunit protein S2	962	16	0.50	2.5E-02
Rmet_1979	RpsF	30S ribosomal subunit protein S6	694	8	0.20	6.0E-04
Rmet_2412	Efp	Translation elongation factor P	402	7	0.34	4.1E-07
Rmet_2432	RpmF	50S ribosomal subunit protein L32	296	2	0.21	8.0E-04
Rmet_2455	RpsU1	30S ribosomal subunit protein S21	113	2	0.32	7.9E-03
Rmet_2630	ValS	Valyl-tRNA synthetase	831	11	0.37	1.7E-04
Rmet_2885	IleS	Isoleucyl-tRNA synthetase	1072	15	0.49	2.7E-02
Rmet_2904	RpsT	30S ribosomal subunit protein S20	466	6	0.27	1.0E-04
Rmet_3290	RplQ	50S ribosomal subunit protein L17	286	5	0.25	4.5E-07
Rmet_3293	RpsK	30S ribosomal subunit protein S11	667	7	0.42	3.5E-04
Rmet_3298	RplO	50S ribosomal subunit protein L15	544	8	0.46	1.6E-02
Rmet_3299	RpmD	50S ribosomal subunit protein L30	217	2	0.48	2.5E-04
Rmet_3300	RpsE	30S ribosomal subunit protein S5	957	11	0.44	4.8E-03
Rmet_3301	RplR	50S ribosomal subunit protein L18	631	7	0.44	6.5E-04
Rmet_3302	RplF	50S ribosomal subunit protein L6	1054	14	0.39	5.9E-05
Rmet_3304	RpsN	30S ribosomal subunit protein S14	297	4	0.48	4.4E-02
Rmet_3306	RplX	50S ribosomal subunit protein L24	1005	11	0.34	3.9E-04
Rmet_3307	RplN	50S ribosomal subunit protein L14	523	8	0.43	3.7E-05
Rmet_3308	RpsQ	30S ribosomal subunit protein S17	253	3	0.38	7.5E-06
Rmet_3310	RplP	50S ribosomal subunit protein L16	302	4	0.47	7.7E-03
Rmet_3312	RplV	50S ribosomal subunit protein L22	503	7	0.25	1.0E-04
Rmet_3313	RpsS	30S ribosomal subunit protein S19	470	5	0.35	3.4E-07
Rmet_3314	RplB	50S ribosomal subunit protein L2	1303	16	0.31	1.6E-05
Rmet_3316	RplD	50S ribosomal subunit protein L4	1027	13	0.40	3.7E-05
Rmet_3327	RpsL	30S ribosomal subunit protein S12	329	5	0.50	1.1E-02
Rmet_3336	RplJ	50S ribosomal subunit protein L10	938	12	0.39	7.5E-04
Rmet_3337	RplA	50S ribosomal subunit protein L1	1252	18	0.34	9.0E-04

Continued on next page

Table B.14 – Proteins down-regulated in P-Mg co-limited media compared to optimal media

Locus tag	Protein name	Description	No. peptides	Score	FC	P value
Rmet_3338	RplK	50S ribosomal subunit protein L11	241	5	0.37	5.2E-04
Purines, pyrimidines, nucleosides and nucleotides						
Rmet_0506	PurK	Phosphoribosylaminoimidazole carboxylase ATPase subunit	578	7	0.38	5.7E-03
Transcription						
Rmet_0302	RpoX	Sigma 54 modulation protein, ribosome-associated	489	6	0.35	2.3E-02
Rmet_1232	YhgF	Putative RNA-binding transcription accessory protein	200	4	0.44	1.3E-02
Transport and binding proteins						
Rmet_0452	PhoL	Putative enzyme with nucleoside triphosphate hydrolase domain	73	2	0.28	9.9E-05
Rmet_2945	VajC	Preprotein translocase auxiliary subunit YajC transmembrane	435	6	0.49	2.4E-03
Rmet_5616	Bug	Extra-cytoplasmic solute receptor protein	110	2	0.44	1.8E-06
Unassigned						
Rmet_0097		Conserved hypothetical protein	74	2	0.16	5.5E-04
Rmet_0408		Conserved hypothetical protein	208	4	0.48	1.4E-04
Rmet_0665	LemA	LemA like protein	67	2	0.05	2.1E-02
Rmet_0972		Putative aminoglycoside phosphotransferase	227	4	0.27	5.2E-03
Rmet_0986		Putative ATPase, AAA family	726	11	0.44	2.3E-02
Rmet_1135		Conserved hypothetical protein	505	7	0.39	2.0E-04
Rmet_1600		Conserved hypothetical protein; putative exported protein	224	4	0.32	1.5E-04
Rmet_1808	PepM	Phosphoenolpyruvate phosphomutase	420	8	0.46	5.8E-03
Rmet_2440	Rne	Fused ribonucleaseE: endoribonuclease	1441	21	0.50	3.1E-02
Rmet_2452	TrxB2	Thioredoxin reductase	741	13	0.47	9.7E-05
Rmet_2657		Conserved hypothetical protein	84	2	0.48	3.9E-02
Rmet_3697		Conserved hypothetical protein	163	3	0.42	1.2E-05
Rmet_5074		Conserved hypothetical protein	363	7	0.24	2.4E-04
Rmet_6408		Putative rhodanese-related sulfurtransferase	145	2	0.34	4.4E-02

Table B.14 – Proteins down-regulated in P-Mg co-limited media compared to optimal media

B.8 Proteins differentially regulated in the iron and magnesium co-limited treatment

B.8.1 Up-regulated compared to the control

Table B.15 – Proteins up-regulated in Fe-Mg co-limited media compared to optimal media

Locus tag	Protein name	Description	No. peptides	Score	FC	P value
Amino acid synthesis and metabolism						
Rmet_0398	GdhA	Glutamate dehydrogenase	11	979.25	2.9	1.4E-04
Rmet_2471	Asd	Aspartate-semialdehyde dehydrogenase, NAD(P)-binding	17	1658	2.0	2.3E-03
Rmet_4537	SerA2	D-3-phosphoglycerate dehydrogenase, NAD-binding	9	596.04	7.6	7.4E-07
Rmet_4606	MetY	O-acetylhomoserine/O-acetylserine sulfhydrylase	15	1569.52	2.3	1.4E-03
Rmet_5602		Putative threonine dehydratase	5	349.31	6.3	9.8E-05
Biological processes						
Rmet_4084	PhoA1	Alkaline phosphatase	10	665.11	2.8	2.1E-02
Biosynthesis of cofactors, prosthetic groups, and carriers						
Rmet_0839		(S)-2-hydroxy-acid oxidase 1	6	410.34	6.3	3.3E-04
Rmet_1110	SbnH	Diaminopimelate decarboxylase implied in the biosynthesis of staphyloferrin B	9	695.13	11.7	8.1E-05
Rmet_1111	SbnG	2-dehydro-3-deoxyglucarate aldolase implied in the biosynthesis of staphyloferrin B	8	474.17	7.6	2.6E-04
Rmet_1112	SbnF	IucC-like protein implied in the biosynthesis of staphyloferrin	17	1286.67	9.1	8.2E-06
Rmet_1113	SbnE	Siderophore synthetase component protein IucA-like implied in the biosynthesis of staphyloferrin B	15	993.57	7.1	1.4E-04
Rmet_1115	SbnC	IucC-like protein implied in the biosynthesis of staphyloferrin B	11	793.89	7.4	8.3E-05
Rmet_1116	SbnB	Ornithine cyclodeaminase implied in the biosynthesis of staphyloferrin B	26	2563.42	17.0	3.0E-06
Rmet_1117	SbnA	Cysteine synthase implied in the biosynthesis of staphyloferrin B	7	553.84	4.0	4.9E-04

Continued on next page

Table B.15 – Proteins up-regulated in Fe-Mg co-limited media compared to optimal media

Locus tag	Protein name	Description	No. peptides	Score	FC	P value
Rmet_1118	AleB	Staphyloferrin B receptor	8	441.68	18.9	2.0E-05
Cell envelope						
Rmet_0712	OmpA	Outer membrane protein or related peptidoglycan-associated (lipo)protein	11	907.33	2.1	5.0E-03
Rmet_1352	ComL	DNA uptake lipoprotein	4	214.19	2.5	6.0E-05
Rmet_1455	YbbK	Putative protease, membrane anchored	11	981.74	4.2	4.0E-04
Rmet_5339		CsgG family protein; Curli production assembly/transport component	2	105.84	2.1	1.4E-02
Cellular process						
Rmet_3346	UspA8	Universal stress protein, UspA family	4	371.14	2.7	1.1E-02
Rmet_1951	AhpD	Alkyl hydroperoxide reductase D	7	546.24	2.4	4.4E-02
Rmet_3574	CstA	Starvation-induced protein involved in peptide utilization during carbon starvation	3	172.28	2.1	1.5E-02
Rmet_3616		Osmotically inducible protein	3	217.56	2.2	1.2E-02
Rmet_5981	CzcB	CzcB,membrane fusion protein, three components cation proton antiporter efflux system involved in Cd(II), Zn(II), Co(II) resistance	4	231.95	2.1	2.3E-03
Central intermediary metabolism						
Rmet_0967	GstI	Glutathione S-transferase	12	887.65	6.2	1.1E-05
Rmet_1498	CbbO	Rubisco activation protein	7	384.51	4.0	5.2E-03
Rmet_4929	GstI	Glutathione S-transferase enzyme with thioredoxin-like domain	4	271.72	2.2	1.9E-02
Rmet_5402		Putative alkyl sulfatase	15	987.49	3.4	3.3E-03
DNA metabolism						
Rmet_2101	Hfq	Host factor I protein	4	188.73	5.3	6.8E-03
Rmet_2940	DpsA	DNA protection during starvation or oxydative stress transcription regulator protein	7	859.35	2.9	5.5E-04
Rmet_4549	UvrA2	Excinuclease ABC, A subunit	6	392.59	2.2	8.0E-03
Energy metabolism						
Rmet_0386		Putative 3-hydroxyacyl-coa dehydrogenase oxidoreductase protein	4	236.7	2.3	2.1E-03
Rmet_1093	Adh	Alcohol dehydrogenase, 1-propanol preferring	16	1304.04	3.3	2.8E-04
Rmet_1511	CbbF2	Fructose-1,6-bisphosphatase I	6	419.29	8.6	1.1E-03
Rmet_1512	CbbP	Phosphoribulokinase	4	309.8	5.6	3.4E-05
Rmet_1513	CbbT1	Transketolase 1, thiamin-binding	4	252.45	3.1	5.9E-04

Continued on next page

Table B.15 – Proteins up-regulated in Fe-Mg co-limited media compared to optimal media

Locus tag	Protein name	Description	No. peptides	Score	FC	P value
Rmet_1515	CbbG1	Glyceraldehyde-3-phosphate dehydrogenase A	8	585.07	6.5	3.0E-04
Rmet_1521	CbbI1	Ribose 5-phosphate isomerase	2	151.18	5.1	3.5E-04
Rmet_4859		Putative NADH-depentdent flavin oxidoreductase	9	548.87	3.0	2.8E-03
Rmet_5128	AldB	Aldehyde dehydrogenase 2	8	507.12	2.0	1.1E-02
Rmet_0565	FabI	Enoyl-acyl-carrier-protein reductase, NADH-dependent	6	610.42	2.3	2.5E-02
Rmet_1200	PhaP	Phasin (PHA-granule associated protein)	27	3727.04	2.0	3.3E-03
Rmet_2643	Cfa	Cyclopropane-fatty-acyl-phospholipid synthase	5	258.01	5.2	3.3E-05
Mobile and extrachromosomal element functions						
Rmet_1516	Pgk1	Phosphoglycerate kinase	3	269.93	2.2	9.0E-05
Phosphorus metabolism						
Rmet_2177	Ppx	Exopolyphosphatase	3	193.13	2.5	3.8E-02
Rmet_2178	Ppk	Polyphosphate kinase	2	95.54	3.9	1.2E-02
Rmet_2182	PstB	Phosphate transporter subunit	5	218.11	4.1	2.5E-03
Rmet_2185	PstS	Phosphate transporter subunit	25	2141.92	2.2	2.5E-04
Rmet_2992	PtxD	Phosphonate dehydrogenase	12	858.78	2.1	3.5E-04
Protein fate						
Rmet_0283		Peptidase M16-like protein	4	282.94	2.2	3.8E-02
Rmet_0876	PepN	Aminopeptidase N	7	464.8	2.2	2.8E-02
Rmet_1026	IscU	FeS cluster assembly scaffold protein	9	570.08	4.3	3.1E-06
Rmet_1028	HscB	DnaJ-like molecular chaperone specific for IscU	3	162.62	3.2	2.9E-02
Rmet_1029	HscA	DnaK-like molecular chaperone specific for IscU	8	458.66	3.5	8.8E-04
Protein synthesis						
Rmet_0448	GlyQ	Glycine tRNA synthetase, alpha subunit	3	131.94	3.9	2.1E-02
Rmet_0831	AlaS	Alanyl-tRNA synthetase	19	1089.21	2.1	3.4E-04
Rmet_1025	IscS	Cysteine desulfurase (tRNA sulfurtransferase)	11	798.26	2.7	8.7E-05
Rmet_1160	ThrS	Threonyl-tRNA synthetase	20	1366.05	3.6	7.4E-06
Rmet_5930	FusA2	Elongation factor G2	16	1795.41	5.0	3.8E-05
Purines, pyrimidines, nucleosides and nucleotides						
Rmet_3087	NrdB	Ribonucleoside-diphosphate reductase beta subunit	6	262.79	4.7	1.9E-03
Rmet_3088	NrdA	Ribonucleoside-diphosphate reductase alpha subunit	31	2312.57	3.2	6.4E-05
Regulation						

Continued on next page

Table B.15 – Proteins up-regulated in Fe-Mg co-limited media compared to optimal media

Locus tag	Protein name	Description	No. peptides	Score	FC	P value
Rmet_0001	DnaA	Chromosomal replication initiator protein	2	123.23	4.5	4.1E-02
Rmet_2952	PhcB	Regulatory protein	5	289.86	2.4	1.1E-02
Rmet_5746	Fur1	Ferric uptake regulator	6	418.3	3.2	2.9E-05
Transcription						
Rmet_4773		Putative endoribonuclease L-PSP	2	135.37	2.4	3.8E-03
Transport and binding proteins						
Rmet_1121	AcrD	Aminoglycoside/multidrug efflux system	4	208.87	8.9	3.2E-03
Rmet_2277	ExbA	TonB-like protein, membrane spanning	3	204.27	12.7	9.5E-06
Rmet_2279	ExbD1	Biopolymer transport protein	6	484.31	8.5	5.2E-06
Rmet_3549	TctC	Periplasmic tricarboxylate binding receptor	9	584.04	2.6	8.8E-04
Rmet_5329	ZneA	Heavy metal cation tricomponent efflux pump	4	279.26	8.0	2.2E-04
Rmet_5330	ZneB	Membrane fusion protein heavy metal cation tricomponent efflux	9	558.78	19.5	1.0E-05
Rmet_5376	HmuT	Hemin-binding periplasmic protein	8	770.49	4.9	1.0E-04
Rmet_5378	HmuV	Putative Hemin ABC transport system, ATP-binding protein	7	370.99	10.3	4.9E-05
Rmet_5890	FeoB	Fe^{2+} transport system protein B	5	269.16	4.2	7.2E-05
Rmet_6209	CnrB	Membrane fusion protein, three components cation proton antiporter efflux system, involved in Co(II), Ni(II) resistance	4	237.57	2.7	2.1E-03
Unassigned						
Rmet_0421		Conserved hypothetical protein; putative exported protein	12	1250.66	4.1	3.9E-04
Rmet_0563	Ptb	Phosphate acetyltransferase	6	373.48	2.6	3.7E-02
Rmet_0838	PiuC	PKHD-type hydroxylase (Iron-uptake factor)	6	378.89	9.5	7.9E-04
Rmet_1050		Conserved hypothetical protein	3	182.11	2.2	9.0E-03
Rmet_1063	TrxB1	Thioredoxin reductase	4	277.45	7.5	2.4E-04
Rmet_1109		Conserved hypothetical protein	3	169.19	37.7	2.8E-03
Rmet_1187		Hypothetical protein	4	447.13	2.1	1.8E-02
Rmet_1394		Acyl-CoA-binding protein	4	241.19	5.7	1.0E-02
Rmet_1499	CbbQ	Rubisco activation protein	13	863.76	2.1	2.0E-05
Rmet_1518	CbbA2	Fructose-bisphosphate aldolase	6	505.66	5.7	2.1E-05
Rmet_1695		Conserved hypothetical protein; putative exported protein	3	256.67	2.4	1.0E-02
Rmet_1790	GlcD	Glycolate oxidase subunit	4	253.01	2.6	2.0E-03
Rmet_1830	GcvT	Putative glycine cleavage T protein	3	111.19	3.0	2.2E-03

Continued on next page

Table B.15 – Proteins up-regulated in Fe-Mg co-limited media compared to optimal media

Locus tag	Protein name	Description	No. peptides	Score	FC	P value
Rmet_1864		Conserved hypothetical protein	2	113.97	2.1	1.7E-02
Rmet_2071	YggX	Fe(II) trafficking protein	2	82.65	4.0	3.8E-03
Rmet_2278	ExbB	Biopolymer transport exbB protein MotA/TolQ/ExbB proton channel	7	542.98	5.9	3.0E-04
Rmet_2614		Putative GTP cyclohydrolase	5	411.38	2.9	1.1E-03
Rmet_2875	Scd	Fatty-acid desaturase	4	256.39	13.4	8.1E-06
Rmet_3358		Conserved hypothetical protein	2	86.17	96.6	1.5E-04
Rmet_3904	PrkA	Serine protein kinase	10	486.89	7.0	1.0E-05
Rmet_4200		Conserved hypothetical protein	3	199.78	6.2	2.2E-03
Rmet_5007		Conserved hypothetical protein	2	198.63	3.1	1.8E-02
Rmet_5043		Conserved hypothetical protein	10	800.71	2.3	9.9E-03
Rmet_5267		Putative alpha/beta hydrolase; putative prolyl aminopeptidase	2	118.64	3.7	8.0E-03
Rmet_5374		Hypothetical protein	7	617.66	15.0	1.8E-05
Rmet_5375	HmuS	Hemin transport protein; putative Hemin-degrading	8	570.87	7.2	1.9E-05
Rmet_5405		Conserved hypothetical protein; putative periplasmic protein	8	702.91	3.4	1.5E-04
Rmet_5578		Conserved hypothetical protein; putative signal peptide	11	733.3	10.4	7.6E-07
Rmet_5638		ABC-type transporter, periplasmic component	11	878.84	9.0	4.1E-05
Rmet_5639		Conserved hypothetical protein; putative exported protein	2	123.94	11.7	6.4E-04
Rmet_5753		Conserved hypothetical protein	7	430.49	4.8	1.2E-03
Rmet_5936		Putative monooxygenase with luciferase-like ATPase activity	2	80.31	5.3	2.7E-04

Table B.15 – Proteins up-regulated in Fe-Mg co-limited media compared to optimal media

B.8.2 Down-regulated compared to the control

Table B.16 – Proteins down-regulated in Fe-Mg co-limited media compared to optimal media

Locus tag	Protein name	Description	No. peptides	Score	FC	P value
Amino acid synthesis and metabolism						
Rmet_0140	ArgB	Acetylglutamate kinase	9.0	598	0.45	1.1E-02
Rmet_2815	CysO	Protein involved in cysteine metabolism	3.0	149	0.35	2.4E-02
Rmet_2473	LeuD	3-isopropylmalate isomerase subunit	7.0	357	0.34	6.0E-03
Rmet_2475	LeuC	3-isopropylmalate isomerase subunit, dehydratase component	8.0	630	0.28	1.3E-04
Rmet_2480	LivK1	Leucine/isoleucine/valine transporter subunit	30.0	2760	0.50	9.6E-04
Rmet_3181	TrpC	Indole-3-glycerol phosphate synthase	2.0	95	0.38	4.1E-02
Rmet_3241	HisI	Phosphoribosyl-AMP cyclohydrolase	2.0	105	0.38	6.9E-03
Rmet_3249	HisG	ATP phosphoribosyltransferase	4.0	143	0.49	8.9E-03
Rmet_3262	GltD	Glutamate synthase, 4Fe-4S protein, small subunit	18.0	1298	0.29	4.9E-05
Rmet_3263	GltB	Glutamate synthase, large subunit	43.0	2962	0.27	3.5E-05
Biological processes						
Rmet_3513		ABC-type transporter, periplasmic component	6.0	450	0.30	2.4E-03
Rmet_1206	YkgE	Putative hydroxyacid oxidoreductase (Fe-S centre)	2.0	120	0.08	3.0E-02
Biosynthesis of cofactors, prosthetic groups, and carriers						
Rmet_0114	BioA	7,8-diaminopelargonic acid synthase, PLP-dependent	6.0	351	0.39	5.0E-04
Rmet_0115	BioF	8-amino-7-oxononanoate synthase	2.0	128	0.35	2.7E-02
Rmet_2106	IspG	1-hydroxy-2-methyl-2-(E)-butenyl 4-diphosphate synthase	3.0	227	0.30	1.7E-03
Rmet_2688	RibD	Fused diaminohydroxyphosphoribosylaminopyrimidine deaminase	3.0	85	0.41	1.9E-02
Rmet_2868	IspH	1-hydroxy-2-methyl-2-(E)-butenyl 4-diphosphate reductase, 4Fe-4S protein	3.0	145	0.17	9.6E-04
Rmet_0061	LipA	Lipoate synthase	2.0	93	0.15	1.8E-02
Rmet_0117	BioB	Biotin synthase	14.0	936	0.16	5.8E-05
Cell envelope						
Rmet_0533	KdsB	3-deoxy-manno-octulosonate cytidylyltransferase	3.0	95	0.27	6.5E-03
Cellular process						
Rmet_0458	UspA1	Universal stress protein, UspA family	7.0	535	0.33	2.3E-03

Continued on next page

Table B.16 – Proteins down-regulated in Fe-Mg co-limited media compared to optimal media

Locus tag	Protein name	Description	Score	No. peptides	FC	P value
Rmet_3226	SspB	ClpXP protease specificity-enhancing factor	3.0	170	0.27	4.1E-03
Rmet_3272	PilM	Type IV pilus assembly protein	2.0	101	0.31	1.2E-02
Rmet_4395	UspA9	Universal stress protein	7.0	557	0.34	1.1E-03
DNA metabolism						
Rmet_6191	Bph2	Histone-like DNA-binding protein	5.0	500	0.24	1.2E-04
Energy metabolism						
Rmet_0931	NuoE	NADH dehydrogenase chain E	2.0	130	0.24	4.7E-03
Rmet_0932	NuoF	NADH:ubiquinone oxidoreductase, chain F	7.0	395	0.46	3.8E-05
Rmet_0933	NuoG	NADH dehydrogenase chain G	22.0	1527	0.37	1.3E-04
Rmet_0988		Cytochrome c553	6.0	401	0.29	3.0E-02
Rmet_1146	EtfD	Electron transfer flavoprotein-ubiquinone oxidoreductase	10.0	711	0.30	9.2E-06
Rmet_1297	HoxG	Hydrogenase 1	24.0	1369	0.28	1.9E-05
Rmet_1522	HoxF	NAD-reducing hydrogenase diaphorase moiety large subunit	10.0	799	0.26	1.0E-03
Rmet_1524	HoxY	NAD-reducing hydrogenase	4.0	224	0.41	4.8E-03
Rmet_1539	HypD2	Protein required for maturation of hydrogenases	7.0	342	0.33	3.0E-03
Rmet_2273	FumA	Fumarate hydratase class I	18.0	1326	0.38	6.0E-04
Rmet_2483	SdhB	Succinate dehydrogenase, FeS subunit	15.0	996	0.29	4.4E-03
Rmet_3228	PetC	Cytochrome c1 precursor	6.0	470	0.49	6.6E-05
Rmet_3230	PetA	Ubiquinol-cytochrome c reductase, iron-sulfur subunit	5.0	302	0.38	2.9E-04
Rmet_0987		Cytochrome c, class IC 1	4.0	317	0.16	2.6E-04
Fatty acid and phospholipid metabolism						
Rmet_2464	AccD	Acetyl-CoA carboxylase, beta subunit	3.0	187	0.33	4.0E-03
Mobile and extrachromosomal element functions						
Rmet_1313	TmoD	Toluene-4-monooxygenase system protein D	3.0	241	0.34	4.3E-03
Protein synthesis						
Rmet_2432	RpmF	50S ribosomal subunit protein L32	2.0	296	0.48	2.4E-02
Rmet_2455	RpsU1	30S ribosomal subunit protein S21	2.0	113	0.23	3.6E-03
Rmet_2870	RpmB	50S ribosomal subunit protein L28	4.0	279	0.34	2.7E-03
Rmet_2904	RpsT	30S ribosomal subunit protein S20	6.0	466	0.46	5.6E-03
Rmet_3290	RplQ	50S ribosomal subunit protein L17	5.0	286	0.50	7.8E-03
Rmet_3300	RpsE	30S ribosomal subunit protein S5	11.0	957	0.46	3.5E-04

Continued on next page

Table B.16 – Proteins down-regulated in Fe-Mg co-limited media compared to optimal media

Locus tag	Protein name	Description	Score	No. peptides	FC	P value
Rmet_3313	RpsS	30S ribosomal subunit protein S19	5.0	470	0.44	4.6E-03
Rmet_3327	RpsL	30S ribosomal subunit protein S12	5.0	329	0.48	1.3E-03
Rmet_1163	RplT	50S ribosomal subunit protein L20	2.0	176	0.13	3.8E-03
Purines, pyrimidines, nucleosides and nucleotides						
Rmet_0506	PurK	Phosphoribosylaminoimidazole carboxylase ATPase subunit	7.0	578	0.45	1.1E-02
Transcription						
Rmet_1232	YhgF	Putative RNA-binding transcription accessory protein	4.0	200	0.46	1.6E-02
Transport and binding proteins						
Rmet_0130	Bug	Extra-cytoplasmic Solute Receptor	15.0	1476	0.44	2.7E-03
Rmet_0928	NuoB	NADH dehydrogenase chain B	3.0	278	0.23	9.4E-03
Rmet_0929	NuoC	NADH dehydrogenase chain C	4.0	185	0.44	1.8E-04
Rmet_1769	Bug	Extra-cytoplasmic Solute Receptor	2.0	168	0.44	3.4E-02
Rmet_3488		ABC-type transporter, periplasmic component (branched-chain amino acid transport)	16.0	1251	0.42	1.4E-03
Rmet_5616	Bug	Extra-cytoplasmic solute receptor protein	2.0	110	0.44	1.1E-02
Rmet_6339		Cupin 2 conserved barrel domain protein	2.0	82	0.45	4.3E-02
Rmet_3671	Big	Extra-cytoplasmic Solute Receptor	2.0	56	0.08	3.5E-02
Unassigned						
Rmet_0095		Conserved hypothetical protein	3.0	165	0.27	1.6E-02
Rmet_0298		Conserved hypothetical protein	3.0	242	0.45	1.1E-02
Rmet_0367		Putative Fe-S oxidoreductase FAD/FMN-containing dehydrogenase oxidoreductase	5.0	353	0.28	2.1E-04
Rmet_0492		Conserved hypothetical protein	3.0	210	0.21	4.3E-02
Rmet_0673	PilL2	Type IV pilus protein histidine kinase/response regulator hybrid PilL	4.0	225	0.28	5.6E-04
Rmet_0930	NuoD	NADH-ubiquinone oxidoreductase D subunit	7.0	347	0.48	1.3E-02
Rmet_1600		Conserved hypothetical protein; putative exported protein	4.0	224	0.49	2.5E-03
Rmet_2041	CcoP	cbb3-type cytochrome oxidase, diheme subunit IV	6.0	375	0.24	3.0E-04
Rmet_2043	CcoO	cbb3-type cytochrome oxidase, monoheme subunit II	4.0	203	0.47	1.2E-03
Rmet_2190		RNA-binding protein	3.0	296	0.48	4.5E-03
Rmet_2547		Conserved hypothetical protein	6.0	405	0.47	1.0E-03
Rmet_2626		Conserved hypothetical protein	3.0	116	0.29	6.2E-03

Continued on next page

Table B.16 – Proteins down-regulated in Fe-Mg co-limited media compared to optimal media

Locus tag	Protein name	Description	Score	No. peptides	FC	P value
Rmet_2632		Conserved hypothetical protein	2.0	105	0.43	4.8E-02
Rmet_2657		Conserved hypothetical protein	2.0	84	0.19	1.3E-02
Rmet_3284		Cytochrome c4	5.0	425	0.36	1.8E-03
Rmet_3321		Dienelactone hydrolase	3.0	298	0.48	1.1E-02
Rmet_3424		Cytochrome c551/c552	4.0	358	0.16	2.7E-04
Rmet_3473		Cytochrome c family protein	7.0	420	0.39	3.1E-03
Rmet_5074		Conserved hypothetical protein	7.0	363	0.37	1.3E-04
Rmet_5645	Adh	Alcohol dehydrogenase, zinc-binding	6.0	291	0.35	2.4E-03
Rmet_6408		Putative rhodanese-related sulfurtransferase	2.0	145	0.30	9.3E-03
Rmet_4584		Conserved hypothetical protein	2.0	162	0.14	2.0E-02
Rmet_6090	Bph2	Histone-like DNA-binding protein	3.0	279	0.16	8.7E-04

Table B.16 – Proteins down-regulated in Fe-Mg co-limited media compared to optimal media

B.9 Proteins differentially regulated only iron and phosphorus co-limited treatments

Table B.17 – Proteins differentially regulated only in P-Fe co-limited treatments

Locus tag	Protein name	Description
Up-regulated vs. control		
Cellular processes		
Rmet_4751	MscS	Mechanosensitive ion channel
Central Intermediary Metabolism		
Rmet_0572	CpdB	2':3'-cyclic-nucleotide 2'-phosphodiesterase
Energy metabolism		
Rmet_1511	CbbF2	Fructose-1,6-bisphosphatase I
Rmet_5927	MocA	Aldo/keto oxidoreductase, NADP-binding
Protein fate		
Rmet_0283		Peptidase M16-like protein
Transcription		
Rmet_1601		Regulatory protein, MarR family
Rmet_5818	Csp	Cold-shock responsive transcriptional repressor
Transport and binding proteins		
Rmet_1702	AcrF	Multidrug efflux system protein
Unknown		
Rmet_0564		Conserved hypothetical protein
Rmet_1394		Acyl-CoA-binding protein
Rmet_1418		Hypothetical protein
Rmet_1704		Conserved hypothetical protein
Rmet_1830	GcvT	Putative glycine cleavage T protein
Rmet_4584		Conserved hypothetical protein
Rmet_5311		Isochorismatase hydrolase
Rmet_6396		Hypothetical protein
Down-regulated vs. control		
Amino acid synthesis and metabolism		
Rmet_4583	GltI	glutamate/aspartate transport protein
Biosynthesis of cofactors, prosthetic groups and carriers		
Rmet_0162	ThiC	thiamin biosynthesis protein
Cellular processes		
Rmet_3123	FtsZ	GTP-binding tubulin-like cell division protein
Energy metabolism		
Rmet_2483	SdhB	succinate dehydrogenase, FeS subunit
Fatty acid and phospholipid metabolism		
Rmet_2464	AccD	acetyl-CoA carboxylase, beta subunit
Protein synthesis		
Rmet_3106	RplU	50S ribosomal subunit protein L21
Rmet_3299	RpmD	50S ribosomal subunit protein L30
Rmet_3310	RplP	50S ribosomal subunit protein L16
Rmet_3312	RplV	50S ribosomal subunit protein L22
Rmet_3316	RplD	50S ribosomal subunit protein L4
Rmet_3327	RpsL	30S ribosomal subunit protein S12
Rmet_3336	RplJ	50S ribosomal subunit protein L10
Rmet_3337	RplA	50S ribosomal subunit protein L1
Transcription		

Continued on next page

Table B.17 – Proteins differentially regulated only in P-Fe co-limited treatments

Locus tag	Protein name	Description
Rmet_2034		pseudouridine synthase
Unknown		
Rmet_1135		conserved hypothetical protein
Rmet_2657		conserved hypothetical protein

Table B.17 – Proteins differentially regulated only in P-Fe co-limited treatments

B.10 Proteins differentially regulated only in the magnesium and phosphorus co-limited treatment

Table B.18 – Proteins differentially regulated only in P-Mg co-limited treatments

Locus tag	Protein name	Description
Up-regulated vs. control		
Amino acid synthesis and metabolism		
Rmet_2902	ArgF	Ornithine carbamoyltransferase
Biosynthesis of cofactors, prosthetic groups, and carriers		
Rmet_0728	RfaD	ADP-L-glycero-D-mannoheptose-6-epimerase
Rmet_2689	RibC	Riboflavin synthase alpha chain
Rmet_2976	Fur2	Ferric uptake regulation protein
Cellular processes		
Rmet_2021		NADPH-dependent FMN reductase
Rmet_3618	Ohr	Organic hydroperoxide resistance protein
Central intermediary metabolism		
Rmet_0992	Nit	Nitrilase
Rmet_4943		Putative iron-containing alcohol dehydrogenase
Energy metabolism		
Rmet_1511	CbbF2	Fructose-1,6-bisphosphatase I
Rmet_1537	HypF2	Carbamoyl phosphate phosphatase
Fatty acid and phospholipid metabolism		
Rmet_2850	HutG1	N-Formylglutamate amidohydrolase
Phosphorus metabolism		
Rmet_2177	Ppx	Exopolyphosphatase
Protein synthesis		
Rmet_1085	CysS	Cysteinyl-tRNA synthetase
Rmet_3190	DsbC	Protein-disulfide isomerase
Transport and binding proteins		
Rmet_1701	AcrA	Cation/multidrug efflux system, mebrane-fusion component
Rmet_4789	MetQ	DL-methionine transporter subunit
Unknown		
Rmet_0137		Conserved hypothetical proteinn
Rmet_0186	GlmU	Fused N-acetyl glucosamine-1-phosphate uridyltransferase
Rmet_1021		Conserved hypothetical protein
Rmet_1646		Putative MscS Mechanosensitive ion channel
Rmet_2063		Rhodanese-related sulfurtransferase
Rmet_2587	GstN	Glutathione s-transferase protein
Rmet_2747	HemY	Uncharacterized enzyme of heme biosynthesis
Rmet_3071		Histone H1-like protein HC2
Rmet_3579		Conserved hypothetical protein
Rmet_4086		Conserved hypothetical protein (membrane)
Rmet_5007		Conserved hypothetical protein
Rmet_5267		Putative alpha/beta hydrolase
Rmet_5374		Hypothetical protein
Rmet_5638		ABC-type transporter, periplasmic component
Rmet_6330		Hypothetical protein
Rmet_6396		Hypothetical protein

Continued on next page

Table B.18 – Proteins differentially regulated only in P-Mg co-limited treatments

Locus tag	Protein name	Description
Rmet_6558		Putative hypothetical protein
Down-regulated vs. control		
Amino acid synthesis and metabolism		
Rmet_1134	MetY	O-Acetylhomoserine sulfhydrylase
Rmet_2813	CysD	Sulfate adenylyltransferase
Rmet_0402	GltL	Glutamate and aspartate transporter subunit
Biosynthesis of cofactors, prosthetic groups, and carriers		
Rmet_2688	RibD	5-amino-6-5-phosphoribosylamino uracil reductase
Cell envelope		
Rmet_0727	RfaE	Fused heptose 7-phosphate kinase
Rmet_2674	Pal	Peptidoglycan-associated outer membrane lipoprotein
Rmet_2733	RfbA	Glucose-1-phosphate thymidylyltransferase
Energy metabolism		
Rmet_1524	HoxY	NAD-reducing hydrogenase
Rmet_2483	SdhB	Succinate dehydrogenase, FeS subunit
Fatty acid and phospholipid metabolism		
Rmet_2428	FabG	3-oxoacyl-[acyl-carrier-protein] reductase
Rmet_2464	AccD	Acetyl-CoA carboxylase
Protein synthesis		
Rmet_1435	RpsB	30S ribosomal subunit protein S2
Rmet_2885	IleS	Isoleucyl-tRNA synthetase
Transport		
Rmet_0452	PhoL	Putative enzyme with nucleoside triphosphate hydrolase domain

Table B.18 – Proteins differentially regulated only in P-Mg co-limited treatments

B.11 Proteins differentially regulated only in the iron and magnesium co-limited treatment

Table B.19 – Proteins differentially regulated only in Fe-Mg co-limited treatments

Locus tag	Protein name	Description
Up-regulated vs. control		
Amino acid synthesis and metabolism		
Rmet_4606	MetY	O-acetylhomoserine/O-acetylserine sulfhydrylase
Rmet_2471	Asd	Aspartate-semialdehyde dehydrogenase
Biosynthesis of cofactors, prosthetic groups, and carriers		
Rmet_0839		(S)-2-hydroxy-acid oxidase 1
Cell envelope		
Rmet_0712	OmpA	Outer membrane protein or related peptidoglycan-associated (lipo)protein
Rmet_5339	CsgG	Curli production assembly/transport component
Cellular processes		
Rmet_3346	UspA8	Universal stress protein
Rmet_1951	AhpD	Alkyl hydroperoxide reductase D
Rmet_3616		Osmotically inducible protein
Central intermediary metabolism		
Rmet_1498	CbbO	Rubisco activation protein
Rmet_1499	CbbQ	Rubisco activation protein
Rmet_5402		Putative alkyl sulfatase
Rmet_4929	Gst	Glutathione S-transferase enzyme
DNA metabolism		
Rmet_2101	Hfq	Host factor I protein
Rmet_2940	DpsA	Metalloregulation DNA-binding stress protein
Rmet_4549	UvrA2	Excinuclease ABC, A subunit
Energy metabolism		
Rmet_0386		Putative 3-hydroxyacyl-coa dehydrogenase oxidoreductase protein
Rmet_1511	CbbF2	Fructose-1,6-bisphosphatase I
Rmet_1512	CbbP	Phosphoribulokinase
Rmet_1513	CbbT1	Transketolase 1, thiamin-binding
Rmet_1521	CbbI1	Ribose 5-phosphate isomerase
Rmet_4859		Putative NADH-depentdent flavin oxidoreductase
Rmet_5128	AldB	Aldehyde dehydrogenase 2
Fatty acid and phospholipid metabolism		
Rmet_0565	FabI	Enoyl-[acyl-carrier-protein] reductase, NADH-dependent
Mobile and extrachromosomal element functions		
Rmet_1516	Pgk1	Phosphoglycerate kinase
Phosphorus metabolism		
Rmet_2177	Ppx	Exopolyphosphatase
Rmet_2178	Ppk	Polyphosphate kinase, component of RNA degradosome
Rmet_4084	PhoA1	Alkaline phosphatase
Protein fate		
Rmet_0283		Peptidase M16-like protein
Rmet_0876	PepN	Aminopeptidase N
Rmet_1028	HscB	DnaJ-like molecular chaperone specific for IscU
Rmet_1029	HscA	DnaK-like molecular chaperone specific for IscU
Protein synthesis		

Continued on next page

Table B.19 – Proteins differentially regulated only in Fe-Mg co-limited treatments

Locus tag	Protein name	Description
Rmet_1025	IscS	Cysteine desulfurase
Transport and binding proteins		
Rmet_2071	YggX	Fe(II) trafficking protein
Rmet_3549	TctC	Periplasmic tricarboxylate binding receptor
Rmet_5329	ZnaA	Heavy metal cation tricomponent efflux pump ZneA
Rmet_5330	ZneB	Membrane fusion protein heavy metal cation tricomponent efflux
Unknown		
Rmet_0563	Ptb	Phosphate acetyltransferase
Rmet_1050		Conserved hypothetical protein
Rmet_1109		Conserved hypothetical protein
Rmet_1187		Hypothetical protein
Rmet_1394		Acyl-CoA-binding protein
Rmet_1830	GcvT	Putative glycine cleavage T protein
Rmet_1864		Conserved hypothetical protein
Rmet_5007		Conserved hypothetical protein
Rmet_5043		Conserved hypothetical protein
Rmet_5267		Putative alpha/beta hydrolasee
Down-regulated vs. control		
Amino acid synthesis and metabolism		
Rmet_2480	LivK1	Leucine/isoleucine/valine transporter subunit
Rmet_3181	TrpC	Indole-3-glycerol phosphate synthase
Rmet_3249	HisG	ATP phosphoribosyltransferase
Biological processes		
Rmet_3513		ABC-type transporter, periplasmic component
Biosynthesis of cofactors, prosthetic groups and carriers		
Rmet_2688	RibD	Fused diaminohydroxyphosphoribosylaminopyrimidine deaminase
Cellular processes		
Rmet_3226	SspB	ClpXP protease specificity-enhancing factor
DNA metabolism		
Rmet_6191	Bph2	Histone-like DNA-binding protein (Orf41)
Fatty acid and phospholipid metabolism		
Rmet_2464	AccD	Acetyl-CoA carboxylase
Protein synthesis		
Rmet_2455	RpsU1	30S ribosomal subunit protein S21
Rmet_2904	RpsT	30S ribosomal subunit protein S20
Rmet_3290	RplQ	50S ribosomal subunit protein L17
Rmet_3300	RpsE	30S ribosomal subunit protein S5
Rmet_3313	RpsS	30S ribosomal subunit protein S19
Rmet_3327	RpsL	30S ribosomal subunit protein S12
Purines, pyrimidines, nucleosides and nucleotides		
Rmet_0506	PurK	Phosphoribosylaminoimidazole carboxylase ATPase subunit
Transcription		
Rmet_1232	YhgF	Putative RNA-binding transcription accessory protein
Transport and binding proteins		
Rmet_0130	bug	Extra-cytoplasmic Solute Receptor
Rmet_0929	NuoC	NADH dehydrogenase chain C
Rmet_0930	NuoD	NADH-ubiquinone oxidoreductase D subunit
Rmet_1769	bug	Extra-cytoplasmic Solute Receptor
Rmet_3488		ABC-type transporter, periplasmic component
Rmet_5616	bug	Extra-cytoplasmic solute receptor protein
Unknown		
Rmet_0095		Conserved hypothetical protein

Continued on next page

Table B.19 – Proteins differentially regulated only in Fe-Mg co-limited treatments

Locus tag	Protein name	Description
Rmet_0298		Conserved hypothetical protein
Rmet_2190		RNA-binding protein, containing KH domain
Rmet_2547		Conserved hypothetical protein
Rmet_2626		Conserved hypothetical protein
Rmet_3473		Cytochrome c family protein
Rmet_6408		Putative rhodanese-related sulfurtransferase

Table B.19 – Proteins differentially regulated only in Fe-Mg co-limited treatments

Bibliography

[1] C Bryce, G Horneck, E Rabbow, H Edwards, and C Cockell. Impact shocked rocks as protective habitats on an anoxic early Earth. *Int. J. Astrobiol.*, 14:115–122, 2015.

[2] C Bryce, S Martin, T Le Bihan, J Harrison, T Bush, B Spears, A Moore, B Byloos, N Leys, and C Cockell. Rock geochemistry induces stress and starvation responses in the bacterial proteome. *In Review: Env Microbiol*, 2015.

[3] T LeBihan. Mass spectrometry as tool for protein structure analysis. University Lecture, 2014.

[4] MT Madigan, JM Martinko, PV Dunlap, and D Clark. *Brock Biology of Microorganisms*. Pearson Benjamin Cummings, San Francisco, 2009.

[5] SM Barns, RE Fundyga, MW Jeffries, and NR Pace. Remarkable archaeal diversity detected in a Yellowstone National Park hot spring environment. *P. Natl. Acad. Sci. USA*, 91:1609–1613, 1994.

[6] MJ Ferris and G Muyzer. Denaturing Gradient Gel Electrophoresis profiles of 16S rRNA-defined populations inhabiting a hot spring microbial mat community. *Appl. Environ. Microbiol.*, 62(2):340–346, 1996.

[7] SB Pointing, Y Chan, DC Lacap, MC Lau, JA Jurgens, and RL Farrell. Highly specialized microbial diversity in hyper-arid polar deserts. *P. Natl. Acad. Sci. USA*, 106(47):19964–19969, 2009.

[8] F Reith. Life in the deep subsurface. *Geology*, 39(3):287–288, 2011.

[9] AM Anesio and J Laybourn-Parry. Glaciers and ice sheets as a biome. *Trends Ecol. Evol.*, 27(4):219–225, 2012.

[10] JR Lloyd and DR Lovley. Microbial detoxification of metals and radionuclides. *Curr. Opin. Biotechnol.*, 12:248–253, 2001.

[11] JK Fredrickson, JM Zachara, DL Balkwill, D Kennedy, SW Li, HM Kostandarithes, MJ Daly, MF Romine, and FJ Brockman. Geomicrobiology

of high-level nuclear waste-contaminated vadose sediments at the Hanford site, Washington State. *Appl. Environ. Microbiol.*, 70(7):4230–41, 2004.

[12] BJ Baker and JF Banfield. Microbial communities in acid mine drainage. *FEMS Microbiol. Ecol.*, 44(2):139–52, 2003.

[13] K Kashefi and D Lovely. Extending the Upper Temperature Limit for Life. *Science*, 301:934, 2003.

[14] P Buford Price and T Sowers. Temperature dependence of metabolic rates for microbial growth, maintenance, and survival. *P. Natl. Acad. Sci. USA*, 101(16):4631–4636, 2004.

[15] A Clarke, GJ Morris, F Fonseca, BJ Murray, E Acton, and HC Price. A low temperature limit for life on Earth. *PLoS One*, 8(6):e66207, 2013.

[16] BE Jones, WD Grant, AW Duckworth, and GG Owenson. Microbial diversity of soda lakes. *Extremophiles*, 2(3):191–200, 1998.

[17] J Kuang, L Huang, L Chen, Z Hua, S Li, M Hu, J Li, and W Shu. Contemporary environmental variation determines microbial diversity patterns in acid mine drainage. *ISME J.*, 7(5):1038–50, 2013.

[18] A Oren. Microbial life at high salt concentrations: phylogenetic and metabolic diversity. *Saline Systems*, 4:2, 2008.

[19] TM Hoehler and BB Jorgensen. Microbial life under extreme energy limitation. *Nat. Rev. Microbiol.*, 11(2):83–94, 2013.

[20] G Storz and E Hengge-Aronis, editors. *Bacterial Stress Responses*. ASM Press, Washington, DC, 2000.

[21] WB Whitman, DC Coleman, and WJ Wiebe. Prokaryotes: The unseen majority. *P. Natl. Acad. Sci. USA*, 95:6578–6583, 1998.

[22] JL Wadham, S Arndt, S Tulaczyk, M Stibal, M Tranter, J Telling, GP Lis, E Lawson, A Ridgwell, A Dubnick, MJ Sharp, AM Anesio, and CEH Butler. Potential methane reservoirs beneath Antarctica. *Nature*, 488:633–637, 2012.

[23] PG Falkowski, T Fenchel, and EF Delong. The microbial engines that drive Earth's biogeochemical cycles. *Science*, 320:1034–1039, 2008.

[24] JF Kasting and JL Siefert. Life and the evolution of Earth's atmosphere. *Science*, 296:1066–8, 2002.

[25] C Berney and J Pawlowski. A molecular time-scale for eukaryote evolution recalibrated with the continuous microfossil record. *Proc. Biol. Sci.*, 273:1867–1872, 2006.

[26] CH Wellman, PL Osterloff, and U Mohiuddin. Fragments of the earliest land plants. *Nature*, 425:603–605, 2003.

[27] HL. Ehrlich. How microbes influence mineral growth and dissolution. *Chem. Geol.*, 132:5–9, 1996.

[28] AA Gorbushina. Life on the rocks. *Environ. Microbiol.*, 9(7):1613–1631, 2007.

[29] J Kallmeyer, R Pockalny, RR Adhikari, DC Smith, and S D'Hondt. Global distribution of microbial abundance and biomass in subseafloor sediment. *P. Natl. Acad. Sci. USA*, 109(40):16213–16216, 2012.

[30] M Schidlowski. A 3,800-million-year isotopic record of life from carbon in sedimentary rocks. *Nature*, 333:313–318, 1988.

[31] SJ Mojzsis, G Arrhenius, KD McKeegan, TM Harrison, AP Nutman, and CRL Friends. Evidence for life on Earth before 3,800 million years ago. *Nature*, 384:55–59, 1996.

[32] MT Rosing. Delta 13C-Depleted Carbon Microparticles in less than 3700-Ma Sea-Floor Sedimentary Rocks from West Greenland. *Science*, 283:674–676, 1999.

[33] JW Schopf. Fossil evidence of Archaean life. *Philos. T. Roy. Soc. B.*, 361:869–885, 2006.

[34] M Brasier, O Green, and A Jephcoat. Questioning the evidence for Earth's oldest fossils. *Nature*, 416:76–81, 2002.

[35] EG Nisbet and NH Sleep. The habitat and nature of early life. *Nature*, 409:1083–91, 2001.

[36] HD Holland, B Lazar, and M McCaffrey. Evolution of the atmosphere and oceans. *Nature*, 320:27–33, 2005.

[37] DE Canfield. The Early History Of Atmospheric Oxygen: Homage to Robert M. Garrels. *Annu. Rev. Earth Planet. Sci.*, 33(1):1–36, 2005.

[38] HD Holland. The oxygenation of the atmosphere and oceans. *Philos. T. Roy. Soc. B.*, 361:903–915, 2006.

[39] AL Sessions, DM Doughty, PV Welander, RE Summons, and DK Newman. The continuing puzzle of the great oxidation event. *Curr. Biol.*, 19(14):567–574, 2009.

[40] CS Cockell and G Horneck. The history of the UV radiation climate of the Earth-theoretical and space-based observations. *Photochem. Photobiol.*, 73(4):447–451, 2001.

[41] AL Zerkle, MW Claire, SD Domagal-Goldman, J Farquhar, and SW Poulton. A bistable organic-rich atmosphere on the Neoarchaean Earth. *Nat. Geosci.*, 5(5):359–363, 2012.

[42] R Raiswell and D Canfield. The iron biogeochemical cycle past and present. *Geochemical Perspect.*, 1(1), 2012.

[43] S Moorbath. Oldest rocks, earliest life, heaviest impacts and the Hadean-Archaean transition. *Appl. Geochemistry*, 20:819–824, 2005.

[44] DR Lowe, GR. Byerly, and FT Kyte. Recently discovered 3.42-3.23 Ga impact layers, Barberton Belt, South Africa: 3.8 Ga detrital zircons, Archean impact history, and tectonic implications. *Geology*, 42(9):747–750, 2014.

[45] O Abramov and SJ Mojzsis. Microbial habitability of the Hadean Earth during the late heavy bombardment. *Nature*, 459:419–422, 2009.

[46] KA Maher and DJ Stevenson. Impact frustration and the origin of life. *Nature*, 331:612–614, 1988.

[47] HD Holland. Volcanic gases, black smokers, and the Great Oxidation Event. *Geochim. Cosmochim. Acta*, 66(21):3811–3826, 2002.

[48] R Buick. When did oxygenic photosynthesis evolve? *Philos. T. Roy. Soc. B.*, 363:2731–43, 2008.

[49] DC Catling and MW Claire. How Earth's atmosphere evolved to an oxic state: A status report. *Earth Planet. Sc. Lett.*, 237:1–20, 2005.

[50] PG Falkowski. Tracing oxygens imprint on Earths metabolic evolution. *Science*, 311:1724–1725, 2006.

[51] D Schwartzman and T Volk. Biotic enhancement of weathering and the habitability of Earth. *Nature*, 340:457–460, 1989.

[52] T Fenchel, GM King, and H Blackburn. *Bacterial biogeochemistry: the ecophysiology of mineral cycling.* Elsevier, 2012.

[53] TM Shank, DJ Fornari, KL Von Damm, MD Lilley, RM Haymon, and RA Lutz. Temporal and spatial patterns of biological community development at nascent deep-sea hydrothermal vents (950N, East Pacific Rise). *Deep Sea Res. Part II*, 45:465–515, 1998.

[54] K Kusel, M Blothe, D Schulz, M Reiche, and HL Drake. Microbial reduction of iron and porewater biogeochemistry in acidic peatlands. *Biogeosciences*, 5:1537–1549, 2008.

[55] KJ Edwards, PL Bond, GK Druschel, MM McGuire, RJ Hamers, and JF Banfield. Geochemical and biological aspects of sulfide mineral dissolution: lessons from Iron Mountain, California. *Chem. Geol.*, 169:383–397, 2000.

[56] GM Gadd. Metals, minerals and microbes: geomicrobiology and bioremediation. *Microbiology*, 156(3):609–43, 2010.

[57] PD Tortell, MT Maldonado, J Granger, and NM Price. Marine bacteria and biogeochemical cycling of iron in the oceans. *FEMS Microbiol. Ecol.*, 29(1):1–11, 1999.

[58] JJR Frausto da Silva and RJP Williams. *The Biological Chemistry of the Elements: The Inorganic Chemistry of Life.* Oxford University Press, 2nd edition, 2001.

[59] S Andrews, A Robinson, and F Rodriguez-Quinones. Bacterial iron homeostasis. *FEMS Microbiol. Rev.*, 27:215–237, 2003.

[60] ME Maguire and JA Cowan. Magnesium chemistry and biochemistry. *Biometals*, 15(3):203–10, 2002.

[61] KJ Waldron, JC Rutherford, D Ford, and NJ Robinson. Metalloproteins and metal sensing. *Nature*, 460:823–830, 2009.

[62] L Fiedor, A Kania, B Myśliwa-Kurdziel, L Orze, and G Stochel. Understanding chlorophylls: central magnesium ion and phytyl as structural determinants. *Biochim. Biophys. Acta*, 1777(12):1491–500, 2008.

[63] P Vandevivre, SA Welch, WJ Ullman, and DL Kirchman. Enhanced dissolution of silicate minerals by bacteria at near-neautral pH. *Microb. Ecol.*, 27:241–251, 1994.

[64] LJ Liermann, BE Kalinowski, SL Brantley, and JG Ferry. Role of bacterial siderophores in the dissolution of horneblende. *Geochim. Cosmochim. Acta*, 64(4):587–602, 2000.

[65] J Lee and JB Fein. Experimental study of the effect of Bacillus subtilis on gibbsite dissolution rates under near-neutral pH and nutrient-poor conditions. *Chem. Geol.*, 166:193–202, 2000.

[66] EM Hausrath, A Neaman, and SL Brantley. Elemental release rates from dissolving basalt and granite with and without organic ligands. *Am. J. Sci.*, 309(8):633–660, 2009.

[67] S Uroz, C Calvaruso, M Turpault, and P Frey-Klett. Mineral weathering by bacteria: ecology, actors and mechanisms. *Trends Microbiol.*, 17(8):378–387, 2009.

[68] KO Konhauser, DK Newman, and A Kappler. The potential significance of microbial Fe(III) reduction during deposition of Precambrian banded iron formations. *Geobiology*, 3:167–177, 2005.

[69] M Labrenz, GK Druschel, T Thomsen-Ebert, B Gilbert, SA Welch, KM Kemner, GA Logan, RE Summons, G De Stasio, PL Bond, B Lai, SD Kelly, and JF Banfield. Formation of Sphalerite (ZnS) deposits in natural biofilms of sulfate-reducing bacteria. *Science*, 290:1744–1748, 2000.

[70] F Reith, B Etschmann, C Grosse, H Moors, MA Benotmane, P Monsieurs, G Grass, C Doonan, S Vogt, B Lai, G Martinez-Criado, GN George, DH Nies, M Mergeay, A Pring, G Southam, and J Brugger. Mechanisms of gold biomineralization in the bacterium Cupriavidus metallidurans. *P. Natl. Acad. Sci. USA*, 106(42):17757–62, 2009.

[71] T Kikuchi and S Tanaka. Biological removal and recovery of toxic heavy metals in water environment. *Crit. Rev. Env. Sci. Tech.*, 42(10):1007–1057, 2012.

[72] DK Newman and JF Banfield. Geomicrobiology: How molecular-scale interactions underpin biogeochemical cycles. *Science*, 296:1071–1077, 2002.

[73] K Barbeau, EL Rue, KW Bruland, and A Butler. Photochemical cycling of iron in the surface ocean mediated by microbial iron (III)-binding ligands. *Nature*, 413:409–413, 2001.

[74] AA Gorbushina and WJ Broughton. Microbiology of the atmosphere-rock interface: how biological interactions and physical stresses modulate a sophisticated microbial ecosystem. *Annu. Rev. Microbiol.*, 63:431–50, 2009.

[75] LC Kelly, CS Cockell, T Thorsteinsson, V Marteinsson, and J Stevenson. Pioneer microbial communities of the Fimmvöruháls lava flow, Eyjafjallajökull, Iceland. *Microb. Ecol.*, 68(3):504–18, 2014.

[76] EI Friedmann and R Ocampo. Endolithic blue-green algae in the dry valleys: Primary producers and the Antarctic desert ecosystem. *Science*, 193:1247–1249, 1976.

[77] R Bell. Cryptoendolithic algae of hot semiarid lands and deserts. *J. Phycol.*, 29:133–139, 1993.

[78] T Curtis, W Sloan, and J Scannell. Estimating prokaryotic diversity and its limits. *P. Natl. Acad. Sci. USA*, 99:10494–10499, 2002.

[79] JJ Walker and NR Pace. Endolithic microbial ecosystems. *Annu. Rev. Microbiol.*, 61:331–47, 2007.

[80] N Khan, M Tuffin, W Stafford, C Cary, DC Lacap, SB Pointing, and D Cowan. Hypolithic microbial communities of quartz rocks from Miers Valley, McMurdo Dry Valleys, Antarctica. *Polar Biol.*, 34(11):1657–1668, 2011.

[81] EI Friedmann. Endolithic microorganisms in the Antarctic cold desert. *Science*, 215:1045–1053, 1982.

[82] P Vítek, HGM Edwards, J Jehlicka, C Ascaso, A De los Ríos, S Valea, SE Jorge-Villar, AF Davila, and J Wierzchos. Microbial colonization of halite from the hyper-arid Atacama Desert studied by Raman spectroscopy. *Philos. T. Roy. Soc. A.*, 368:3205–21, 2010.

[83] C Cockell, P Lee, G Osinski, G Horneck, and P Broady. Impact-induced microbial endolithic habitats. *Meteorit. Planet. Sci.*, 1298:1287–1298, 2002.

[84] DA Fike, C Cockell, D Pearce, and P Lee. Heterotrophic microbial colonization of the interior of impact-shocked rocks from Haughton impact structure, Devon Island, Nunavut, Canadian High Arctic. *Int. J. Astrobiol.*, 1(4):311–323, 2002.

[85] S Jorgevillar, H Edwards, and L Benning. Raman spectroscopic and scanning electron microscopic analysis of a novel biological colonisation of volcanic rocks. *Icarus*, 184(1):158–169, 2006.

[86] A Herrera, CS Cockell, S Self, M Blaxter, J Reitner, T Thorsteinsson, G Arp, W Dro, and AG Tindle. A Cryptoendolithic Community in Volcanic Glass. 9(4), 2009.

[87] W Gross, J Kuver, G Tischendorf, N Bouchaala, and W Busch. Cryptoendolithic growth of the red alga Galdieria sulphuraria in volcanic areas. *Eur. J. Phycol.*, 33:25–31, 1998.

[88] PM Gaylarde, AD Jungblut, CC Gaylarde, and BA Neilan. Endolithic phototrophs from an active geothermal region in New Zealand. *Geomicrobiol. J.*, 23:579–87, 2006.

[89] VR Phoenix, PC Bennett, AS Engel, SW Tyler, and FG Ferris. Chilean high-altitude hot-spring sinters: a model system for UV screening mechanisms by early Precambrian cyanobacteria. *Geobiology*, 4:15–28, 2006.

[90] D Papineau, JJ Walker, SJ Mojzsis, and NR Pace. Composition and structure of microbial communities from stromatolites of Hamelin Pool in Shark Bay, Western Australia. *Appl. Environ. Microbiol.*, 71(8):4822–32, 2005.

[91] CJ McNamara, TD Perry, KA Bearce, G Hernandez-Duque, and R Mitchell. Epilithic and endolithic bacterial communities in limestone from a Maya archaeological site. *Microb. Ecol.*, 51(1):51–64, 2006.

[92] U Matthes, Turner S, and DW Larsen. Light attenuation by limestone rock and its constraint on the depth distribution of endolithic algae and cyanobacteria. *Int. J. Plant Sci.*, 162:263–270, 2001.

[93] HW Jannasch, K Eimhjell, CO Wirsen, and A Farmanfa. Microbial degradation of organic matter in the deep sea. *Science*, 171:672–675, 1971.

[94] OU Mason, CA Di Meo-Savoie, JD Van Nostrand, J Zhou, MR Fisk, and SJ Giovannoni. Prokaryotic diversity, distribution, and insights into their role in biogeochemical cycling in marine basalts. *ISME J.*, 3(2):231–242, 2009.

[95] BN Orcutt, W Bach, K Becker, AT Fisher, M Hentscher, BM Toner, CG Wheat, and KJ Edwards. Colonization of subsurface microbial observatories deployed in young ocean crust. *ISME J.*, 5(4):692–703, 2011.

[96] M Nyyssönen, J Hultman, L Ahonen, I Kukkonen, L Paulin, P Laine, M Itävaara, and P Auvinen. Taxonomically and functionally diverse microbial communities in deep crystalline rocks of the Fennoscandian shield. *ISME J.*, 8(1):126–138, 2014.

[97] William J Brazelton, Penny L Morrill, Natalie Szponar, and Matthew O Schrenk. Bacterial communities associated with subsurface geochemical processes in continental serpentinite springs. *Appl. Environ. Microbiol.*, 79(13):3906–16, 2013.

[98] BC Christner, JC Priscu, AM Achberger, C Barbante, SP Carter, K Christianson, AB Michaud, JA Mikucki, AC Mitchell, ML Skidmore, TJ Vick-Majors, WP Adkins, S Anandakrishnan, G Barcheck, L Beem, A Behar, M Beitch, R Bolsey, C Branecky, R Edwards, A Fisher, HA Fricker, N Foley, B Guthrie, T Hodson, R Jacobel, S Kelley, KD Mankoff, E McBryan, R Powell, A Purcell, D Sampson, R Scherer, J Sherve, M Siegfried, and S Tulaczyk. A microbial ecosystem beneath the West Antarctic ice sheet. *Nature*, 512:310–313, 2014.

[99] RP Rastogi, RP Sinha, SH Moh, TK Lee, S Kottuparambil, Y Kim, JS Rhee, E Choi, MT Brown, D Häder, and T Han. Ultraviolet radiation and cyanobacteria. *J. Photoch. Photobio. B*, 141:154–169, 2014.

[100] G Horneck, DM Klaus, and RL Mancinelli. Space microbiology. *Microbiol. Mol. Biol. R.*, 74(1):121–156, 2010.

[101] I Cnossen, J Sanz-Forcada, F Favata, O Witasse, T Zegers, and NF Arnold. Habitat of early life: Solar X-ray and UV radiation at Earth's surface 4–3.5 billion years ago. *J. Geophys. Res.*, 112:E02008, 2007.

[102] L Berkner and L Marshall. History of major atmospheric components. *P. Natl. Acad. Sci. USA*, 53, 1965.

[103] AD Anbar, Y Duan, TW Lyons, GL Arnold, B Kendall, J Garvin, and R Buick. A Whiff of Oxygen Before the Great Oxidation Event. *Science*, 317:1903–1907, 2007.

[104] EE Stüeken, DC Catling, and R Buick. Contributions to late Archaean sulphur cycling by life on land. *Nat. Geosci.*, 5(10):722–725, 2012.

[105] SM Awramik. The oldest records of photosynthesis. *Photosynth. Res.*, 33(2):75–89, 1992.

[106] HJ Hofmann, K Grey, AH Hickman, and RI Thorpe. Origin of 3.45 Ga coniform stromatolites in Warrawoona Group, Western Australia. *Geol. Soc. Am. Bull.*, 111(8):1256–1262, 1999.

[107] JW Schopf, AB Kudryavtsev, AD Czaja, and AB Tripathi. Evidence of Archean life: Stromatolites and microfossils. *Precambrian Res.*, 158:141–155, 2007.

[108] D Lacap, K Warren-Rhodes, C McKay, and S Pointing. Cyanobacteria and chloroflexi-dominated hypolithic colonization of quartz at the hyper-arid core of the Atacama Desert, Chile. *Extremophiles*, 15(1):31–8, 2011.

[109] CS Cockell and JA Raven. Zones of photosynthetic potential on Mars and the early Earth. *Icarus*, 169:300–310, 2004.

[110] F Westall, CEJ de Ronde, G Southam, N Grassineau, M Colas, CS Cockell, and H Lammer. Implications of a 3.472 to 3.333 Gyr old subaerial microbial mat from the Barbeton greenstone belt, South Africa for the UV environmental conditions on the early Earth. *Philos. T. Roy. Soc. B.*, pages 1857–1875, 2006.

[111] T Egli and M Zinn. The concept of multiple-nutrient-limited growth of microorganisms and its application in biotechnological processes. *Biotechnol. Adv.*, 22:35–43, 2003.

[112] JR Rogers and PC Bennett. Mineral stimulation of subsurface microorganisms: release of limiting nutrients from silicates. *Chem. Geol.*, 203:91–108, 2004.

[113] AL N'Guessan, H Elifantz, KP Nevin, PJ Mouser, B Methé, TL Woodard, K Manley, KH Williams, MJ Wilkins, JT Larsen, PE Long, and DR Lovley.

Molecular analysis of phosphate limitation in Geobacteraceae during the bioremediation of a uranium-contaminated aquifer. *ISME J.*, 4(2):253–66, 2010.

[114] WS Harpole, JT Ngai, EE Cleland, EW Seabloom, ET Borer, MES Bracken, JJ Elser, DS Gruner, H Hillebrand, JB Shurin, and JE Smith. Nutrient co-limitation of primary producer communities. *Ecol. Lett.*, 14(9):852–62, 2011.

[115] S Barantal, H Schimann, N Fromin, and S Hättenschwiler. Nutrient and carbon limitation on decomposition in an Amazonian moist forest. *Ecosystems*, 15(7):1039–1052, 2012.

[116] MA Saito, MR McIlvin, DM Moran, and TJ Goepfert. Multiple nutrient stresses at intersecting Pacific Ocean biomes detected by protein biomarkers. *Science*, 345:1173–1178, 2014.

[117] K Olsson-Francis, R Van Houdt, M Mergeay, N Leys, and CS Cockell. Microarray analysis of a microbe-mineral interaction. *Geobiology*, 8(5):446–56, 2010.

[118] CM Moore, MM Mills, KR Arrigo, I Berman-Frank, L Bopp, PW Boyd, ED Galbraith, RJ Geider, C Guieu, SL Jaccard, TD Jickells, J La Roche, TM Lenton, NM Mahowald, E Marañón, I Marinov, JK Moore, T Nakatsuka, A Oschlies, MA Saito, TF Thingstad, A Tsuda, and O Ulloa. Processes and patterns of oceanic nutrient limitation. *Nat. Geosci.*, 6(9):701–710, 2013.

[119] OA Chadwick, LA Derry, PM Vitousek, BJ Huebert, and LO Hedin. Changing sources of nutrients during four million years of ecosystem development. *Nature*, 397:491–497, 1999.

[120] R Amundson, DD Richter, GS Humphreys, EG Jobbágy, and J Gaillardet. Coupling between biota and Earth materials in the critical zone. *Elements*, 3:327–332, 2007.

[121] J Monod. The growth of bacterial cultures. *Annu. Rev. Microbiol.*, 3:371–394, 1949.

[122] B Voigt, T Schweder, M Sibbald, D Albrecht, A Ehrenreich, J Bernhardt, J Feesche, K Maurer, G Gottschalk, JM van Dijl, and M Hecker. The extracellular proteome of Bacillus licheniformis grown in different media and under different nutrient starvation conditions. *Proteomics*, 6(1):268–81, 2006.

[123] A Kolkman, P Daran-Lapujade, A Fullaondo, MMA Olsthoorn, JT Pronk, M Slijper, and AJR Heck. Proteome analysis of yeast response to various nutrient limitations. *Mol. Syst. Biol.*, 2:1–16, 2006.

[124] Q Xia, T Wang, EL Hendrickson, TJ Lie, M Hackett, and JA Leigh. Quantitative proteomics of nutrient limitation in the hydrogenotrophic methanogen Methanococcus maripaludis. *BMC Microbiol.*, 9:149, 2009.

[125] KH Wyatt, RJ Stevenson, and MR Turetsky. The importance of nutrient co-limitation in regulating algal community composition, productivity and algal-derived DOC in an oligotrophic marsh in interior Alaska. *Freshw. Biol.*, 55(9):1845–1860, 2010.

[126] MA Saito, TJ Goepfert, and JT Ritt. Some thoughts on the concept of colimitation: Three definitions and the importance of bioavailability. *Limnol. Oceanogr.*, 53(1):276–290, 2008.

[127] J von Liebig. *Chemistry and its application to Agriculture and Physiology.* Taylor and Walton, London, 1840.

[128] I Poblete-Castro, IF Escapa, C Jäger, J Puchalka, C Ming, and C Lam. The metabolic response of P. putida KT2442 producing high levels of polyhydroxyalkanoate under single- and multiple-nutrient-limited growth: Highlights from a multi-level omics approach. *Microb. Cell Fact.*, 11(24):1–21, 2012.

[129] DJ Vaughan. Arsenic. *Elements*, 2(2):71–75, 2006.

[130] R Van Bogelen, ER Olson, BL Wanner, and FC Neidhardt. Global analysis of proteins synthesized during phosphorus restriction in Escherichia coli. *J. Bacteriol.*, 178(15):4344–4366, 1996.

[131] A Battesti, N Majdalani, and S Gottesman. The RpoS-mediated general stress response in Escherichia coli. *Annu. Rev. Microbiol.*, 65:189–213, 2011.

[132] LU Magnusson, A Farewell, and T Nyström. ppGpp: a global regulator in Escherichia coli. *Trends Microbiol.*, 13(5):236–42, 2005.

[133] F Picard, C Dressaire, L Girbal, and M Cocaign-Bousquet. Examination of post-transcriptional regulations in prokaryotes by integrative biology. *C. R. Biol.*, 332(11):958–73, 2009.

[134] M Ballesteros, S Kusano, A Ishihama, and M Vicente. The ftsQ gearbox promoter of Escheria coli is a major sigma S-dependent promoter in the ddlB-ftsA region. *Mol. Microbiol.*, 30(2):419–430, 1998.

[135] K Potrykus and M Cashel. (p)ppGpp: still magical? *Annu. Rev. Microbiol.*, 62:35–51, 2008.

[136] JW Foster. Microbial responses to acid stress. In G Storz and E Hengge-Aronis, editors, *Bacterial Stress Responses*, pages 99–116. AMS Press, San Francisco, 2000.

[137] JM Wood. Bacterial Osmosensing Transporters. In D Hussinger and H Sies, editors, *Osmosensing and Osmosignaling*, volume 428 of *Methods in Enzymology*, pages 77 – 107. Academic Press, 2007.

[138] DC Walker, BT Smith, and MD Sutton. The SOS response to DNA damage. In G Storz and R Hengge-Aronis, editors, *Bacterial Stress Responses*, pages 131–144. ASM Press, San Francisco, 2000.

[139] T Yura, M Kanemori, and TM Morita. The heat shock response: regulation and function. In G Storz and E Hengge-Aronis, editors, *Bacterial Stress Responses*, pages 3–18. AMS Press, San Francisco, 2000.

[140] S Phadtare, K Yamanaka, and M Inouye. The cold shock response. In G Storz and E Hengge-Aronis, editors, *Bacterial Stress Responses*, pages 33–46. AMS Press, San Francisco, 2000.

[141] DW Deamer. The first living systems: a bioenergetic perspective. *Microbiol. Mol. Biol. R.*, 61(2):239–261, 1997.

[142] A Kirsten, M Herzberg, A Voigt, J Seravalli, G Grass, J Scherer, and DH Nies. Contributions of five secondary metal uptake systems to metal homeostasis of Cupriavidus metallidurans CH34. *J. Bacteriol.*, 193(18):4652–63, 2011.

[143] LJ Rothschild and RL Mancinelli. Life in extreme environments. *Nature*, 409:1092–1101, 2001.

[144] JP Harrison, JE Hallsworth, and CS Cockell. Reduction of the temperature sensitivity of Halomonas hydrothermalis by iron starvation combined with microaerobic conditions. *Appl. Environ. Microbiol.*, 81(6):2156–2162, 2015.

[145] DS Nichols, J Olley, H Garda, RR Brenner, and TA McMeekin. Effect of temperature and salinity stress on growth and lipid composition of Shewanella gelidimarina. *Appl. Environ. Microbiol.*, 66(6):2422–2429, 2000.

[146] NM Mesbah, GM Cook, and J Wiegel. The halophilic alkalithermophile Natranaerobius thermophilus adapts to multiple environmental extremes using a large repertoire of Na(K)/H antiporters. *Mol. Microbiol.*, 74(2):270–81, 2009.

[147] P Laksanalamai and FT Robb. Small heat shock proteins from extremophiles: a review. *Extremophiles*, 8(1):1–11, 2004.

[148] P Monsieurs, H Moors, R Van Houdt, PJ Janssen, A Janssen, I Coninx, M Mergeay, and N Leys. Heavy metal resistance in Cupriavidus metallidurans CH34 is governed by an intricate transcriptional network. *Biometals*, 24(6):1133–1151, 2011.

[149] L Nie, G Wu, DE Culley, JCM Scholten, and W Zhang. Integrative analysis of transcriptomic and proteomic data: challenges, solutions and applications. *Crit. Rev. Biotechnol.*, 27(2):63–75, 2007.

[150] A Mukhopadhyay, Z He, EJ Alm, AP Arkin, EE Baidoo, SC Borglin, W Chen, TC Hazen, Q He, H Holman, K Huang, R Huang, DC Joyner, N Katz, M Keller, P Oeller, A Redding, J Sun, J Wall, J Wei, Z Yang, H Yen, J Zhou, and JD Keasling. Salt stress in Desulfovibrio vulgaris Hildenborough: an integrated genomics approach. *J. Bacteriol.*, 188(11):4068–4078, 2006.

[151] K Riedel and A Lehner. Identification of proteins involved in osmotic stress response in Enterobacter sakazakii by proteomics. *Proteomics*, 7(8):1217–31, 2007.

[152] J Mostertz, C Scharf, M Hecker, and G Homuth. Transcriptome and proteome analysis of Bacillus subtilis gene expression in response to superoxide and peroxide stress. *Microbiology*, 150(2):497–512, 2004.

[153] S Sharma, CS Sundaram, PM Luthra, Y Singh, R Sirdeshmukh, and WN Gade. Role of proteins in resistance mechanism of Pseudomonas fluorescens against heavy metal induced stress with proteomics approach. *J. Biotechnol.*, 126(3):374–82, 2006.

[154] M Mergeay, D Nies, HG Schlegel, J Gerits, P Charles, and F Van Gijsegem. Alcaligenes eutrophus ch34 is a facultative chemolithotroph with plasmid-bound resistance to heavy metals. *J. Bacteriol.*, 162:328–334, 1985.

[155] H Biebl and N Pfenning. Isolation of members of the family Rhodospirillaceae. In MP Starr, H Stolp, HG Truper, A Balows, and HG Schlegel, editors, *The Prokaryotes*, pages 267–273. Springer, New York, 1981.

[156] G Niaura. Raman spectroscopy in analysis of biomolecules. In R Meyers, editor, *Encyclopedia of Analytical Chemistry*. John Wiley & Sons, Ltd, Chichester, 2006.

[157] X Hou and BT Jones. Inductively Coupled Plasma / Optical Emission Spectrometry. In R Meyers, editor, *Encyclopedia of Analytical Chemistry*, pages 9468–9485. John Wiley & Sons, Ltd., Chichester, 2000.

[158] X Hou and B Jones. Inductively Coupled - Opitical Emission Spectrometry. In *Encyclopedia of Analytical Chemistry*, pages 9468–9485. Academic Press, 2000.

[159] TC Walther and M Mann. Mass spectrometry-based proteomics in cell biology. *J. Cell Biol.*, 190(4):491–500, 2010.

[160] KA Neilson, NA Ali, S Muralidharan, M Mirzaei, M Mariani, G Assadourian, A Lee, SC Van Sluyter, and PA Haynes. Less label, more free: approaches in label-free quantitative mass spectrometry. *Proteomics*, 11(4):535–53, 2011.

[161] T Le Bihan, R Grima, S Martin, T Forster, and Y Le Bihan. Quantitative analysis of low-abundance peptides in HeLa cell cytoplasm by targeted liquid chromatography/mass spectrometry and stable isotope dilution: emphasising the distinction between peptide detection and peptide identification. *Rapid Commun. Mass Sp.*, 24(7):1093–1104, 2010.

[162] JV Olsen, S Ong, and M Mann. Trypsin cleaves exclusively C-terminal to arginine and lysine residues. *Mol. Cell. Proteomics*, 3(6):608–14, 2004.

[163] R Aebersold and M Mann. Mass spectrometry-based proteomics. *Nature*, 422:198–207, 2003.

[164] M Scigelova and A Makarov. Orbitrap mass analyzer - overview and applications in Proteomics. *Pract. Proteomics*, 1:17–21, 2006.

[165] CS Ho, CWK Lam, MHM Chan, RCK Cheung, LK Law, LCW Lit, KF Ng, MWM Suen, and HL Tai. Electrospray Ionisation Mass Spectrometry: Principles and clinical applications. *Clin. Biochem. Rev.*, 24:3–12, 2003.

[166] Q Hu, RJ Noll, H Li, A Makarov, M Hardman, and GR Cooks. The Orbitrap: a new mass spectrometer. *J. Mass Spectrom.*, 40(4):430–43, 2005.

[167] McLafferty FW. Tandem mass spectrometry. *Science*, 214:280–287, 1981.

[168] AI Nesvizhskii, O Vitek, and R Aebersold. Analysis and validation of proteomic data generated by tandem mass spectrometry. *Nat. Methods*, 4(10):787–97, 2007.

[169] T Tatusova, S Ciufo, B Fedorov, K O'Neill, and I Tolstoy. RefSeq microbial genomes database: new representation and annotation strategy. *Nucleic Acids Res.*, 42:D553–9, 2014.

[170] H Liu, RG Sadygov, and JR Yates. A model for random sampling and estimation of relative protein abundance in shotgun proteomics. *Analytical*, 76(14):4193–4201, 2004.

[171] MJ Anderson. A new method for non-metric multivariate analysis of variance. *Ausralian J. Ecol.*, 26:32–46, 2001.

[172] PJ Janssen, R Van Houdt, H Moors, P Monsieurs, N Morin, A Michaux, MA Benotmane, N Leys, T Vallaeys, A Lapidus, S Monchy, C Médigue, S Taghavi, S McCorkle, J Dunn, D van der Lelie, and M Mergeay. The complete genome sequence of Cupriavidus metallidurans strain CH34, a

master survivalist in harsh and anthropogenic environments. *PLoS One*, 5(5):e10433, 2010.

[173] E Rabbow, P Rettberg, S Barczyk, M Bohmeier, A Parpart, C Panitz, G Horneck, J Burfeindt, F Molter, E Jaramillo, C Pereira, P Weiss, R Willnecker, R Demets, J Dettmann, and G Reitz. The astrobiological mission EXPOSE-R on board of the International Space Station. *Int. J. Astrobiol.*, pages 1–14, 2014.

[174] R Demets, M Bertrand, A Bolkhovitinov, K Bryson, C Colas, H Cottin, J Dettmann, P Ehrenfreund, A Elsaesser, E Jaramillo, M Lebert, G van Papendrecht, C Pereira, T Rohr, K Saiagh, and M Schuster. Window contamination on EXPOSE-R. *Int. J. Astrobiol.*, 14(01):33–45, 2014.

[175] E Jessberger. 40Ar-39Ar dating of the Haughton impact structure. *Meteorit. Planet. Sci.*, (23):233–234, 1988.

[176] C Chyba, T Owen, and WH Ip. Impact delivery of volatiles and organic molecules to Earth. In T Gehrels, M Shapley Matthews, and A Schumann, editors, *Hazards Due To Comets Asteroids*, pages 9–58. University of Arizona Press, Tucson, 1995.

[177] L Dor, N Carl, and I Baldinger. Polymorphisms and salinity tolerance as criterion for differentiation of three new species of Chrococcidiopsis (Chrococcales). *Arch. Hydrobiol.*, 64:411–421, 1991.

[178] J Komarek and F Hindak. Taxonomy of the new isolated strains of Chroococcidiopsis (Cyanophyceae). *Arch. Hydrobiol.*, 13:311–329, 1975.

[179] EI Friedmann. Endolithic microbial life in hot and cold deserts. *Orig. Life*, 10:223–235, 1980.

[180] EI Friedmann and R Ocampo-Friedmann. Blue-green algae in arid crytoendolithic habitats. *Arch. Hydrobiol*, 71(2), 1985.

[181] B Budel and D Wessels. Rock inhabiting blue-green algae/cyanobacteria from hot arid regions. *Arch. Hydrobiol.*, 64:385–398, 1991.

[182] EI Friedmann and R Ocampo Friedmann. A primitive cyanobacterium as pioneer microorganism for terraforming Mars. *Adv. Space Res.*, 15(3):3–6, 1995.

[183] CS Cockell, P Rettberg, E Rabbow, and K Olsson-Francis. Exposure of phototrophs to 548 days in low Earth orbit: microbial selection pressures in outer space and on early earth. *ISME J.*, 5(10):1671–82, 2011.

[184] G Britton. Structure and properties of carotenoids in relation to function. *FASEB J.*, 9:1551–1558, 1995.

[185] G Wang, Z Hao, Z Huang, L Chen, X Li, C Hu, and Y Liu. Raman spectroscopic analysis of a desert cyanobacterium Nostoc sp. in response to UVB radiation. *Astrobiology*, 10(8):783–787, 2010.

[186] Y Tamaru, Y Takani, T Yoshida, and T Sakamoto. Crucial role of extracellular polysaccharides in desiccation and freezing tolerance in the terrestrial cyanobacterium Nostoc commune. *Appl. Environ. Microbiol.*, 71:7327–7333, 2005.

[187] KA Hughes and B Lawley. A novel Antarctic microbial endolithic community within gypsum crusts. *Environ. Microbiol.*, 5:555–565, 2003.

[188] JP de Vera, U Boettger, R De La Torre, FJ Sánchez, D Grunow, N Schmitz, C Lange, HW Hübers, D Billi, M Baqué, P Rettberg, E Rabbow, G Reitz, T Berger, R Möller, M Bohmeier, G Horneck, F Westall, J Jänchen, J Fritz, C Meyer, S Onofri, L Selbmann, L Zucconi, N Kozyrovska, T Leya, B Foing, R Demets, CS Cockell, C Bryce, D Wagner, P Serrano, HGM. Edwards, J Joshi, B Huwe, P Ehrenfreund, A Elsaesser, S Ott, J Meessen, N Feyh, U Szewzyk, R Jaumann, and T Spohn. Supporting Mars exploration: BIOMEX in Low Earth Orbit and further astrobiological studies on the Moon using Raman and PanCam technology. *Planet. Space Sci.*, 74(1):103–110, 2012.

[189] LC Kelly, CS Cockell, YM Piceno, GL Andersen, T Thorsteinsson, and V Marteinsson. Bacterial diversity of weathered terrestrial Icelandic volcanic glasses. *Microb. Ecol.*, 60(4):740–52, 2010.

[190] P Vandamme and T Coenye. Taxonomy of the genus Cupriavidus: a tale of lost and found. *Int. J. Syst. Evol. Microbiol.*, 54:2285–9, 2004.

[191] M Mergeay, C Houba, and J Gerits. Extrachromosomal inheritance controlling resistance to cadmium, cobalt, copper and zinc ions: evidence from curing in a Pseudomonas. *Arch. Int. Physiol. Biochim.*, 86:440–442, 1978.

[192] L Diels, S Van Roy, S Taghavi, and R Van Houdt. From industrial sites to environmental applications with Cupriavidus metallidurans. *Antonie Van Leeuwenhoek*, 96(2):247–58, 2009.

[193] T von Rozycki and DH Nies. Cupriavidus metallidurans: evolution of a metal-resistant bacterium. *Antonie Van Leeuwenhoek*, 96(2):115–39, 2009.

[194] S Wuertz and M Mergeay. The impact of heavy metals on soil microbial communities and their activities. In D van Elsas, E Wellington, and J Trevors, editors, *Modern Soil Microbiology*, pages 607–642. Marcel Dekker Publisher, New York, 1997.

[195] MI Sarró, AM García, and DA Moreno. Biofilm formation in spent nuclear fuel pools and bioremediation of radioactive water. *Int. Microbiol.*, 8:223–230, 2005.

[196] M La Duc, W Nicholson, R Kern, and K Venkateswaran. Microbial characterization of the Mars Odyssey spacecraft and its encapsulation facility. *Environ. Microbiol.*, 5(10):977–985, 2003.

[197] K Mijnendonckx, A Provoost, CM Ott, K Venkateswaran, J Mahillon, N Leys, and R Van Houdt. Characterization of the survival ability of Cupriavidus metallidurans and Ralstonia pickettii from space-related environments. *Microb. Ecol.*, 65(2):347–60, 2013.

[198] T Coenye, T Spilker, R Reik, P Vandamme, and JJ Lipuma. Use of PCR analyses to define the distribution of Ralstonia species recovered from patients with cystic fibrosis. *J. Clin. Microbiol.*, 43(7):3463–6, 2005.

[199] MM Bradford. A rapid and sensitive method for the quantitation of microgram quantities of protein utilizing the principle of protein-dye binding. *Anal. Biochem.*, 72:248–254, 1976.

[200] K Clarke and R Gorley. PRIMER v6: User Manual/Tutorial., 2006.

[201] MJ Anderson, RN Gorley, and KR Clarke. PERMANOVA+ for PRIMER: Guide to software and statistical methods., 2008.

[202] MJ Anderson. Distance-based tests for homogeneity of multivariate dispersions. *Biometrics*, 62:245–253, 2006.

[203] J Murphy and JP Riley. A modified single solution method for the determination of phosphate in natural waters. *Anal. Chim. Acta*, 27:31–36, 1962.

[204] RG Wetzel and GE Likens. Inorganic Nutrients: Nitrogen, Phosphorus, and Other Nutrients. In *Limnlogical Analalysis*, pages 85–111. Springer, New York, 2000.

[205] WW Metcalf and BL Wanner. Involvement of the Escherichia coli phn (psiD) gene cluster in assimilation of phosphorus in the form of phosphonates, phosphite , Pi esters , and Pi. 173(2):587–600, 1991.

[206] RW Titball. Bacterial Phospholipase C. *Microbiol. Rev.*, 57(2):347–366, 1993.

[207] S Banerji and A Flieger. Patatin-like proteins: a new family of lipolytic enzymes present in bacteria? *Microbiology*, 150(3):522–525, 2002.

[208] LP Wackett, SL Shames, CP Venditti, and CT Walsh. Bacterial carbon-phosphorus lyase: products, rates, and regulation of phosphonic and phosphonic acid metabolism. *J. Bacteriol.*, 169(2):710–717, 1987.

[209] CM Chen, QZ Ye, ZM Zhu, BR Wanner, and CT Walsh. Molecular-biology of carbon phosphorus bond cleavage cloning and sequencing of the Phn (PsiD) genes involved in alkylphosphonate uptake and C-P lyase activity in Escheria-coli. *J. Biol. Chem.*, 8265(8):4461–4471, 1990.

[210] B Hove-Jensen, DL Zechel, and B Jochimsen. Utilization of glyphosphate as phosphate source: biochemistry and genetics of bacterial carbon-phosphorus lyase. *MMBR*, 78(1):176–197, 2014.

[211] MT Pellicer, MF Nun, J Aguilar, J Badia, and L Baldoma. Role of 2-Phosphoglycolate Phosphatase of Escherichia coli in metabolism of the 2-Phosphoglycolate formed in DNA repair. 185(19):5815–5821, 2003.

[212] J Zhou, Q He, CL Hemme, A Mukhopadhyay, K Hillesland, A Zhou, Zi He, JD Van Nostrand, TC Hazen, DA Stahl, JD Wall, and AP Arkin. How sulphate-reducing microorganisms cope with stress: lessons from systems biology. *Nat. Rev. Microbiol.*, 9(6):452–66, 2011.

[213] EH Oelkers and SR Gislason. The mechanism, rates and consequences of basaltic glass dissolution: I. An experimental study of the dissolution rates of basaltic glass as a function of aqueous Al, Si and oxalic acid concentration at 25 degrees C and pH 3 and 11. *Geochim. Cosmochim. Acta*, 65(21):3671–3681, 2001.

[214] E Frossard, M Brossard, MJ Hedley, and A Metherell. Reactions controlling the cycling of P in soils. In H Tiessen, editor, *Phosphorus in the Global Environment: transfers, cycles and management*, pages 107–137. Wiley, Chichester, 1995.

[215] R Ram, NC Verberkmoes, MP Thelen, GW Tyson, BJ Baker, RC Ii, M Shah, RL Hettich, and JF Banfield. Community proteomics of a natural microbial biofilm. *Nature*, 37:1915–1920, 2005.

[216] H Lambers, JA Raven, GR Shaver, and SE Smith. Plant nutrient-acquisition strategies change with soil age. *Trends Ecol. Evol.*, 23(2):95–103, 2008.

[217] J Huisman, N Pham Thi, DM Karl, and B Sommeijer. Reduced mixing generates oscillations and chaos in the oceanic deep chlorophyll maximum. *Nature*, 439:322–325, 2006.

[218] CM Bethke, D Ding, Q Jin, and RA Sanford. Origin of microbiological zoning in groundwater flows. *Geology*, 36:739–742, 2008.

[219] PW Boyd, AJ Watson, CS Law, ER Abraham, T Trull, R Murdoch, DCE Bakker, AR Bowie, KO Buesseler, H Chang, M Charette, P Croot, K Downing, Rl Frew, M Gall, M Hadfield, J Hall, M Harvey, G Jameson, J Laroche, M Liddicoat, R Ling, MT Maldonado, RM Mckay, S Nodder, S Pickmere, R Pridmore, S Rintoul, K Safi, P Sutton, R Strzepek, K Tanneberger, S Turner, A Waite, and J Zeldis. A mesoscale phytoplankton bloom in the polar Southern Ocean stimulated by iron fertilization. *Nature*, 407, 2000.

[220] HJW de Baar, PW Boyd, KH Coale, MR Landry, A Tsuda, P Assmy, DCE Bakker, Y Bozec, RT Barber, MA Brzezinsku, KO Buesseler, M Boye, PL Croot, F Gervais, MY Gorbnov, PJ Harrison, WT Hiscock, P Laan, C Lancelot, CS Law, M Levasseur, A Marchettie, FJ Millero, J Nishioka, Y Nojiri, T van Oijen, U Riebesell, MJA Rijkenberg, H Saito, S Takeda, KR Timmermans, MJW Veldhuis, AM Waite, and C Wong. Synthesis of iron fertilization experiments: From the Iron Age in the Age of Enlightenment. *J. Geophys. Res.*, 110:C09S16, 2005.

[221] S Poulton and D Canfield. Ferruginous conditions: A dominant feature of the ocean through Earth's history. *Elements*, 7(2):107–122, 2012.

[222] PM Vitousek, S Porder, BZ Houlton, OA Chadwick, and Z Houlton. Terrestrial phosphorus limitation: mechanisms, implications, and nitrogen–phosphorus interactions. *Ecol. Appl.*, 20(1):5–15, 2015.

[223] TW Walker and JK Syers. The fate of phosphorus during pedogenesis. *Geoderma*, 15:1–19, 1976.

[224] MD Krom, S Brenner, N Kress, and LT Gordon. Phosphorus limitation of primary productivity in the Eastern Mediterranean Sea. *Limnol. Oceanogr.*, 36:424–432, 1991.

[225] TF Thingstad, MD Krom, RFC Mantoura, GAF Flaten, S Groom, B Herut, N Kress, C Law, A Pasternak, P Pitta, S Psarra, F Rassoulzadegan, T Tanaka, A Tselipides, P Wassmann, EMS Woodward, C Wexels Risers, G Zodiatis, and T Zohary. Nature of phosphorus limitation in the ultraoligotrophic Eastern Mediterranean. *Science*, 309:1068–1071, 2005.

[226] DM Karl, R Letelier, L Tupas, J Dore, J Christian, and DV Hebel. The role of nitrogen fixation in the biogeochemical cycling in the subtropical North Pacific Ocean. *Nature*, 388:533–538, 1997.

[227] J Wu, W Sunda, EA Boyle, and DM Karl. Phosphorus depletion in the western North Atlantic. *Global Biogeochem. Cy.*, 17:1008–1016, 2000.

[228] J Xu, K Yin, L He, X Yuan, A Ho, and PJ Harrison. Phosphorus limitation in the northern South China Sea during late summer: Influence of the Pearl River. *Deep Sea Res. Part I*, 55(10):1330–1342, 2008.

[229] AMP Romani. Cellular magnesium homeostasis. *Arch. Biochem. Biophys.*, 512(1):1–23, 2011.

[230] A Gilis, MA Khan, P Cornelis, JM Meyer, M Mergeay, and D van der Lelie. Siderophore-mediated iron uptake in Alcaligenes eutrophus CH34 and identification of aleB encoding the ferric iron-alcaligin E receptor. *J. Bacteriol.*, 178(18):5499–507, 1996.

[231] BM Hopkinson, KL Roe, and KA Barbeau. Heme uptake by Microscilla marina and evidence for heme uptake systems in the genomes of diverse marine bacteria. *Appl. Environ. Microbiol.*, 74(20):6263–70, 2008.

[232] KL Roe, SL Hogle, and KA Barbeau. Utilization of heme as an iron source by marine Alphaproteobacteria in the Roseobacter Clade. *Appl. Environ. Microbiol.*, 79(18), 2013.

[233] KD Krewulak and HJ Vogel. Structural biology of bacterial iron uptake. *Biochim. Biophys. Acta*, 1778(9):1781–804, 2008.

[234] A Gaballa, H Antelmann, C Aguilar, SK Khakh, K Song, GT Smaldone, and JD Helmann. The Bacillus subtilis iron-sparing response is mediated by a Fur-regulated small RNA and three small, basic proteins. *P. Natl. Acad. Sci. USA*, 105(33):11927–32, 2008.

[235] AK White and WW Metcalf. The htx and ptx operons of Pseudomonas stutzeri WM88 are new members of the pho regulon. *J. Bacteriol.*, 186(17):5876–82, 2004.

[236] M Sun, J Sun, J Qiu, H Jing, and H Liu. Characterization of the proteomic profiles of the brown tide alga Aureoumbra lagunensis under phosphate- and nitrogen-limiting conditions and of its phosphate limitation-specific protein with alkaline phosphatase activity. *Appl. Environ. Microbiol.*, 78(6):2025–33, 2012.

[237] O Dalmas, P Sompornpisut, F Bezanilla, and E Perozo. Molecular mechanism of Mg2+-dependent gating in CorA. *Nat. Commun.*, 5, 2014.

[238] C Grosse, S Friedrich, and DH Nies. Contribution of extracytoplasmic function sigma factors to transition metal homeostasis in Cupriavidus metallidurans strain CH34. *J. Mol. Microb. Biotech.*, 12:227–40, 2007.

[239] A Matin. MicroReview The molecular basis of carbon-starvation-induced general resistance in Escherichia coii. *Mol. Microbiol*, 5(1):3–10, 1991.

[240] AB Flavier, M Clough, and TP Denny. Identification of 3-hydroxypalmitic acid methyl ester as a novel autoregulator controlling virulence in Ralstonia solanacearum. *Mol. Microbiol*, 26(2):251–259, 1997.

[241] S Kiyokawa, T Ito, M Ikehara, and F Kitajima. Middle Archean volcano–hydrothermal sequence: bacterial microfossil–bearing 3.2 Ga Dixon Island Formation, coastal Pilbara terrane, Australia. *GSA Bulletin*, 118(1):3–22, 2006.

[242] KE Fishbaugh, F Poulet, V Chevrier, Y Langevin, and JP Bibring. On the origin of gypsum in the Mars north polar region. *J. Geophys. Res*, 112:1–17, 2007.

Publication

International Journal of Astrobiology 14 (1): 115–122 (2015)
doi:10.1017/S1473550414000123

Impact shocked rocks as protective habitats on an anoxic early Earth

Casey C. Bryce[1], Gerda Horneck[2], Elke Rabbow[2], Howell G. M. Edwards[3,4] and Charles S. Cockell[1]

[1]*UK Centre for Astrobiology, School of Physics and Astronomy, University of Edinburgh, Edinburgh, Scotland, UK*
e-mail: Casey.Bryce@ed.ac.uk
[2]*German Aerospace Center DLR, Institute of Aerospace Medicine, Koeln, Germany*
[3]*Centre for Astrobiology and Extremophiles Research, School of Life Sciences, University of Bradford, Bradford, UK*
[4]*Department of Physics and Astronomy, Space Science Research Centre, University of Leicester, Leicester, UK*

Abstract: On Earth, microorganisms living under intense ultraviolet (UV) radiation stress can adopt endolithic lifestyles, growing within cracks and pore spaces in rocks. Intense UV irradiation encountered by microbes leads to death and significant damage to biomolecules, which also severely diminishes the likelihood of detecting signatures of life. Here we show that porous rocks shocked by asteroid or comet impacts provide protection for phototrophs and their biomolecules during 22 months of UV radiation exposure outside the International Space Station. The UV spectrum used approximated the high-UV flux on the surface of planets lacking ozone shields such as the early Earth. These data provide a demonstration that endolithic habitats can provide a refugium from the worst-case UV radiation environments on young planets and an empirical refutation of the idea that early intense UV radiation fluxes would have prevented phototrophs without the ability to form microbial mats or produce UV protective pigments from colonizing the surface of early landmasses.

Received 12 February 2014, accepted 27 March 2014, first published online 14 May 2014

Key words: chroococcidiopsis, early life, EXPOSE-R, impacts, ISS, low Earth orbit, UV.

Introduction

For the last 2.5 billion years, the Earth has been protected from harmful ultraviolet (UV) radiation by the ozone shield (Kastings & Siefert 2002). However, the first 1 billion years of life's evolution occurred under a nitrogen and carbon dioxide atmosphere which does not have the same ability to absorb UV radiation (Cockell & Horneck 2001). Organisms attempting to survive on the Earth's surface prior to the rise in oxygen would receive a radiation dose up to 1000 times more damaging to DNA than today (Cockell & Horneck 2001). Indeed, it was originally proposed that the intense UV radiation flux experienced on the early Earth might have prevented the colonization of the land masses (Berkner & Marshall 1965).

In high-UV environments on Earth today a number of survival strategies are observed. One such strategy is the matting habitat, whereby organisms achieve protection within thick laminated structures such as stromatolites. This has long been recognized as a potential means for early surface-dwelling organisms to have been protected from early intense UV radiation (Margulis *et al.* 1976; Westall *et al.* 2006). Alternatively, organisms commonly grow in the interior of rocky substrates or under them (Friedmann 1980). These organisms are known as endoliths and hypoliths, respectively.

The depth of penetration of UV radiation into a rock will depend on the substrate. One rock substrate suitable for colonization is crystalline rocks shocked by asteroid and comet impacts, including gneisses, which become more porous as a result of the intense pressures and temperatures of impact shock (Cockell *et al.* 2002). Cockell *et al.* (2002) calculated that organisms at 2 mm depth in porous impact-shocked gneiss under these early Earth radiation conditions would only encounter a maximum of one tenth of the DNA damage encountered on the surface of the Earth today, whilst still receiving sufficient photosynthetically active radiation for (anoxygenic or oxygenic) photosynthesis.

Previous work has only tested the protection afforded by rocks to UV radiation for a short period (Cockell *et al.* 2003) and only using the present-day terrestrial flux. One location in which the putative early earth UV radiation flux can be simulated is low Earth orbit (LEO) (Rettberg *et al.* 1998), where cut-off filters can be used to attenuate the extraterrestrial UV flux to simulate early Earth UV fluxes.

In the study presented here, we used the long-term exposure facility, EXPOSE-R, aboard the International Space Station to test the ability of an impact shocked endolithic substrate to provide adequate protection for phototrophs under a simulated worst-case prediction for early Earth's UV radiation regime. Here oxygenic phototrophs are studied. There are numerous lines of evidence which suggests oxygenic photosynthesis had evolved well before the atmosphere became oxygenated on a large scale (Buick 2008). Therefore oxygenic photosynthesis would almost certainly have existed before

UV-protection from the ozone shield was achieved. However, the principle we demonstrate is equally applicable to anoxygenic photosynthesizers.

Materials and methods

Organism and substrate selection

In this exposure experiment impact-shocked gneiss from the Haughton Impact Crater in the Canadian High Arctic was selected as a test substrate. A detailed outline of the geology of the Haughton Impact Structure from which the rocks were obtained can be found in Osinski *et al*. (2005). For a rock to be colonized it has to be suitably porous. Sandstones or vesicular volcanic rocks are porous under normal geological conditions making them good candidates for colonization (Cockell & Osinski 2007). Crystalline rocks are generally low porosity and a poor prospect for colonization. However, asteroid and comet impacts, widely considered to be a purely destructive force, have the ability to alter crystalline rocks in a way which increases the porosity, and therefore the availability of microhabitats within the rock structure (Cockell *et al*. 2002, 2003; Fike *et al*. 2002; Pontefract *et al*. 2012). Cockell *et al*. (2002) describe a 25 times increase in the porosity of gneiss (a crystalline, low-porosity metamorphic rock) which had been highly shocked by impact compared to nearby lightly shocked or non-shocked gneiss of the same parent material. They observe that this increased porosity allows bands of phototrophic cyanobacteria to colonize below the surface of the rock in a high-radiation natural environment.

The exposed land on the early Earth, whilst containing some sedimentary lithologies, would most likely have been predominantly comprised of crystalline rocks (Moorbath 2005). In the period between 4.1 and 3.8 billion years ago, asteroid impacts were many orders of magnitude more common than today (Chyba & Owen 1994). Thus, when life appeared, impacts would have been widespread and could have altered the crystalline surface to provide suitable habitats in which the first microbes could survive under the harsh UV conditions encountered on the Earth's land masses.

Since asteroid and comet impacts are ubiquitous throughout the universe, we can extend our hypothesis that impact-shocked rocks provide important habitats to any rocky planet which lacks atmospheric oxygen and is therefore subject to intense UV radiation exposure. This could be particularly important on planets where the geology is dominated by low-porosity crystalline rocks rather than sedimentary lithologies and thus where potential endolithic habitats would be in short supply.

Further details on the shocked gneiss can be found in Fike *et al.* (2002) and Cockell *et al.* (2002). Cockell *et al.* (2002) discuss the improvements for life which resulted from the impact which altered the gneiss used here to its current state.

The polyextremotolerant cyanobacterium *Chroococcidiopsis* sp.029 was selected as a model organism. *Chroococcidiopsis* is one of the most tolerant to extremes of all of the known cyanobacteria. It is remarkably versatile with strains having been described from a wide range of extreme habitats such as hot springs (Geitler 1933), hypersaline (Dor *et al*. 1991) and freshwater (Komarek & Hindak 1975) environments, hot and cold deserts (Friedmann 1980; Friedmann & Ocampo-Friedmann 1985; Budel & Wessels 1991) and within lichens as cyanobionts (Budel & Henssen 1983). In the most extreme hot, cold, arid and saline habitats on Earth, it is generally found to be the dominant cyanobacterium (Friedmann & Ocampo-Friedman 1995). *Chroococcidiopsis* commonly adopts an endolithic lifestyle. The rocks it inhabits act as a shield from harmful environmental conditions (Friedmann 1980).

The long-term survival of *Chroococcidiopsis* aboard the ISS was demonstrated as part of the ESA EXPOSE-E mission (Cockell *et al.* 2011). Cells of *Chroococcidiopsis* sp. 029 were used to artificially augment a natural phototroph biofilm which was exposed to space conditions. These cells were shown to be viable after 534 days in LEO exposed to the full extraterrestrial UV radiation spectrum. This survival was attributed to the high numbers of *Chroococcidiopsis* cells relative to the abundance of other species in the natural phototroph community and protection of live cells by dead cells under a biofilm of cells, which was not a monolayer. In the experiment reported here, the exposure time was extended (22 months compared to 18 for EXPOSE-E) and pure cultures of *Chroococcidiopsis* used in sample preparation. The samples on glass discs have both high numbers of *Chroococcidiopsis* cells and a thin layer of cells so we will be able to test if these are the only attributes contributing to survival in the previous EXPOSE-E experiment.

Sample preparation

Chroococcidiopsis sp. CCMEE 029 was obtained from the Culture Collection of Microorganisms from Extreme Environments (CCMEE) established by E. Imre Friedmann and now maintained at the University of Rome 'Tor Vergata'. Cells were cultured in BG-11 media as described previously (Cockell *et al*. 2005). An aliquot of cells ($\sim 1.5 \times 10^6$ cells) were transferred evenly onto the surface of 0.5 cm-diameter sterile glass discs or 1 cm-diameter discs of impact-shocked gneiss (Fig. 1). The impact-shocked gneiss was 5 mm thick, a thickness within which visible light transmission in the majority of the substrate is sufficient to support photosynthetic growth in natural communities that inhabit these rocks (*Cockell et al*. 2002).

Exposure conditions

The International Space Station (ISS) orbits the Earth at an altitude of around 450 km, in a region termed 'low Earth orbit' (LEO). In this region, our organisms are exposed to a variety of extremes: space vacuum, intense radiation bombardment from both solar and galactic sources as well as extreme and variable temperatures (Horneck *et al*. 2010).

The samples were fixed into the European Space Agency Expose-R facility in March 2009. The technical specifications of this facility have been described previously by Rabbow *et al.* (2009). The EXPOSE facility, run by the European Space

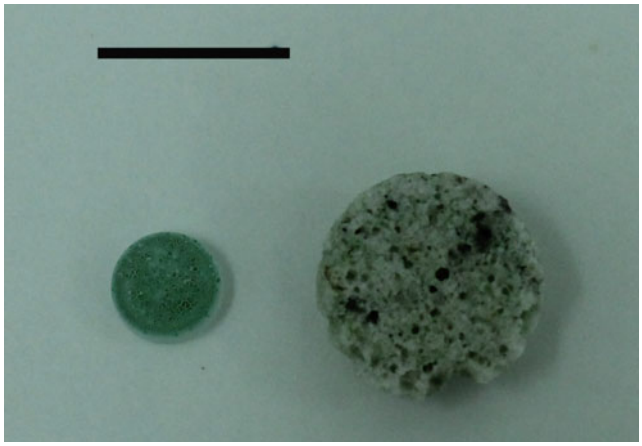

Fig. 1. Image displaying the impact-shocked gneiss (right) and borosilicate glass (left) used as substrates for the experiment.

Agency (ESA), is a multi-user facility which was designed to host medium- to long-term experiments (around 1.5 years) aboard the ISS. It is comprised of three trays containing hundreds of individual compartments in which samples are housed. The trays can be vented to the space environment or sealed and pressurized with defined gases to simulate an atmosphere. A variety of filters are used to control the wavelength and intensity of radiation the samples are exposed to. A range of bacteria, cyanobacteria, fungi, plants and some invertebrates have previously been shown to survive exposure to the full range of space conditions or selected parameters of it (summarized in Horneck *et al.* 2010).

A total of 36 glass discs and 12 rock discs were tested. Half of the glass discs were housed in containers which were vented to allow exposure to the vacuum of space whilst half were in sealed containers filled with argon gas. These experiments therefore investigate the effects of UV radiation alone, but do not take into account any potential confounding effects of interactions between UV radiation and atmospheric components that might have been present in the early Earth atmosphere such as carbon dioxide. Twelve glass discs in each condition were exposed to UV radiation whilst the rest were kept dark. MgF_2 or Suprasil windows were used which let through UV > 110 nm or >170 nm, respectively. In the Suprasil windows further cut-off filters were used to reduce the final UV cut-off to >200 nm. Neutral density filters were used to control radiation dose to 0.01, 1 or 100% of the total radiation (no neutral density filter). Three glass discs in each container (sealed or vented) were exposed to 100% UV > 200 nm, two exposed to 1% UV > 200 nm and three exposed to 0.01% UV > 200 nm. These conditions were repeated for UV > 110 nm to investigate the effects of very short wavelengths of UV radiation.

The UV conditions encountered by each sample type are summarized in Table 1. For the glass discs we report the averages across the two compartments (vented or sealed) as this should not influence the UV flux. The method of calculating UV fluences throughout the experiment are discussed in detail in Rabbow *et al.* (2014, this issue).

All of the samples on rock discs were housed in vented containers. Six rock discs were exposed to 100% of the UV radiation >110 nm and the remaining six kept dark. These rocks were exposed to 80 nm (110–190 nm) of UVC radiation not expected to have been encountered on the early Earth and therefore experienced a UV spectrum on their surface more severe than the worst-case early Earth spectrum. Identically prepared control samples were kept dark in the laboratory for the duration of the experiment. The experiment was conducted for 22 months (10 March 2009–21 February 2011).

Raman spectroscopy

Raman spectroscopy was used to investigate the destruction of biomolecules on exposure to the extreme conditions in LEO. We used the presence or absence of carotenoids as a proxy for biomolecule destruction in our experiments. Carotenoids are a group of coloured pigments which are ubiquitous in nature, particularly in photosynthetic organisms like cyanobacteria and plants. Excitation of a carotenoid containing sample at 514 nm will reveal a characteristic spectrum (Fig. 2), where the Raman shifts relate to the stretching of the C=C and C–C bonds and to the bending of the C–CH groups within the conjugated molecule (Jorge Villar & Edwards 2006).

The observed Raman peaks arise from a resonance effect which causes an amplification of the band intensities above the background. This has proved to be extremely effective in the analysis of biological samples which are complex, of low concentration or which, as is common in cyanobacteria, are prone to being obscured by the significantly stronger fluorescence emission excited by visible laser wavelengths. The technique is particularly suited to the analysis of organic materials in mineral matrices, is also non-destructive and is therefore excellent for studies such as these where samples are extremely precious. It has been used on numerous occasions to detect cyanobacterial biomarkers from extreme environments (e.g. Jorge Villar & Edwards 2006; Wang *et al.* 2010; Vitek *et al.* 2010; Cockell *et al.* 2011).

A Renishaw inVia laser Raman microscope (Renishaw, UK) was used and samples were excited at a wavelength of 514 nm. The laser was typically operated at 5% power with each spectrum being an average of ten acquisitions. Data were analysed using the commercial WiRE 3.2 software package (Renishaw, UK)

Before analysis of the rock discs, a cross-section was obtained with a sterile chisel. A positive or negative result for the carotenoid spectra both on the UV-exposed surface of the disc and the interior was recorded. Selection of the spot on which to sample within the rock was guided by the location of patches of cells as, owing to irregularities in pore spaces, they are not homogeneously distributed throughout the rock. For samples which were highly fluorescent at this level, the laser power was reduced to 1% to ensure that the signal was not hidden by the attendant fluorescence generated. Control spectra were also obtained from a segment of rock on which there were no cells and from dried cells of *Chroococcidiopsis* sp.029 on BG-11 agar.

Table 1. *Average radiation doses experienced by each sample type during the experiment*

Sample type	Cut-off wavelength	% of exposure	External irradiation (kJ m^2)	UVA at sample site (kJ m^2)	UVB at sample site (kJ m^2)	UVC at sample site (kJ m^2)	UV (100–400 nm) at sample site (kJ m^2)	PAR at sample site (kJ m^2)	Total irradiation at sample site (kJ m^2)
Glass disc	110 nm	100	1.7×10^7 ($\pm$ 5 116)	4.6×10^5 $\pm$ 1×10^5)	8.5×10^4 ($\pm$ 2.2×10^4)	3.1×10^4 ($\pm$9266)	5.7×10^5 ($\pm$ 1.3×10^5)	3.7×10^6 ($\pm$ 7×10^5)	8.2×10^6 ($\pm$ 1.5×10^6)
		1	1.7×10^7 ($\pm$ 5392)	4×10^3 ($\pm$ 777)	867 ($\pm$ 176)	205 ($\pm$ 52)	6034 ($\pm$ 1004)	5.1×10^4 ($\pm$ 5055)	1.3×10^5 ($\pm$ 1×10^4)
		0.01	1.7×10^7 ($\pm$ 5116)	51 ($\pm$ 9.1)	8.8 ($\pm$ 2)	2.1 ($\pm$ 0.6)	61 ($\pm$ 12)	521 ($\pm$ 70)	1314 ($\pm$ 160)
Glass disc	200 nm	100	1.7×10^7 ($\pm$ 3×10^5)	3.9×10^5 ($\pm$ 8×10^4)	6.9×10^4 ($\pm$ 1.7×10^4)	2.4×10^4 ($\pm$6732)	4.8×10^5 ($\pm$ 1×10^5)	3.3×10^6 ($\pm$ 6.2×10^5)	7.3×10^6 ($\pm$ 1.3×10^6)
		1	1.7×10^7 ($\pm$ 3×10^5)	4270 ($\pm$ 487)	709 ($\pm$ 129)	166 ($\pm$ 37)	5132 ($\pm$ 649)	4.6×10^4 ($\pm$ 3499)	1.1×10^5 ($\pm$ 7588)
		0.01	1.7×10^7 ($\pm$ 3×10^5)	44 ($\pm$ 6.6)	7.3 ($\pm$ 1.5)	1.7 ($\pm$ 0.4)	53 ($\pm$ 8)	479 ($\pm$ 58)	1176 ($\pm$ 137)
Rock disc	110 nm	100	1.7×10^7	3.7×10^5 ($\pm$ 7×10^4)	5.2×10^4 ($\pm$9676)	1.5×10^4 ($\pm$ 2.9×10^3)	4.3×10^5($\pm$$8.1\times10^4$)	3.8×10^6 ($\pm$ 7×10^5)	8.7×10^6 ($\pm$ 1.6×10^6)

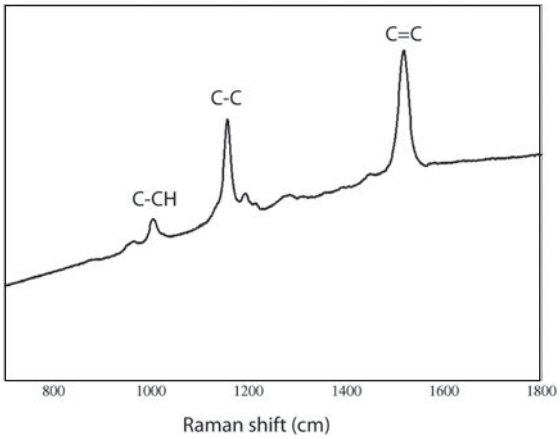

Fig. 2. Raman spectra taken from *Chroococcidiopsis* cells displaying the typical carotenoid signature where peaks correspond to the stretching of the C = C and C–C bonds and the bending of the C–CH group.

One glass disc from each condition was probed in triplicate with a positive or negative result for the typical carotenoid spectra recorded.

Both the glass and the rock used for this experiment were investigated in an identical manner to the experimental samples to ensure that the substrate did not have an independent signal which could confuse the results.

Amplification of 16S rRNA genes from Chroococcidopsis on glass discs

To assess the effect of direct UV radiation exposure on DNA preservation, 16S rRNA was amplified from the glass discs in UV radiation exposed and dark conditions. Cells were recovered from glass discs by vortexing the discs in 200 µl of sterile MilliQ water. Cells were lysed by cryogenic grinding to a fine powder following sequential freeze–thawing cycles in liquid N_2.

Polymerase chain reaction (PCR) was performed using cyanobacteria specific primers, forward primer CYA106F and reverse primer CYC781R (Nubel *et al.* 1997). CYA718 was an equimolar mixture of CYA781R(a) and CYA781R (b). The primers were synthesized commercially (Sigma-Aldrich, UK).

PCR amplifications were performed with an Eppendorf epgradient S mastercycler. Touchdown PCR was performed (Korbie & Mattick 2008), to maximize sensitivity and specificity. 100 µl PCR reactions contained 50 pmoles of each primer, 25 nmol each of dNTP (Roche, Penzberg, Germany), 200 µg of BSA (New England Biolabs, Herts, UK), 10 µl of 10 × PCR buffer and 20 µl of DNA sample. The $MgCl_2$ concentration present in the reaction mixture was supplemented to give a final concentration of 2.5 mM. Reactions were started by the addition of 4 U of SuperTaq DNA polymerase (Cambio, Ltd, Cambridge, UK) after an initial denaturation step (5 min at 94 °C), at 80 °C. The first incubation cycle was 1 min at 94 °C, 1 min at 65 °C and 1 min at 72 °C. In the second cycle, the annealing temperature was decreased by 1–64 °C, in the third cycle by 1–63 °C, and so on in the same stepwise

manner until the annealing temperature was 54 °C (after 12 cycles). Twenty-five further cycles were performed at this annealing temperature followed by a final elongation step of 10 min at 72 °C. The results shown are of a minimum of two independent amplifications. The amplification products were resolved on a 1% TAE agarose gel (40 mM Tris-acetate, 1 mM EDTA, pH 8.0) stained with SYBR Safe DNA gel stain (Invitrogen).

The PCR aims only to provide a qualitative assessment of DNA destruction. Since each sample was prepared identically, a negative result indicates DNA destruction compared to the control samples which consistently display a band.

Post-flight culturing

On return, one-third of each rock disc was placed in 100 ml of BG-11 media with triplicate cultures for each exposure condition. Subsequent growth was identified using bright field microscopy. Since the rock could not be broken into segments with adequate accuracy and cells were unevenly distributed throughout the pore space, calculation of the exact number of cells on each fragment of rock used for the inoculation was not possible. Therefore, only a positive or negative result for growth could be obtained. For the glass discs, one disc for each exposure condition was added to fresh BG-11 media.

Scanning electron microscopy

Both rock discs and glass discs were imaged using scanning electron microscopy. The rock discs were coated in gold before imaging using a Philips XL30CP scanning electron microscope (SEM) (Philips, UK) operated at 1 mbar pressure. Images were obtained using the absorbed current detector (AEI) at a voltage of 20 kV.

Observations on the glass discs were carried out using a CamScan MX2500 SEM (CamScan, UK) operated in controlled pressure mode (Envac, 30 Pa) and coupled to energy dispersive X-ray analysis (EDX) with Noran Vantage system and Vista software. Images were recorded at a working distance of 20 mm using the AEI at a voltage of 20 kV.

Results

Post-flight culturing

Within 4 weeks of inoculation of the fragments of rock discs, numerous 0.5–1 mm green specks were observed on the rock fragments. After 2 months, growth was clearly observed in the media of all experimental samples whether stored in the laboratory, kept dark in LEO or UV exposed in LEO. *Chroococcidiopsis* cells were confirmed under bright field microscopy. Some variability in the growth rates and concentrations of cells between conditions was observed but this was not quantifiable due to the necessary inaccuracies in the number of cells used for inoculation.

It was found that no samples on glass discs, whether in LEO or stored in the lab, had remained viable for the duration of the experiment.

Fig. 3. Image showing colour change in UV-exposed rocks (left) compared to rock kept dark in LEO (right).

Raman spectroscopy

In our samples, we found that glass discs which had been inoculated with cells of *Chroococcidiopsis* and either stored under laboratory conditions or kept dark whilst in the EXPOSE-R facility clearly exhibited the characteristic carotenoid bands described above. This indicates that despite the death of the cells during the period of desiccation the biomolecular carotenoids had not undergone degradation.

In the UV-exposed samples on glass discs the carotenoid peaks were only detectable at a very low level in one sample which had been exposed to 0.01% of the incoming radiation >110 nm in a vented container. All other UV-exposed samples tested exhibited no spectral peaks. Variations in the background fluorescence emission intensity were observed in several of these UV-exposed samples.

Rock discs which had been exposed to UV in LEO exhibited a browning of the surface which was not observed in rock discs which had been kept dark (Fig. 3). The spectra obtained from cells in the rock discs are displayed in Fig. 4. For cells on rock discs stored in the lab or kept dark in LEO the carotenoid signal was detected both on the surface and in the subsurface (Fig. 4(a) and (b)). In the rock discs it was found that cells on the UV-exposed surfaces of the rocks had experienced similar destruction to carotenoids as that exhibited by cells on glass UV-exposed discs (Fig. 4(c)). Cells on the surface of the rocks imaged through the Raman microscope had turned brown during exposure and they did not exhibit any characteristic Raman peaks when probed (Fig. 4(c)). However, below the surface in the cleaved samples, green flecks were observed which when probed at 514 nm exhibited the typical carotenoid Raman spectral signals (Fig. 4(c)). This demonstrates that the rocks were effective in shielding the cells housed internally from 100% exposure to the full extraterrestrial radiation dose >110 nm. We have determined that whilst some fluorescence contribution from glassy minerals in the rocks is present there is no interference that would confuse the interpretation of these characteristic carotenoid spectral signals.

Polymerase chain reaction

The results of the PCR reactions are displayed in Fig. 5. 16S rRNA was successfully amplified from all of the cells on glass

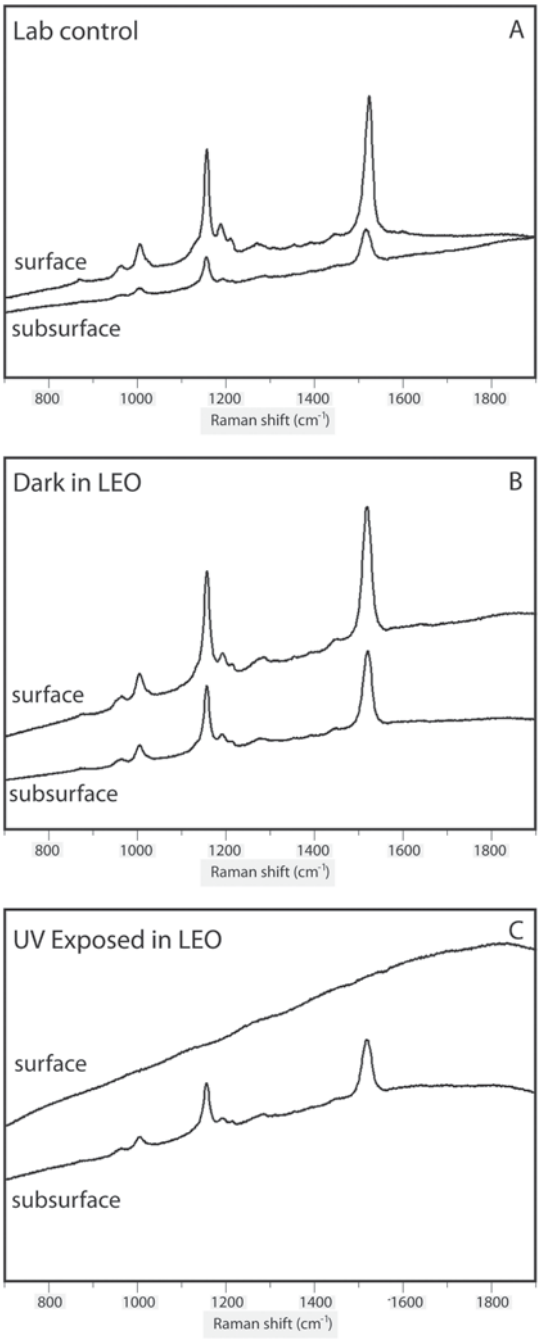

Fig. 4. Raman shift at 514 nm of the patches of cells in the surface and subsurface of rock discs from each condition. The spectral bands indicative of carotenoids is present in the surface and subsurface of the laboratory controls and the dark samples from low Earth orbit as well as the subsurface of the UV-exposed rocks. The brown cells on the surface of the UV-exposed rocks do not show any distinct peaks but exhibit an increased fluorescence.

discs which had been kept in dark conditions, but not on any exposed to UV radiation. There was some variation between the intensity of the bands that were detected. The use of the PCR aimed to provide a proxy for DNA damage to the samples. The successful imaging of bands gives a qualitative assessment of the destruction of DNA since all discs were

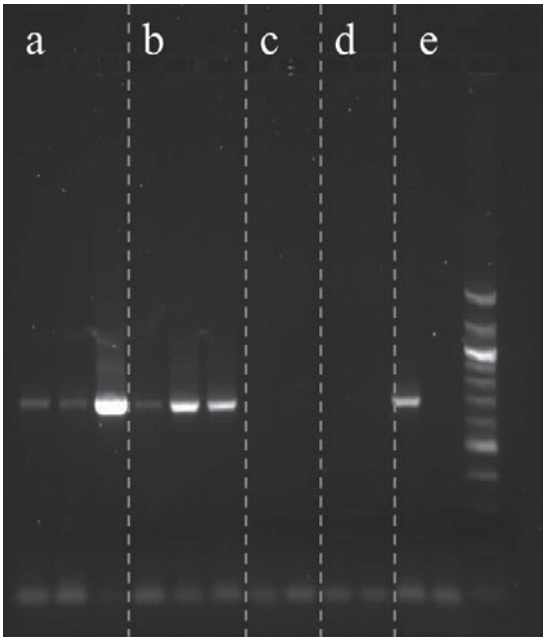

Fig. 5. Amplification of 16S rRNA genes from *Chroococcidiopsis* on glass discs exposed to various space conditions. (a) Amplification of genes from cells on three glass discs kept dark in sealed containers, (b) amplification of genes from cells on three glass discs kept dark in vented containers, (c, d) no gene bands observed from cells on UV-exposed glass discs in sealed (c) or vented, (d) containers, (e) positive control (left), negative control (middle) and marker lane (right).

originally inoculated with the same numbers of cells. For this reason normalization of the DNA was not required.

Scanning electron microscopy

Figure 6 displays SEM images of cells in the pore space of the rocks in the control (a), dark (b) and UV exposed (c) samples. It was observed in the UV-exposed rocks that morphologically intact cells were present even in pores directly exposed to the surface. This could suggest that UV bleaching of the cells had occurred and the biomolecules destroyed whilst the cells still maintained their shape.

SEM images of the glass discs reveal that samples which had been kept dark, despite being dead on their return to Earth, had also retained their morphology (not pictured). This was also the case for the glass discs exposed to UV radiation within vented containers but intact cells were not observed on glass discs which had been kept sealed.

Discussion

In this study, we used the UV radiation conditions found in low Earth orbit (LEO) to determine if an endolithic lifestyle could provide suitable shelter for phototrophs on the anoxic early Earth, or on other anoxic planets, which receive a higher UV radiation dose than the Earth's surface today. Impact shocked gneiss was chosen as the rock substrate to determine whether

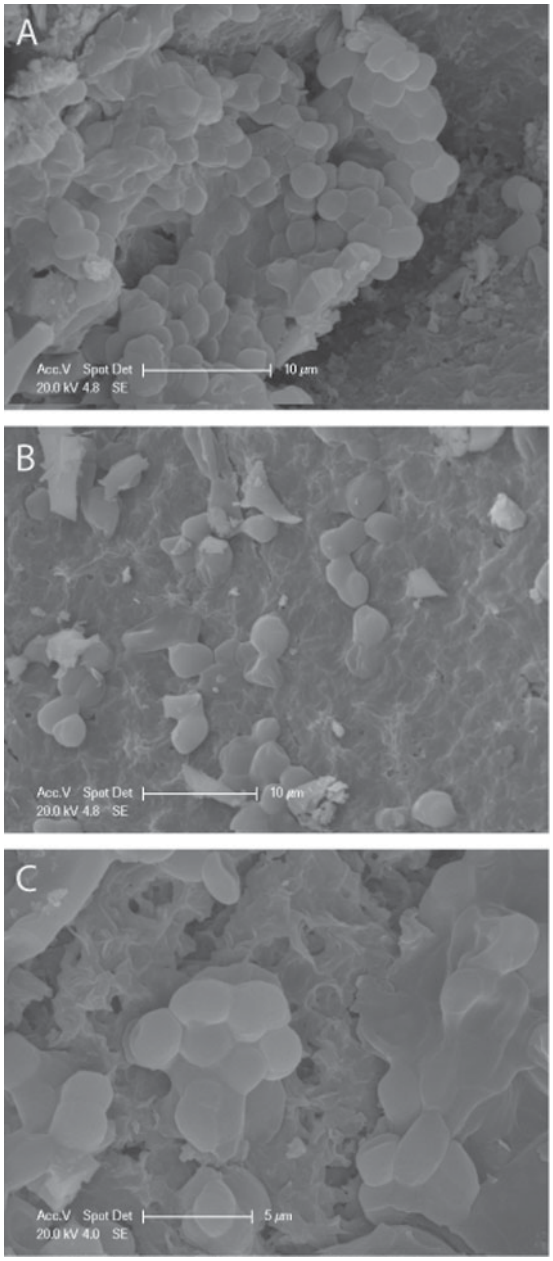

Fig. 6. SEM images of the rock discs show that cell morphology observed in the control was preserved during exposure to space conditions, both dark and UV radiation exposed (a) rock control disc kept dark in the lab for the duration of the experiment, (b) rock disc kept dark in LEO and(c) rock disc exposed to 100% UV > 110 nm in LEO.

new habitats created by impact events could provide adequate protection from the higher UV radiation.

Phototrophs have the requirement for photosynthetically active radiation (PAR) for growth, meaning that they must be exposed to sunlight with the concomitant exposure to UV radiation. Therefore, simply growing at a depth where UV radiation is completely extinguished is not an option.

We report that organisms within impact-shocked gneiss exposed to the intense UV radiation environment in LEO for 22 months were viable on their return to Earth. This reveals that it would be possible for cyanobacteria to persist in a desiccated state for almost 2 years in these rocks under the worst-case UV radiation conditions.

The complete loss of viability in cells on all of the glass discs regardless of exposure conditions (and in controls) could be a result of extreme desiccation of the thin layer of cells on the glass disc. Cells within clumps inside the rocks might have been protected by the extracellular polysaccharide of other cells as observed with other cyanobacteria (Tamaru *et al.* 2005) or have had reduced rates of desiccation when they were prepared. The thin layer of cells desiccated onto the flat glass surface will have dried out quickly. Inside the rocks, cells contained within the liquid would have pooled in pore spaces allowing cells to desiccate more slowly, where it would form thick clumps as seen in Fig. 6(a).

Our results on the UV-exposed glass discs show that direct exposure to the worst-case early Earth UV radiation conditions over a long period will have a destructive effect on biomolecules, destroying both essential pigments and breaking up DNA even when this was attenuated to only 0.01% of the incoming UV. Our PCR and Raman spectroscopy results demonstrate that this damage was not as extensive in discs which had been kept dark compared to those exposed to UV radiation. This supports the general consensus that UV radiation exposure is the most destructive aspect of exposure to space conditions (Horneck *et al.* 2010). This also emphasizes the low survivability of photosynthetic life on the surface of the early Earth in the absence of active repair.

The positive detection of carotenoid signatures observed by Raman spectroscopy in cells exposed to 0.01% UV radiation of >110 nm in vented containers suggests that the radiation dose received at this level may have been close to a threshold level at which biological molecules can survive.

We also observed that UV radiation exposure, death and biomolecule destruction does not necessarily destroy the morphology of cells. SEM images of the rock discs showed that the morphology of some cells within the rocks remained intact regardless of exposure condition or proximity to the surface. The morphology could also be discerned from cells on glass discs from all conditions in vacuum but not on discs housed in argon gas. This could suggest that space vacuum might be advantageous to the preservation of morphology under extreme UV radiation stress. With only one sample available for this imaging analysis this result would require further confirmation; however, this could suggest that the presence of a thick atmosphere may be detrimental to biomarker preservation and detection on a planetary surface with a high-UV flux.

The extent of carotenoid destruction on directly exposed cells (either on the glass discs or the surface of the rocks) compared to those within the impact-shocked rocks highlights the importance of a shielding mechanism in high-UV radiation conditions whether on the early Earth or other rocky planetary surfaces. These data show that impact-shocked rocks provide protection against biomolecule destruction and ultimately loss of cell viability.

We conclude that the protection afforded to organisms within impact-shocked rocks is adequate to preserve viable cyanobacterial cells in a desiccated state for at least 22 months under a UV flux at least equal to the worst-case scenario on the early Earth. This result could extend to other terrestrial-type rocky planets lacking a sufficient atmospheric UV radiation shield. Cells actively growing, unlike the desiccated cells we studied here, would have the potential to actively repair UV radiation-induced damage (assuming the dose is sublethal), suggesting that our results are conservative. This work highlights the potential of impact craters and endolithic habitats as protective habitats on rocky planets with a high-UV radiation flux and it empirically demonstrates that phototrophic microorganisms could have colonized early land masses under a worst-case UV radiation flux even without a matting ability.

Acknowledgements

The authors thank Angela Dawson for her contribution to the PCR, Peter Chung for assistance with the Raman spectroscopy and Lore Troalen for assistance with the SEM on the glass discs. The PhD studentship for C. Bryce is funded by EPSRC.

References

Berkner, L.V. & Marshall, L.C. (1965). History of major atmospheric components. *Proc. Natl. Acad. Sci. USA* **53**, 1215–1225.

Budel, B. & Henssen, A. (1983). *Chroococcidiopsis* (*Cyanophyceae*), a phycobiont in the lichen family *Lichinaceae*. *Phycologia* **22**, 367–375.

Budel, B. & Wessels, D. (1991). Rock inhabiting blue-green algae Cyanobacteria from hot arid regions. *Algolog. Stud.* **64**, 85–398.

Buick, R. (2008). When did oxygenic photosynthesis evolve? *Philos. Trans. R. Soc. Lond. B Biol. Sci.* **363**, 2731–2743.

Chyba, C.F. & Owen, T.C. (1994). Impact delivery of volatiles and organic molecules to Earth. In *Hazards Due To Comets and Asteroids*, ed. Gehrels, T., pp. 9–58. University of Arizona Press, Arizona.

Cockell, C.S. & Horneck, G. (2001). The history of the UV radiation climate of the Earth – theoretical and space-based observations. *Photochem. Photobiol.* **73**(4), 447–451.

Cockell, C.S. & Osinski, G.R. (2007). Impact-induced impoverishment and transformation of a sandstone habitat for lithophytic microorganisms. *Meteorit. Planet. Sci.* **42**, 1985–1993.

Cockell, C.S., Lee, P., Osinski, G., Horneck, G. & Broady, P. (2002). Impact-induced microbial endolithic habitats. *Meteor. Planet. Sci.* **37**, 1287–1298.

Cockell, C.S., Rettberg, P., Horneck, G., Scherer, K. & Stokes, D.M. (2003). Measurements of microbial protection from ultraviolet radiation in polar terrestrial microhabitats. *Polar Biol.* **26**, 62–69.

Cockell, C.S., Schuerger, A.C., Billi, D., Friedmann, E.I. & Panitz, C. (2005). Effects of a simulated Martian UV flux on the cyanobacterium, *Chroococcidiopsis* sp 029. *Astrobiol.* **5**, 127–140.

Cockell, C.S., Rettberg, P., Rabbow, E. & Olsson-Francis, K. (2011). Exposure of phototrophs to 548 days in low Earth orbit: microbial selection pressures in outer space and on early Earth. *ISME J.* **5**, 1671–1682.

Dor, L., Carl, N. & Baldinger, I. (1991). Polymorphisms and salinity tolerance as criterion for differentiation of three new species of *Chroococcidiopsis* (*Chrococcidiopsis Chrococcales*). *Algolog. Stud.* **64**, 411–421.

Fike, D.A., Cockell, C.S., Pearce, D. & Lee, P. (2002). Heterotrophic microbial colonization of the interior of impact-shocked rocks from Haughton impact structure, Devon Island, Nunavut, Canadian High Arctic. *Int. J. Astrobiol* **1**, 311–323.

Friedmann, E.I. (1980). Endolithic microbial life in hot and cold deserts. *Orig. Life* **10**, 223–235.

Friedmann, E.I. & Ocampo-Friedmann, R. (1995). A primitive cyanobacterium as pioneer microorganism for terraforming Mars. *Adv. Space Res.* **15**(3), 243–246.

Geitler, L. (1933). Diagnosen neuer Blaualgen von den Dunda Inseln. *Arch. Hydrobiol. – Suppl* **12**, 622–634.

Horneck, G., Klaus, D.M. & Mancinelli, R.L. (2010). Space microbiology. *Microbiol. Mol. Biol. Rev.* **74**, 121–156.

Jorge-Villar, S.E. & Edwards, H.G.M. (2006). Raman spectroscopy in Astrobiology. *Anal. Bioanal. Chem.* **384**, 100–113.

Kasting, J.F. & Siefert, J.L. (2002). Life and the evolution of Earth's atmosphere. *Science* **296**, 1066–1068.

Komarek, J. & Hindak, J. (1975). Taxonomy of the new isolated strains of *Chroococcidiopsis* (*Cyanophyceae*). *Arch. Hydrobiol.* **13**, 311–329.

Korbie, D.J. & Mattick, J.S. (2008). Touchdown PCR for increased specificity and sensitivity in PCR amplification. *Nat. Protoc.* **3**(9), 1452–1454.

Margulis, L., Walker, J.C.G. & Rambler, M. (1976). Reassessment of roles of oxygen and ultraviolet light in Precambrian evolution. *Nature* **264**, 620–624.

Moorbath, S. (2005). Oldest rocks, earliest life, heaviest impacts and the Hadean–Archaean transition. *Appl. Geochem.* **5**, 819–824.

Nubel, U., Garcia-Pichel, F. & Muyzer, G. (1997). PCR primers to amplify 16S rRNA genes from Cyanobacteria. *Appl. Environ. Microbiol.* **63**(8), 3327–3332.

Osinski, G.R., Lee, P., Spray, J.G., Parnell, J., Lim, D.S.S., Bunch, T.E., Cockell, C.S. & Glass, B. (2005). Geological overview and cratering model for the Haughton impact structure, Devon Island, Canadian High Arctic. *Met. Planet. Sci.* **40**, 1759–1776.

Pontefract, A., Osinski, G.R., Lindgren, P., Parnell, J., Cockell, C.S. & Southam, G. (2012). The effects of meteorite impacts on the availability of bioessential elements for endolithic organisms. *Met. Planet. Sci.* **47**, 1681–1691.

Rabbow, E. *et al.* (2009). EXPOSE, an astrobiological exposure facility on the International Space Station – from proposal to flight. *Orig. Life. Evol. Biosph.* **39**, 581–98.

Rabbow, E., Rettberg, P., Barczyk, S., Bohmeier, M., Parpart, A., Panitz, C., Horneck, G., Burfeindt, J., Molter, M., Jaramillo, E., Pereira, C., Weiß, P., Willnecker, R., Demets, R., Dettmann, J. &, Reitz, G. (2014). *The Astrobiological Mission EXPOSE-R on board of the International Space Station*.

Rettberg, P., Horneck, G., Strauch, W., Facius, R. & Seckmeyer, G. (1998). Simulation of planetary UV radiation climate on the example of the early Earth. *Adv. Space Res.* **22**, 335–339.

Tamaru, Y., Takani, Y., Yoshida, T. & Sakomoto, T. (2005). Crucial role of extracellular polysaccharides in desiccation and freezing tolerance in the terrestrial cyanobacterium *Nostoc commune*. *Appl. Environ. Microbiol.* **71**, 7327–7333.

Vítek, P., Edwards, H.G.M., Jehlicka, J., Ascaso, C., De los Ríos, A., Valea, S., Jorge-Villar, S.E., Davila, A.F. & Wierzchos, J. (2010). Microbial colonization of halite from the hyper-arid Atacama Desert studied by Raman spectroscopy. *Philos. Trans. R. Soc. A* 368(1922), 3205–3221.

Wang, G., Hao, Z., Huang, Z., Chen, L., Li, X., Hu, C. & Liu, Y. (2010). Raman spectroscopic analysis of a desert cyanobacterium *Nostoc* sp. in response to UVB radiation. *Astrobiology* **10**(8), 783–787.

Westall, F., de Ronde, C. E. J., Southam, G., Grassineau, N., Colas, M., Cockell, C. S. & Lammer, H. (2006). Implications of a 3.472–3.333-Gyr-old subaerial microbial mat from the Barbeton greenstone belt, South Africa for the UV environmental conditions on the early Earth. *Philos. Trans. R. Soc. B* **361**, 1857–1875.